Advanced PID Control Optimisation and System Identification for Multivariable Glass Furnace Processes by Genetic Algorithms

Kumaran Rajarathinam

A thesis submitted in partial fulfillment of the requirements of
Liverpool John Moores University for the degree of
Doctor of Philosophy

February 2016

To My Parents, Wife and Two Little Angles

Sekaran, Sarojini, Annaletchumy, Niranjanaa and Hamssini

Acknowledgements

First and foremost, I would like to extend my gratitude and great appreciation to my first Supervisor, Dr. Barry Gomm for his continual support, guidance and invaluable advice throughout the duration of this PhD project. I would also like to thank my second Supervisor Prof. DingLi Yu for his support and encouragement throughout this research investigation.

Many individuals have unknowingly helped me in my research throughout my PhD and therefore I would like to thank all of my fellow researchers and academics at the Control Research Group at the Liverpool John Moores University for their insight and experience. Without the fantastic research environment created by these individuals, the completion of this project would not have been possible.

I would also like to acknowledge the support and encouragement of my friends for their valuable contributions. Most importantly, my special thanks and deepest appreciation to my parents, wife, children and all my family members. It is a hackneyed theme to thank loved ones for patience and understanding while a project is being undertaken, but now I know why, and do give heartfelt thanks.

Trademarks

Abstract

This thesis focuses on the development and analysis of general methods for the design of optimal discrete PID control strategies for multivariable glass furnace processes, where standard genetic algorithms (SGAs) are applied to optimise specially formulated objective functions. Furthermore, a strong emphasis is given on the realistic model parameters identification method, which is illustrated to be applicable to a wide range of higher order model parameters identification problems.

A complete, realistic and continuous excess oxygen model with nonlinearity effect was developed and the model parameters were identified. The developed excess oxygen model consisted of three sub-models to characterise the real plant response. The developed excess oxygen model was evaluated and compared with real plant dynamic response data, which illustrated the high degree of accuracy of the developed model.

A new technique named predetermined time constant approximation was proposed to make an assumption on the initial value of a predetermined time constant, whose motive is to facilitate the SGAs to explore and exploit an optimal value for higher order of continuous model's parameters identification. Also, the proposed predetermined time constant approximation technique demonstrated that the population diversity is well sustained while exploring the feasible search region and exploiting to an optimal value. In general, the proposed method improves the SGAs convergence rate towards the global optimum and illustrated the effectiveness.

An automatic tuning of decentralised discrete PID controllers for multivariable processes, based on SGAs, was proposed. The main improvement of the proposed technique is the ability to enhance the control robustness and to optimise discrete

PID parameters by compensating the loop interaction of a multivariable process. This is attained by adding the individually optimised objective function of glass temperature and excess oxygen processes as one objective function, to include the total effect of the loop interaction by applying step inputs on both set points, temperature and excess oxygen, at two different time periods in one simulation.

The effectiveness of the proposed tuning technique was supported by a number of simulation results using two other SGAs conventional tuning techniques with 1^{st} and 2^{nd} order control oriented models. It was illustrated that, in all cases, the resulting discrete PID control parameters completely satisfied all performance specifications.

A new technique to minimise the fuel consumption for glass furnace processes while sustaining the glass temperature is proposed. This proposed technique is achieved by reducing the excess oxygen within the optimum thermal efficiency region within 1.7% to 3.2%, which is approximately equal to about 10% to 20% of excess air. Therefore, by reducing the excess oxygen set point within the optimum region, 2.45% to 2%, the fuel consumption is minimised from $0.002942kg/sec$ to $0.002868kg/sec$ while the thermal efficiency of the glass temperature is sustained at the desired set point ($1550K$).

In addition, a reduction in excess oxygen within methane combustion guidelines will assure that undesirable emissions are in control throughout the combustion process. The efficiencies of the proposed technique were supported by a number of simulation results applying the three SGAs controller tuning techniques. It was illustrated that, in all cases, the fraction of excess oxygen reduction results in a great minimisation of fuel consumption over long plant operating periods.

Contents

List of Figures

List of Tables

Glossary of Symbols

Nomenclature

α_1	Gas flame zone
α_2	Gas non-flame zone
β_1	Glass surface flame zone (half inch thickness)
β_2	Glass surface non-flame zone (half inch thickness)
Δ_{GO}	Genetic operator for convergence precision
δ_1	Glass volume flame zone (bottom half)
δ_2	Glass volume non-flame zone (bottom half)
$\delta(\%)$	Settling band
ε_g	Emissivity coefficient of real gas
ζ	Zeta, damping ratio
θ_i	Angle of surface elements, i
θ_j	Angle of surface elements, j
k	Emissivity coefficient of gas
λ	Lambda, weighting factor, combustible mixture
ρ	Density
σ	Stephan-Boltzman constant
ϕ	Equivalent ratio combustible mixture
χ_1	Glass volume flame zone (top half)
χ_2	Glass volume non-flame zone (top half)
ω_n	Natural frequency
ω_{pc}	Phase crossover frequency
A_i	Area of surface element i

A_j	Area of surface element j
$a_n ... a_1$	Coefficients of denominator polynomials
a_g	Gray gases
a_j	Lower boundary of individual chromosome's
a	Time constant
b_j	Upper boundary of individual chromosome's
C_i	Constant by set of initial conditions
Css	Zero steady-state
c	Specific heat
Dec	Decimal value of respective binary string
E_i	Black emissive power of surface i
E_j	Black emissive power of surface j
$E(s)$	Control error
$E_{g,i}$	Black emissive power of gas
f	Fuel-air ratio
f_s	Stoichiometric fuel-air ratio
f_1	Algebraic expression of fuel controller (kg/s)
f_2	Algebraic expression of thermal energy demand (K)
$f(t-\theta)$	Input signal or forcing function with time delay
$G_C(s)$	Control strategies
G_i	Heat flux gas zone i
G_j	Heat flux gas zone j
$G_P(s)$	System's process
h	Radiation heat transfer coefficient
J_i	Performance criterion
K_D	Derivative gain
K_I	Integral gain
K	Number of parameters
K_p	Process gain
K_P	Proportional gain

$\dot{m}$	Fuel flow (kg/s)
$\dot{m}$	Fuel flow (kg/s)
$Maxfuel_{(constant)}$	Maximum fuel flow (constant) (kg/s)
m_j	Number of bits of individual chromosome's
n	Sample size
P_f	Internal pressure of furnace (psi)
P_i	Incident power
p_i	Root of denominator
P	Partial pressure of gray gases
Q	Generated heat
Q_{i_G,j_G}	Heat transfer between gas zone i and gas zone j
Q_{i_G,j_S}	Heat transfer between gas zone i and surface zone j
Q_{i_S,j_S}	Heat transfer between surface zone i and gas surface j
$q_{rad,}$	Net rate of heat flow
q	Power loss
Q_{Fuel}	Pressurised fuel flow as energy
$\underline{R}$	Methane gas constant $(ft.Ibf/Ibm.R)$
$R(s)$	Reference input
r_{ij}	Size of vector that connects the centres of two elements
S_i	Heat flux surface zone i
S_j	Heat flux surface zone j
T_1, T_2	Absolute temperature of involved regions
ts	Settling time
t	Time
u	Temperature feedback error
$\bar{V}$	Mean methane temperature (K)
$\dot{V}$	Methane flow rate in volumetric (ft^3/hr)
V_i	Volume of gas element i
V_j	Volume of gas element j
X_i	Optimal value
x_j	Respective real value of the chromosome's

$X_i^{'}$	Sub-optimal value
$Y(s)$	Controlled output
$YoutN(t)$	Model process output signal
$y(t)$	Output Signal
$Y(t)$	Real process output signal

Abbreviations

AFR	Air-fuel ratio
$AFR_{(Mass)}$	Air-fuel ratio in mass (kg)
$AFR_{stoichiometric)}$	Stoichiometric Air-fuel ratio
$AFR_{(Volumetric)}$	Air-fuel ratio in volumetric (ft^3)
AIC	Akaike information criterion
$AICc$	Akaike information criterion with correction
BIC	Bayesian information criterion
BLT	Biggest log modulus
C	Carbon
CFD	Computational fluid dynamics
C_g	Glass temperature control
CH_4	Methane fuel
CO_2	Carbon dioxide
$DCSs$	Distributed Control Systems
DR_P	Process's dynamic period
DS	Direct-Synthesis
EA	Excess air
ED	Thermal energy demand (K)
EO_2	Excess oxygen (%)
EOP	Effective open-loop
$FOPDT$	First-order plus dead-time
FPE	Akaike's Final prediction error criterion
GM	Gain Margin

H	Hydrogen
H_2O	Hydrogen oxide (Water)
IAE	Integral absolute error
IMC	Internal model control
ISE	Integral sum error
LHV	Lower calorific heat value (MJ/kg)
$MIMO$	Multiple-input multiple-output
$MOEA$	Multi-objective evolutionary algorithm
$MRAC$	Model reference adaptive control
N_2	Nitrogen
O_2	Oxygen
PID	Proportional, Integral, Derivative
PLC	Programmable Logic Controllers
POD	Proper orthogonal decomposition
PSO	Particle swarm optimiser
$PTcA$	Predetermined time constant approximation
$RETF$	Reduced effective transfer function
RGA	Relative gain array
S	Sulphur
SAE	Sum of absolute error
SB_{Lower}	Lower search boundary
SB_O	Optimum search boundary
SB_{Upper}	Upper search boundary
$SGAs$	Standard genetic algorithms
$SISO$	Single-input single-output
SO_2	Sulphur dioxide
$SOPDT$	Second-order plus dead-time
SSE	Sum of square error
T_{amb}	Ambient temperature (K)
T_g	Glass temperature (K)
$Ts_{p(Initial)}$	Initial predetermined time constant

$TITO$	Two-input two-output
T_{SET}	Primary temperature setting (K)

Algorithm Definitions

$FitnV$	Fitness value, chromosomes evolution
G_{gap}	Generation gap
L_{ind}	Length of chromosome
N_{ind}	Number of individuals
N_{keep}	Number of selected group of fitter chromosomes
N_{keep1}	Offspring chromosomes matrix of new population
N_{pop}	Number of population size
N_{va}	Number of variables
$PRECI$	Precision, number of bits depends on desired accuracy
$SEL-F$	Selection function
S_{rate}	Selection rate, fraction of number of population
SUS	Stochastic universal sampling, selection process
$XOV-F$	Crossover function
X_{rate}	Probability of recombination rate

Chapter 1

INTRODUCTION – OVERVIEW AND THESIS OUTLINE

This chapter begins with a brief review of the obstacles faced in glass furnace industries to optimise the desire performances. In particular, the tight environmental regulations to control undesirable emissions associated with burning fossil fuels and excess oxygen. Finally, the project scope and the structure of this thesis are outlined.

1.1 Review of Glass Furnace Processes and Control

Glass manufacturing represents a challenge for automation and for control engineers as it is a very complex, long dynamic process with complicated, nonlinear and not completely understood dynamical behaviour. So it is still common that glass furnaces are controlled by simple controllers such as PID regulators or by manual interventions of furnace operators. As a result, the process may be kept in suboptimal conditions and acting disturbances may not be effectively rejected.

However, market competition creates a need for tighter control of the process towards optimum. Glass furnaces are usually energised by fossil fuels or electricity. The massive furnaces with multiple port burners cause the glass manufacturing industries to consume high energies in glass production. Most glass industries are

operating at maximum daily through-put to fulfil the market demand and requirement. High energy costs and severe competition amongst glass manufacturers has resulted in the emergence of several solutions to reduce the fuel consumption of these furnaces.

Apart from high energy consumption, undesirable emission from glass industries is another setback to consider as the entire world is greatly concerned about green house effects. Tight environmental regulations are now applied to reduce carbon monoxide, sulphur dioxide, nitrogen oxides and particles that are undesirable emissions associated with burning fossil fuels. These compounds are toxic, contribute to pollutions and can ultimately cause health problems.

In the USA, federal and state laws govern the permissible emission rates for these pollutants under the guidance of the Clean Air Act and oversight of the federal Environmental Protection Agency (EPA), National Risk Management Research Laboratory, (2004). State and local environmental agencies also exert authority in regulating the emissions of these pollutants.

Globally, 191 states have signed and ratified the Kyoto Protocol (1998) to execute themselves in a reduction of four green-house gases (carbon dioxide, methane, nitrous oxide and sulphur hexafluoride) which would badly interfere with the global climate system and human health. According to article 2 of the Kyoto Protocol, the reduction of emissions is focused on industrial combustion emission. As a result, the industries which are related to combustion processes are tightly observed by environmental agencies to ensure stabilization of green house gases emission.

To act in accordance with emission guidelines and for clean emission, most process industries are emphasising in reduction of the excess oxygen (EO_2) by controlling the air-fuel ratio (AFR). EO_2 is an important element in combustion products that would lead to formation of sulphur dioxide (SO_2) and nitrous oxide (NO_2). According to the combustion emission guideline, the permissible EO_2 is not more than 3% from combustion, excluding Japan which allows not more than 5% of EO_2 from combustion.

1.2 Problem Statement

Literature survey reveals that there has been no research undertaken on EO_2 model parameter identification and control parameter optimisation. Also, an insignificant number of works has been undertaken on control parameter optimisation for glass furnaces. Further, the glass and other process industries generally operate within emission guidelines which are regulated by environmental agencies (SEPA, 2005). Thus, a necessity of an EO_2 model parameters identification has not arisen and has not been considered. However, at maximum operating conditions with high energy consumption, the probability of producing undesirable emission is high. Any occurrence of sudden undesirable disturbances can cause more problems for existing furnaces which are operating in poor thermal conditions.

Therefore, it is clear that in order to bridge the gap between EO_2 and the glass furnace, a multivariable process with the respective discrete control parameters will be designed to minimise the fuel consumption while sustain the desired glass temperature. The research presented in this thesis is focused on this problem and delivers solutions that satisfy these criteria.

1.3 Research Novelty and Methodology

The primary endeavour of this research is to design a multivariable glass furnace model for fuel consumption minimization and EO_2 reduction while sustaining the desired output. The strategy of this work is developed using standard genetic algorithms (SGAs), a heuristic optimisation technique based on Darwin's theory [1]. The developed models and control methods will be evaluated applying simulation and Matlab software.

More specifically, this thesis addresses the distinct objectives below and as de-

[1] Darwin's theory of biological evolution, stating that all species of organisms arise and develop through the natural selection of small, inherited variations that increase the individual's ability to compete, survive and reproduce

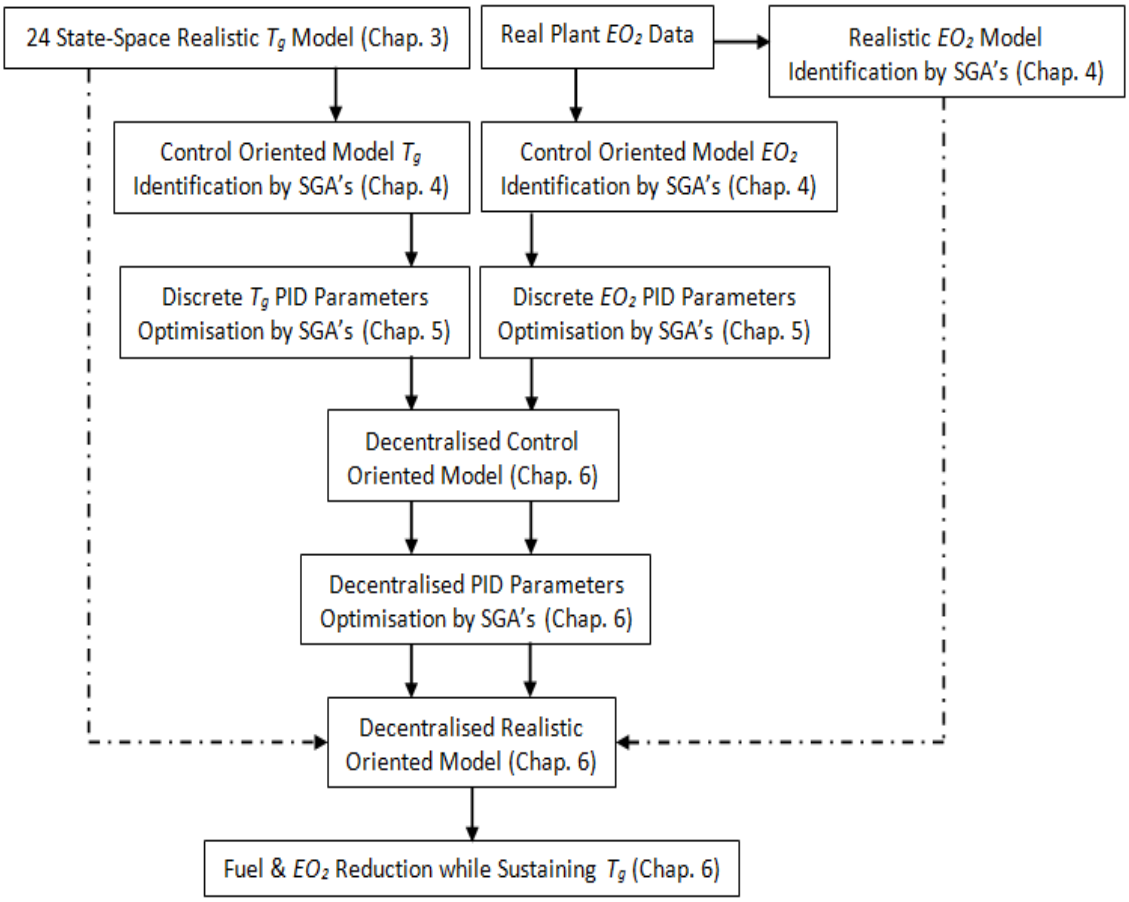

Figure 1.1: Schematic Flow of Research Methodology

scribed in schematic flow (Figure 1.1):

1. Identify and investigate the dynamic characteristics of a realistic 24 state-space glass temperature (T_g) model. Then, develop a control oriented glass T_g simulation model.

2. Develop and investigate a realistic simulation model with nonlinear effect and a control oriented simulation model without nonlinear effect of excess oxygen (EO_2) from numerical data of real plant.

3. Optimise the discrete control parameters according to the performance criteria of T_g and EO_2, individually.

4. Develop the discrete decentralised control strategies by control oriented models of T_g and EO_2. Then, improve and optimise the dynamic discrete control strategies by three tuning approaches.

5. Implement and evaluate the optimised discrete control strategies on realistic multivariable process for attaining the desired performances.

1.4 Thesis Outline

The structure of this thesis is outlined below. Most of the material contained in chapters 2 and 3 is standard and is only intended as a brief review of the current state of affairs in the field of GAs as function optimisers. The main contributions and novel aspects of this work are contained in chapters 4 to 6 and are summarised in Chapter 7.

- ***Chapter 2 - Literature Review of Standard Genetic Algorithms***

This chapter commences with a brief overview of optimisation algorithms as applied to the solution of control engineering problems. Standard Genetic Algorithms (SGAs) as function optimisers are then introduced, focusing on their fundamental differences and advantages over conventional algorithms. The relevance of SGAs to control systems is then illustrated by a number of successful applications in different areas of process modelling and control optimisation. Finally, applications of SGAs for glass furnace and furnace type processes are outlined.

- ***Chapter 3 - Review of Glass Furnace Modelling***

This chapter begins with a brief literature review of designing the combustion chamber, which is fundamental to the developed methods for the glass furnace models. Computational fluid dynamics method derived from radiative heat transfer were applied here to analyse the temperature distribution within the combustion chamber, which is divided into finite zones. Linearised energy balance equations in steady-state improve the prediction and accuracy of temperature distribution within finite zones. An assessment on the selected glass furnace model, which is designed by a zone method, provides a deeper insight of model understanding and quantitative performance.

- ***Chapter 4 - Model Parameters Identification of Glass Temperature and Excess Oxygen***

This chapter is primarily focused on optimal control oriented model's parameter identification for glass temperature and excess oxygen. A common phenomenon of premature convergence, which is the search space constraint, in SGAs is reviewed. A novel technique, predetermined time constant approximation, is proposed to enhance the search mechanism to optimise the search boundaries to locate optimal values of model parameters. Further, a full scale realistic excess oxygen model which consists of air-fuel ratio conversion model, dynamic transfer function model and excess oxygen look-up table, is developed by using a real plant's numerical data of excess oxygen.

According to the literature survey, there is no realistic excess oxygen model available for further research. Therefore, the development of a realistic excess oxygen model is essential for further research here. Also, control oriented models of both glass temperature and excess oxygen processes are developed for control parameter optimisation.

- ***Chapter 5 - Control Parameters Optimisation of Glass Temperature and Excess Oxygen***

In this chapter, the discrete control (PID) parameters optimisation by SGAs for control oriented models of glass temperature and excess oxygen, which are identified in chapter 4, is primarily focused on. A literature review of PID control strategies and tuning issues are briefly discussed and addressed. The control parameters of both control oriented models are optimised individually without loop interaction according to the desired performance criteria. The improved search space boundaries and modified objective function are subsequently introduced for excess oxygen and glass temperature respectively, to improve the discrete PID parameters to attain the desired dynamic performance criteria.

The search space boundaries are improved by resizing the upper and lower boundaries with an assist of conventional tuning techniques, Ziegler-Nichols and Direct

Synthesis, for an initial knowledge of PID parameters. For the glass temperature, the objective function is modified by adding a weighting factor with input term to achieve the desired characteristic response. Further, three other modified objective functions are analysed and compared with the selected objective function for better dynamic characteristics of glass temperature response.

- ***Chapter 6 - Decentralised PID Controller Tuning for Multivariable Glass Furnace Process***

In this chapter, the decentralised discrete PID control tuning techniques are investigated for the multivariable glass furnace process. A literature review of multivariable PID control strategies and tuning issues are briefly discussed and addressed. Three tuning approaches with respective objective functions are investigated to optimise the control performances for control oriented multivariable glass furnace models. An improved and modified objective function which includes the total effect is proposed with other conventional tuning techniques, based on SGAs. This modified objective function is shown to exhibit improved control robustness and disturbance rejection under loop interaction. This is achieved by combining both optimal objective functions of T_g and EO_2 on control oriented models which were developed individually in chapter 5.

Further, the set of discrete PID parameters are applied on the multivariable realistic model of T_g and EO_2 to optimise fuel consumption reduction and excess oxygen while sustaining the glass temperature. Simulation results are presented to illustrate the effectiveness of the proposed method.

- ***Chapter 7- Conclusions - Main Contributions and Further Work***

The first part of this chapter summarises the key results and main contributions of this research project. A number of recommendations for further work in this direction, which will extend an improvement of SGAs in the area of model parameters identification and state-space model extension with respective thermal energy as input, are given in the second part of this chapter.

1.5 Dissemination of Research Contributions

During this research an endeavour has been made in order to suggest the ideas and methodologies proposed in this thesis to a variety of different audiences through both peer reviewed publications and presentations. The publications made throughout the duration of research are listed below:

- Rajarathinam K., Gomm J. B. and Yu D. L, "*Identification, Simulation and Control Optimisation of a Glass Furnace by Genetic Algorithm*", Proceeding of the GERI 8th Annual Research Symposium (GARS 2013), LJMU, UK, 2013,

- Rajarathinam K., Gomm J. B., Yu D. L. and Abdelhadi A. S., "*Minimisation of Fuel Consumption in a Glass Furnaces Industry by Standard Genetic Algorithms*", Proceeding of the GERI 9th Annual Research Symposium (GARS 2014), LJMU, UK, 2014.

- Rajarathinam K., Gomm J. B., Yu D. L. and Abdelhadi A. S., "*Decentralised Control Optimisation for a Glass Furnace by SGA's*", Proceeding of the 15th International Conference on Computer Systems and Technologies (CompSysTech'14), Ruse, Bulgaria, 2014. Also published in ACM International Conference Proceeding Series, vol. 883, pp. 248-255, 2014. (Best Paper Award)

- Rajarathinam K., Gomm J. B., Yu D. L. and Abdelhadi A. S., "*Decentralised PID Control Tuning for a Multivariable Glass Furnace by Genetic Algorithm*", Proceeding of the 20th International Conference on Automation and Computing (ICAC), Bedfordshire, UK, pp. 14-19, 2014.

- Rajarathinam K., Gomm J. B., Yu D. L. and Abdelhadi A. S., "*PID Controller Tuning for a Multivariable Glass Furnace Process by Genetic Algorithm*", International Journal of Automation and Computing (IJAC), vol. 13 (1), pp. 64-72, 2016. (accepted, June 2015).

- Rajarathinam K., Gomm J. B., Yu D. L. and Abdelhadi A. S., "*Predetermined Time Constant Approximation Method for Model Identification Search Space*

Boundary by Standard Genetic Algorithm", SIAM Conference on Control and Its Applications, Paris, France, CP22, pp. 73, 2015. (Abstracts accepted).

- Rajarathinam K., Gomm J. B. and Yu D. L., "*Predetermined Time Constant Approximation Method for Optimising Search Space Boundary by Standard Genetic Algorithm*", Proceeding of the 16$^{\text{th}}$ International Conference on Computer Systems and Technologies (CompSysTech'15), Dublin, Ireland, 2015. Also published in ACM International Conference Proceeding Series, vol. 1008, pp. 38-45, 2015.

- Rajarathinam K., Gomm J. B., Yu D. L. and Abdelhadi A. S., "*An Improved Search Space Resizing Method for Model Identification by Standard Genetic Algorithm*", Proceeding of the 21$^{\text{st}}$ International Conference on Automation and Computing (ICAC), Glasgow, UK, pp. 1-6, 2015.

This chapter begins with an overview of challenges that are face by glass furnace industries in higher fuel consumption and undesirable emission. The research methodologies and the structure of this thesis are outlined, and related research publications are listed.

Chapter 2

Literature Review of Optimisation and Genetic Algorithms

2.1 Introduction

This chapter commences with a brief overview of optimisation algorithms as applied to the solution of control engineering problems. Standard Genetic Algorithms (SGAs) as function optimisers are then introduced, focusing on their fundamental differences and advantages over conventional algorithms. The relevance of SGAs to control systems is then illustrated by a number of successful applications in different areas of process modelling, control optimisation, multiobjective optimisation and the negative aspect of optimisation by premature convergence factors are reviewed. Further, the single-input single-out and multi-variable PID tuning strategies are reviewed. Finally, applications of SGAs for glass furnace and furnace type processes are outlined.

2.2 Definition of Optimum

In general, an optimisation is applied to locate the finest promising solutions to a specified difficulty. In the simplest case, an optimisation problem consists of maximising or minimising an objective function, J_i, by systematically selecting the input variables from within a feasible parameter set depending on the desired criterion.

The generalization of optimization theory and techniques to other formulations comprises a large area of control theory or applied mathematics.

In mathematics, maxima and minima are the prime values (maximum) or least values (minimum) that a function brought in a point either within a given local minima or on the function domain in its global maximum. Figure 2.1 illustrates the local and global maxima and minima for a random function, $f(x) = exp^{-x}.cos(2\pi x)$ for $0.2 \leq x \leq 2.7$.

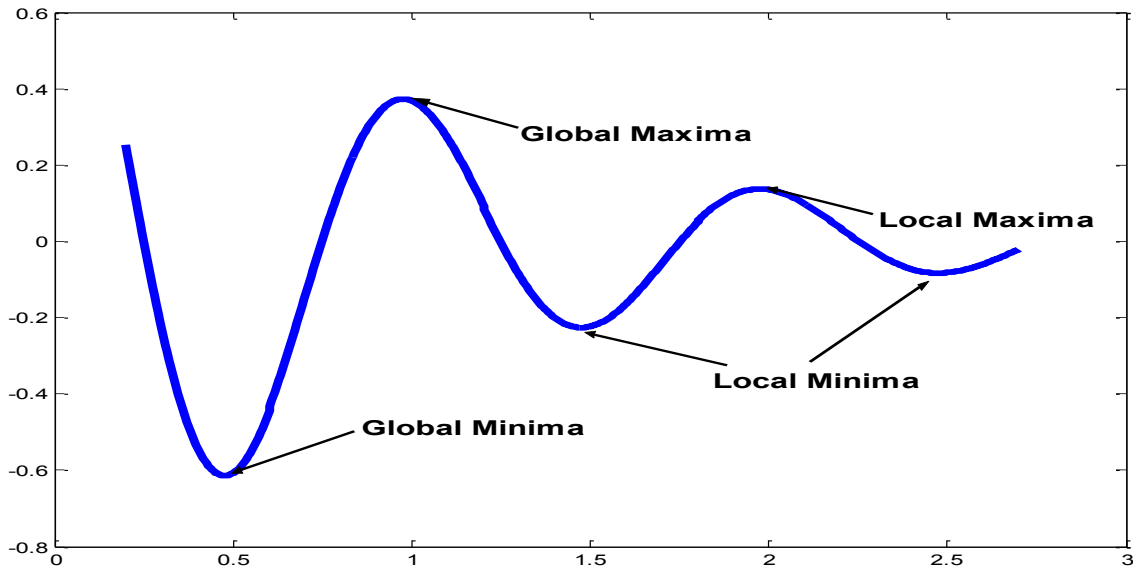

Figure 2.1: Global and local maxima and minima

Furthermore, the classification of an optimal solution is problem dependent. For instance, single objective optimisation can be classified either minimum or maximum. Whereas, for multi objective optimisations minimum or maximum perceptions are rather applied to sets F consisting of $n =\mid F \mid$objective functions f_i, each representing one criterion to be optimised [Kalyanmoy, 2001].

$$F = \{f_i : X \rightarrow Y_i : 0 < t < n, Y_i \subseteq R\} \tag{2.1}$$

2.3 Overview of Optimisation Algorithms

It is difficult to visualize the selection of existing computational tasks and the number of algorithms developed to resolve them. In general, the heuristic can be categor-

ised into two groups of techniques; deterministic and probabilistic techniques. The overview begins with deterministic search algorithm. The straightforward searching algorithm is known as exhaustive search, which endeavours all potential solutions from a predetermined set and consequently selects the optimal value.

- **Local search** is an uncomplicated search technique, however with limited search space. This technique is constantly examining the current solution and replacing it if the neighbour's solution is better than the current one. If the solution is not improved further, the current solution can be considered as a local optimal solution [Kokash and Natallia, 2005]. Popular hill-climbing techniques belong to this class. For instance, heuristics for the problem of intergroup replication for multimedia distribution service based on Peer-to-Peer network is based on a hill-climbing strategy [Xiang et. al., 2004].

- **Divide & Conquer (D&C)** is an algorithm attempt to resolve in effortlessly by partitioning a problem into sub-problems. Subsequently, the resolution of the sub-problems should be combinable to provide a resolution to the original problem. Although this method is an efficient algorithm and applicable for any problems, the shortcoming is that it is time consuming to comprehend and design D&C. Also, it is difficult to partition and combine back the sub-problem in such an approach [Cormen et. al., 2000].

- **Branch-and-Bound (B&B)** is an algorithm design paradigm for discrete and combinatorial optimisation problems. This algorithm consists of a systematic enumeration of candidate solutions by means of state space search, which the set of candidate solutions is thought of as forming a rooted tree with the full set at the root. The algorithm explores branches of this tree, which characterise subsets of the solution set. Before enumerating the candidate solutions of a branch, the branch is ensured against upper and lower estimated bounds on the optimal solution, and is discarded if it cannot produce a better solution than the best one found so far by the algorithm. But the B&B algorithm is extremely time-consuming if the numbers of nodes in

branches of the tree are large [Kokash and Natallia, 2005].

- **Dynamic programming (DP)** is a very influential algorithmic paradigm in which a problem is solved by identifying a collection of sub-problems and attempting them one at a time. Then using the solution to sub-problems to assist solving larger ones, until the whole problem is solved. The key point for applying this technique is formulating the solution process as a recursion [Bertsekas, 2000]. The biggest drawback of dynamic programming is that is time consuming due to dimensionality. In higher dimensions, a generalized implementation is applied that explicitly checks for legal operators at each node. This introduces a constant factor to the time complexity of DP since processing each node takes longer than it would in an implementation tailored to a specific dimension [Hohwald et. al., 2003].

- **Greedy algorithm** is perhaps the most uncomplicated and influential method that is based on the evident principle of taking the (local) best selection at each stage of the algorithm in order to locate the global optimum of some objective function. For large complex cases this method is time consuming and does not always provide the best solution as its only search and select the best choice from current search state [Cormen et. al., 2000].

The deterministic heuristic techniques are relatively effective but their time-complexity often is too high and unacceptable for NP-complete tasks. Also, the deterministic techniques are tending to premature convergence and generally locate the nearest local optimum which maybe a low quality. The summary of deterministic heuristic techniques are tabulated in table 2.1 for comparison.

The purpose of probabilistic heuristics is to overcome these drawbacks. The comparative studies of probabilistic heuristics are illustrated and simplified in Gamal et. al., (2014).

- **Evolutionary Algorithms (EAs)** are succeeding in evading premature convergence by considering a number of solutions simultaneously which will be discussed more elaborately in the next section.

Table 2.1: Comparison of the deterministic techniques

Methods	Positive Aspect	Negative Aspect	Reference
Local Search	Uncomplicated search technique, Move to next state if have better solution	Applicable only for limited search space	Kokash & Natallia, 2005
Divide & Conquer	Resolve a problem by partitioning into sub-problem, Applicable to any problem	Time consuming, Difficult to partition and combine back if problem is complex	Cormen et. al., 2000
Branch & Bound	Explores branch of tree which characterise subset of solution set and discarded if cannot produce a better solution than the best	Extremely time consuming	Kokash & Natallia, 2005
Dynamic Programming	Solving sub-problems one at time to assist solving bigger problem	Time consuming due to dimensionality	Hohwald et. al., 2003
Greedy Algorithm	Uncomplicated and influential technique, Taking best solution at each stage to locate global optimum.	Time consuming if problem is complex, Always do not provide best solution	Cormen et. al., 2000

- **Simulated annealing (SA)** is a generic probabilistic, meta-heuristic algorithm which applies an approach similar to hill-climbing, but irregularly admits solutions that are worse than the present solution. The probability of such admittance is decreasing with time. At each step, the SA heuristic considers some neighboring state s' of the present state s, and probabilistically decides between moving the system to state s' or staying in state s. These probabilities ultimately lead the system to move to states of lower energy. Typically this step is repeated until the system reaches a state that is good enough for the application [Aydin and Fogarty, 2004].

- **Tabu search** is another meta-heuristic search method which extends the idea to avoid local optima by using memory structures. The problem of simulated annealing is that after a "jump" the algorithm can simply repeat its own track. Tabu search prohibits the repetition of moves that have been made recently [Battiti, 1996].

- **Swarm intelligence (SI)** is the discipline that deals with natural and artificial systems composed of many individuals that coordinate using decentralized control and self-organization. In particular, the discipline focuses on the collective behaviors that result from the local interactions of the individuals with each other and with their environment [Beni and Wang, 1989]. Two of the most successful types of this approach are Ant Colony Optimization (ACO) [Dorigo, 1992] and Particle Swarm Optimization (PSO) [Kennedy and Eberhart, 1995]. The ACO is inspired by the behavior of ants which is used to find the shortest path from nest to food source. During the foraging process ants move randomly from their nest to food source, during that period the ants leave a chemical substance called pheromone. This pheromone path helps other ants to reach the food source and this repeating process produces a positive feedback and makes a pheromone trail [Bijaya and Gyanesh Das, 2011]. The PSO deals with problems in which a best solution can be represented as a point or surface in an n-dimensional space. The main advantage of swarm intelligence techniques is that they are resistant to the local optima problem.

2.3.1 Evolutionary Algorithm

Evolutionary algorithms (EAs) are techniques that develop ideas of biological evolution for searching the solution of an optimisation problem, founded on the principles of natural selection [Darwin, 1859] and population genetic [Fisher, 1930]. They relate to the principle of survival on a set of potential solutions to generate gradual approximations to the optimum. A new set of approximations is created by the process of selecting individuals according to their fitness and breeding them together with operators stimulated from genetic processes. Figure 2.2 illustrates a schematic of generalised EA techniques.

The main loop of EA includes the following steps:

1. Initialize and evaluate the initial population.

2. Perform competitive selection.

3. Apply genetic operators to generate new solutions.

4. Evaluate solutions in the population.

5. Start again from point 2 and repeat until convergence criteria is satisfied or solution is attained.

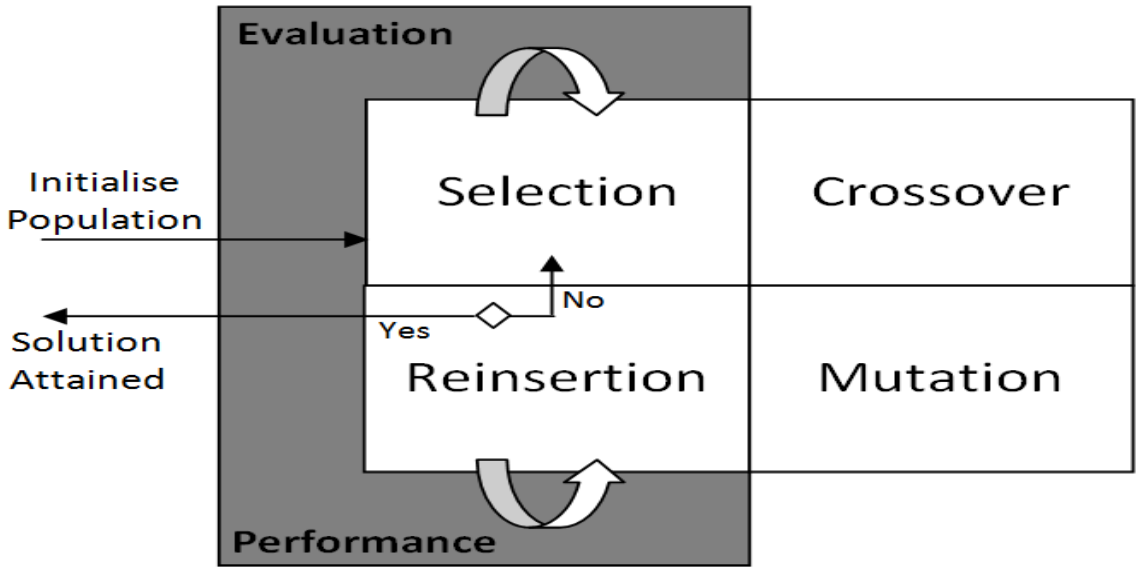

Figure 2.2: Schematic of generalised evolutionary algorithm (Fleming and Purshouse, 2002)

Therefore, any iterative, population based technique that applies the random variation and selection to produce new solutions can be classified as an EA. The EAs field has its genesis in four landmark evolutionary approaches: evolutionary programming (EP) [Fogel et. al., 1966], evolution strategies (ES) [Rechenberg, 1973], genetic programming (GP) [Koza, 1992] and genetic algorithms (GAs) [Holland, 1975].

Even though EA share a general scheme, evolutionary techniques can be differentiated according to the implementation and the problems to which they are applied. GP explores for a solution in the form of computer programs. Their fitness is determined by the ability to solve a computational problem. The only difference from EP is that the latter fixes the structure of the program and allows their numerical parameters to evolve. ES works with vectors of real numbers as representations of solutions, and applies self-adaptive mutation rates. The most well known and

successful among evolutionary algorithms are genetic algorithms (GAs). They have been explored by John Holland in 1975 and exhibit the necessary effectiveness.

Further, GAs were popularised by Goldberg (1989) and consequently, the majority of control applications are approved and implemented by this approach. GAs are based on the fact that the role of mutation improves the individual quite seldom and, therefore, they rely mostly on applying recombination operators.

2.4 Standard Genetic Algorithms

Standard genetic algorithms (SGAs) are a stochastic global search technique based on the metaphor of natural biological evolution. This technique sustains a set of candidate solutions to a specified problem, which then evolve applying artificial genetic operators such as selection, crossover and mutation. SGAs work by merging the Darwinian "survival of the fittest" principle with a probabilistic information exchange approach encouraged by the processes of natural genetics, to form a structured yet randomised search algorithm that assures to be well competent of identifying optimal, or near-optimal solutions, to a wide range of search, optimisation and machine learning problems.

As discussed earlier, SGAs have been developed by John Holland, his colleagues, and his students at the University of Michigan. Studies by Holland (1975), De Jong (1975), Goldberg (1989), and others have demonstrated its superiority performance of SGAs by theory and experimentation. More information on SGAs and a list of practical applications can be found in Shopova and Vaklieva-Bancheva (2006) Fogel (1994), Goldberg (1994), Randy and Sue (2004) and the introductory textbooks by Goldberg (1989) and Mitchell (1996). Because of their exclusive structure and function, SGAs diverge from more traditional and modern search procedures and algorithms in some very fundamental ways, making them ideal candidates as global function optimisers.

Recent studies illustrated the SGAs performed reasonably well compared to other evolutionary algorithms (Wu and Ji, 2007) (Kachitvichyanukul, 2012) (Silberholz and Golden, 2010) (Adewole et. al., 2012) (Bajeh and Abolarinwa, 2011) (Gamal

et. al., 2014) (Nagaraj and Murugananth, 2010).

Another attribute of SGAs that distinguishes them from most conventional and modern search methods is that they work with a coding of the parameter set and not with the parameters themselves. This gives them direct applicability to an exceptionally wide range of non-numerical, discrete, combinatorial, and mixed optimisation problems. Kachitvichyanukul (2012) has suggested that SGAs are more suitable for discrete PID optimisation than the PSO and DE, which are suitable for continuous PID optimisation.

Most conventional and modern optimisers based on continuous parameter variations cannot normally be used for the solution of such problems. The influences of SGAs come from the statement that they are robust and thus, have the prospective to apply and solve efficiently many difficult problems without constraints. As expected, SGAs are not certain to locate the globally optimal solution to a specific problem, but are generally excellent in locating reasonably fine solutions to a wide range of problems which is rapidly acceptable.

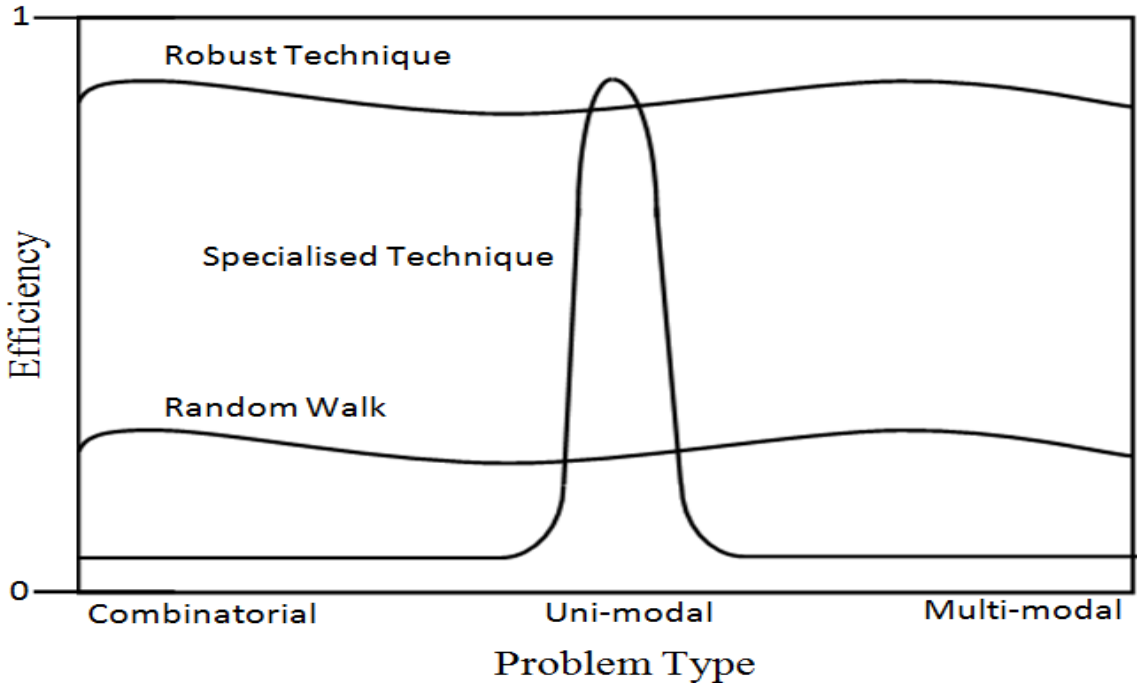

Figure 2.3: Efficiency of different classes of search techniques across a problem continuum (Goldberg, 1989)

Figure 2.3 illustrates the better perception of the significance of robustness in a search technique. According to the figure, the specialised technique is well per-

forming in the problem area it has been designed for, but its efficiency drops rapidly when applied in different problem areas. On the contrary to that, entirely randomised techniques, such as random walk, are executing consistently in a wide range of problem areas, but their efficiency is in general low. Robust techniques, such as SGAs, unite efficiency with consistency and achieve a suitable performance across a wide range of domains. Even though other specialised techniques are probably perform better than SGAs for solving specific problems but the SGAs can provide a very effective, efficient and fast solution.

2.4.1 Multi-Objective Optimisation by SGAs

Being a population-based approach, SGAs are well suited to solve multi-objective optimization problems. A generic single-objective SGAs can be modified to locate a multiple non-dominated solutions set in a single execution. The ability of SGAs to simultaneously search different regions of a solution space makes it possible to locate a diverse set of solutions for difficult problems with non-convex, discontinuous, and multi-modal solutions spaces. In addition, most multi-objective SGAs do not require the user to prioritize, scale, or weigh objectives. Therefore, SGAs have be en the most popular heuristic approach to multi-objective design and optimization problems.

The first multi-objective SGAs, called vector evaluated SGAs (or VEGA), was proposed by Schaffer (1985). Afterwards, several multi-objective evolutionary algorithms were developed including Multi-objective Genetic Algorithm (MOGA) (Fonseca and Fleming, 1995). Since then many research works has been undertaken to improve the MOGA (Fonseca and Fleming, 1998) (Jensen, 2003) (Xiujuan and Zhongke, 2004). However, the MOGA is not considered here as a part of this research work.

2.4.2 Premature Convergence

One of the most general phenomena that encountered in optimisation is premature convergence in modern heuristic algorithm (Vanaret et. al, 2013). A process of

optimisation prematurely converged to a local optimum if the initial population is generated randomly from poorly selected search space region [Ursem, 2003] [Vanaret et. al., 2013] [Chaiwat and Prabhas, 2011]. In another term, if population is not selected from optimal search region it becomes complicated to locate the elite solution of the problem whether in the case of initial population selection or the selection of population for the next generation. Figure 2.4 illustrates several common phenomena (factors) to take into account when the initial population is generated randomly.

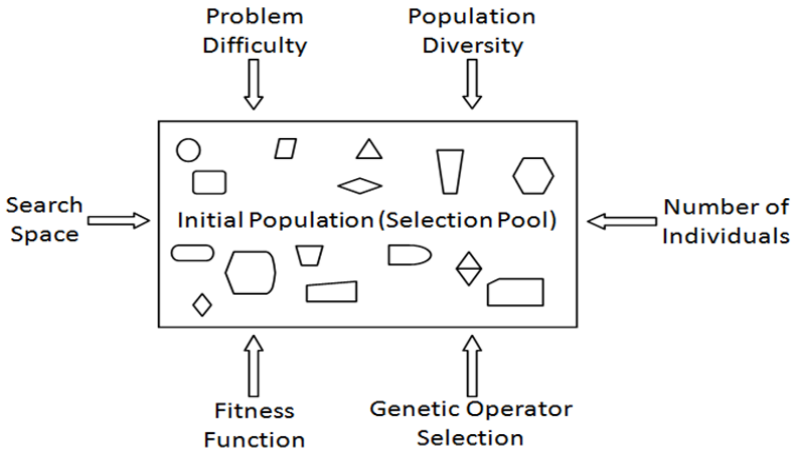

Figure 2.4: Phenomenon of initial population

The search space selection is one of the grounds that lead to premature convergence. Well selected search space region will brought the elite group within the feasible region to avoid premature convergence [Rajarathinam et. al., 2015]. In fact, the well selected search space regions will sustain the population diversity. Preservation of search space and population diversity is correlated with sustaining a well balance between exploration and exploitation [Weise, 2009]. An exploration is applied to examine new and unknown region in the search space, and exploitation applies the previously visited and identified information to assist locate the elite solution [Rajarathinam et. al., 2015].

A brief knowledge about variety methods of sustaining the population diversity and selective pressure to avoid the premature convergence were proposed (Deepti and Shabina, 2012). Nakisa et. al., (2014) presented a comprehensive survey of the various PSO-based algorithms such that PSO is a computational search and optimization method based on the social behaviours of birds flocking or fish schooling.

Chaiwat and Prabhas (2011) proposed the self-adaption technique to control the population diversity without explicit parameter setting. The technique is based on the competition of preference characteristic in mating. Based on simulation results, the adaptive technique has potential to adapt the diversity of the population for a given problem without the knowledge of correct parameter setting. Also, it has a good performance in finding the solution.

A number of basic variations have been developed due to solve the premature convergence problem and improve quality of solution founded by the PSO. Suri et. al., (2013) proposed that Elitism technique was augmented within Genetic Algorithm allowing the best solution from any generation to be carried across the new population allowing it to sustain. Social Disaster Techniques (SDT) was used when premature convergence occurred and the problem of premature convergence may be avoided by creating random offspring and inserting diversity in the population (Ramadan, 2013). This paper attempted to use the both concepts of Elitism and Social Disaster techniques spanning across various generations. A previous solution was chosen and it has been looked upon how Elitism and Social Disaster techniques fares towards the same problem. Malik and Wadhwa (2014) proposed a collaboration of dynamic genetic clustering algorithm (SGCA) and elitist technique for preventing premature convergence. This proposed technique provides a strong immunity to mutation and crossover operators to be trapped in local optima.

Based on the complex Box technique, a boundary search method for optimisation problems in the case of the optimal solution at the boundary was proposed (Zhu et. al., 1984). It has been demonstrated and verified, if there is an optimal solution at the boundary constraint set. Recently, a modified GAs is applied in solving the n-Queens difficulty in chessboard (Heris and Oskoei, 2014). The holism and random choices cause solving difficulties for SGAs in searching a large space. To improve the solving difficulty, the minimal conflicts algorithm is collaborated with SGAs. The minimal conflicts algorithm gives a partial view for SGAs by a locally searching space. But, the collaboration of algorithms consumed time for searching.

An approach called the self-adaptive boundary search strategy for penalty factor

selection within SGAs was proposed (Wu and Simpson, 2002). This approach guides the SGA to preserve around constraint boundaries and improves the efficiency of attaining the optimal or near optimal solution. A technique for resolving the structural optimisation difficulties in quantising the subjective uncertainties of active constraints is proposed by fuzzy logic formulation (Wu and Wang, 1992).

Another method to improve the prematurity and to sustain the diversity population was proposed by Niche Genetic Algorithm (NGM) associated with isolation mechanism (Lin et. al., 2000). A comparison study was done on NGM and Annealing Genetic Algorithm where the Annealing Genetic Algorithm has better premature convergence (Tu and Mei, 2008). However, the Annealing Genetic Algorithm is time consuming by extra procedures.

Another method, named Accelerating Genetic Algorithm (AGM) was proposed to resizing the feasible region into the elite individual's adjacent region for better local searching and convergence (Jin et. al., 2001). Search space boundary reduction for the candidate diameter for each link by pipe index vector and critical path method, along with modified genetic operator's derivatives, was proposed (Mahendra et. al., 2008) (Vairavamoorthy and Ali, 2005). Further, an improved AGM based on the saddle distribution by which adding random individuals into the initial population to increase the searching ability of optimal solution was proposed (Xu et. al., 2012).

2.4.3 SGAs in Model Parameter Identification

The SGAs have been employed succesfully in the process model parameter identification of both linear and non-linear system's models. Kampisios et. al., (2008) applied off-line GAs in identification of linear induction motor electrical parameters in function of flux levels based on experimental transient measurements from a vector controlled induction motor (I.M.) drive. Liu et. al., (2014) demonstrated a parameter identification for the determination of hydraulic and water quality parameters such as the longitudinal dispersion coefficient, the pollutant degradation coefficient, velocity by coupling the GAs with finite difference method (FDM).

Wong et. al., (2011) applied the GAs to generalise and learn protein-DNA bind-

ing sequence representations. The generalized pairs are shown to be more meaningful than the original transcription factors and transcription factor binding sites (TF-TFBS) binding sequence pairs. The proposed method by GAs assists to extract such many-to-many information from the one-to-one TF-TFBS binding sequence pairs found in the previous study, providing further knowledge in understanding the bindings between TFs and TFBSs.

Kiperwasser et. al., (2013) improved and proposed the dense pixel matching using the GAs in rectifying the image scenario. An elegant approach is allowing, optimising and matching fitness functions has recently shown a 20% of quality improvement while performing fast convergence. The effectiveness and efficiency of GAs has been well demonstrated by Roeva (2008) and Benjmin et. al., (2008) for model parameters identification of fed-batch cultivation processes. Further, Maria et. al., (2011) applied SGAs and multi-population GAs for a parameter identification of a yeast fed-batch cultivation of S, (*cerevisiae*).

Mathew et. al., (2014) successfully applied the GAs based a segmentation approach in identification of defects in glass bottles. The GAs has produced high sensitivity, high specificity and high accuracy of 92%, 93% and 93% respectively. The method produced effective results and hence this tool shall be useful for food processing industries for the Quality Inspection of the glass bottles.

Aloysius et. al., (2012) successfully applied the GAs in order to maximize the revenue of airline by optimizing the flight booking and transportation terminal open/close decision system. Gondro and Kinghorn, (2007) aligned the multiple sequence alignment which plays an important role in molecular sequence analysis. An alignment is the arrangement of two (pair-wise alignment) or more (multiple alignment) sequences of 'residues' (nucleotides or amino acids) that maximizes the similarities between them. Algorithmically, the problem consists of opening and extending gaps in the sequences to maximize an objective function (measurement of similarity). The GAs is well suited for problems of this nature since residues and gaps are discrete units.

Further, the SGAs have been successfully applied in the field of medicine and

biology. Wang et. al., (2007) demonstrated an exploitation of different methods for intergenic distance, cluster of orthologous groups (COG) gene functions, metabolic pathway and microarray expression data. The GAs is applied for integrating the four types of data of predicting operons in prokaryote. Nur et. al., (2012) proposed and demonstrated GAs to estimate the parameter of warranty cost model with warranty claim data collected from Malaysian automotive industry. Further, Scarf and Majid, (2011) introduced the mixed exponential distribution with GAs since zero delay time may occur in some defects. As a result, they found that the mixed exponential models is better than ordinary exponential.

2.4.4 SGAs in Control Parameter Optimisation

Numerous GA-based techniques have been developed for the optimal control design and control parameter optimisation. Altinten et. al., (2008) successfully applied the GAs to optimise the PID parameters for temperature control of a jacketed batch polymerization reactor and to track performance of optimal temperature profile. Further, Altinten et. al., (2010) applied the GAs for self-tuning PID control for the complex semi-batch polymerisation reactor processes. The change of monomer concentration is causing a change in reaction rate varies nonlinearly over the time. The simulation results assured that GAs control the temperature very well.

Slavov and Roeva, (2012) applied binary coded SGAs to optimise the discrete PID parameters for sustaining the glucose concentration during the *E. Coli* fed-batch cultivation process. Jan et. al., (2008) proposed and demonstrated robust PID control scheme by SGAs for the permanent magnet synchronous motor is implemented by a DSP-based fully discrete controller.

Kim et. al., (2008) proposed an improved GAs technique to tune an optimal PID parameter to control the reverse osmosis (RO) plant with minimum overshoot and fast settling time compared with conventional tuning techniques. Yin et. al., (2004) successfully applied GAs to tune PID parameter for low damping and slow response process. Zain et. al., (2009) applied GAs for optimizing PID parameters to control a single-link flexible manipulator in vertical motion. Simulation results

revealed that the optimum PID parameters by GAs enable the system to perform well in reducing vibration at the end-point of the manipulator.

Nithyrani et. al., (2013) applied SGAs to tune an optimal discrete PID parameters for liquid tank process temperature. Simulation reveled that the binary coded SGAs performed well to sustain the liquid temperature and compared with conventional techniques. Zhang et. al., (2010) proposed a PID parameter optimization by performance index based on integral of absolute error, rise time, controller output and overshoot. Simulation results indicate that the GAs is a practical and effective method in optimizing the control parameters.

Perez and Basterrechea, (2004) demonstrated an application of SGAs for predicting the far-field radiation of an antenna from synthetic near-field data. Simulation results compared and revealed that the binary coded SGAs well performed for large antennas as it applies small population size than real coded genetic algorithms (RCGAs). Gauri and Kulkarni, (2013) well applied the binary coded SGAs to optimize the discrete PID parameters for missile altitude control system.

Valarmathi et. al., (2012) demonstrated an optimisation of PID parameters by binary coded SGAs for a non-linear liquid conical tank system. Jayachitra and Vinodha, (2014) well applied binary coded SGAs to optimise the discrete PID control for continuous stirred tank reactor (CSTR) process. The control performance of CSTR process has enhanced by integrating weighting factor with combined conventional objective functions. Patrascu et. al., (2011) applied the discrete PID parameters which are optimised by SGAs for non-linear 3D crane multi-input multi-output (MIMO) systems.

In recent years, the GAs is well applied in control strategy for robotics technology. Abo-Hammour et. al., (2011) demonstrated binary coded GAs based control suitability for autonomous selection of a collision free path for the manipulator that minimizes the deviation between the generated and the desired Cartesian path. The control parameters are satisfies the joints limits of the manipulator, and maximize the minimum distance between the manipulator links and the obstacles. Ghanbari and Noorani, (2011) proposed a control technique for a new crawling gait to develop

in a modular robot by GAs. Wang et. al., (2012) proposed a new approach to generate the original motion data for humanoid motion planning by binary coded GAs.

The state generator is developed based on the GAs, which enables users to generate various motion states without using any reference motion data. By specifying various types of constraints such as configuration constraints and contact constraints, the state generator can generate stable states that satisfy the constraint conditions for humanoid robots. Arturo et. al., (2013) proposed a technique of integration of gain-phase margin method with the binary coded GAs for discrete control strategy of industrial robot and computer numerical control (CNC) machines. The proposed technique is performed well as expected and compared with RCGAs and conventional gain-phase margin method. Some other applications to multivariable process control are reviewed in chapter 6.

2.4.5 An Application of SGAs for Furnace Type Processes

Literature survey revealed that not numerous research works has been undertaken on an application of SGAs for the glass furnace or furnace type processes in model parameters identification and control parameters optimisation.

Joao and Pedro, (2003) introduced an architecture for the operation system of industrial recuperative-type glass furnace. The expert control is integrated with GAs for control optimisation and solves the multi-objective optimisation problems, respectively. Zarko et. al., (2010) presented an application of GAs with fuzzy control for optimising PID parameters for fluidized bed combustion (FBC) chamber. The results revealed that the closed-loop systems have a fast rise response with small overshoot.

Srisertpol et. al., (2011) proposed an estimation method for the mathematical model using the open-loop identification for the slab reheating furnace walking hearth type with GAs in heating curve up process. The responses of experimental and simulation are consistent. Liu and Guo, (2013) presented the fuzzy neural network temperature control system based on SGAs for resistance furnace which has

nonlinear characteristics with big inertia and great delay.

The artificial neural network structure and parameters are trained with fuzzy control rules. The membership functions of fuzzy control rules are determined by using the neural network's self-learning and adaptive ability. The SGAs is adopted to train the controller's connecting weights. The simulated results indicate that the fuzzy neural network temperature control system is more dynamic, robust, and highly precise.

Ping et. al., (2014) presented and applied the dynamic matrix predictive control based on GA to the electrode regulator systems of industrial arc furnace. The optimal control law is obtained by rolling optimization. The simulation result shows a significant improvement on the dynamic performance and the robustness of the system.

2.5 Review of PID Control Strategies

The PID controllers have been at the heart of control engineering practices for the last seventy-five years. The first tuning rule for setting up controller parameters was defined by Callender (1935). The proposed technique comprises design of a PD controller for a process which is exactly modelled by an integrator plus delay time. After eight years of Callendar work, Zeigler-Nicholas proposed two classical techniques for PI/PID control parameters identification. These techniques are still extensively applied, either in novel structure or with some improvement. The first technique was derived from an open-loop step response of the process, which is characterised by two unknown parameters. The unknown parameters were established from a unit step response of a process and applied to identify the controller parameters (Zeigler-Nicholas, 1942).

The second technique of Zeigler-Nicholas (1943) was derived from frequency response of a process. The parameters of P/PI/PID controller were determined from gain margin, GM and phase crossover frequency, ω_{pc}. Chien et. al., (1952) personalized the Zeigler-Nicholas step response technique by applying fastest response without overshoot or with 20% overshoot as design criteria. The proposed technique

made a significant observation that tuning for set-point response or load disturbance response should be different. Cohen and Coon (1953) designed a technique which was derived from First-Order plus Dead-Time (FOPDT) model structure. The proposed technique does suffer, nevertheless, from the decay ratio being too small, which means that the closed-loop systems obtained have low damping and high sensitivity.

In the beginning of twenty first century, the applications of PID parameters on complex and higher order processes are well enhanced. Majhi and Atherton (2000) developed a controller design technique on a modified smith predictor strategy, which leads to significant improvements in its regulatory capacities for reference inputs and disturbances. The first order or second order response of the plant model is assumed and the controller parameters are approximated by applying precise analysis from the peak amplitude and frequency of the process output obtained from a single relay feedback test. The robustness of controller is noticeable from results obtained using incorrect time delay values in the plant model.

Wang and Shao (2000) proposed a technique for PI controller based on load disturbance rejection with constraint which is the Nyquist curve of the loop transfer function is tangent to a line parallel to the imaginary axes in the left-half of the complex plane. The method satisfies both robustness and performance requirements, but is restricted to PI controller and does not provide an extension to the PID controllers.

Wang et. al., (2001) developed internal model control-based (IMC) single-loop controller design technique. The model reduction technique was applied to approximate the best single loop controller for the IMC controller. This technique can be automatic for on-line tuning. The technique gives an alternative to attain specified closed-loop performance at the cost of controller complexity or retain simple PID controller with possible deterioration in the closed-loop performance. So, this technique is not well applicable for higher order processes to get the desired closed-loop response with PID controllers.

Skogestad (2003) developed an analytic rule for PID controller tuning which

is simple and still gives good closed-loop behaviour. The starting point has been the IMC-PID tuning rules that have achieved widespread industrial acceptance. The rule for integral term has been modified to improve disturbance rejection for integrating processes. Furthermore, rather than deriving separate rules for each transfer function model, there is a single tuning rule for FOPDT or Second-Order plus Dead-Time (SOPDT) model. The only drawback of the method is that the model order reduction is required for higher order systems.

The design of PI controllers to achieve desired frequency and time domain specifications simultaneously was proposed by Hamamci and Tan (2006). The performance of frequency domain, GM and phase margin (PM), and the performance of time domain, settling time and overshoot were defined prior to the design. To meet the specified performance values, a method which presents a graphical relation between the required performance values and the parameters of the PI controller for a given model. The graphical relations are limited to the design of PI controller and extension to the PID controller is not cleared.

An alternative PID auto-tuning approach had been proposed to the popular step response and relay-based technique by Gyongy and Clarke (2006). The approach involves injection of a variable-frequency probing signal into the closed-loop. The technique differs from most existing methods in that the tuning was performed online, which is whilst; the controller was undertaking closed-loop control. As a result, it is providing single-shot auto-tuning while continuous adaptation of the controller. In this approach, ease-of-use was ensured by a semi-automatic initialization procedure only, which employs the results and knowledge of a prior step-test.

Bitschnau and Kozek (2009) applied a PID controller with feed-forward compensation technique for continuous heat treatment steel strips type furnace. Simulation result revealed that the PID with feed-forward compensation technique is able to react to temperature parameter variation of the proposed material in reasonable time. In model based design of PID controllers, Malwatkara et. al., (2009) proposed for higher-order oscillatory systems. This method has no limitations regarding systems order, load changes, time delays and oscillatory behaviour. Selection of

coefficients through the use of frequency responses with reduced model is achieved based on third-order modelling. The tuning of the PID parameters is obtained from a reduced higher-order model. This technique seems to be simple, effective, and improved performance of the overall system.

Improved Electromagnetism-like (EM) algorithm with genetic algorithm (GA) technique (IEMGA), for optimization of fractional-order PID (FOPID) controller is proposed by Ching and Chang (2010). IEMGA is a population-based metaheuristic algorithm originated from the electromagnetism theory. For FOPID control optimization, IEMGA simulates the "attraction" and "repulsion" of charged particles by considering each controller parameters as an electrical charge. The neighborhood randomly local search of EM algorithm is improved by using GA and the competitive concept. IEMGA has the advantages of EM and GA in reducing the computation complexity of EM. This method gives effective performance.

A novel fractional order (FO) fuzzy-PID controller has been proposed by Saptarshi et al. (2011), which works on the closed loop error and its fractional derivative as the input and has a fractional integrator in its output. The fractional order differ-integrations in the proposed fuzzy logic controller (FLC) are kept as design variables along with the input–output scaling factors (SF) and are optimized with genetic algorithm (GA). The closed loop performances and controller efforts in each case are compared with conventional PID, fuzzy PID and PI Dm controller subjected to different integral performance indices. Simulation results show that the proposed fractional order fuzzy PID controller out performs the others in most cases.

In the literature review of Hitay et. al., (2012) a classical proper PID controllers are designed for linear time invariant plants whose transfer functions are rational functions of s^a, where $0 < a < 1$, and s is the laplace transform variable. Effect of input–output time delay on the range of allowable controller parameters is investigated. The allowable PID controller parameters are determined from a small gain type of argument for finite dimensional plants.

There are many online automatic PID parameters tuning methods have been proposed to improve the control performances, Nevertheless, satisfactory control

performances are not able to attain by above mentioned methods due to inapplicability of wide operating region of the controller. Also, a high mathematical approach is complicating the implementation to industrial process.

Heuristic optimization is a technique of locating good solutions at a reasonable computational cost without being able to guarantee either feasibility or optimality, or even in many cases to state how close to optimality a particular feasible solution is (Reeves, 1995). By means of superiority for global optimisation and better robustness, the SGA is applied here to enhance the capabilities of conventional PID tuning techniques in online identification without complicated mathematics. Recently, SGAs has been extensively studied by many researchers in searching for optimal PID parameters due to its high potential of escaping being trapped a local minimum as discussed in detail at chapter 2.

2.6 Review of Multivariable PID Tuning Strategies

For a complex multivariable process, a decentralised control strategy is generally applied, and has always been in the attention of many researchers, for developing a precise control strategy to enhance the performance of multivariable processes. However, difficulties are encountered in designing the decentralised control due to the loop interactions.

A literature survey reveals that there are several classified tuning methods suggested to tune decentralised controllers for multivariable processes such as detuning (Monica et. al., 1998), sequential design (Hovd and Skogestad, 1994) and independent design (Lee et. al., 2001) methods.

In the detuning method, the individual controllers of the multi-loop control system are first designed without considering the interactions between control loops, and then, all settings are detuned taking into account the interactions until some stability criterions are satisfied. A well-known method of this type is the biggest log modulus tuning (BLT) method (Luyben W. L., 1986).

Initially, the single-input, single-output (SISO) controllers are obtained by using the Ziegler-Nichols settings. Detuning is then performed by adjusting one parameter

F, where F is determined via a Nyquist-like plot of the closed-loop characteristic polynomial. Since the biggest log-modulus, which measures how far the control system is from being unstable, is obtained equal to $2N$ (N is the order of system) by adjusting F, the controller parameters for multi-loop control systems are determined.

In the sequential design method, each controller is designed sequentially with the previously designed controllers implemented. Basically, a controller is first designed by considering the selection of an input-output pair and this loop is closed. A second controller is designed by considering the second input-output pairing since the first loop closed and so on. The sequential design method can be used for complex interactive problems where the independent design method does not work. A potential disadvantage of this design method is that failure tolerance is not guaranteed when the previous loops fail. When the system outputs can be decoupled in time, the sequential design method can be effectively used for the design of multi-loop controllers.

In the independent design method, each controller is designed based on the corresponding diagonal element of the multivariable process transfer function model, while the off-diagonal interactions should be taken into account by considering some inequality constraints on the process interactions. The main advantage of independent design is that the failure tolerance is guaranteed automatically. However, it is conservative due to the assumptions of the design method. This design method is effective when the system is diagonally dominant.

In general, these tuning methods have achieved a certain degree of success in the design approach. However, these tuning methods do exhibit weaknesses and can suffer in compensating the couplings between loop interactions of a multivariable system. To improve the compensation of loop interactions, the effective open-loop (EOP) method was introduced (Huang et. al., 2003). The EOP method considers all other loop interactions while adapting the $i-th$ control parameters for the $i-th$ EOP. But, the EOP method produces model approximation error due to mathematical complications as the model dimensions are increased. Thus, the EOP method is mainly applicable for low dimension models.

Another successful approach is that of relay auto-tuning, which is a combination of single loop relay auto-tuning and the sequential tuning method (Loh et. al., 1993). This method appears to perform well, but a multivariable system with large multiple dead times exhibits poor performance.

In recent years, to improve the entire control performance and robust stability, systematic approaches based on the generalised IMC-PID design method (Grosdidier and Morari, 1987) and the reduced effective transfer function (RETF) by inverse response behaviour method (Truong et. al., 2009) have been introduced for multivariable processes. But, both methods involve a complex mathematical approach to design the decentralised controllers. In general, a question always arises about the wellness of control optimisation and the flexibility due to the application constraints by these design methods.

In decentralized control of 2×2 MIMO systems, the control system consists of two such controllers. Each of them takes care of a single loop only and the interaction between the two loops is greatly reduced, unlike the centralized PID control where a similar 2×2 controller structure is assumed to stabilize a two-input two-output (TITO) process (Tavakoli et. al., 2006) (Fernando et. al., 2008). However, the decentralized controller design can be easily applied if the loops do not heavily interact with each other, i.e. the corresponding Relative Gain Array (RGA) should have a dominating principal diagonal. If the loop interaction changes the process gains of the individual loops considerably, then well-tuned controllers for the individual loops fail to keep the controlled variables at their respective set-points. In such cases, pairing of any manipulated variable with any controlled variable results in poor controller performance.

Applications of evolutionary algorithms have become very prominent to improve the decentralised control for multivariable processes. Iruthayarajan and Baskar (2009) and Wei (2007) used evolutionary algorithms and multi-crossover genetic algorithms to minimize the summed integrated absolute error (IAE) for each loop while tuning the PID controller parameters. Ramin et. al., (2008) designed a decentralized PID controller by minimizing total IAE for all loops using the colonial

competitive algorithm. Kai et. al., (2008) tuned PID controllers based on a closed loop particle swarm optimizer (PSO) algorithm. Zhao et. al., (2012) minimized integral square error (ISE) employing "two-*lbests*" based PSO for designing robust PID controller for MIMO systems.

Vijula and Devarajan (2014) proposed the model reference adaptive control (MRAC) technique for a multivariable quadruple tank process. The linearized model of the quadruple tank system has a multivariable transmission zero and it is much more difficult to control the system in non minimum phase condition than minimum phase condition. The proposed controller can adjust the controller parameters in response to changes in plant uncertainties and disturbances based on the specified reference model and prevent the system from interaction between process variables. It is shown by the simulation results that MRAC technique solves the dynamic problem of the quadruple tank process and it is convenient for controller design under the requirement of the system.

A promising decentralised controller by SGAs was proposed for a multivariable process (Vlachos et. al., 1999). The controller performance was defined by closed-loop response in terms of time-domain bounds for both reference following and loop interactions. An integrity theorem with SGAs to enhance the closed-loop system stability when certain loops are failing or breaking down was proposed by Li et. al., (2007). Recently, improved convergence of genetic algorithms was achieved by introducing the multi-objective evolutionary algorithm (MOEA) which combines two fitness assignments methods; global rank and dominance rank (Rani et. al., 2012).

2.7 Why SGAs?

As discussed in section 2.4, the SGAs are selected for its united efficiency with consistency, robustness and an ability of achieving a suitable performance across a wide range of domains. As a result, in cases where other expert techniques exist for solving specific problems and possibly perform better than SGAs, but SGAs can provide a very effective and efficient solution. Further, the literature survey reveals

that the SGAs are not well applied and explored for glass furnace process neither in model identification and control parameter optimisation.

On the subject of SGAs coding selection, the real-coded may have outperformed the binary-coded in several cases. However, the literature reveals that the binary-coded is predominantly applied for discrete control parameter identification for its suitability and flexibility than the real-coded. In particular, exceptionally complex processes such as robotics for humanoid motion and missile trajectory for defence system. Therefore, the SGAs associate with binary-coded is selected for model parameters identification and control parameter optimisation as the discrete PID control will be designed for research.

2.8 Chapter Summery

In this chapter, an overview of optimisation algorithms as applied to the solution of control engineering problems was discussed, followed by a brief introduction to standard genetic algorithms (SGAs) as global function optimisers, with emphasis on their fundamental differences and advantages over conventional search algorithms. The most attribute of SGAs that distinguishes them from conventional and modern search methods is that they work with a coding of the parameter set and not with the parameters themselves. This gives SGAs direct applicability to an exceptionally wide range of non-numerical, discrete, combinatorial, and mixed optimisation problems.

A literature survey was then presented, indicating a successful applicability of SGAs in process model parameters identification and control parameters optimisation problems. On the subject of SGAs coding selection, the binary-coded SGAs is selected as it is predominantly applied for discrete control parameter identification in exceptionally complex processes such as robotics for humanoid motion and missile trajectory for defence system for its suitability and flexibility than the real-coded. Further, other applications of SGAs for glass furnace and furnace type processes were outlined. Finally, a successful tuning strategies in single-input single-out and multi-variable PID are reviewed.

Chapter 3

Glass Furnace Modelling Validation

3.1 Introduction

This chapter begins with a brief literature review of designing the combustion chamber, which is fundamental to the developed methods for the glass furnace models. Computational fluid dynamics method derived from radiative heat transfer were applied here to analyse the temperature distribution within the combustion chamber, which is divided into finite zones.

Linearised energy balance equation in steady-state is improving the prediction and accuracy of temperature distribution within finite zones. An assessment on selected glass furnace model, which is designed by zones method is, provides a deeper insight of model understanding and performance quantitative.

3.2 Review of Combustion Chamber

Literally, two main modelling techniques are strongly involved in furnace modelling research; 1 – Empirical modelling techniques (Data-based) and, 2 – First-principles-based modelling utilizing computational fluid dynamics (CFD) techniques. Empirical Modeling Technique (Data-based) is a common and general approach that was successfully applied in the glass industry and they result in fast models (Müller et.

al., 2003). This technique is able to learn and simulate the process behaviour just from data, no further description is necessary. Parameters of these models have to be determined from data measured on a real process.

There are some prominent empirical identification methods to determine the model from measured data, such as Genetic Algorithm, AR, ARX, ARMAX, etc (Ljung, 1999). A mathematical model using open-loop identification for the slab reheating furnace by genetic algorithm was developed (Srisertpol et. al., 2011). The responses of experimental and simulation systems were consistent. The approximate mathematical model can be used to design an open-close burner to control the suitable temperature with heating curve up and save energy of the slab reheating furnace.

Another method of model identification of a process is performed by a learning system, based on a fuzzy learning-by-examples algorithm (Joao and Pedro, 2003). Process optimisation is carried out by an expert controller, and uses genetic algorithms to solve a multi objective optimisation problem. Results of real and simulated experiments with the glass manufacturing process are blended with artificial data. Even though the empirical modelling technique results a fast model for real time simulation, difficulties arise in model identification due to long and painful tests operation and the models are only valid for particular operating points. Moreover, no glass companies are willing or allowing to perform the model identification tests while the production is scheduled.

On the other hand, Computational fluid dynamics (CFD) solvers based on first-principles are well established tools in the glass industry and highly prominent for thermodynamics. Depending on the fineness of the used grid for discretization of the partial differential equations describing the process, the model of, e.g., a melter, is typically described by tens of thousands equations. Hence, computation takes a long time and simulators run only at a speed comparable to a real time. Also, a lot of parameters, initial and boundary conditions have to be specified prior to the simulation. Mostly for speed reasons the full-order CFD models are inappropriate for real time design purposes.

A Proper Orthogonal Decomposition (POD) method is proposed for the collection of measurements of physical quantities (such as temperature) in position and time (signals) to reduce the complexity of CFD models (Astrid, 2004). Following ideas from Fourier series expansions, signals are represented as series of orthonormal functions. These so-called basis functions approximate the spatial distribution of the signal while the coefficients of the basis functions represent the time-varying dynamics. A similar POD technique was applied to a CFD model of a glass feeder (Astrid and Weiland, 2005). The original CFD model of a feeder described by 3800 differential equations was reduced to a non-linear model only with 18 equations, resulting in significantly increased simulation speed. Turbulent combustion models for fine CFD are extensively developed (Veynante, 2002). The model represents how the turbulence influences the combustion. In particular, the Eddy-Break-Up and the mixture fraction approaches are implemented in glass furnaces models.

Another simplified CFD and thermodynamic modelling approach by using POD was proposed, which can be used to simulate glass melt temperatures, velocities and chemical composition as a function of time and position from a given furnace geometry, composition of raw materials, refractory properties and (time varying) boundary conditions (Huisman, 2005). These models are able to calculate the time dependent behaviour of the temperature profile more than 10000 times faster than the initial CFD model.

Regardless of how accurately the CFD model reduction method is applied, there is still a need for calibration of the CFD model so that it sufficiently simulates the real furnace (Müller et. al., 2005). With the validated model they use black-box identification to obtain suitable linear models for controller design. Research in the CFD field is still going on model reduction, but accuracy of such a model is dependent on the accuracy of the original CFD model.

3.3 Combustion Chamber Modelling Approach

The initial classical CFD approach, where conservation laws on energy, momentum, mass and mass fraction constitute the backbone of the model is applied in model-

ling a combustion chamber (Ungan, 1996). The model consists of tens of thousands equations for the combustion chamber. Today, with growth of computer processing power combined with simplified CFD models, the combustion chamber model operates at a very fine scale (Auchet, 2005). However, the computation time is high and inadequate for real time. The structure of combustion chamber models follows the different physical phenomenon in terms of characteristics, which are combustion space, bath and walls (Carvahlo et. al., 1997).

In a combustion chamber, a radiative heat transfer is a common occurrence and predominant. Therefore, identification of the combustion chamber geometry is playing a great importance task to describe the decomposition of a chamber into zones having uniform temperature and radiative properties (either gas volumes, molten glass surfaces or refractory wall surfaces) (Auchet et. al., 2008).

The most common radiative heat transfer method for analysing the temperature and heat flux is Hottel zone method (Hottel and Cohen, 1958). This method was used to analyse the radiation heat transfer in an enclosure containing gray gas. Later, the zone method was applied and developed for more complex geometries (Hottel and Sarofim, 1967). Since then, the zone method is widely applied by researchers to identify the combustion chamber due to low computational time and great model accuracy. Therefore, the developed combustion chamber by zone method is presented here.

The zone method was employed for predicting heat flux on the side walls of enclosures and temperature distribution within the combustion chamber. In this method, the whole space of the combustion chamber is split into zones and the enclosure's walls are divided into some finite surface parts (zones). By writing energy balance equations for all surface and volume zones in steady state, a system of linear equations are derived for the temperature fields on volume and surface zones.

3.3.1 Radiative Heat Transfer between Zones

The heat transfer between a pair of zones is known as directed heat flux area coefficients. The amount of heat transfer between surface to surface (SS), gas to surface

(GS) and gas to gas (GG) in a combustion chamber can written as,

$$Q_{i_S,j_S} = S_i\vec{S_j}E_i - S_i\overleftarrow{S_j}E_j \tag{3.1}$$

$$Q_{i_G,j_S} = G_i\vec{S_j}E_{g,i} - G_i\overleftarrow{S_j}E_j \tag{3.2}$$

$$Q_{i_G,j_G} = G_i\vec{G_j}E_{g,i} - G_i\overleftarrow{S_j}E_{g,j} \tag{3.3}$$

where $\vec{S_iS_j}$ and $\overleftarrow{S_iS_j}$ are heat flux area between surface zone i and surface zone j, $E_{g,i}$ is black emissive power of gas and E_j is black emissive power of surface. The radiative emissive power of each zone depends on temperature ($E_i = \sigma T^4$; where σ is the Stephan-Boltzman constant).

Apart from directed flux area, there are two more important coefficients in radiation calculation that are applied in zone method; total exchange area and directed exchange area. Table 3.1 illustrates the coefficients of radiation and respective effective parameters.

Table 3.1: Radiation Coefficients of Zone Method

Coefficients	Symbols	Effective Parameters
Directed Flux Area	$\vec{S_iS_j}, \vec{G_iS_j}, \vec{G_iG_j}$	Enclosure's geometry, Absorption coefficient of gray gas, Surface emissivity coefficient, Temperature of radiation source.
Directed Exchange Area	$\overline{s_is_j}, \overline{g_is_j}, \overline{g_ig_j}$	Enclosure's geometry, Absorption coefficient of gray gas.
Total Exchange Area	$\overline{S_iS_j}, \overline{G_iS_j}, \overline{G_iG_j}$	Enclosure's geometry, Absorption coefficient of gray gas, Surface emissivity coefficient.

The directed exchange area coefficient is also known as photometric coefficient and this coefficient quantifies how the elements radiate each other, and is only depending on the geometry and the photometric coefficients of the gas and the different surfaces filling the chamber. In the present model, all elements are assumed grey, i.e. with directed exchange area coefficients not depending on the wavelength. This means that the heat transfer computations can be done globally on the whole spectrum.

Directed exchange areas are kind of visibility factors, and following expressions shows the case of visibility factor between,

A surface element A_i and a surface element A_j,

$$\overline{s_i s_j} = \int_{A_i} \int_{A_j} \frac{\cos\theta_i \cos\theta_j \exp\left(-kr_{ij}\right)}{\pi r_{ij}^2} dA_i dA_j \tag{3.4}$$

A gas element V_i and a surface element A_j,

$$\overline{g_i s_j} = \int_{V_i} \int_{A_j} \frac{k \cos\theta_j \exp\left(-kr_{ij}\right)}{\pi r_{ij}^2} dV_i dA_j \tag{3.5}$$

A gas element V_i and a gas element V_j,

$$\overline{g_i g_j} = \int_{V_i} \int_{V_j} \frac{k^2 \exp\left(-kr_{ij}\right)}{\pi r_{ij}^2} dV_i dV_j \tag{3.6}$$

where, r_{ij} is the size of the vector that connects the centres of two elements to each other, θ_i and θ_j are the angle between the normal vector of surface elements and aforementioned vector, and k is emissivity coefficient of gas.

So far, the total exchange area been calculated by gray gas assumption from combustion product. But, the gray gas is not the main product of combustion. Thus, using gray gas assumption caused an unrealistic real gas model. Therefore, the weight summation of gray gases method is applied. In this method, the following expression is considered for emissive coefficient of real gas:

$$\varepsilon_g = \sum_{i=0}^{n} a_{g,i}(1 - \exp(k_i PL)) \tag{3.7}$$

where k, P and L represents the emissivity, partial pressure and effective path length of the gray gases, respectively. Term $i = 0$ is related to limpid gas.

By using and considering this method, the water vapour and carbon dioxide (CO_2)and a limpid gas as the main products of combustion the coefficients of $a_{g,i}$ have been calculated for several states of partial pressures (Viskanta and Mengue, 1987).

These coefficients are employed for calculating directed flux area from total exchange area by the following expressions, for

Surface-Surface zones:

$$\overrightarrow{S_iS_j} = \sum_{n=1}^{N} a_{s,n}(T_i) \left[\overline{S_iS_j}\right]_{k=k_n} ; \overleftarrow{S_iS_j} = \sum_{n=1}^{N} a_{s,n}(T_j) \left[\overline{S_iS_j}\right]_{k=k_n} \tag{3.8}$$

Surface-Gas zones:

$$\overrightarrow{G_iS_j} = \sum_{n=1}^{N} a_{g,n}(T_{g,i}) \left[\overline{G_iS_j}\right]_{k=k_n} ; \overleftarrow{G_iS_j} = \sum_{n=1}^{N} a_{s,n}(T_j) \left[\overline{G_iS_j}\right]_{k=k_n} \tag{3.9}$$

Gas-Gas zones;

$$\overrightarrow{G_iG_j} = \sum_{n=1}^{N} a_{g,n}(T_{g,i}) \left[\overline{G_iG_j}\right]_{k=k_n} ; \overleftarrow{G_iG_j} = \sum_{n=1}^{N} a_{g,n}(T_{g,j}) \left[\overline{G_iS_j}\right]_{k=k_n} ; \tag{3.10}$$

3.3.2 Energy Balance Equation

The first law gives a quantitative relation of energy balance equation by the variation with time, t, of the heat generated in the sample, Q, due to the absorption of light of incident power P_i, is given by

$$\partial Q/\partial t = P_i - q \tag{3.11}$$

where, q is the power losses by radiation, convection and conduction.

For research, radiation is the only mechanism taken into account for energy balance formulation due to its predomination. Thus, the parameter q should be some function of the temperatures, T_1 and T_2, of both the regions involved. It is denoted as the heat flux. In general, the dependence of the heat flux on the temperature is non-linear.

The continuous energy interchange between separated bodies by means of electromagnetic waves, the net rate of heat flow, q_{rad}, radiated by a body surrounded by a medium at a temperature T_1 is given by the Stefan-Boltzmann Law,

$$q_{rad} = \varepsilon\sigma A\left(T_2^4 - T_1^4\right) \tag{3.12}$$

where A is the surface area of the radiating object and ε is the total emissivity of its surface having absolute temperature T_2.

To compute the rise of temperature, ΔT, of the back sample's surface, the heat term of equation 3.1 must be expressed as a function of that increase. It is given by the relationship,

$$Q = \rho c V \Delta T \tag{3.13}$$

where ρ is the density, c is the specific heat and $V = AL$ is the sample's volume.

Differentiation of equation 3.13 with respect to time and substitution into equation 3.11 leads to:

$$\frac{\partial \Delta T}{\partial t} + \frac{q}{\rho c V} - \frac{P_i}{\rho c V} = 0 \tag{3.14}$$

where q_{rad} is specified as radiation terms given by equation 3.12.

As described by non-linear relationships, the rates of radiative heat flow are dependence on the temperature. This non-linearity makes complicated the analytical solution of the energy conservation law as given by equation 3.14. A glimpse at equation 3.12 shows that if the temperature difference $\Delta T = T_2 - T_1$ is small, then one could expand it as a Taylor series around T_1 obtaining a linear relationship:

$$q = 4\varepsilon\sigma A T_1^3 \left(T_2 - T_1\right) = hA\Delta T \tag{3.15}$$

The $h = 4\varepsilon\sigma T_1^3$ can be considered as a radiation heat transfer coefficient. This linearised energy balance equation is accurate above 1300K (Holladay, 2005).

3.4 Simulated Combustion Chamber Model

The combustion chamber that is identified and applied for further research here is modelled from Fenton Art Glass Company, USA (Morris, 2007). This is an extended

research work of Holladay (2005) and was applied to develop a state space model of an end-fired furnace in which the furnace was divided longitudinally into two zones. The Zone 1 contains the burner flame "cylinder", while Zone 2 is beyond the end of the flame cylinder. Separate states are identified for the temperatures of the refractory in the crown, the walls above the glass melt, the walls adjacent to the two primary melt zones, and the floor of the furnace.

The furnace ends are also divided into similar zones constituting discrete states. The glass melt itself contains a thin, surface layer and two thicker layers of stratification. In all, 24 state variables are included in the model. The inputs are the net thermal power provided by the flame and the ambient temperature.

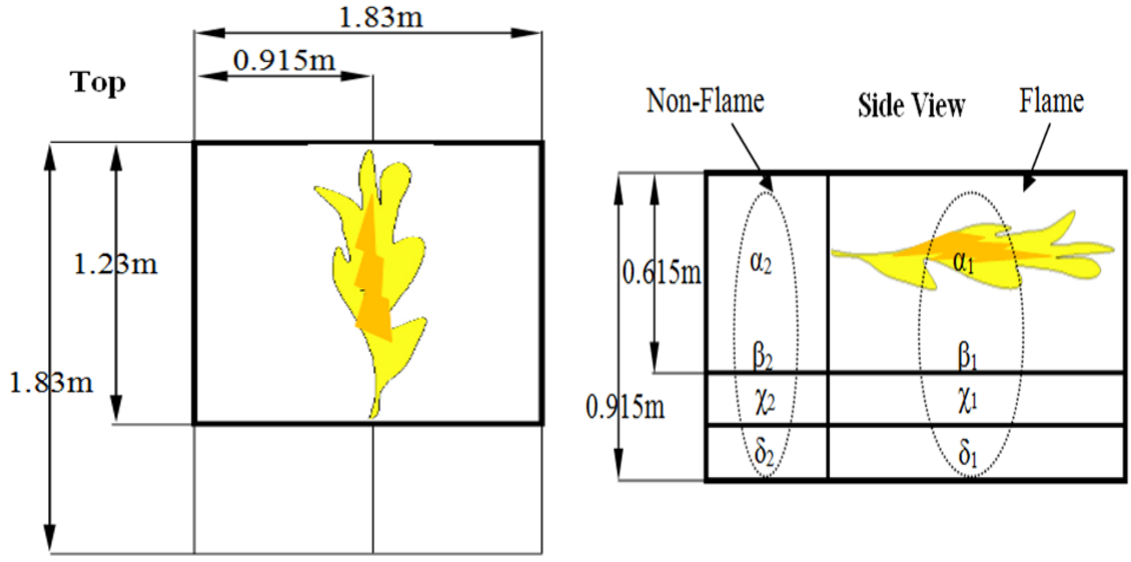

Figure 3.1: 3D Furnace Combustion and Zone Divisions (Morris, 2007)

Simulations were performed in Simulink and Matlab and the results were verified with real furnace from Fenton Art Glass Company. As illustrated in figure 3.1, the dimensions of the furnace were approximated as $1.83m \times 1.83m \times 0.915m$ ($6ft \times 6ft \times 3ft$).

The chamber is divided into two main zones; non-flame and flame zone. The gas zone (α) consists of with and without flame. This division is kept steady as the furnace is further divided throughout the depth of the glass. The glass surface (β) is half inch thickness. This small thickness allows the assumption of no lateral heat transfer. The final volume is the top half of the glass volume (χ) and the bottom of

the glass in the chamber (δ). The temperature within each volume of glass and gas is assumed uniform.

Consequently, the heat transfer equation is simpler and gives fewer temperature states within the furnace. However different volumes have different temperatures, which allows for variations in temperature along the length and height of the furnace. Refractory volumes consist of only the inner high temperature layer. A furnace is constructed using two layers of refractory. The inner layer is an extreme temperature refractory that is designed to resist the corrosion of the glass. The outer layer consists of a lighter and insulating refractory.

The top half of the glass volume of non-flame zone temperature (Tg_{x2}) is preferred as a final product output and feedback to controller to sustain the glass temperature. The linearised energy balance equation 3.15 is applied and modified with related variables for each gas and surface zones to identify 24 state-space variables corresponding to temperatures as listed in table 3.2. For example, the energy balance equation of combustion zone α_1 can be written as,

$$Qa_{\alpha 1} = Ca_{\alpha 1}\frac{dTa_{\alpha 1}}{dt} \tag{3.16}$$

$$Ca_{\alpha 1}\frac{dTa_{\alpha 1}}{dt} = \begin{array}{c} Qbw_{\alpha 1} + Qc_{\alpha 1} + Qsw_{\alpha 1} + Qa_{\alpha 2} + Qg_{\beta 1} + \\ Qg_{\beta 2} + Qg_{x1} + Qg_{\chi 2} + Qg_{\delta 1} + Qg_{\delta 2} + Q_{Fuel} \end{array} \tag{3.17}$$

$$\begin{aligned} Ca_{\alpha 1}\tfrac{dTa_{\alpha 1}}{dt} = {} & \tfrac{Abw_{\alpha 1}}{Rbw_{\alpha 1}}(Ta_{\alpha 1} - Tbw_{\alpha 1}) + \tfrac{Ac_{\alpha 1}}{Rc_{\alpha 1}}(Ta_{\alpha 1} - Tc_{\alpha 1}) \\ & + \tfrac{Asw_{\alpha 1}}{Rsw_{\alpha 1}}(Ta_{\alpha 1} - Tsw_{\alpha 1}) + \tfrac{Aa_{\alpha 2}}{Ra_{\alpha 2}}(Ta_{\alpha 1} - Ta_{\alpha 2}) \\ & + \tfrac{OF_\beta Ag_{\beta 1}}{Rg_{\beta 1}}(Ta_{\alpha 1} - Tg_{\beta 1}) + \tfrac{(SF)OF_\beta Ag_{\beta 2}}{Rg_{\beta 2}}(Ta_{\alpha 1} - Tg_{\beta 2}) \\ & + \tfrac{OF_\chi Ag_{\chi 1}}{Rg_{\chi 1}}(Ta_{\alpha 1} - Tg_{\chi 1}) + \tfrac{(SF)OF_\chi Ag_{\chi 2}}{Rg_{\chi 2}}(Ta_{\alpha 1} - Tg_{\chi 2}) \\ & + \tfrac{OF_\chi Ag_{\chi 1}}{Rg_{\chi 1}}(Ta_{\alpha 1} - Tg_{\chi 1}) + \tfrac{(SF)OF_\delta Ag_{\delta 2}}{Rg_{\delta 2}}(Ta_{\alpha 1} - Tg_{\delta 2}) + Q_{Fuel} \end{aligned}$$

After expansion and rearrangement the heat transfer equation for the combustion gases in $\alpha 1$ is,

$$\begin{aligned} \tfrac{dTa_{\alpha 1}}{dt} = {} & \tfrac{1}{Ca_{\alpha 1}}\left[\tfrac{Abw_{\alpha 1}}{Rbw_{\alpha 1}} + \tfrac{Ac_{\alpha 1}}{Rc_{\alpha 1}} + \tfrac{Asw_{\alpha 1}}{Rsw_{\alpha 1}} + \tfrac{Aa_{\alpha 2}}{Ra_{\alpha 2}} + \tfrac{OF_\beta Ag_{\beta 1}}{Rg_{\beta 1}} + \tfrac{(SF)OF_\beta Ag_{\beta 2}}{Rg_{\beta 2}} + \tfrac{OF_\chi Ag_{\chi 1}}{Rg_{\chi 1}}\right. \\ & \left. + \tfrac{(SF)OF_\chi Ag_{\chi 2}}{Rg_{\chi 2}} + \tfrac{OF_\delta Ag_{\delta 1}}{Rg_{\delta 1}} + \tfrac{(SF)OF_\delta Ag_{\delta 2}}{Rg_{\delta 2}}\right] + Ta_{\alpha 1} + \tfrac{Abw_{\alpha 1}}{(Ca_{\alpha 1})Rbw_{\alpha 1}}Tbw_{\alpha 1} \\ & + \tfrac{Ac_{\alpha 1}}{(Ca_{\alpha 1})Rc_{\alpha 1}}Tc_{\alpha 1} + \tfrac{Asw_{\alpha 1}}{(Ca_{\alpha 1})Rsw_{\alpha 1}}Tsw_{\alpha 1} + \tfrac{Aa_{\alpha 2}}{(Ca_{\alpha 1})Ra_{\alpha 2}}Ta_{\alpha 2} \end{aligned}$$

$$+\frac{OF_{\beta}Ag_{\beta 1}}{(Ca_{\alpha 1})Rg_{\beta 1}}Tg_{\beta 1}+\frac{(SF)OF_{\beta}Ag_{\beta 2}}{(Ca_{\alpha 1})Rg_{\beta 2}}Tg_{\beta 2}+\frac{OF_{\chi}Ag_{\chi 1}}{(Ca_{\alpha 1})Rg_{\chi 1}}Tg_{\chi 1}$$
$$+\frac{(SF)OF_{\chi}Ag_{\chi 2}}{(Ca_{\alpha 1})Rg_{\chi 2}}Tg_{\chi 2}+\frac{OF_{\delta}Ag_{\delta 1}}{(Ca_{\alpha 1})Rg_{\delta 1}}Tg_{\delta 1}+\frac{(SF)OF_{\delta}Ag_{\delta 2}}{(Ca_{\alpha 1})Rg_{\delta 2}}Tg_{\delta 2}+\frac{Q_{Fuel}}{Ca_{\alpha 1}}$$

where, OF is the absorption factor based on capacity, SF is the shape factor relating to radiation heat transfer, $Ca_{\alpha 1}$ is the capacitance of combustion gas in $\alpha 1$.

The other 23 state-space variables are listed in appendix.

Table 3.2: 24 State-space Variables of the Simulated Furnace Model

Order	State Variables	Order	State Variables	Order	State Variables
1	$Ta_{\alpha 1}$	9	$Tg_{\beta 1}$	17	$Tg_{\delta 1}$
2	$Tbw_{\alpha 1}$	10	$Tg_{\beta 2}$	18	$Tbw_{\delta 1}$
3	$Tc_{\alpha 1}$	11	$Tg_{\chi 1}$	19	$Tsw_{\delta 1}$
4	$Tsw_{\alpha 1}$	12	$Tbw_{\chi 1}$	20	$Tfl_{\delta 1}$
5	$Ta_{\alpha 2}$	13	$Tsw_{\chi 1}$	21	$Tg_{\delta 2}$
6	$Tc_{\alpha 2}$	14	$Tg_{\chi 2}$	22	$Tsw_{\delta 2}$
7	$Tsw_{\alpha 2}$	15	$Tsw_{\chi 2}$	23	$Tfw_{\delta 2}$
8	$Tfw_{\alpha 2}$	16	$Tfw_{\chi 2}$	24	$Tfl_{\delta 2}$

3.4.1 Brief Introduction of Glass Furnace

Figure 3.2 illustrates the block diagram of multivariable glass furnace which consists of 24 states-space furnace model with feedback-loop and open-loop EO_2 model. f_1 and f_2 is algebraic expression, f_1 includes controller output and saturation, f_2 is thermal or energy demand (ED) includes specific heat (Cp) and low fuel calorific heat value (LHV) for determining the combustion energy, T_{SET} is primary temperature setting, C_g is glass control, AFR is air-fuel ratio, T_{amb} is ambient temperature, $\dot{m}$ is fuel flow in mass, Q_{Fuel} is pressurised fuel based on ED for combustion, T_g is glass temperature and EO_2 is excess oxygen.

The glass temperature of the furnace is designed and controlled by primary input vectors, $\dot{m}$ (based on T_{SET} with feedback error and AFR) and a secondary input vector, T_{amb}. Any variation within these input variables could affect the T_g. The EO_2 is part of product element of methane combustion. The input vector of EO_2 model is based on the AFR in mass (kg). The EO_2 are developed based on the real data collected from the Quinn Glass Limited, Chester by empirical technique for $1000sec$ with $5sec$ sampling interval (discussed in detail in section 4.5). The data

was gathered by the step input of increasing air ratio from 9.5 to 10.5 in volumetric (ft^3).

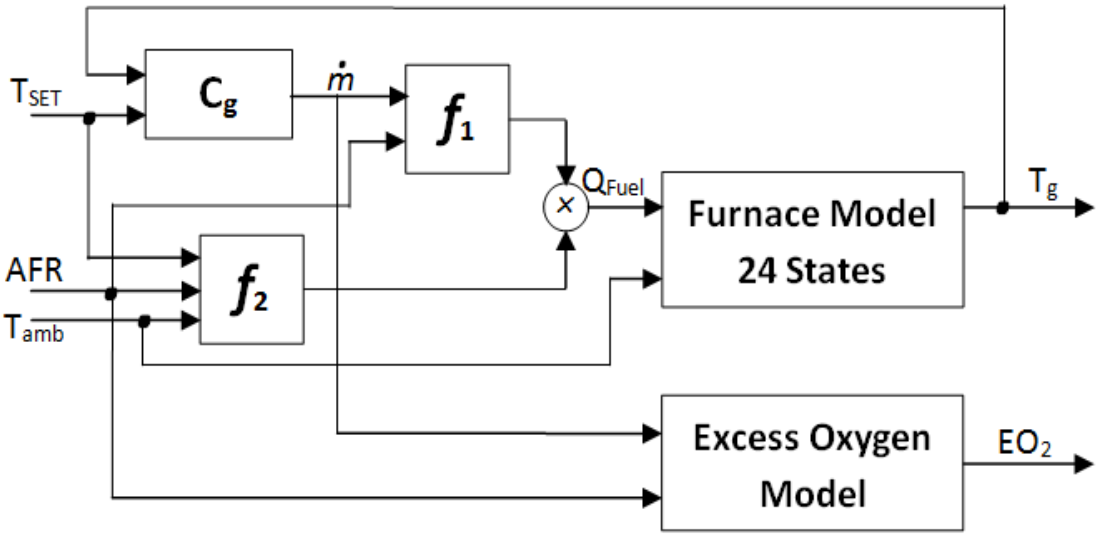

Figure 3.2: Block Diagram of Multivriable Glass Furnace

3.4.2 Validation of Combustion Chamber Model

The physical properties of the combustion chamber model were studied and the main findings are as follows;

- The numerical coefficients of 24 state-space variables given in Morris (2007), are unstable as an eigenvalue is located at right-side on s-plane (+45.3) as shown in figure 3.3. Further close observation was carried out for each element of the state matrix and it was found that 4 elements ($Tg_{\chi 1}$, $Tg_{\chi 2}$, $Tg_{\delta 1}$, $Tg_{\delta 2}$) were absent (zero) for the non-flame forward wall temperature state-space variable ($Tfw_{\alpha 2}$).

- Another, state matrix element $Tg_{\chi 2}$ was mistakenly identified as $Tg_{\chi 1}$ and displaced for the non-flame glass surface temperature state-space variable ($Tg_{\beta 2}$). Those missing and mistakenly identified elements were recalculated and the 24 state-space matrices updated. Cross reference was done with the updated

24 state-space variables simulation results and real data. Figure 3.4 shows the corrected combustion model is now stable as expected as all the eigenvalues are located at left-side on s-plane.

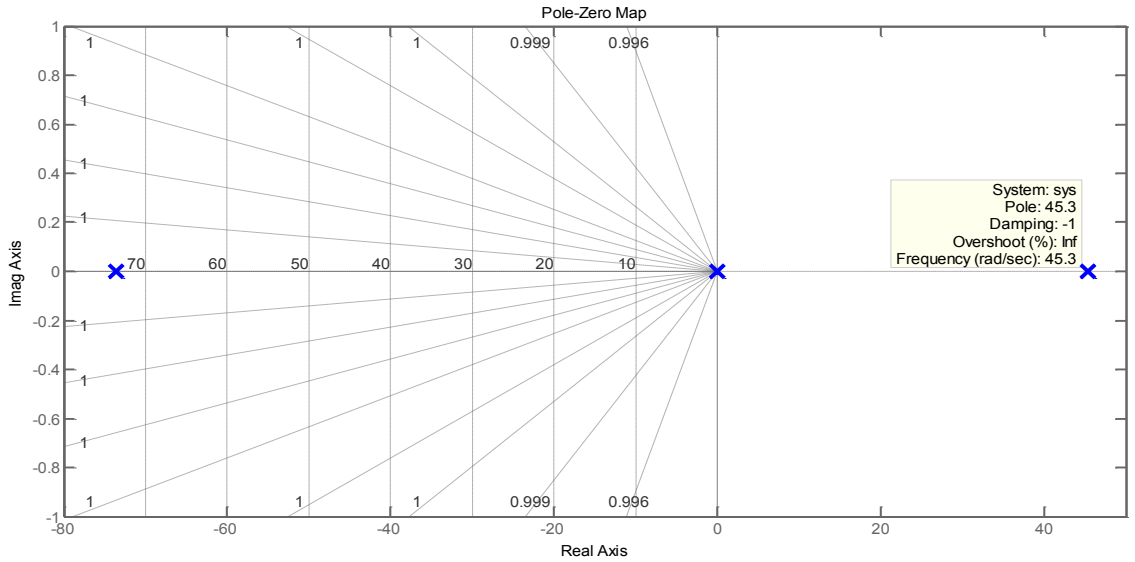

Figure 3.3: Eigenvalues of 24 Original State-Space Variables (Unstable)

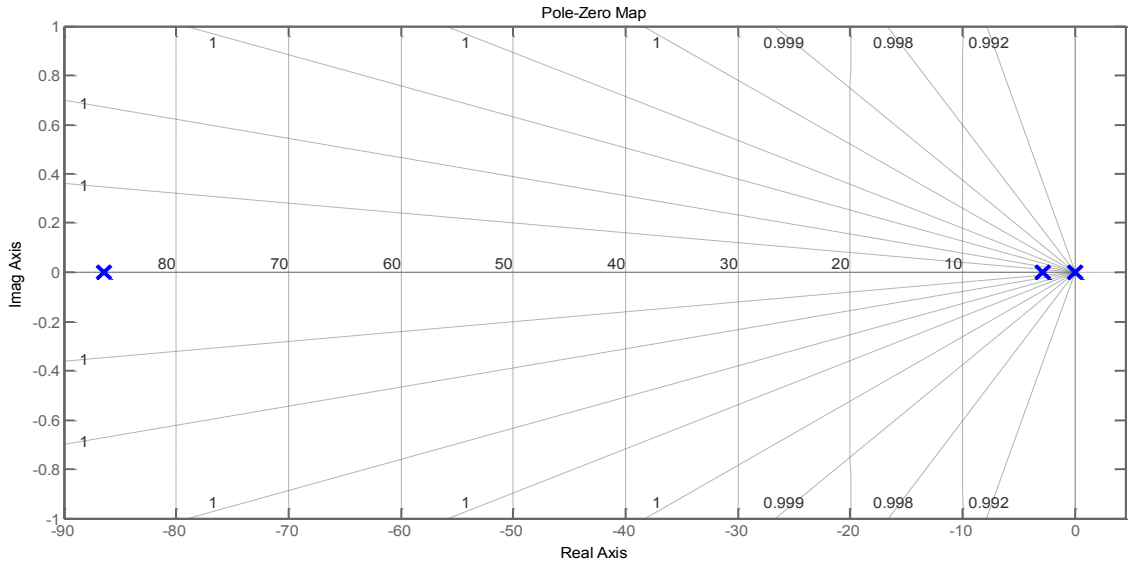

Figure 3.4: Eigenvalues of Corrected 24 State-Space Variables (Stable)

- All the stable 24 eigenvalues are identified. An eigenvalue located at -86.4, another eigenvalue located at -2.87 and the rest of the eigenvalues are located between -5.06×10^{-6} to -3.47×10^{-3}. No complex poles. The eigenvalue at

-86.7 which is temperature of flame combustion gas zone ($Ta_{\alpha 1}$) is dynamic and has fastest response. Then is followed by the eigenvalue at -2.87, which is temperature of non-flame combustion gas zone ($Ta_{\alpha 2}$). The rest of the 22 eigenvalues are between -0.5×10^{-5} to -3.5×10^{-3}.

- The glass furnace model was simulated on a computer using the simulation package MatLab/Simulink. The time taken to complete a simulation tended to be slowed and stopped when applying the default simulink solver options (*ode*45 or *ode*23; standard variable step integration algorithms) as the simulation model exhibits a stiffness problem. This is evident in the large variation of the system eigenvalues, as discussed for figure 3.4 above. The *ode*23*t* (moderately stiff/Trapezoidal) algorithm was therefore applied and was observed to improve the simulation period and accuracy. The variable step was applied in the simulation parameters as it is more robust than fixed step for stiff problems (MathWorks, 2015).

- Open-loop step response of 24 state-space matrix combustion model has $54hrs$ ($2days$ and $6hrs$) of 5% settling time for the glass temperature. According to Morris (2007), the closed-loop response has $7.5hrs$. Further simulation testing carried out found that the controller gain used was excessive. With excessive controller gain, the temperature of flame combustion gas zone ($Ta_{\alpha 1}$) has high overshoot ($1750K$). Thus, these cause the refratories of chamber (crown and walls) to have fast rise time and settling time in temperature less than 1hr. A sudden, rise in temperature could cause a lessening in the life time of chamber refratories (Carniglia, 1992). Appropriate controller tuning is required to enhance the life time of refratories while making a concession on the settling time of system response.

- A difficulty arose in understanding the input-output bounds to the glass furnace process. The main fuel controller section has two sub-sections to determine Q_{Fuel} for combustion. As shown in figure 3.5, the first section is the total

ED section (f_2), which is estimated by thermal parameters such as LHV, AFR, C_p and T_{SET}, gives $ED_{(f_2)} = \left(\frac{LHV}{C_p \times AFR} + T_{amb}\right) - T_{SET}$. The T_{SET} is set by operator, manually according to the daily throughput. The second section is the fuel control section to control the $\dot{m}$ according to the temperature feedback error. Further, the $\dot{m}$ is integrated with AFR and C_p, gives $f_1 = C_p \times \left[\left(\dot{m} \times AFR\right) + \dot{m}\right]$. The T_{Fuel} is total fuel consumption for total period of simulation, gives $T_{Fuel} = \int_0^t \dot{m}(t)dt$. As per thermal demand necessity, the control should change when reset the T_{SET} to attain the steady-state temperature. These two sections are dependable and both T_{SET} and $\dot{m}$ values are correlated. But, the main controller of Fenton Glass furnace was designed as two different separate sections and not dependable. Therefore, the f_1 and f_2 are applied to estimate the Q_{Fuel} for an optimum combustion. Further, the T_{SET} and $\dot{m}$ values are calculated separately to modify the main controller and for model parameter identification.

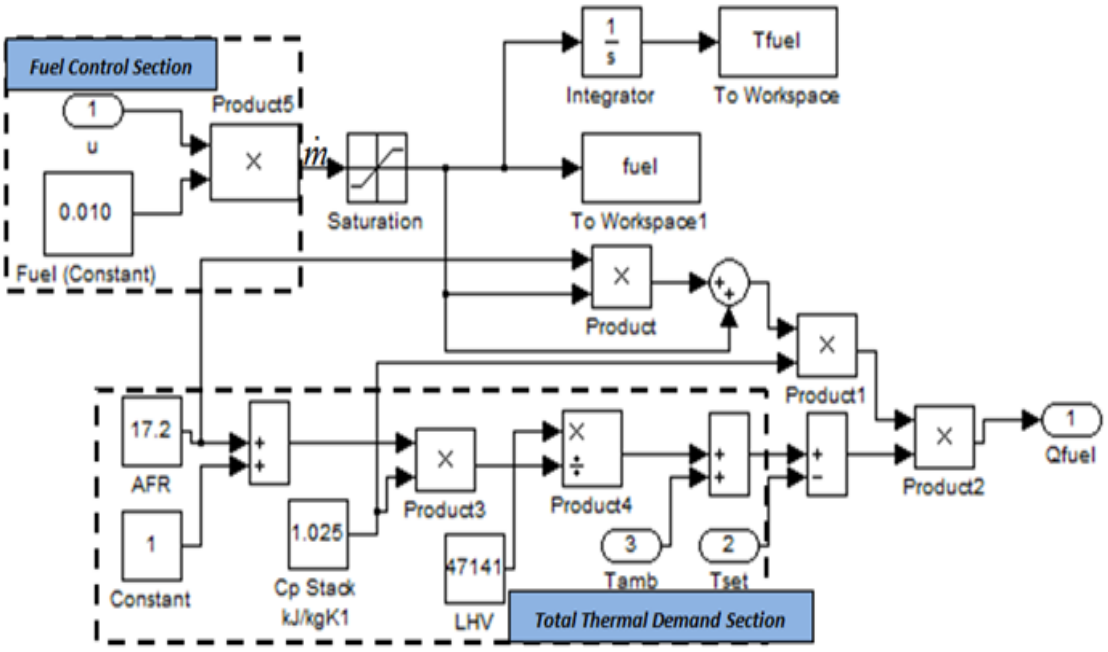

Figure 3.5: Simulink Diagram of the Subsystem in the Open-Loop Model of Furnace

Figure 3.6 illustrates the three different input configurations by open-loop process step responses with statement below,

1. $1500K$ steady-state – both T_{SET} and $\dot{m}$ values are changed accordingly. The response attained the desired steady-state value.

2. $1550K$ steady-state – only fuel $\dot{m}$ value is changed. The response attained $1600K$.

3. $1550K$ steady-state – only T_{SET} value is changed. The response attained $1450K$.

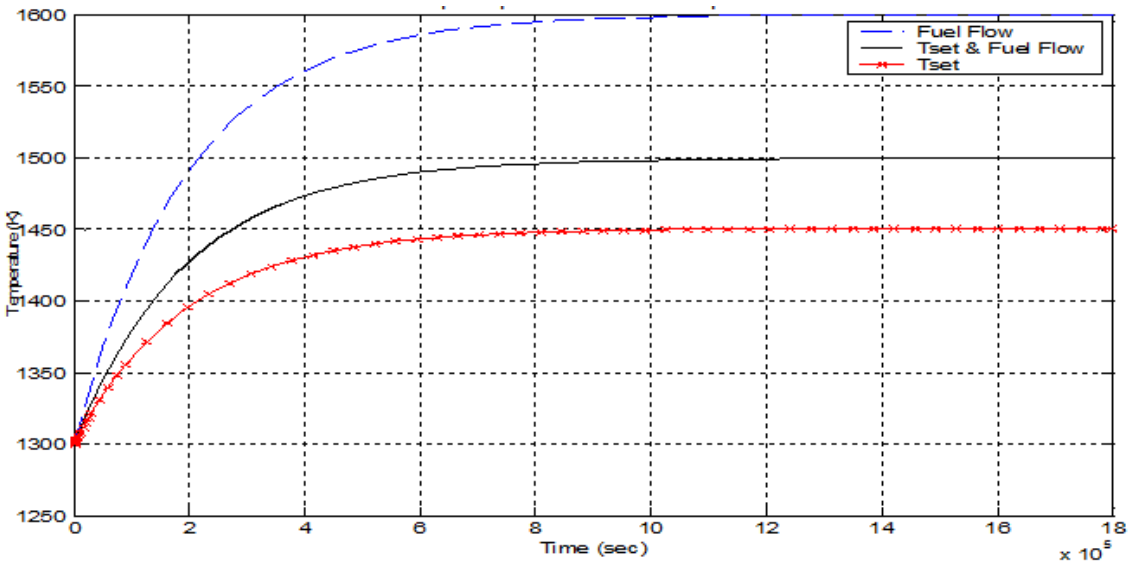

Figure 3.6: Step Responses of Glass Temperature of 3 Input Configurations

3.5 Chapter Summary

In this chapter, the selected glass furnace model's design methodologies by CFD method were outlined. The developed combustion chamber based on radiative heat transfer in finite zones and the enclosures walls surface parts, improved the heat flux and temperature distribution within the combustion chamber. Further, a non-linearity relationship in energy balances (conservation law) exhibits an analytical complication due to the dependency of radiative heat flow rates on the temperature.

Thus, an application of Taylor series expansion around temperature differences, improved the linear relationship in energy balances. The physical properties of selected combustion chamber model is studied.

Further, the unstable eigenvalues of 24 state space variables are corrected by recalculating by energy balance equation and verified. The main equations are applied for glass furnace modelling and simulation are, 1). Radiative heat transfer between zones (equ. 1 to equ. 3), 2). 24 states of energy balance equation of combustion (equ. 3.17), 3). Total ED section (f_2) and 4). Fuel control section $\dot{m}$ with AFR and C_p (f_1).

Chapter 4

Model Parameters Identification of Glass Temperature and Excess Oxygen

4.1 Introduction

This chapter is primarily focused on optimal control oriented model parameter identification for glass temperature and excess oxygen. Common phenomenon of premature convergence which is the search space constraint in SGAs is reviewed. A novel technique named, predetermined time constant approximation, is proposed to enhance the search mechanism to optimise the search boundaries to locate optimal values of model parameters.

Further, a full scale of realistic excess oxygen model parameters which are consists of air-fuel ratio conversion model, dynamic transfer function model and excess oxygen look-up table is developed by using real plant's numerical data of excess oxygen. According to the literature survey, there is no realistic excess oxygen model available for further research. Therefore, the development of a realistic excess oxygen model is essential for further research here. Also, the control oriented model parameters of both glass temperature and excess oxygen processes are developed for control parameter optimisation.

4.2 Model Parameter Identification

In general, a system identification dilemma can be categorised into two optimisation tasks; Structural identification of the equations and Model parameter estimation. The vicinity of model parameters identification has received great attention over the last three decades as in control engineering [Juang and Phan, 1994]. The primary perception of optimal model parameters identification is the progression of altering the input variables of model parameter characteristics or process to locate the minimum or maximum output or product as illustrated in figure 4.1. For this motivation numerous researchers consider that optimisation is one of the oldest sciences which even extends into daily life [Neumaier et. al., 2006] [Haupt and Haupt, 2004]. It can be noticed that as an input consists of variables, the function is known as the objective function or fitness function and the output is the cost or fitness.

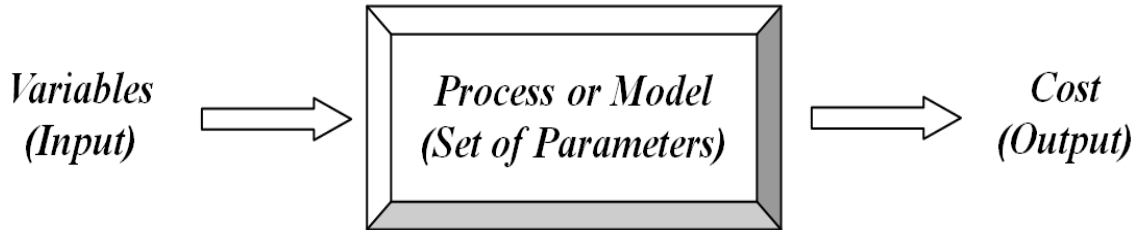

Figure 4.1: Schematic diagram of model parameters to be optimised

A mathematical approach is inevitable for validation if there is something significant and has to be optimised. As a result, the global optimisation is the part of mathematical and numerical analysis that concerns on the optimisation of a set of criterion which expressed in a fitness function [Weise, 2009]. Therefore, the foremost endeavour of the global optimisation is to locate a set of parameters for which these fitness functions will return the optimal values [Okaeme, 2008]. Therefore, with the aim of attain these optimal values, the optimisation algorithms are in application. In general, the optimisation algorithms technique can be categorised into two groups; deterministic and probabilistic algorithms.

The deterministic algorithm is generally applied if there is an understandable, predictable behaviour and not excessively complex relation between a solution candidate and its fitness. Or else, it is really difficult to be resolved deterministically

and dimensionality if the search space is too high which could lead to local minima. While, the probabilistic or randomized algorithms is applied based on a degree of randomness as part of its logic. In other word, the probabilistic algorithms violate the constraint of determinism. This algorithm typically applies uniformly random bits as an auxiliary input to guide its behaviour, in the hope of achieving good performance in over all possible choices of random bits [Weise, 2009].

In contrast, current problems are likely to be extremely complex and relate to analysis of great sets of data. Even if a precise algorithm can be developed its time or space complexity may be undesirable. But in reality it is often adequate to locate an estimated or partial solution. Such admission extends the set of techniques, known heuristic algorithms to manage with the problem. Heuristics applied in global optimisation function that to produce an acceptable solution to a problem in many practical situations without any guarantee of its correctness. If there is an unknown technique to locate an optimal values to a given desired criterion, under the given constraints of time or space, then the heuristic algorithm is a better preference [Weise, 2009], [Michalewicz and Fogel, 2004].

4.2.1 Primary Elements of SGAs

Goldberg (1989) illustrated that SGAs involve nothing more composite than copying and substituting partial strings. There are a number of prime matters that should be considered when applying SGAs (Whitely, 1993). These prime elements are discussed in the followings subsections.

4.2.1.1 Population Initialisation

The beginning point of the search is to generate a group of individuals to form a population, called initial population. Generally, the initial population can be generated by four different methods; Random Initialisation, Grid Initialisation, Knowledge-based Random Initialisation and Knowledge-based Grid Initialisation. The most familiar setup commences by generating the number of individuals applying a random number generator that uniformly distributes numbers in the required range.

For instance, if there is a binary population of N_{ind} individuals whose chromo-

somes are L_{ind} bits long, then $N_{ind} \times L_{ind}$ random numbers uniformly distributed from the set $\{0 : 1\}$ would be produced.

The prime objective is to produce a population with a better search space to have a gene pool with good prospective for breeding better solutions. Otherwise, genomes can be distributed to the entire search space according to a regular grid-layout. However, an entirely new selection of beginning points can be an improvement to a random setup while executions are repeated.

A further approach is that experts typically can approximate a realistic solution to a specific problem. By introducing this realistic solution as one of the initial individuals, then the remaining individuals will be randomly distributed in a grid close to the best known solution. So, a problem with such an initialisation can attain to have a search area near the best solution.

Therefore, the selection of initialisation methods can be concluded that it depends on the specific problem itself and the approach to be applied. Nevertheless, expert knowledge plays a significant role in initialisation for the real life application [Chipperfield et. al., 1994b], [Ursem, 2003].

4.2.1.2 Objective Function

As soon as a population of solutions is generated, each of the chromosomes or individuals in the population has to be evaluated according to their performance. The performance evaluation process can be attained with the objective function which decodes the chromosome. Then, the process evaluates it and returns the performance to the SGAs. The evolution process's successes are based on the fittest chromosomes which have the lowest numerical value of the associated objective function. This numerical value is applied to identify the relative performance of individuals in SGAs.

In order to transform the objective function value into a measurable relative fitness (*fitness function*), the total relative population is applied in which the individual fitness, $F(x_i)$, of each individual is calculated as the individual's raw performance, $f(x_i)$,:

$$F(x_i) = \frac{f(x_i)}{\sum_{i=1}^{N_{ind}} f(x_i)} \tag{4.1}$$

where N_{ind} is the population size and x_i is the phenotypic value of individual i. Nevertheless, one of the weaknesses of this fitness function is that it fails to account for negative objective function values because it make sure that each individual has a probability of reproducing according to its relative fitness. Then, a linear transformation which offsets the objective function is often applied to guarantee that the resulting fitness values are non negative. The function used is illustrated below:

$$F(x) = a \cdot f(x) + b \tag{4.2}$$

where a is a positive factor if the optimisation has to be maximised or negative factor if the optimisation has to be minimised. The offset b is chosen to compensate the non negative results. Figure 4.2 illustrates how the fitness of the best individual improves over time and the fitness value approaches gradually the zero point towards the end of the execution.

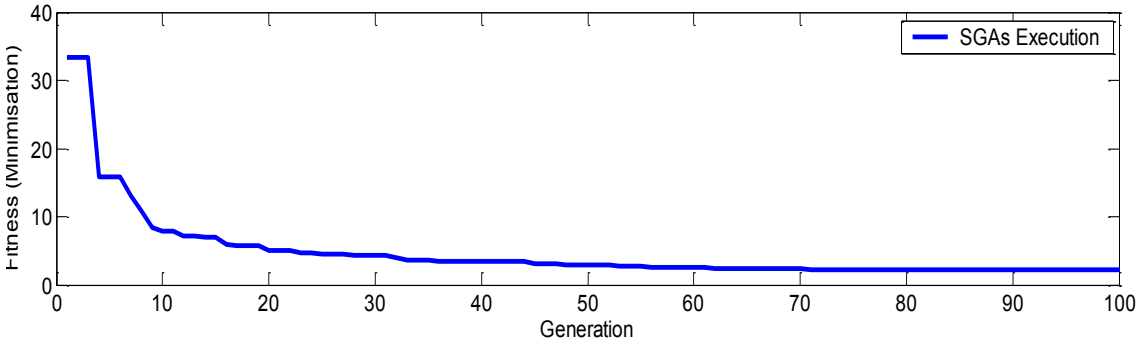

Figure 4.2: Gradual fitness improvements by SGAs execution (minimisation)

4.2.1.3 Selection

When the evaluation procedure is completed for all the possible solutions, two or more must be selected to be a parent string with high fitness value from the current population, to create fitter offspring for the next generation. The selection process

is usually a random process of determining the number of trials; a particular individual is selected for reproduction and subsequently the number of offspring that an individual will create. The main goal is to create a new generation of individuals that are potentially better solutions or fitter than their parents.

The selection process is correlated with the fitness assignment of each individual. In other words, each individual is inspected and evaluated applying the fitness function and the output value will quantify the fitness of each individual. There are a number of ways to implement the selection. Some of the most accepted and well studied selection processes are; Roulette Wheel Selection Method, Tournament Selection and Stochastic Universal Sampling.

Here the stochastic universal sampling (SUS) is selected for further works. SUS is a development of roulette-wheel selection (RWS) which exhibits no bias and minimal spread. The individuals are mapped to adjacent parts of a line, such that each individual's part is equal in size to its fitness exactly as in RWS. In this case, depending on the number of individuals to be selected, the same number of equally spaced pointers is placed over the line. Consider $N - Pointer$ as the number of individuals to be selected, then the distance between the pointers is $1/N - Pointer$ and the position of the first pointer is given by a randomly generated number in the range $[0, 1/N - Pointer]$.

Figure 4.3 illustrates the selection of the choice of 6 individuals where the distance between the pointers is $1/6 = 0.167$. Sample of 1 random number in the range [0, 0.167]:0.18. After selection, the mating population consists of the individuals: 1, 2, 3, 4, 6 and 8. Stochastic universal sampling ensures a selection of offspring which is closer to what is deserved than roulette wheel selection [Chipperfield et. al., 1994b].

4.2.1.4 Crossover

Crossover is one of the essential operators for reproducing new chromosomes in SGAs. Crossover produces new individuals that have some characteristics of parent strings. The recombination operator is applied to exchange genetic information between pairs of individuals and produce offspring for the next generation. Two

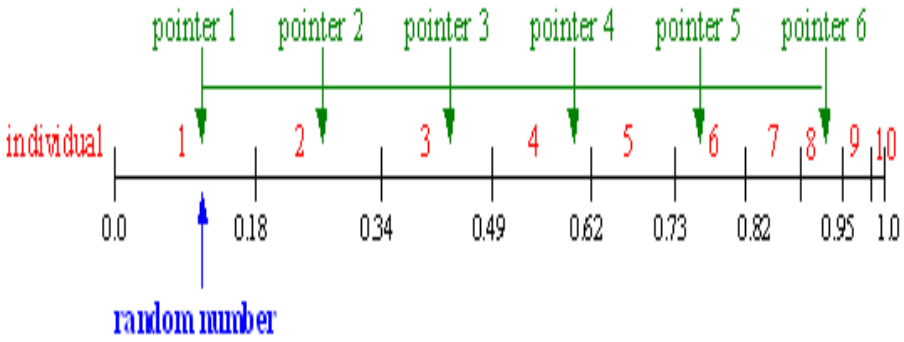

Figure 4.3: Stochastic Universal Sampling (SUS)

strings are selected randomly from the mating pool. The crossover rate or probability, X_{rate}, will decide if crossover should take place and how frequently, within any generation, the crossover function is carried out on pairs of individuals. This value is generally selected to be in the range 0.5 - 1.0 [Srinivas and Patnaik, 1994].

The simplest recombination operator is the single-point crossover, although there are some other variations of crossover such as multi-point crossover, uniform crossover, intermediate recombination and line recombination. The differences between them are the generated crossover points. In this section the single-point crossover will be described.

Consider the two parent binary strings:

$$P_1 = 10010110$$

$$P_2 = 10111000$$

As referred above, when crossover occur the two new offspring strings are created. An integer point, i, is selected randomly between 1 and the string length, l, minus one $[1, l-1]$, therefore, the genetic information is exchanged between the individuals about this point, i. The two offspring from the below figure 4.4 are produced when the crossover points $i = 5$ is selected.

This crossover operator is not performed on all strings in the population. Instead, it is applied when the pairs are selected for breeding with probabilities X_{rate} [Chipperfield et. al., 1994b]. Figure 4.5 illustrates the crossover for real-coded

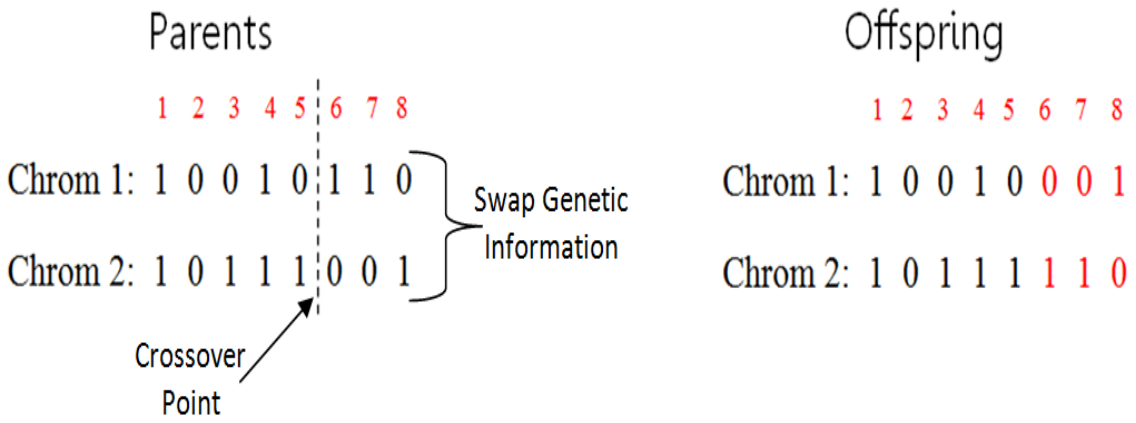

Figure 4.4: Single-Point crossover (Binary-Coded)

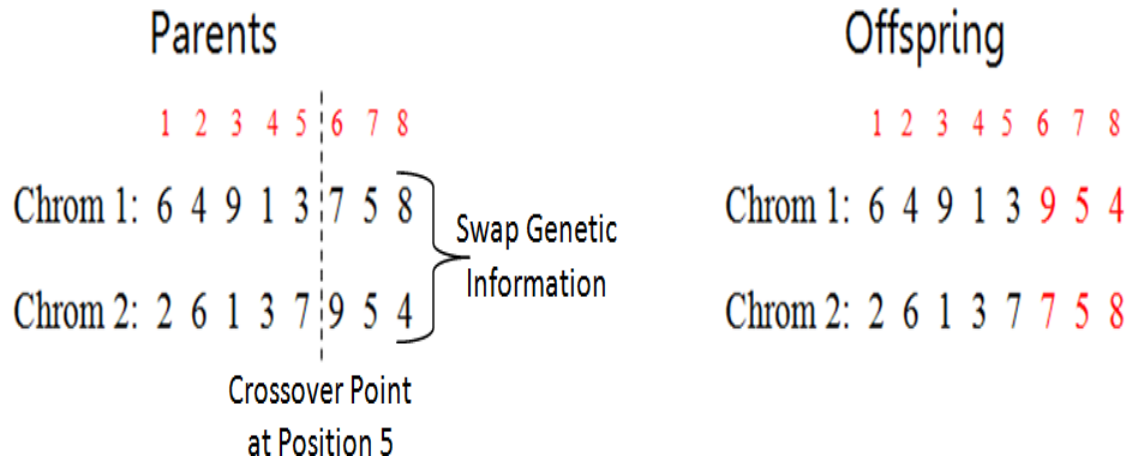

Figure 4.5: Single-Point crossover (Real-Coded)

representation of individuals for single-point crossover. In this case, during the simulation of the single-point crossover, the two individuals selected randomly for reproduction are paired off. The crossover point is selected at 5 and all the digits of one individual to the right of the crossover point are exchanged with those of the other. The resulting individuals, termed offspring, form the individual of the population of the new generation.

4.2.1.5 Mutation

Mutation is a random process where one allele of a gene is substituted by another to produce a new genetic configuration and is applied to the new chromosomes with a set mutation rate, M_{rate}. The mutation operation does not occur as often as the crossover function and it is applied generally by applying a low M_{rate}, typically in

the range 0.005 - 0.05 [Srinivas and Patnaik, 1994]. Therefore, the role of mutation is often providing a certainty that the probability of searching on any string set will never be zero and acting as a safety net to recover good genetic material that may be lost through the selection and crossover processes [Goldberg, 1989].

Mutation causes the individual genetic representation to be changed according to some probabilistic criteria. So, if l is the length of the chromosome then a number between 1 and l is selected randomly as the mutation point. In the binary-coded representation, mutation will cause a single bit to change its state, $0 \longrightarrow 1$ or $1 \longrightarrow 0$. Figure 4.6 illustrates the process of binary-coded mutation. According to the figure 4.6, the mutation point on the 3^{rd} bit of the binary individual is mutated by flipping the value of the bit.

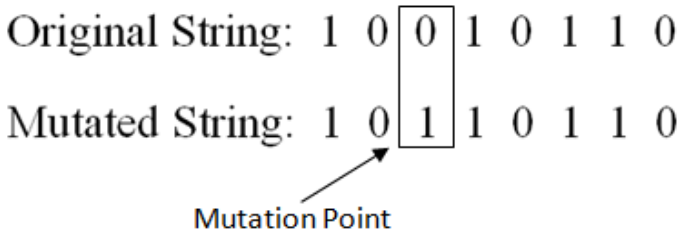

Figure 4.6: Binary-coded mutation

Given that mutation is generally applied uniformly on entire population of strings, it is possible that a given binary string may be mutated at more than one point. Figure 4.7 illustrates the mutation for real-coded representation of individuals. The application of real-coded mutation includes randomly selecting a position to execute the operation and then changing the figure in that position to any of its complementary values. For the decimal population, any figure (in any position) would have nine complementary values.

4.2.2 Prior Knowledge of Specific Problem

In numerous optimisation problems, the functional information related to the problem may have exist, and can frequently be applied a priori to effectively assist SGAs to execute well in terms of rate of convergence. If there exists prior information about regions in the search space where the optimal points may located, a percent-

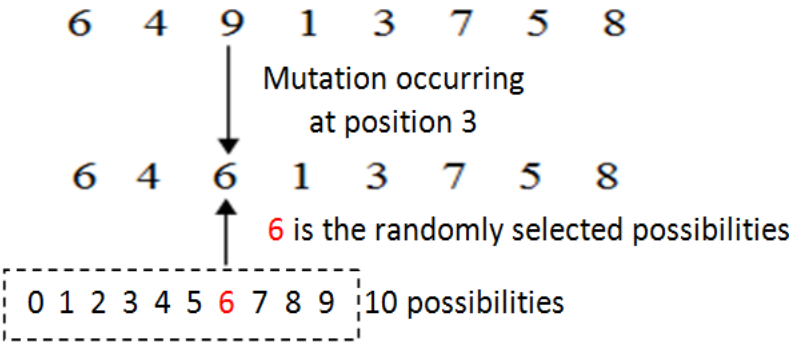

Figure 4.7: Real-valued mutation

age of the population at time $t = 0$ can be initialised by selecting candidate solutions from these promising regions. This approach can be applied whenever one searches to improve on previously identified 'optimal' solutions.

As follows, the SGAs commence with a set of potentially above-average solutions, which can significantly improve the rate of convergence of the SGAs. Whereas the crossover and mutation operators theoretically ensures the SGAs still able to explore different regions in the search space (Vlachos, 2000). Such heuristic initialisations of the population should be applied carefully, in order to avoid premature convergence, the situation where the SGAs may convergence to a sub-optimal region in the search space.

4.2.3 Convergence Constraints by Search Space Boundary

In most situations, selecting the search space boundary regions is delicate if there is no prior knowledge of optimum value location. Thus, a randomly selected search space boundary is a significant factor which leads the SGAs to often converge and get trapped in local optima, resulting in suboptimal solutions. Particularly, if it locates near the boundary or outside of the boundary.

As illustrated in figure 4.8, the SB_{Lower} is lower search boundary, SB_{Upper} is upper search boundary Δ_{GO} is the genetic operator for convergence precision and X_i is optimal value. The SGAs convergences by search space boundary constraints can be classified by three states;

- State 1 – If the optimal value(X_i) is located within uniformly distributed elite group around boundary region $[X_i - \Delta_{GO}, X_i + \Delta_{GO}]$, the genetic operators

have higher probability of converging to global optimum. Thus, the randomly generated initial population within well distributed elite group search boundary has higher probability exploring and exploiting a better parent chromosome. Further, the selected parent chromosome will be evaluated by genetic precision process (selection, crossover and mutation) to produce fitter offspring without any convergence constraint.

- State 2 – If the X_i is located near SB_{Lower}, $[SB_{Lower}, X_i - \Delta_{GO}]$ or SB_{Upper}, $[X_i + \Delta_{GO}, SB_{Upper}]$ the SGAs possibly will converge to local minima. The elite group which is distributed near the boundary may have located a part of the elite group at the outer boundary. If the elite group at the outer part have the genetic information of an optimal value, the genetic operators will suffer to exploit the optimal value and the exploration process will retard. As a result, the search space boundary constraints will lead the SGAs to converge to local minima.

- State 3 – If the X_i is located outside the boundary region $[SB_{Lower} > X_i > SB_{Upper}]$, the SGAs will fail to explore and exploit the optimal value. The simulation may be retarded and stopped.

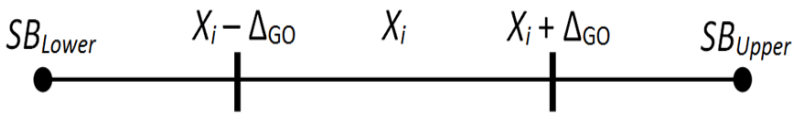

Figure 4.8: Schematic diagram of feasible search space boundary region (Xu B. et.al., 2012)

4.2.4 Predetermined Time Constant Approximation

To improve search space boundaries for optimal model parameters identification, a new boundary resizing technique without a complex mathematical constraint is introduced here, named predetermined time constant approximation,($PTcA$). The

proposed $PTcA$ method provides a prior knowledge of higher order poles coefficients of transfer function, named initial predetermined time constant $\left(Ts_{p(Initial)}\right)$ value from dynamic response of a process. Applying the $Ts_{p(Initial)}$, gives an approximation of the elite group distribution within a feasible boundary region by resizing the boundary region is at the initial stage. This gives the genetic operators opportunity to locate the optimal value rapidly without any constraint. Author primarily considered identification of the denominator polynomial coefficients provide a foundation for determining a system's dynamic response characteristics.

Consider a system can be modelled by the general order transfer function is of the form,

$$G(s) = \frac{Y(s)}{F(s)} = \frac{K_p}{a_n s^n + a_{n-1} s^{n-1} + \cdots + a_1 s + 1} e^{-\theta s} \tag{4.3}$$

where $Y(s)$ is the output signal, $F(s)$ is the input signal or forcing function, K_p is process gain, θ is the time delay and $a_n \ldots a_1$ are coefficients of the denominator polynomial which is particularly defining the components in the homogeneous response.

For the $PTcA$ method application, the denominator of equation 4.1 is approximated as follows,

$$G(s) = \frac{Y(s)}{F(s)} = \frac{K_p}{\left(Ts_{p(Initial)} s + 1\right)^n} e^{-\theta s} \tag{4.4}$$

By applying the $PTcA$ method, the coefficients of the denominator polynomial, $a_n ... a_1$ in equ. 4.1 are to be substituted with $Ts_{p(Initial)}$ values in expansion of equ. 4.2, gives,

$$G(s) = \frac{Y(s)}{F(s)} = \frac{K_p}{Ts_{p(Initial)n} s^n + Ts_{p(Initial)n-1} s^{n-1} + \cdots + Ts_{p(Initial)1} s + 1} e^{-\theta s} \tag{4.5}$$

where the $Ts_{p(Initial)} = a$. As discussed earlier, it's difficult to approximate the higher order model's denominator polynomial coefficients without a prior knowledge. Whereas, the initial value of K_p and θ can be easily approximated by observing the

magnitude of response from $C(t) = 0$ to $C(t) = Css \pm \delta(\%)$ and delay of transmission from $t = 0$ to $t = \theta$, respectively. Therefore, only the denominator polynomial coefficients are considered here.

The $PTcA$ method can be divided into two sup-processes. First sub-process is an identification of $Ts_{p(Initial)}$ from dynamic response for initial boundary setting. The identification process as illustrated in figure 4.9 and described as follows;

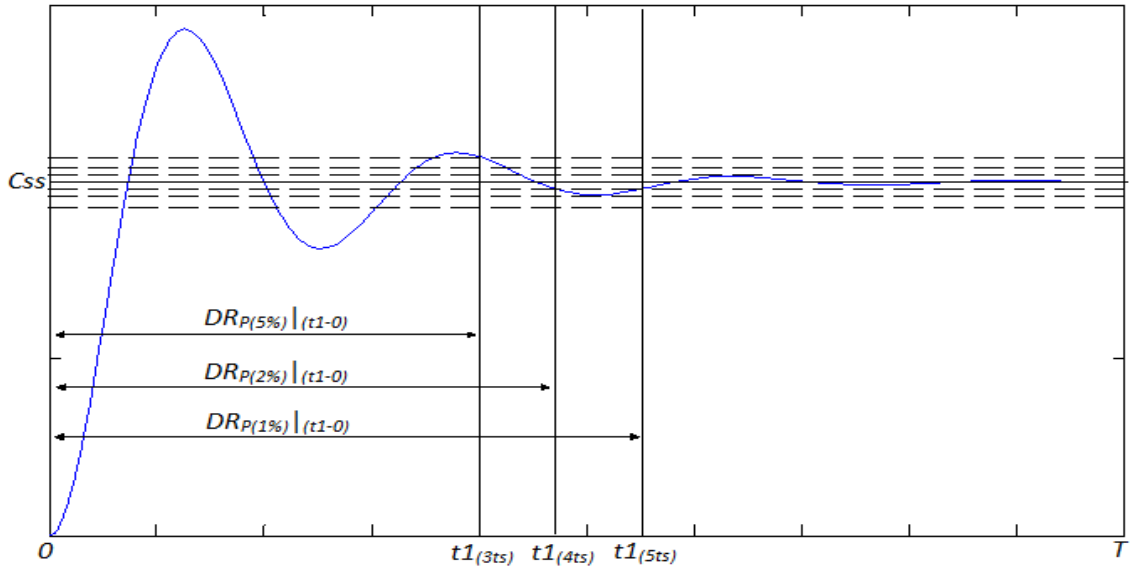

Figure 4.9: Sub-process of $Ts_{p(Initial)}$ identification from dynamic response

- Selecting $ts_{(\delta\%)}$, where ts is settling time and δ is the settling band in % ($\delta = 1$, 2 and 5). The selection of desired δ is according to the raggedness of dynamic response. The ts is defined as and in α, time constants for which the response remain within $\delta\%$ of the final value. This can be approximated as, $\zeta\omega_n ts \cong \alpha$. Hence, the $ts_{(\delta\%)} = 1\%$, 2% and $5\% \rightarrow \alpha = 5$, 4 and 3, respectively.

- Estimating process's dynamic response period $(DR_P)_{(t_1-0)}$. At $C(t) = 0_{(t=0)}$ to $C(t) = Css \pm \delta(\%)_{(t=t_1)}$.

- Approximaing a $Ts_{p(Initial)} = DR_{P(t_1-0)}/\alpha_{(\delta\%)}$.

- Applying $Ts_{p(Initial)}$ according to the respective transfer function coefficients, $a_n s^n + a_{n-1}s^{n-1} + ... + a_1 s + 1 \rightarrow Ts_{p(Initial)n}s^n + Ts_{p(Initial)n-1}s^{n-1} + ... + Ts_{p(Initial)1}s + 1$

The second sub-process of $PTcA$ method is the search space boundary optimisation by resizing the upper and lower search boundary based on $Ts_{p(Initial)}$. As illustrated in figure 4.10, the SB_O is optimum search space boundary, SB_{Lower} is lower search boundary and SB_{Upper} is upper search boundary. An optimum search space boundary as illustrated in figure 4.10 can be expressed as;

$$SB_O = \left\{SB_O; SB_{Lower} \leq Ts_{p(Initial)} \leq SB_{Upper}\right\} \tag{4.6}$$

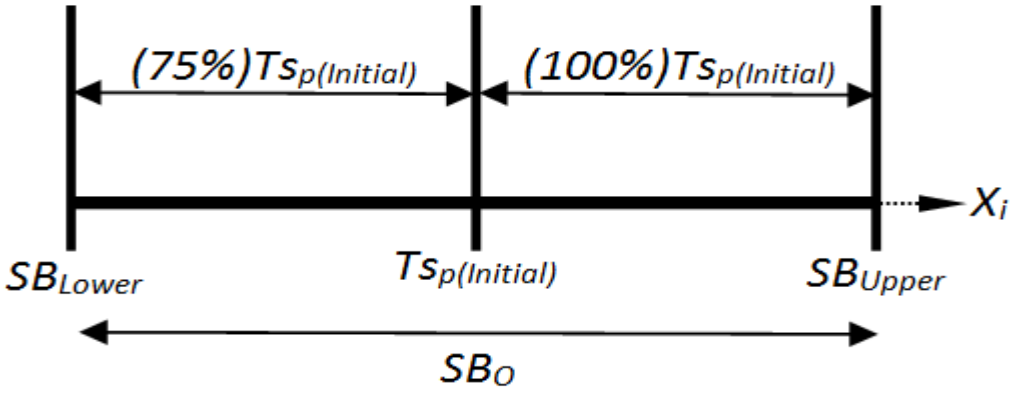

Figure 4.10: Sub-process of search space boundary optimisation by $Ts_{p(Initial)}$

For an SB_O, the SB_{Upper} and SB_{Lower} are extended by 100% and 75% from $Ts_{p(Initial)}$, respectively. Especially, 100% of extension for SB_{Upper} is required as the optimal solution can be mostly located near to the upper boundary region. Such a search space extension is required for SGAs to explore the elite groups which are uniformly distributed within boundaries and to exploit the X_i.

As illustrated in figure 4.10, the $Ts_{p(Initial)}$ is only applies for initial search boundary resizing and 1st SGAs execution. For further search boundary resizing is decided by previously executed sub-optimal value (X_i'), which is presumed as Ts_p. The sub-process of search space boundary adjustment and an optimal X_i identification can be stated as follows;

- Initial attempt – Identified $Ts_{p(Initial)}$ according to the respective denominator polynomial coefficients are applied with 100% extension on SB_{Upper}. The SB_{Lower} is extended to approximately 95% instead of 75% for better exploration at the beginning stage. Execute the SGAs.

- Second attempt – Genetically identified X_i' by initial attempt (1st execution) of respective denominator polynomial coefficients are applied for next execution to extend (which, $Ts_p = X_i'$) accordingly (SB_{Upper} to 100% and SB_{Lower} to 75%) to optimise SB_O. Execute the SGAs.

- Subsequent attempt – Continuing the SGAs execution with unchanged boundary search approximation by second attempt, until optimal X_i and minimum sum of square error (SSE) attained.

- *Subsequent attempt – If the extended boundary in second attempt is not a SB_O, consecutive boundary resizing is essential until SB_O is achieved. Then, continuing the SGAs execution until optimal X_i and SSE attained.

4.2.5 Application of SGAs in Model Parameters Identification

SGAs can be applied in model parameters identification if each individual (chromosome), in the population must represent a model of the plant. The quality of the model is based on the ability of predicting the evolution of the measured outputs. The measured outputs are compared with the real process measurement and the individual's quality is a function of the error [Ursem, 2003] [Vladu, 2003]. The measured output predictions are compared with the real plant's measurements. The SGAs model parameters identification procedure used as illustrated in the schematic flow in figure 4.11.

The discrete SGAs begins by defining a chromosome of binary string or an array of variable values to be optimised and $PRECI$ is number of bits depends on desired accuracy. For an instance, a 3rd orders transfer function with delay;

$$G(s) = \frac{C(s)}{R(s)} = \frac{A_1}{A_2 s^3 + A_3 s^2 + A_4 s + 1} e^{-A_5 s} \tag{4.7}$$

The model chromosome has 5 numbers of variables (N_{var}) dimensional optimisation variables can be written as an N_{var} element row vector.

$$chromosome = \{A_1, A_2, A_3, A_4, A_5\} \tag{4.8}$$

The SGAs starts by creating an initial population which consist a group of random binary matrix of size chromosome known as the population.

$$N_{pop} = N_{ind} \times L_{ind}; \qquad L_{ind} = (N_{var} \times PRECI)\,; \qquad N_{var} = 5 \tag{4.9}$$

where N_{pop} is number of population size, N_{ind} is number of individuals and L_{ind} is the length of the chromosome.

Good initial populations are smoothening the progress of a SGAs convergence, whereas poor initial populations can obstruct SGAs convergence. For SGAs converge better, the fitness values ($FitnV$) of all chromosomes are evaluated by the rank based objective function of entire initial population in a decoded form. This process is known as natural selection, which occurs at each iterations of the algorithm. Only the best are selected to pursue further, while the rest are discarded.

The selection rate (S_{rate}) is the fraction of N_{pop} that survives for the further survival process. A selected group of fitter chromosomes (N_{keep}) in iteration are applied further in the genetic operators and unfit chromosomes ($N_{pop} - N_{keep}$) are discarded to create room for new offspring. The number chromosomes are kept at each iteration is,

$$N_{keep} = S_{rate} \times N_{pop}; \qquad S_{rate} = SEL\_F \times FitnV \times G_{gap} \tag{4.10}$$

where SEL_F is selection function to hence the chromosome breeding and G_{gap} is generation gap to create new individuals.

SEL_F are performed and emphasised to keep the population size constant by selecting two chromosomes from the mating pool of N_{keep} chromosomes to produce new offspring. Selection has to be balanced with variation from crossover and mutation for continuing the progression. A strong selection will take over the population due to highly fit individuals. This selection will reduce or may stop the diversity needed for further progression.

While, a weak selection will resulting in slow evolution process. Author selected stochastic universal sampling (SUS) for selection process. SUS applies a single random value to sample all of the solutions by selecting chromosomes at evenly spaced intervals. This process gives weaker chromosomes a possibility to be selected and not allowing the fittest chromosomes to saturate the candidate space.

Crossover is a paring process of selected chromosomes of parents to produce one or more new chromosomes of offspring and integrated into the population (Syswerda, 1989). Single-point crossover function is selected by author for chromosomes matrix recombination. It performs between pairs of parent chromosomes contained in the current population (N_{keep}) according to the crossover probability (X_{rate}) and returns a pair offspring which is a new population after mating (N_{keep1}). The pair of new offspring chromosomes are created and kept at each iteration is,

$$N_{keep1} = XOV\_F \times N_{keep} \times X_{rate} \tag{4.11}$$

where N_{keep1} is the offspring chromosomes matrix of the new population, XOV_F is crossover function and X_{rate} is the probability of recombination rate.

Higher rate of probability crossover will rigorously trade large bits of binary string between two parent chromosomes. This could discard the best binary string from parent chromosomes to appear in offspring chromosomes for SGAs converges better. While, a lower rate will resulting in reappearing most of binary string in offspring chromosomes.

Mutation is a process modifying the binary string of chromosomes by certain percentage of mutation probability rate.

$$N_{keep1} = N_{keep} \times M_{rate}; \qquad M_{rate} = 0.7/L_{ind} \tag{4.12}$$

where M_{rate} is probability of mutation rate.

In SGAs, the mutation is a source of variability and a higher M_{rate} results in distraction the algorithm of converging efficiently. On other hand, it also tends to increases the searching freedom of algorithms at outside current region of variable

space. In general, mutation does not occur on the elite solution. Such elitism is very frequent in SGAs and propagates the solutions unchanged.

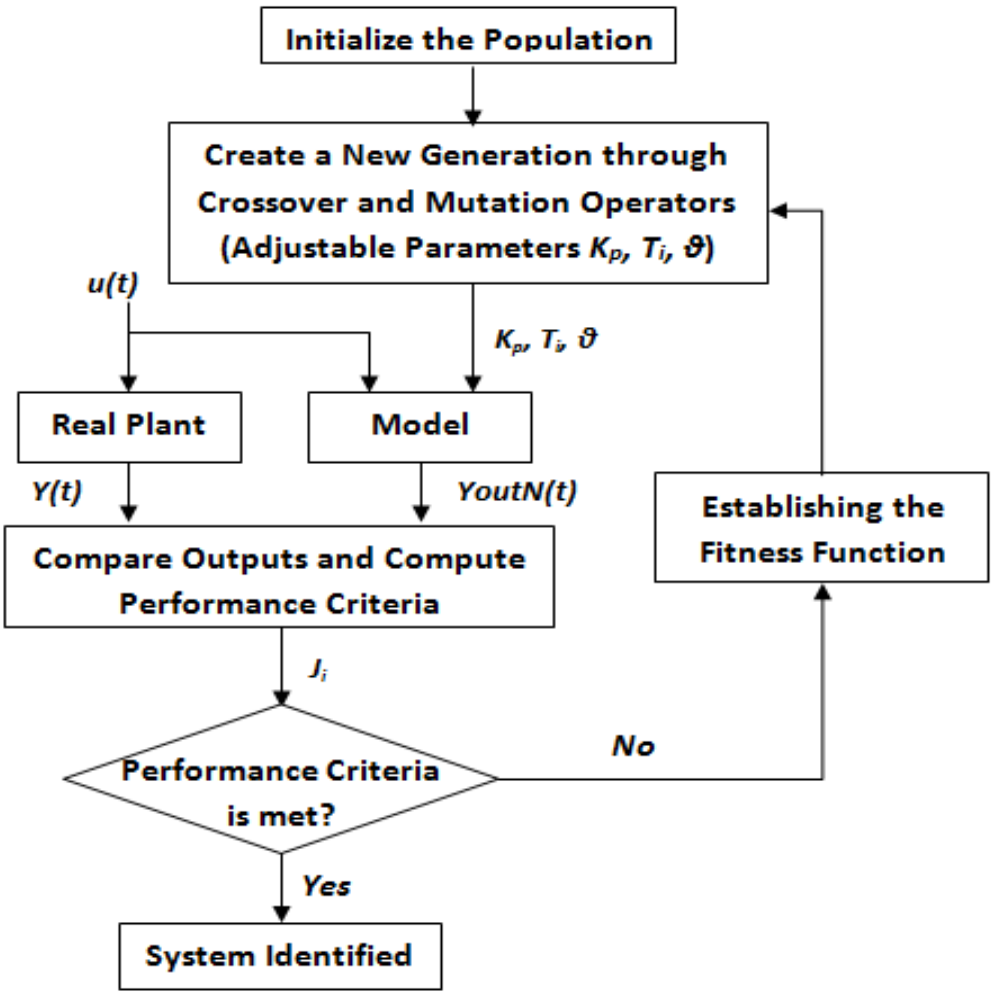

Figure 4.11: The principle scheme of SGAs for model parameters estimation (Vladu E. E., 2003)

According to the figure 4.11, the block named Real Plant has the known parameters, which are the real plant gathered data, $Y(t)$. The block Model has adjustable parameters, K_p, T_i and θ which are transmitted from SGAs in the evaluation step. By comparing the $Y(t)$ and $YoutN(t)$ outputs, a measure of the performance criterion, J_i is obtained, on the basis of which the chromosome, i has assigned the $Fitness_i$ function. If the obtained performance criterion is not met, the fitness function is established to re-estimate the model parameters until the performance criterion is met (Pereira, 2005).

4.3 Glass Temperature (T_g) Model

For glass temperature, an identification of control oriented model is necessary for control parameter optimisation which will be discussed in next chapter. Whereas, realistic model identification is not necessary as the 24 state space glass furnace model is presumed as realistic model. As described in section 3.4.1, a difficulty rose in understanding the input-output bounds to the process.

The 24 state space realistic model consists of two secondary inputs, the $\dot{m}$ and ED are correlated and driving the state-space model with different dynamic input responses over the simulation time period. Both secondary inputs are controlled by a primary input, directly and indirectly which is the T_{SET}. The T_{SET} is set by operator, manually according to the daily throughput. The total ED input is estimated by thermal parameters such as LHV, AFR, Cp and controlled directly by T_{SET}.

As illustrated in equation 4.13, the LHV, AFR, Cp and T_{amp} are constant; the T_{SET} is directly affecting the ED.

$$ED(f_2) = \left(\frac{LHV}{Cp \times AFR} + T_{amb}\right) - T_{SET} \tag{4.13}$$

$$ED(f_2) = \left(\frac{47.141MJ/kg}{1.025kJ/kgK \times 17.2} + 300K\right) - T_{SET}(K) \tag{4.14}$$

Another secondary input is the fuel control section to control the $\dot{m}$ according to the temperature feedback error (u) and controlled indirectly by T_{SET}.

$$f_1 = Cp \times \left[\left(\dot{m} \times AFR\right) + \dot{m}\right] = 1.025kJ/kgK \times \left[\left(\dot{m} \times 17.2\right) + \dot{m}\right] \tag{4.15}$$

$$*\dot{m} = u \times Maxfuel_{(constant)} = u \times 0.01kg/s \tag{4.16}$$

Figure 4.12 illustrates the control oriented model's parameters identification procedure used by SGAs, where the Plant is representing as realistic plant of 24 state-

space combustion chamber (chapter 3) and the Model is representing the parameters to be identified. According to the simulation diagram of realistic furnace model (chapter 3, figure 3.5), the $\dot{m}$ and ED should vary as per throughput energy demand necessity, when retune the T_{SET} to attain the steady-state T_g. Also, the simulation result of realistic furnace model (chapter 3, figure 3.6) illustrated that the simulation result reveals that the dynamic response of time constant (Ts) of both $\dot{m}$ and T_{SET} are similar.

Therefore, both $\dot{m}$ and T_{SET} input dynamics are considered to identify the transfer function gains (K_{p1}, K_{p2}) and 1st order Ts, individually. The parameters are experimentally tested to enhance the function of error. This is done by calibrating the genetic operator parameters, at each testing to reduce the J_i between the realistic 24 state space plant and 1st order model.

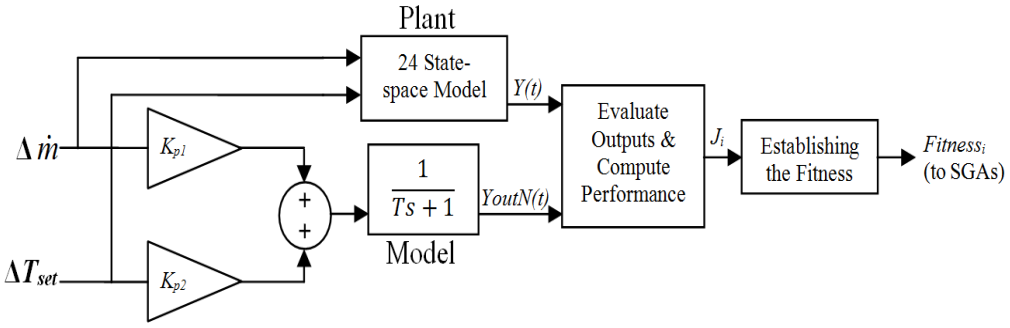

Figure 4.12: Control oriented model parameter identification by SGAs

4.3.1 Operating Point Selection of T_g

For an optimal operating point for the methane combustion, the selected $AFR_{(Mass)}$ is 17.2. According to linearised energy balance equation (section 3.3.2), the identified furnace model is accurate above $1300K$ (Holladay, 2005). While, based on the environmental agencie's (SEPA, 2005) guideline for the glass furnace industries, the formation of undesirable emissions has higher probability and severe if the T_g ascend beyond $1600K$. Thus, the selected operating point for T_g is $1500K$ to $1600K$. Table 4.1 illustrates the numerical relations of secondary inputs with combustion energy.

Another secondary input (u) is decided with closed loop system by regulating the T_g accordingly. As the Q_{Fuel} is product of both $\dot{m}$ and ED and an primary

input in form of combustion energy, both secondary inputs are has to be selected specifically.

Table 4.1: Selection of Operating Point of T_g and u with $AFR_{(Mass)}$ (17.2)

$T_{SET}(K)$	u	Q_{Fuel}	$\dot{m}(kg/s)$
1300	0.1985	56.55	0.001985
1350	0.2151	59.27	0.002151
1400	0.2329	61.99	0.002329
1450	0.2519	64.71	0.002519
1500	**0.2723**	**67.4**	**0.002723**
1550	**0.2942**	**70.09**	**0.002942**
1600	**0.3179**	**72.77**	**0.003179**
1650	0.3435	75.43	0.003435
1700	0.3713	78.06	0.003713

4.3.2 Selection of Genetic Parameters

There are many research papers have been published in deciding the genetic operators for an optimum models parameter. Related research works of first-order with and without dead time processes are reviewed as a guideline for selection of genetic parameters (Shin et. al., 2007) (Yang and Seested, 2013). But, most identified genetic operators were unique and only applicable to the related problem instead for general application. For well SGAs execution, the probabilities of crossover and mutation, an appropriate string encoding, population size are to be needed and precised.

Similarly, there are no precise strategies of determining these parameters to related problem or task. Fortunately, practice has illustrated that, in most optimisation problems, SGAs are robust adequate that the SGAs parameters do not severely affect their performance [Vlachos et. al., 2000]. Thus, the author preferred to calibrate the genetic operator parameters, at each testing to reduce the performance criterion (J_i) between the real plant and model as simplified in follows;

1. For the number of individuals, the J_i has improved when the N_{ind} from $10 \rightarrow 50$. While, the J_i has sustained and the simulation time slowed when N_{ind} from $50 \rightarrow 100$.

2. For the maximum number of generation, the J_i has sustained well within

45 $\longleftrightarrow$ 60. However, higher number of generation is selected for further evolution.

3. For the generation gap, the J_i and simulation time are improved when G_{gap} from 0.1 $\rightarrow$ 0.7. However, higher generation gap, $G_{gap} > 0.7$, has not the improved the J_i. Thus, the $G_{gap} = 0.7$ is selected.

4. For precision of binary rep., selection, crossover and mutation, the default values are selected due to the J_i has not improved as expected and also generally suggested by selected research papers for first-order without dead time process.

The calibrated genetic operator parameters and SGAs optimal model parameters identification procedure applied as illustrated in the flow chart in figure 4.6. the selected genetic operator parameters (table 4.2) are;

Table 4.2: Selected genetic operators of T_g

Genetic Operators	$T_g(K)$
Number of Individuals	50
Maximum No. of Generation	100
Generation Gap	0.7
Precision of Binary Rep.	19
Selection	SUS
Crossover	Single Point, 0.7
Mutation	Binary Rep., $0.7/L_{ind}$

4.3.3 Model Order Selection of T_g

The realistic 24 state space model exhibits first order system response without transport delay and disturbance. Thus, first order model is optimal and selected to represent system's homogeneity as control oriented model for T_g. Equation 4.15 illustrates the T_g control oriented model's transfer function with respective process gain and time constant.

$$\triangle T_g(s) = \frac{K_{p1}}{Ts+1}\triangle \dot{m}(s) + \frac{K_{p2}}{Ts+1}\triangle T_{SET}(s) \tag{4.17}$$

4.3.4 Simulation Results of T_g

As discussed in section 4.2.2, a prior knowledge of SB_O is required to assist the SGAs to locate the optimal control oriented model parameter values. To obtain SB_O, the first sub-process of an $Ts_{p(Initial)}$ identification from dynamic response is not required here as the open-loop technique is applied to approximate the initial K_{p1}, K_{p2} and Ts.

4.3.4.1 SB_O Approximation for T_g by Open-Loop Technique

The K_{p1}, K_{p2} of both inputs are determined by the change in steady-state of T_g respective to $\dot{m}$ and T_{SET}. With no transport delay, the Ts is determined as the time interval between the application of the step input and the time when the process output attains 63.2% of its final value.

The identified 1st order control oriented T_g model's parameters by open-loop technique is;

$$\triangle T_g(s) = \frac{4566.2}{1.98e5s+1}\triangle\dot{m}(s) + \frac{-0.92}{1.98e5s+1}\triangle T_{SET}(s) \tag{4.18}$$

4.3.4.2 Model Parameter Identification for T_g by SGAs

The identified T_g model's parameters (equation 4.16) by open-loop technique can be applied to approximate the K_{p1}, K_{p2} and Ts model's parameters and can be substituted with $Ts_{p(Initial)}$ to extent the SB_{Upper} (100%) and SB_{Lower} (75%); $K_{p1} \in [1141.55, 9132.4]$, $K_{p2} \in [-0.23, -1.84]$ and $Ts \in [4.95e4, 3.96e5]$ to improve the search mechanism. Two objective function, sum of square error (SSE) and sum of absolute error (SAE) are assigned and evaluated to reduce the differences between the $Y(t)$ and $YoutN(t)$.

The mathematical form of the objective function used is given by the relation,

$$J_i(SAE) = \sum_{k=0}^{k=max} \mid e(k) \mid \tag{4.19}$$

$$J_i(SSE) = \sum_{k=0}^{k=max} e^2(k) \tag{4.20}$$

where k is the simulation time and $e(k)$ is the differences between $Y(t)$ and $YoutN(t)$. To locate the X_i for control oriented model parameters, three SGAs tuning approaches are applied in open-loop step input tests.

The three tuning approaches are:

- SGAs[1]: the model parameter values of both K_{p1}, K_{p2} with Ts are identified concurrently by varying the respective step-inputs simultaneously.
- SGAs[2]: the model parameter values of both K_{p1}, K_{p2} with Ts are identified individually by varying the respective step-inputs simultaneously.
- SGAs[3]: the model parameter values of both K_{p1}, K_{p2} with Ts are identified individually by varying the respective step-inputs individually.

Each tuning approaches are tested by approximated initial Ts_p with SB_O. Table 4.3, 4.4 and 4.5 illustrates the SGAs execution of locating X_i for K_{p1}, K_{p2} with Ts by three tuning approaches. According to the tables 4.3, 4.4 and 4.5, the initially executed $X_i^{'}$ values (K_{p1}, K_{p2} and Ts) by SGAs for all three tuning approaches are illustrates the similarities with initial approximated $Ts_{p(Initial)}$ by open-loop technique is SB_O.

As discussed earlier in section 4.2.3 (state 1), all SGAs tuning approaches explored well the entire search space boundaries (SB_O) and exploited the elite group within the selected boundary region $[X_i - \triangle_{GO}, X_i + \triangle_{GO}]$ for Ts_P values of K_{p1}, K_{p2} and Ts at the initial attempt.

This can be seen by the consistency of the Ts_P values of K_{p1}, K_{p2} and Ts in further execution with readjusted boundaries at the 2$^{\text{nd}}$ attempt. Also, SB_O ensured that the solution space is well searched at early stage of locating the X_i. This has sustained the population diversity and enhanced the exploitation of an optimal X_i at each subsequent attempt by the SGAs.

Figure 4.8 illustrated that the dynamic response of T_g by open-loop technique exhibits a 8% overshoot. This variation is caused by the K_{p1} is 2.6%$_{\text{(approximately)}}$ more than the SGAs. While, the K_{p2} is 4.7%$_{\text{(approximately)}}$ less than SGAs. This is

exhibiting an ineffectiveness of open-loop technique to correlate the both dynamic inputs, $\dot{m}$ and T_{SET} to sustain the steady-state of T_g. Also, the application of open-loop technique here for an approximation of prior knowledge of model's parameters ($Ts_{p(Initial)}$), not for a performance comparison with SGAs.

Further, an open-loop model sensitivity is tested on controlled oriented models which are identified by three tuning approaches. The T_g responses by three tuning approaches are exhibiting similar sensitivities. Table 4.6 illustrates the

Table 4.3: Model Parameters Identification by SGAs[1] Execution

Exe	K_{p1}		K_{p1}		Ts	
	SB_U	SB_L	SB_U	SB_L	SB_U	SB_L
1	9132	280	-1.84	-0.06	3.96e5	1.24e4
2	8850	1100	-1.88	-0.23	3.92e5	4.90e4
3	**8850**	**1100**	**-1.88**	**-0.23**	**3.92e5**	**4.90e4**
4	8850	1100	-1.88	-0.23	3.92e5	4.90e4
5	8850	1100	-1.88	-0.23	3.92e5	4.90e4

Exe	$Ts_p(K_{p1})$	$Ts_p(K_{p2})$	$Ts_p(Ts)$	SSE	SAE
1	4429.1	-0.9391	1.973e5	3.5784e3	1.7973e3
2	4408.3	-0.9443	1.961e5	3.5731e3	1.7324e3
3	**4401.5**	**-0.9450**	**1.965e5**	**3.5612e3**	**1.7806e3**
4	4403.8	-0.9382	1.971e5	3.5811e3	1.8017e3
5	4402.4	-0.9430	1.964e5	3.5615e3	1.7811e3

Table 4.4: Model Parameters Identification by SGAs[2] Execution

Exe	K_{p1}		K_{p1}		Ts	
	SB_U	SB_L	SB_U	SB_L	SB_U	SB_L
1	9132	280	-1.84	-0.06	3.96e5	1.24e4
2	8870	1100	-1.97	-0.25	3.90e5	4.90e4
3	8870	1100	-1.97	-0.25	3.90e5	4.90e4
4	**8870**	**1100**	**-1.97**	**-0.25**	**3.90e5**	**4.90e4**
5	8870	1100	-1.97	-0.25	3.90e5	4.90e4

Exe	$Ts_p(K_{p1})$	$Ts_p(K_{p2})$	$Ts_p(Ts)$	SSE	SAE
1	4434.8	-0.9833	1.9521e5	3.5681e3	1.7883e3
2	4450.3	-0.9594	1.9663e5	3.5617e3	1.7822e3
3	4453.9	-0.9715	1.9655e5	3.5636e3	1.7846e3
4	**4451.5**	**-0.9672**	**1.9652e5**	**3.5586e3**	**1.7796e3**
5	4459.1	-0.9681	1.9661e5	3.5657e3	1.7871e3

Table 4.5: Model Parameters Identification by SGAs^3 Execution

Exe	K_{p1}		K_{p1}		Ts	
	SB_U	SB_L	SB_U	SB_L	SB_U	SB_L
1	9132	280	-1.84	-0.06	3.96e5	1.24e4
2	**8960**	**1120**	**-1.97**	**-0.25**	**3.97e5**	**4.96e4**
3	8960	1120	-1.97	-0.25	3.97e5	4.96e4
4	8960	1120	-1.97	-0.25	3.97e5	4.96e4
5	8960	1120	-1.97	-0.25	3.97e5	4.96e4

Exe	$Ts_p(K_{p1})$	$Ts_p(K_{p2})$	$Ts_p(Ts)$	SSE	SAE
1	4483.8	-0.9841	1.9852e5	3.6518e3	1.8811e3
2	**4488.4**	**-0.9834**	**1.9920e5**	**3.4722e3**	**1.7735e3**
3	4479.4	-0.9782	1.9871e5	3.5377e3	1.8487e3
4	4485.3	-0.9841	1.9914e5	3.4871e3	1.7858e3
5	4486.7	-0.9837	1.9918e5	3.4733e3	1.7741e3

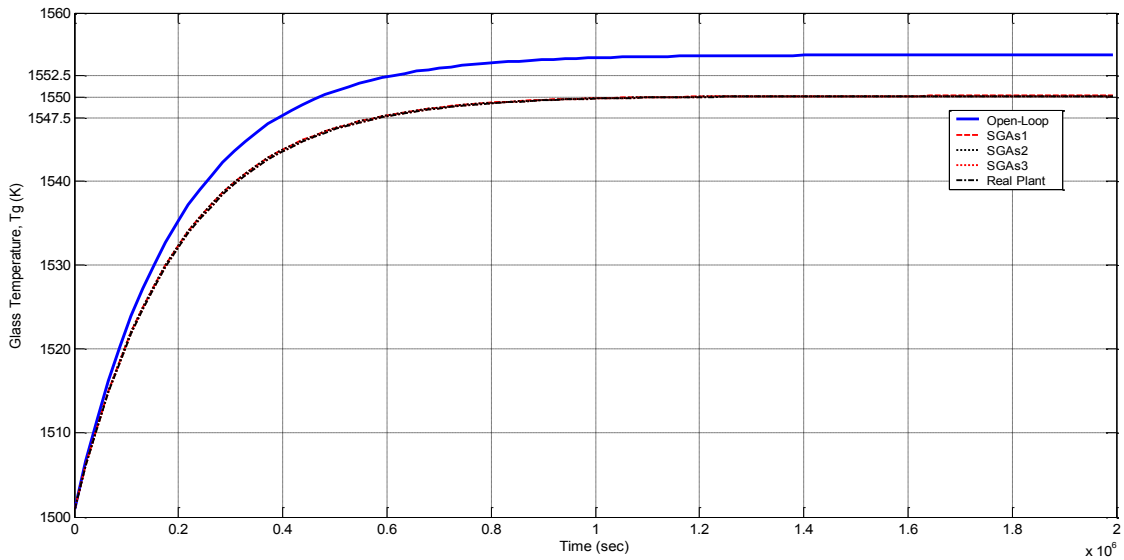

Figure 4.13: Transient responses of T_g real plant with open-loop technique and three tuning of SGAs

In general, the transient responses of three SGAs tuning approaches are completely overlapped and well fitted with realistic plant response. The best model parameter values of K_{p1}, K_{p2} and Ts by three SGAs tuning approaches are bold with respective tables. However, the identified K_{p1}, K_{p2} and Ts by SGAs^3 is well consolidated and minimise the SSE and SAE. As a result, it is selected as T_g optimal model parameter values for control oriented model.

4.4 Excess Oxygen (EO_2) Model

As illustrates in chapter 3, section 3.4.1, the EO_2 is part of product element of methane combustion. The input vector of EO_2 model is based on the air and fuel ratio. Literature survey reveals that there is no EO_2 realistic model of glass furnace is available for research. It is due to most glass industries are not emphasising on continuous monitoring as there are operating within the operating guideline limits (SEPA, 2005). Therefore, an identification of model parameters for higher order as a realistic model and low order as a control oriented model is required and concerned here.

The realistic and control oriented model of excess oxygen are developed based on the real data collected from the Quinn Glass Limited, Chester by empirical technique for $1000sec$ with $5sec$ sampling interval. As illustrated in figure 4.9, the process response of EO_2 is the first-order plus dead-time (FOPDT) system. The dead time (θ) can be approximated as $160sec$. The data was gathered by the step input of increasing air ratio from 9.5 to 10.5 in volumetric (ft^3).

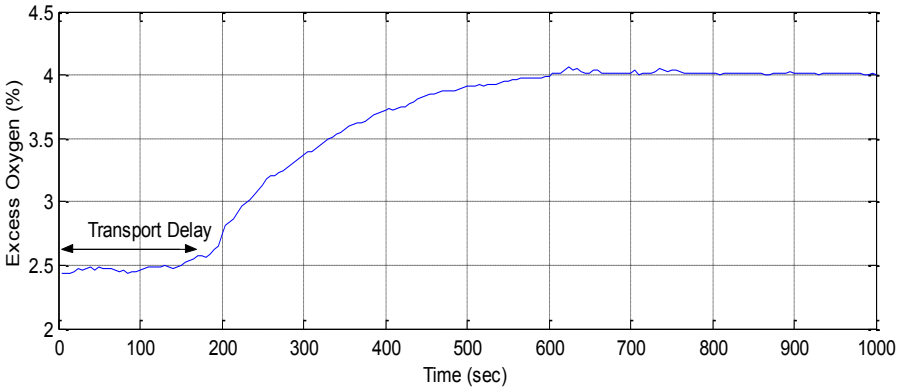

Figure 4.14: Step response of real industry response of EO_2

4.4.1 Methane Combustion Process

Combustion is the conversion of a substance called a fuel (methane) into chemical compounds known as products of combustion by combination with an oxidizer (air). The stoichiometric combustion is the ideal combustion mixture where fuel is combusted completely. This ideal mixture approximately yields the maximum flame temperature, as all the energy released from combustion is applied to melt the glass.

By balancing the atomic abundance on both the reactant and product sides, one can find the coefficient for each species. Complete combustion is a process of burning all the carbon (C) to carbon dioxide (CO_2), all the hydrogen (H) to hydrogen dioxide (H_2O) and all the sulphur (S) to sulphur dioxide (SO_2). The chemical equation for combustion of methane (CH_4) with air can be expressed as

$$CH_4 + 2(O_2 + 3.76N_2) \rightarrow CO_2 + 2H_2O + 7.52N_2 \tag{4.21}$$

According to the atomic weights of methane and oxygen, the carbon (C) has $12.01g/mol$, the oxygen (O) has $16g/mol$ and hydrogen (H) has $1.008g/mol$. Thus, one molecular weight of methane and oxygen are $16.042g/mol$ and $32g/mol$, respectively. Based on the oxygen-methane mass ratio, $1kg$ of methane requires $3.99kg$ of oxygen. Since 23.2 mass-percentage of air is oxygen, the stoichiometric air-fuel ratio ($AFR_{(stoichiometric)}$) $1kg$ of methane requires $17.2kg$ ($9.52ft^3$) of air. This is an ideal AFR if natural gas were 100% methane.

However, in reality it is difficult to obtain pure methane as it contains heavier hydrocarbons and are often combusted with an amount of air different from the stoichiometric ratio. As illustrated in figure 4.15, if less air than the stoichiometric amount is used, the mixture is described as fuel rich. If excess air (EA) is used, the mixture is described as fuel lean. For this reason, lambda (λ) is frequently used to quantify the combustible mixture based on the AFR. The λ is the ratio of the actual AFR to the $AFR_{(stoichiometric)}$ defined as

$$\lambda = \frac{AFR}{AFR_s} = \frac{1/f}{1/f_s} = \frac{1}{f/f_s} = \frac{1}{\phi} \tag{4.22}$$

The subscript s indicates a value at the stoichiometric condition, f is fuel-air ratio (FAR) and ϕ is equivalence ratio. $\lambda < 1$ is a rich mixture, $\lambda = 1$ is a stoichiometric mixture, and $\lambda > 1$ is a lean mixture. Similar to f, the range of ϕ is bounded by zero and ∞ corresponding to the limits of pure air and fuel respectively.

Theoretically, oxygen should not be traced in EA if the combustion is complete. But, factually the oxygen does traced in EA even though $AFR_{(stoichiometric)}$ is ap-

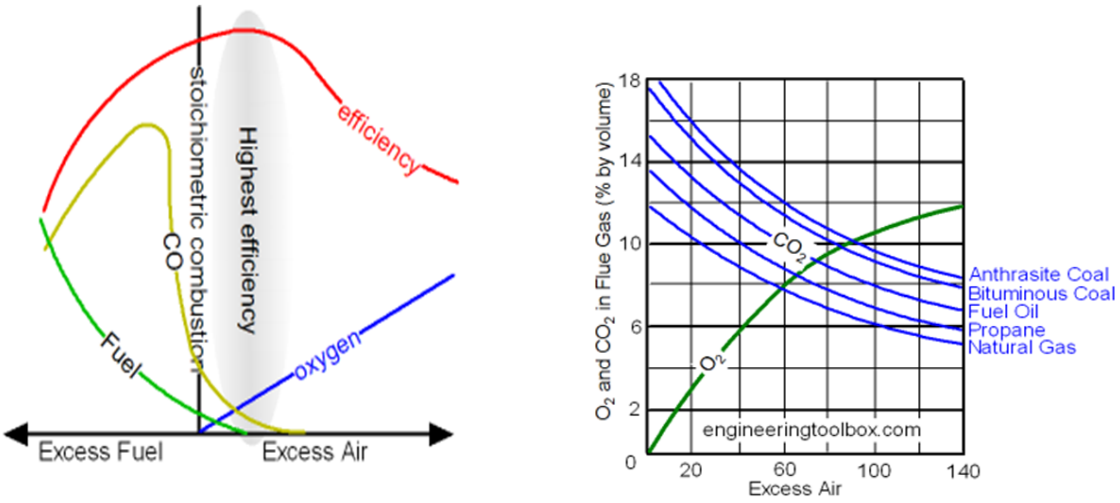

Figure 4.15: Stoichiometric combustion processes (Engneeringtoolbox)

plied for combustion EO_2. For example, by increasing 20% of EA for combustion, the related AFR is increases $11.4ft^3$. According to the combustion chemistry of methane, the volumetric of carbon (C) and water vapour (H_2O) are unchanged. Thus, the combustion products are $9.003ft^3$ of nitrogen (N_2) and $0.3971ft^3$ of EO_2 according to the element composition of air. That is equivalent to the 3.2% of EO_2. The stoichiometric methane combustion equation,

$$CH_4 + 2(O_2 + 3.76N_2) \rightarrow CO_2 + 2H_2O + 7.52N_2$$

The analysis of $EO_{2(\%)}$ can be simplified and generalised;

$$EO_{2(\%)} = \frac{EO_2(ft^3)}{EO_2(ft^3) + [[EA(ft^3) - EO_2(ft^3)] + 7.52] + CO_2 + 2H_2O} \tag{4.23}$$

The methane combustion equation with 20% EA;

$a = EA\,(ft^3) = \left(EA_{(\%)}\right)\left(AFR_{(stoichiometric)}\right) = \left(20_{(\%)}\right)\left(9.5_{(ft^3)}\right) = 1.9ft^3$

$b = O_{2(\%)(Air\ Composition)} = 20.9\%$

$EO_2(ft^3) = a \times b = (1.9ft^3)\,(20.9\%) = 0.3971ft^3$

$Excess\ Nitrogen = EA\,(ft^3) - EO_2(ft^3) = 1.503ft^3$

$AFR_{\left(20\%_{(EA)}\right)(Volumetric)} = AFR_{(stoichiometric)} + EA(ft^3) = 11.4$

*Total methane combustion product with $EA_{(20\%)}$;

$$CO_{2(unchanged)} + 2H_2O_{(unchanged)} + 9.023N_2 + 0.3971O_2$$

$$EO_{2(\%)} = \frac{0.3971ft^3}{0.3971ft^3 + [[1.9ft^3 - 0.3971ft^3] + 7.52] + 1 + 2} = 3.197\%$$

With $EO_2(\%) \approx 3.2\%$, gives $AFR_{(Volumetric)} = 11.4$ and $AFR_{(Mass)} = 20.58$.

According to the chemical properties of methane, the sulphur is not present in atomic structure (EHS Guidelines, 2007). Thus, the formation of sulphur dioxide is not concerned and completely can be ignored. For research, the EO_2 due to lean-rich mixture by combustion is taken into further consideration. As discussed earlier, the EO_2 does traceable in $AFR_{(stoichiometric)}$ methane combustion. Therefore, AFR increment and reduction must be carefully controlled to prevent formation of nitrous dioxide (NO_2) and incomplete combustion, respectively.

The AFR is theoretically known in mass ratio of air and fuel. But, most of industries are evaluating the AFR in volumetric. To identify a model and optimize the EO_2 emission and AFR, the complete numerical identification for the EA and EO_2 with related AFR conversion between mass to volumetric is essential. The ideal gas law for methane in mass can be expressed (Engneeringtoolbox),

$$\dot{m} = \frac{\dot{V}P_f}{\underline{R}\overline{T}} \tag{4.24}$$

where $\underline{R}$ is the gas constant of methane ($96.32ft \cdot Ibf/Ibm \cdot R$), P_f is the internal pressure of the furnace ($14.2psi$), $\dot{V}$ is the volumetric flow rate of methane (ft^3/hr) and $\overline{T}$ is the mean methane temperature (540^oR5) ($*1^oR = 5/9K$). The Fenton Art Glass furnace was recorded at steady flow rate of $1.98 \times 10^{-3}kg/sec$. That is equivalent to $15.73Ibm/hr$. By applying equation 4.24, the steady flow rate of methane in volumetric is $400ft^3/hr$.

Therefore, the AFR of methane in volumetric and mass can be evaluated as,

$$\dot{V} = \frac{1.056ft^3/sec}{0.1111ft^3/sec} = 9.5 \quad ; \quad \dot{m} = \frac{34.06 \times 10^{-3}kg/sec}{1.98 \times 10^{-3}kg/sec} = 17.2 \tag{4.25}$$

According to the ideal gas law for methane the P (pressure), $\underline{R}$ (gas constant) and $\overline{T}$ (temperature) are constant. By simplifying the equation 4.25, the mass $\leftrightarrow$ volumetric conversion AFR model in this research has been designed as an input to the EO_2 transfer function.

Table 4.6: $AFR_{(stoichiometric)}$with relative EA and EO_2

$AFR_{(Volumetric)}(ft^3)$	$AFR_{(Mass)}(kg)$	$EA(\%)$	$EO_2(\%)$
9.5	17.2	0	0
10	18.06	5	0.905
10.45	18.86	10	1.734
10.93	19.76	15	2.504
11.4	20.58	20	3.2
11.87	21.43	25	3.865
12.35	22.3	30	4.462
12.83	23.16	35	5.04

Table 4.6 illustrates the complete methane stoichiometric combustion interaction mass and volumetric of AFR with $EA_{(\%)}$ and $EO_{2(\%)}$ by applying equation 4.23 and 4.25. Figure 4.16 illustrates the insignificant nonlinear response of stoichiometric $EO_{2(\%)}$ with respective $AFR_{(Volumetric)}$.

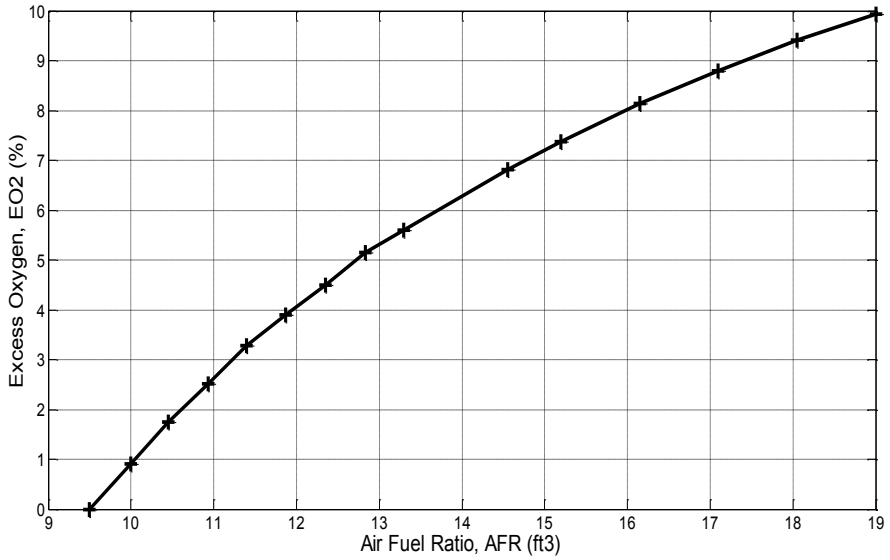

Figure 4.16: Insignificant nonlinear effect of $AFR_{(stoichiometric)}(ft^3)$ Vs $EO_{2(\%)}$

4.4.2 Complete EO_2 Model Development

A major concern of this section is about three specific issues. First issue is related

to the non-zero initial steady state condition. In general, model's parameter is developed derived from the deviation of zero initial condition. However, the real industry responses are not available in zero initial condition. According to the Quinn Glass EO_2 data response, the output response initialised at non-zero initial condition (2.45%) as shown in figure 4.9. Second issue is related to the input and output synchronisation. Along with the Quinn Glass, the prime input of AFR is in kg/sec at the controller board. While, at firing port the AFR is decided by actuator in ft^3/sec and fused for the complete combustion.

The combustion process is represented by transfer function which is decided by the step-input deviation of $AFR_{(Volumetric)}$. After combustion the absolute output is EO_2 in percentage. Third, the relation of $AFR_{(Volumetric)}$ and $EO_{2(\%)}$ which are exhibits an insignificant nonlinear effect with EO_2 as illustrated in figure 4.14. Thus, a complete realisation of EO_2 model is necessary for non-zero initial steady state condition, input-output synchronisation and nonlinear effect.

The complete realistic EO_2 model consists of three sub-model; AFR conversion model, transfer function and EO_2 look-up table as shown figure 4.17. The AFR conversion model particularly designed to convert the real value of $AFR_{(Mass)}$ to respective $AFR_{(Volumetric)}$ derived from the methane gas law equation 4.25. The transfer function is modified as illustrated in equation 4.26 to avoid zero initialisation as real EO_2 dynamic response initialised at 2.45% for stoichiometric $AFR_{(Volumetric)}$. The EO_2 look-up table is designed based on methane chemical relationship of stoichiometric $AFR_{(Volumetric)}$ as an input and $EO_{2(\%)}$ as an output by using linear interpolation block from simulink.

$$\begin{aligned} \frac{Y(s)}{U(s)} &= \frac{K_p e^{-\theta}}{a_n s^n + a_{n-1} s^{n-1} + \cdots + a_1 s + 1} \\ \frac{dy}{dt} &= \frac{1}{a_n}\left[K_p u\left(t-\theta\right) - a_{n-1}\frac{d^{n-1}y}{dt^{n-1}} - \cdots - a_n \frac{dy}{dt} - y\right] \end{aligned} \tag{4.26}$$

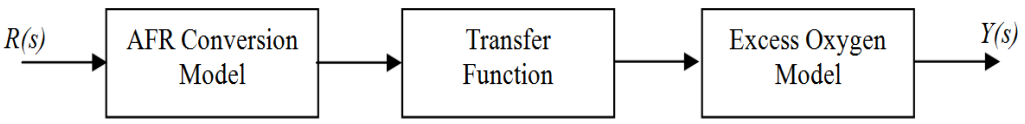

Figure 4.17: Block Diagram of Complete Realised EO_2 Model

4.4.3 Operating Point Selection of EO_2

As illustrated in figure 4.14, the real EO_2 response is initialised at 2.45% and attain steady-state at 4% with respective step-input of stoichiometric $AFR_{(Volumetric)}$ $9.5ft^3$ to $10.5ft^3$. Therefore, the step-input $9.5ft^3$ to $10.5ft^3$ is selected as operating point to characterise the dynamic and homogeneous of real EO_2 response with modified transfer function (equation 4.26).

4.4.4 Selection of Genetic Parameters

As discussed in 4.3.2, similar related research works of first-order with and without dead time processes are reviewed as a guideline for selection of genetic parameters (Shin et. al., 2007) (Yang and Seested, 2013) (Seested, 2013). For well SGAs execution, the genetic operator parameters are calibrated accordingly to reduce the performance criterion (J_i) between the real plant and model. The selected genetic operators for EO_2 are identical as discussed in the section 4.3.2 (for T_g) as the are exhibiting a similarities in reducing the J_i when calibrated.

The calibrated and selected genetic operator parameters (table 4.7) are,

Table 4.7: Selected genetic operators of EO_2

Genetic Operators	$EO_2(\%)$
Number of Individuals	50
Maximum No. of Generation	50
Generation Gap	0.7
Precision of Binary Rep.	17
Selection	SUS
Crossover	Single Point, 0.7
Mutation	Binary Rep., $0.7/L_{ind}$

4.4.5 Simulation Results of EO_2

Although the real EO_2 response exhibits FOPDT process, the open-loop method may not well applicable for $Ts_{p(Initial)}$ approximation for realistic higher order model's parameter. Especially, the curvature dynamic of the initial rising of the output response after the transport delay, around the point of inflexion. Thus, both sub-processes of $PTcA$ are required and applied for an initial value approximation and search space boundary optimisation for EO_2.

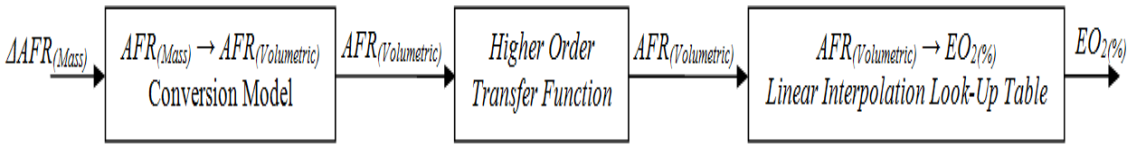

Figure 4.18: Realistic EO_2 model set-up for parameter identification

Figure 4.19: Control oriented EO2 model set-up for parameter identification

The parameters identification process of both realistic and control oriented models are implemented in two different approach as illustrated in figure 4.18 and 4.19. For realistic model, the linear interpolation look-up table is used to incorporated with the nonlinear effect by methane chemical relationship of stoichiometric $AFR_{(Volumetric)}$ and $EO_{2(\%)}$. Also, the higher order transfer function is required for characterising the homogeneous of EO_2 real plant response.

Whereas, for the control oriented model, the nonlinear effect is not included and low order transfer function is selected. Further, the parameters identification process of both realistic and control oriented models by SGAs are similar as discussed for T_g. However, the output of control oriented model is in $AFR_{(Volumetric)}$. Therefore, a constant is added at output to synchronise the control oriented model output according to the realistic plant.

4.4.5.1 SB_O Approximation for EO_2 by $PTcA$ Method

The process gain (K_p) and transport delay (θ) can be approximated by close observation of the EO_2 real plant transient response. As illustrated on the transient response of EO_2, $K_p \approx 1.54$ and $\theta \approx 160sec$. As a result, an extension on the search space boundaries are approximated for $K_p \in [1:2]$ and $\theta \in [50:200]$. If a process has transport delay, then the DR_P need to be calculated from $t = \theta$ to $t = t1$.

For better approximation, the θ is selected $100sec$. Thus, the EO_2 dynamic response, the $DR_{P(t1-\theta)} = 700sec - 100sec = 600sec$. Selecting $ts_{(\delta\%)} = 1\%$, as the

desired α is 5, gives the $Ts_{p(Initial)} = 120s$. In favour of both optimal EO_2's realistic and control oriented model's parameters selection, the $Ts_{p(Initial)}$ approximation method is tested on 1st, 2nd, 3rd, 4thand 5thorder transfer function models.

For instance, the 3rd order $Ts_{p(Initial)}$ polynomial coefficients model can be approximated as;

$\therefore Ts_{p(Initial)} = 120s;$

$$\begin{gathered}\left(Ts_{p(Initial)}s+1\right)^3 = (Ts_{p(Initial)}s)^3 + 3(Ts_{p(Initial)}s)^2 + 3Ts_{p(Initail)}s + 1 \\ Ts_{p(Initial)} = 1.728e6s^3 + 4.32e4s^2 + 3.6e2s + 1\end{gathered} \tag{4.27}$$

Based on 2nd sub process of $PTcA$ method, initially approximated as S^3, S^2 and S^1 polynomial coefficients by $Ts_{p(Initial)}$, respectively are applied to extent the SB_{Upper} (100%) and SB_{Lower} (75%), $S^3 \in [4.32e5 : 3.456e6]$, $S^2 \in [1.1e4 : 8.6e4]$ and $S^1 \in [90 : 720]$ to improve the search mechanism to locate the optimal X_i.

According to the $PTcA$ technique, genetically identified $X_i^{'}$ by 2nd execution for the respective polynomial coefficients illustrates that the resized search boundary by initially identified $X_i^{'}$ at 1st execution is SB_O. Therefore, further resizing of search boundary is not required as the $X_i^{'}$ will evolve well within SB_O to attain the X_i.

As illustrated in table 4.8, the distribution of elite groups within boundary region $[X_i - \triangle_{GO}, X_i + \triangle_{GO}]$, the exploitation of optimal X_i and the consistency of the $X_i^{'}$ values of S^2 and S^1 in further execution by SGAs are exhibiting similar process characteristics as 3rdtransfer function model.

Based on the initial attempt, the elite groups of $X_i^{'}$ values of S^3 are uniformly distributed around $X_i - \triangle_{GO}$ region. The simulation results shows that the $X_i^{'}$ values of S^3 is still continuously evolving within the boundary SB_O region at each execution.

Therefore, further readjustment of SB_O boundaries is not required as the elite groups are still within the boundary range (state 1) as discussed in section 4.2.3. So, the 3rd order model of EO_2, the $X_i^{'}$ values by the 5th execution are selected as the SSE and Gen (generation) is minimum and optimal (X_i).

Table 4.8: 3rd Order Model Polynomial Coefficient Approximation by SGAs Execution

Exe	$Ts_p(S^3)$		$Ts_p(S^2)$		$Ts_p(S^1)$	
	SB_U	SB_L	SB_U	SB_L	SB_U	SB_L
1	3.5e6	10	8.6e4	10	7.2e2	10
2	1.6e4	2e3	2e4	2e3	3.5e2	40
3	1.6e4	2e3	2e4	2e3	3.5e2	40
4	1.6e4	2e3	2e4	2e3	3.5e2	40
5	1.6e4	2e3	2e4	2e3	3.5e2	40
6	1.6e4	2e3	2e4	2e3	3.5e2	40
7	1.6e4	2e3	2e4	2e3	3.5e2	40
8	1.6e4	2e3	2e4	2e3	3.5e2	40
9	1.6e4	2e3	2e4	2e3	3.5e2	40

Exe	$X_i'(S^3)$	$X_i'(S^2)$	$X_i'(S^1)$	SSE	Gen
1	8088.2	10085	178.73	0.86796	70
2	4039.7	14074	180.02	0.49128	20
3	2699.7	13304	180.38	051873	40
4	4875.7	14995	183.64	0.49413	40
5	8187.7	14524	181.41	0.48654	20
6	8079.1	16513	184.16	0.53421	35
7	4330.5	14555	177.2	0.5109	90
8	4137.2	15028	181.88	0.48758	22
9	9903.9	16043	182.3	0.51771	80

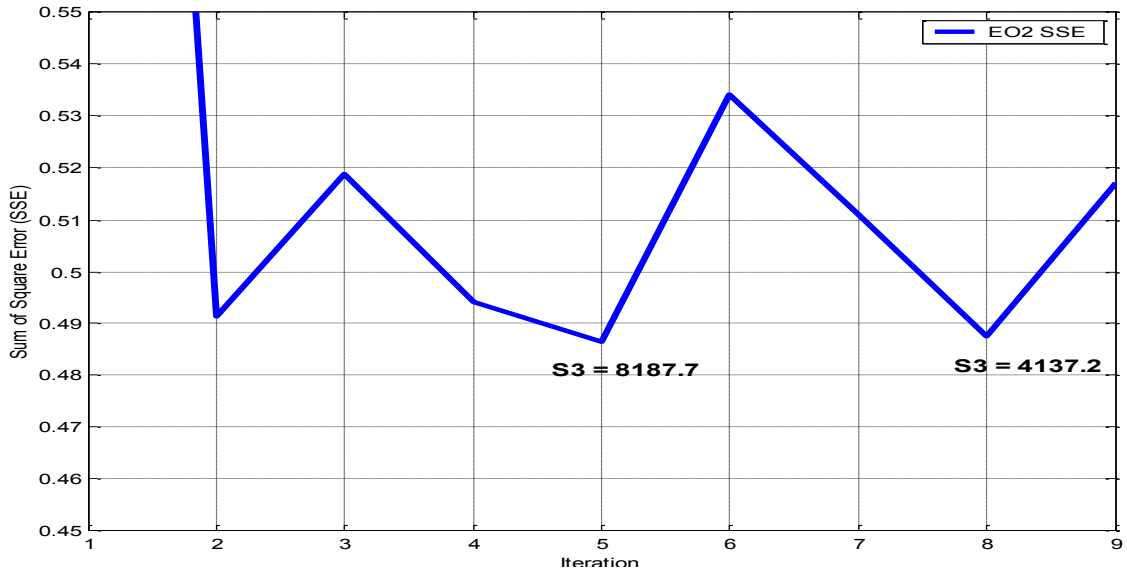

Figure 4.20: Two global optima of X_i values of S^3 for EO_2

However, the inconsistency of S^3 shows that there are two optimal values of X_i' ($X_i' = 8187.7; 4137.2$), which frequently appear within the SB_O region at 1st, 2nd,

4^{th}, 5^{th}, 6^{th}, 7^{th} and 8^{th} execution.

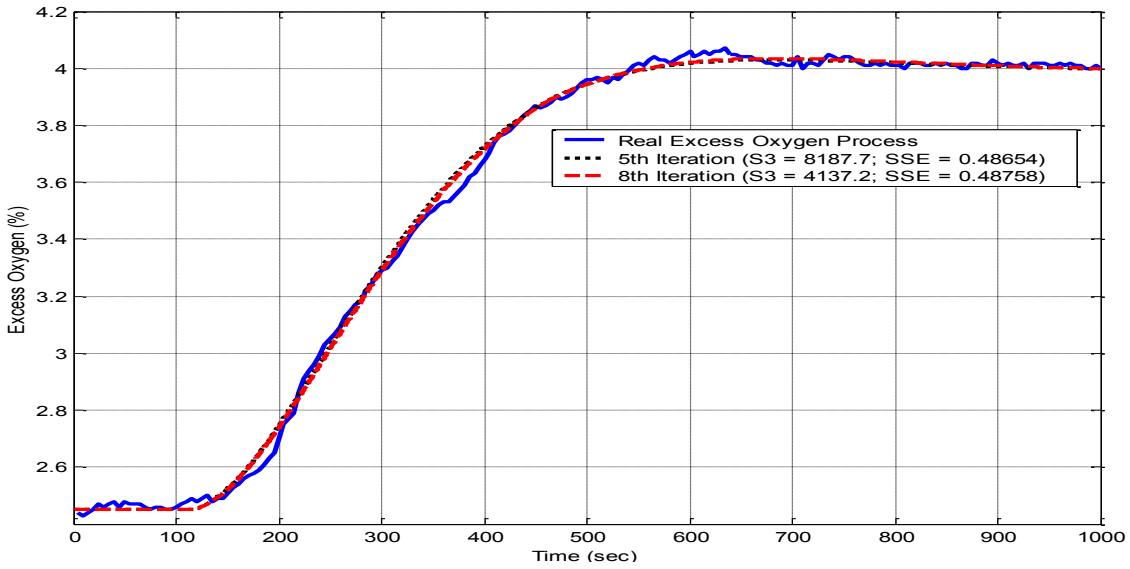

Figure 4.21: Transient responses of 2 global optimal X_i with real process of EO_2

This has been verified by simulation results in figure 4.15 and 4.16 of both optimal X_i' values of S^3 are minimum SSE. Furthermore, the inconsistency of S^3 demonstrated that the SGAs with improved boundaries well sustaining the population diversity by exploring the feasible search region and exploiting to optimal X_i.

Table 4.9: EO_2 Control Oriented Model's Parameters (Linear)

Model Order	K_p	S^5	S^4	S^3	S^2	S^1	θ	SSE
1	1.6299	-	-	-	-	152.35	173.35	2.3827
2	1.5544	-	-	-	14460	181	109.73	0.48646
3	1.5547	-	-	8187.7	14524	181.41	109.36	0.48654
4	1.56	-	8.418e6	2.453e5	17203	198.32	96.391	0.45175
5	1.682	1.7593e8	2.9028e6	7.1561e5	11997	251.42	97.01	4.6942

Table 4.10: EO_2 Realistic Model's Parameters (Nonlinear)

Model Order	K_p	S^5	S^4	S^3	S^2	S^1	θ	SSE
1	1.1438	-	-	-	-	153.5	175.11	2.1501
2	1.392	-	-	-	15057	185.46	108.13	0.50095
3	1.1388	-	-	3.7525e5	19632	206.49	84.32	0.50345
4	1.1374	-	2.7321e7	8.2689e5	26895	224.99	55.75	0.48284
5	1.324	6.4098e4	6.8715e2	2.0629e7	20.013	1586.8	0	8.3027

Similar process of optimal model parameter identification by $PTcA$ method is applied for 1st, 2nd, 4th and 5th orders control oriented model and for 1st, 2nd, 3rd, 4th and 5th orders realistic model. The table 4.9 and 4.10 illustrates, the optimally identified model parameters for each control oriented and realistic model orders by SGAs with 10 executions.

4.4.5.2 Model Order Selection of EO_2

As discussed earlier, two parametric models are to be selected; a control oriented model for control optimisation without nonlinear effect and a realistic model for final application with nonlinear effect. The selection of realistic model order is primarily concern here. However, the selection of model order has always been a difficult matter. Particularly, models complexity. A non-complex model is easier for approximation, but it may not able to entirely extrapolate the characteristics of the real data.

Alternatively, a complex model requires a great computational endeavour due to model dimensionality, but it may able to explicate the characteristics of real data significantly. The common methodology for model order selection involves selecting a model order that minimizes one or more information criteria estimated over a range of model orders.

The information criteria's are applied;

- Akaike Information Criterion with correction (AIC_C): $AIC + \frac{2K(K+1)}{n-K-1}$,
- Akaike's Final Prediction Error Criterion (FPE): $SSE \times \frac{1+K/n}{1-K/n}$,
- Bayesian Information Criterion (BIC): $K\ell n(n) - 2\ell n(SSE)$

where K is number of parameters, n is sample size (200), ℓn is natural logarithm and SSE is sum of square error.

Table 4.11 illustrates the three information criterions and SSE with respective model orders. For control oriented model, the selection assessment is not essential as the 1st order model is generally applied for control optimisation. However, the 1st order model has a significant error value. While, the 2nd order model has 79.5%

better SSE criterion than 1st order model. Also, the 2nd order model is well characterising the curvature dynamic of the initial rising of the output response after the θ, around the point of inflexion of EO_2 real plant.

Therefore, the 2nd order model is selected alongside with 1st order model for optimal control parameters consideration. Based on the figure 4.22 and table 4.11, the 1st and 5th orders of realistic model (nonlinear) are completely discarded for selection assessment as the model orders has a significant error value. Also, the realistic model is generally higher than 1st order model to characterise the real data. Thus, 2nd, 3rd and 4th orders are considered for optimal model selection assessment. Based on the table 4.11, the SSE and FPE are exhibiting the information criterions of 4th order model has better model characteristics with real data.

Table 4.11: Information Criterion of Model Orders

Model Order	SSE		AIC_C	
	Realistic	Control Oriented	Realistic	Control Oriented
1	2.1501	2.3827	0.4892	0.2837
2	0.50035	0.48646	5.443	5.503
3	0.50945	0.48654	7.471	7.563
4	0.48284	0.45175	9.661	9.794
5	8.3027	4.6942	6.076	7.215

Model Order	FPE		BIC	
	Realistic	Control Oriented	Realistic	Control Oriented
1	2.194	2.431	3.767	3.562
2	0.5162	0.5013	11.98	12.04
3	0.5302	0.5064	17.24	17.34
4	0.5076	0.4749	22.65	22.78
5	8.816	4.988	22.26	23.40

But, the AIC_C and BIC are futile due to the penalty term increases the information criterion as the number of model parameters increases. Based on the SSE, the 4th order model has 3.6% and 5.2% better extrapolation the real data than 2nd and 3rd order, respectively. Also, the 3rd order model is not improving the accuracy by increasing the model parameters. Concurrently, the 4th order model has better accuracy by FPE about 1.7% and 4.3% than 2nd and 3rd order, respectively. Even though, the 4th order model is generally finalised for realistic model selection, the information criteria of FPE and SSE is not sufficient for realistic model assessment.

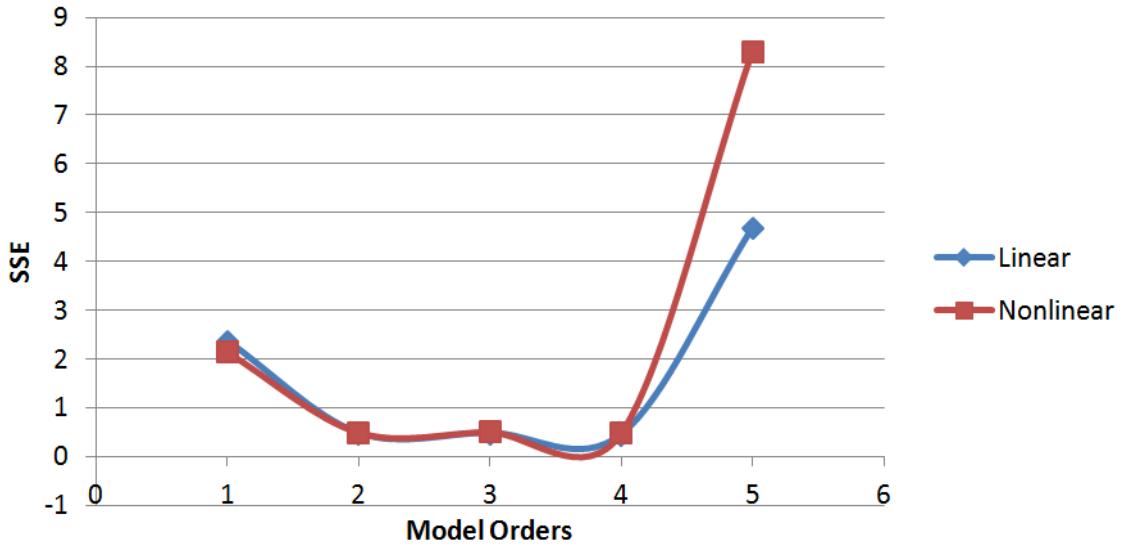

Figure 4.22: Control oriented (Linear) and realistic (Nonlinear) model orders with respective SSE

Therefore, the roots of denominator of model orders are assessed for model selection. In particular, the system poles are directly exhibiting the homogeneous response of transfer function. The homogeneous response of transfer function can be written as,

$$y(t) = \sum_{i=1}^{n} C_i e^{p_i t} \tag{4.28}$$

where C_i is constant by set of initial conditions, p_i is root of denominator. The location of the poles in the s-plane therefore describes the n components in the homogeneous response of transfer function.

As illustrated in table 4.12, the choice made to discard the 1^{st} and 5^{th} order for model selection was well verse. Especially, the 5^{th} order model is exhibiting instabilities of system as a pair of complex pole located on right-side of s-plane. On other hand, the 2^{nd}, 3^{rd} and 4^{th} order models are having an indistinguishable a pair of complex pole on left-side of s-plane which exhibiting dominant characteristics of real data. Thus, the 2^{nd}, 3^{rd} and 4^{th} order models are possibly will suitable for model selection.

However, the 2^{nd} order model is not extrapolating entirely the homogeneous response of real data. While, the 3^{rd} order model's real pole (-0.0403) is exhibiting

Table 4.12: Roots of Denominator of Model Orders

Model Order	Roots of Denominator [Realistic(Nonlinear)]
1	-0.0065
2	-0.0062±0.0053i
3	-0.0403; -0.0060±0.0055i
4	-0.00102±0.0251i; -0.0049±0.0051i
5	-0.0054±17.94i; 0.0003±0.0088i; -0.0006

Model Order	Roots of Denominator [Control Oriented (Linear)]
1	-0.0066
2	-0.0063±0.0055i
3	-1.761; -0.00627±0.00548i
4	-0.0082±0.0412i; -0.0064±0.0052i
5	-0.0214±0.0141i; 0.0018±0.0048i; -0.0023

inconsequential domination in homogeneous response, which causes an insignificant rise in SSE. Whereas, the 4$^{\text{th}}$ order model's another pair of complex pole is enhancing the extrapolation on the real data characteristic. The identified models parameters of EO_2 by SGAs are,

1$^{\text{st}}$ order control oriented model;

$$G(s) = \frac{\triangle EO_2}{\triangle AFR} = \frac{1.6299}{152.4s + 1} e^{-174s}$$

2$^{\text{nd}}$ order control oriented model;

$$G(s) = \frac{\triangle EO_2}{\triangle AFR} = \frac{1.5544}{1.446e4s^2 + 181s + 1} e^{-110s}$$

4$^{\text{th}}$ order realistic model;

$$G(s) = \frac{\triangle EO_2}{\triangle AFR} = \frac{1.1374}{2.7321e7s^4 + 8.2689e5s^3 + 2.6895e4s^2 + 224.99s + 1} e^{-55.75s}$$

The selected model order for realistic and control oriented models are optimal and has better performance criterion and well fitted the real plant response while reducing the J_i by adapting $fitness_i$ to the respective step input. Despite the

4^{th} order realistic model has higher response accuracy than the 2^{nd} order control oriented model, both models of EO_2 are relatively insensitive to model parameter orders variation by exhibiting similarities in their transient responses and performance criterion ($J_{i(SSE)} = 0.48284_{(Realistic)}; 0.48646_{(Control)}$).

Further, the EO_2 models parameter insensitivities are well exhibited in the 3^{rd} order model parameter identification by SGAs. Inconsistency of the 3^{rd} polynomial coefficient (S^3) shows that there are two optimal values of X_i' ($X_i' = 8187.7; 4137.2$) for EO_2 with minimum J_i. However both of these 3^{rd} order models have very similar transient responses. Figure 4.23 illustrates the selected model's homogeneous response with real numerical data response.

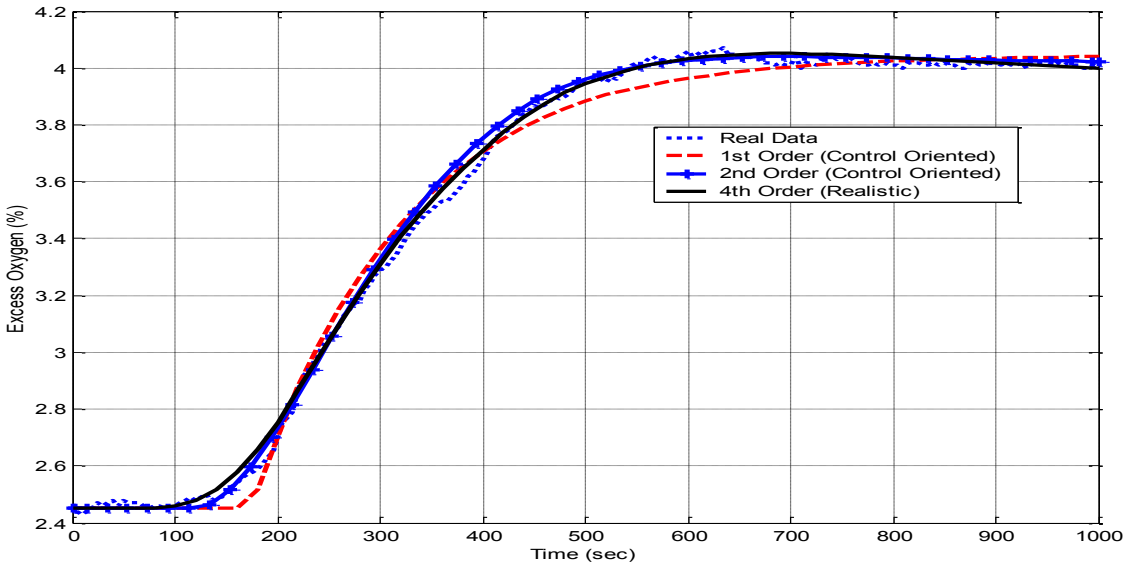

Figure 4.23: Selected Models Order for Realistic and Control Oriented Models

Complete realisation of input output EO_2 models can be simplified by simulation results as follows:

Figure 4.24 illustrates with constant input of $AFR_{(Mass)}$;

- $AFR_{(Mass)}$, $17.2kg$ is fed to conversion model as an input. According to the methane gas law, the $AFR_{(Mass)}$ is converted to $AFR_{(Volumetric)}$, $9.5ft^3$ as an output. $AFR_{(Volumetric)}$, $9.5ft^3$ is fed into the modified transfer function as an input. With the process gain (K), the output of transfer function is initialised

at $10.9ft^3$ without negative deviation. As $AFR_{(Volumetric)}$, $10.9ft^3$ is fed into the EO_2 look-up table, the final output of EO_2 interpolates at 2.45%.

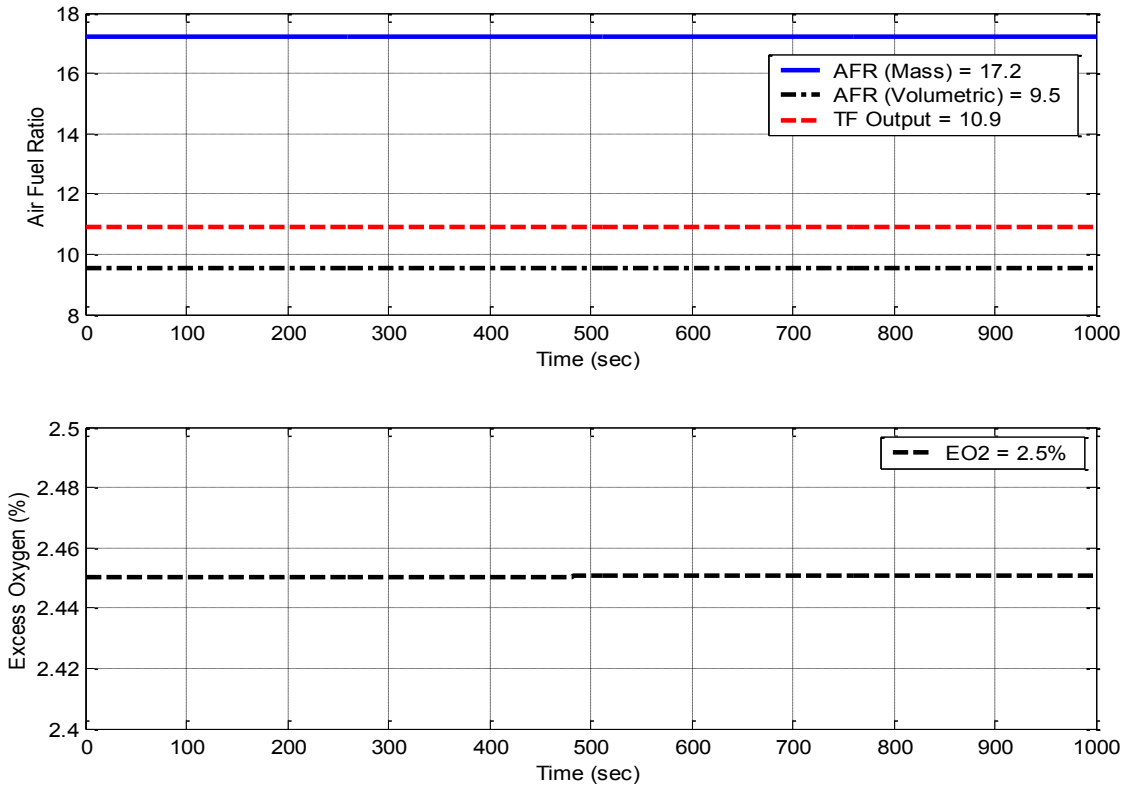

Figure 4.24: Non-Zero Initialised Constant Input of Complete Model Realisation

Figure 4.25 illustrates with step-up input of $AFR_{(Mass)}$;

- $AFR_{(Mass)}$, $17.2kg$ is step-upped to $18.93kg$ in conversion model. Thus, $AFR_{(Volumetric)}$, $9.5ft^3$ is increased to $10.5ft^3$ as an input to transfer function. With unchanged K the output of transfer function is raised from $10.9ft^3$ to $11.99ft^3$ after $167sec$ of dead time. As a result, the EO_2 model initialised at 2.45% and settled at 4.05% without negative deviation.

Figure 4.5 assured that the EO_2 response is initialised at non-zero initial state as expected. Apart from that, the input output responses of complete model is well synchronised according to the real glass industry response. While the figure 4.20

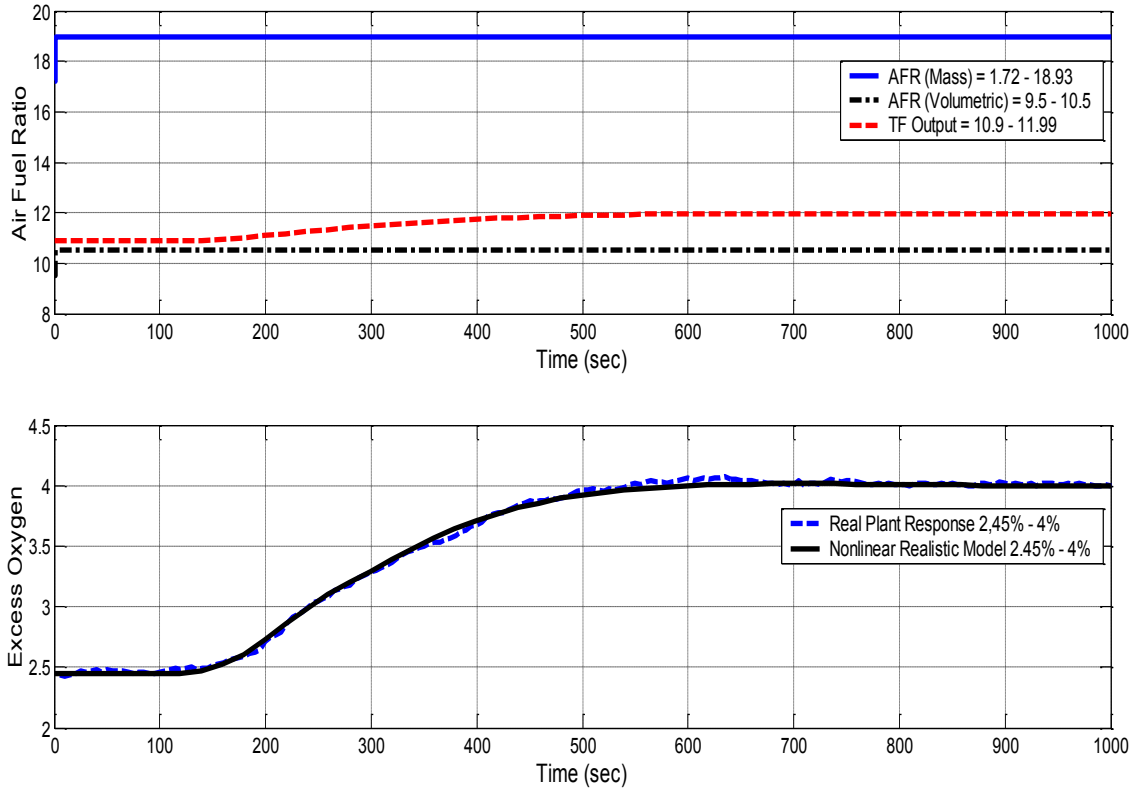

Figure 4.25: Non-zero Initialised Step Responses of Identified EO_2 Models

illustrates, the realistic model response is well fitted and completely realised with real plant response.

4.5 Summary

The proposed predetermined time constant approximation, $PTcA$ method enhanced the optimisation of search space boundaries for global optima convergence. The response's dynamic period and time constant of settling time provides better presumption of prior knowledge of an initial predetermined time constant for search space optimisation. The resized lower and upper search boundary for an optimal search boundary (SB_O) derived from an initial predetermined time constant well brought the elite group within a feasible bounded search region. Further, SGAs execution improved the exploration of elite groups to locate and exploit the optimal values for the model parameters of T_g and EO_2. Particularly, higher order polynomial coefficients identification for realistic EO_2 model with nonzero initial condition,

input-output synchronisation and nonlinearity effect. Moreover, the population diversity and search space are consolidated well with sustaining a balance between exploration and exploitation by improved feasible search region technique.

As expected, an optimum control oriented model's parameters for 1st order T_g and 1st and 2nd orders of EO_2 (as illustrated in section 4.5.5.2) are well identified by the improved search space approximation technique for control parameter optimisation. For T_g, control oriented model parameters which is identified by SGAs^{3}exhibits 3.1% and 3.6% better J_i than SGAs^{2}and SGAs^1, respectively. While, for the EO_2, the 2nd order model has 79.5% better SSE criterion than 1st order model. Also, the 2nd order model is well characterising the curvature dynamic of the initial rising of the output response after the delay, θ, around the point of inflexion of the EO_2 real plant data. Therefore, the 2nd order model is selected alongside with 1st order model for optimal control parameters consideration.

Further, the 4th order realistic model's parameters of EO_2 with nonlinear effect are well identified. Based on the SSE, the 4th order model has 3.6% and 5.2% better extrapolation of the real data than 2nd and 3rd order, respectively. Also, based on the roots of the denominator of model orders assessment, the 4th order model has another pair of complex poles which enhances the extrapolation on the real data characteristic. The higher order model of EO_2 is essential to characterise the homogeneous of real plant response as no realistic model is available for further work.

Chapter 5

CONTROL PARAMETERS OPTIMISATION OF GLASS TEMPERATURE AND EXCESS OXYGEN

5.1 Introduction

In this chapter, the discrete control (PID) parameters optimisation by SGAs for control oriented models of glass temperature and excess oxygen which are identified in chapter 4 are focused on. A literature review of PID control strategies and tuning issues are briefly discussed and addressed. The control parameters of both control oriented models are optimised individually without loop interaction according to the desired performance criteria. The improved search space boundaries and modified objective function is subsequently introduced for excess oxygen and glass temperature, respectively to improve the discrete PID parameters to attain the desired dynamic performance criteria.

The search space boundaries are improved by resizing the upper and lower boundaries with an assist of the conventional tuning techniques, Ziegler-Nichols and Direct Synthesis for an initial knowledge of PID parameters. For the glass temperature,

the objective function is modified by adding the weighting factor with input term to achieve the desired characteristic response. Further, the three other modified objective functions were analysed and compared with selected objective function for better dynamic characteristics of glass temperature response.

5.2 Brief Introduction of PID Control

A Proportional–Integral–Derivative (PID) controller has an extensive history, beginning from last century in the automatic control field (Bennett, 2000). As a result of its comparative straightforwardness and satisfactory performance, it is capable to endow with a wide range of processes; and also it has become in tradition the standard controller in industrial settings. The PID controller has been evolving along with the current technology advancement and frequently implemented in discrete structure rather than with pneumatic or electrical components. It can be established in virtually all category of control equipments, either as a stand-alone (single-station) controller or as a functional block in Programmable Logic Controllers (PLCs) and Distributed Control Systems (DCSs).

In point of fact, the latest PID potentialities are provided by the advancement of the discrete technology and the software packages has guided to a significant growth of the research in control field. The achievement of the PID controllers is also enhanced by the fact that they often represent the fundamental component for more sophisticated control schemes that can be implemented when the basic control law is not sufficient to obtain the required performance or a more complicated control task is of concern (Patel and Chaphekar, 2012). Recently, efficient tools and heuristic algorithms have been developed for the improvement of the PID control analysis and design methods.

Figure 5.1 illustrates a general structure of closed-loop negative-feedback control system. The $R(s)$ is reference input, $Y(s)$ is controlled output, $E(s)$ is control error, $G_P(s)$ is system's process and $G_C(s)$ is control strategies which are consist of K_P, K_I and K_D parameters. The desired control parameters/conditions for a closed loop system are normally attained by tuning the process to the inherent conditions

without precise knowledge of a plant model. Stability can frequently be ensured using only the proportional term. Pure proportional action will result in control offset.

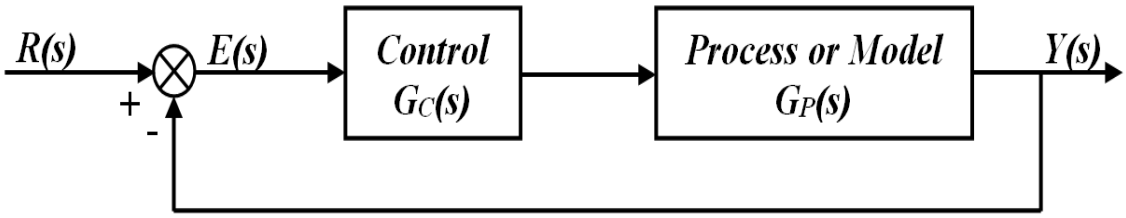

Figure 5.1: Schematic diagram of closed-loop negative-feedback control system

Thus, the integral term eliminates the offset. It does this by repeating the action of the proportional band every integral time constant. This enables the system to recover more quickly from a disturbance in conditions. The derivative term is used to provide damping or shaping of the response. The action of derivative is to cater for disturbances and sudden changes. In effect, it is used to predict what is going to happen within the process and takes quicker action than the integral term to correct it.

5.3 Discrete PID Parameters Optimisation

The textbook or in classical PID controller, can be described as an input–output relation expressed in standard forms,

$$u(t) = K_c \left(e(t) + \frac{1}{T_i} \int_0^t e(\tau) d\tau + T_d \frac{de(t)}{dt} \right) \tag{5.1}$$

where K_c is controller gain, T_i is called integral time, T_d is derivative time, u is the control signal and e is the error signal ($e = r - y$). The reference value is also called the set-point.

The proportional part acts on the present value of the error, the integral represent an average of past errors and the derivative can be interpreted as a prediction of future errors based on linear extrapolation. By using the finite difference approximations, equation 5.1 is expressed to its discrete equivalent in positional form.

For more accurate approximations, the trapezoidal and backward rules are ap-

plied here to develop discrete expressions for integral and derivative terms, respectively ($K_P = K_c; K_I = {}^1/_{T_i}; K_D = T_d$),

$$G_C(z) = \frac{U(z)}{E(z)} = K_P \left(1 + K_I \frac{T}{2}\frac{(z+1)}{(z-1)} + K_D \frac{1}{T}\frac{(z-1)}{z}\right) \tag{5.2}$$

5.4 SGAs Configuration for Control Optimisation

The SGAs approach is applied for optimisation of the discrete PID control parameters as illustrated in figure 5.2. At initial state, the chromosomes of an array of variable values of T_g and EO_2 to be optimised individually are defined as:

$$Chromosome = \left(\underbrace{K_P, K_I, K_D}_{T_g}\right) \quad ; \quad \left(\underbrace{K_P, K_I, K_D}_{EO_2}\right) \tag{5.3}$$

The binary coding is encoded to the discrete controller parameters into binary strings to generate the initial population randomly in the beginning. The length of each chromosome (L_{ind}) is determined based on the binary precision or resolution:

$$res_j = \frac{(b_j - a_j)}{2^{m_j} - 1} \tag{5.4}$$

where m_j is the number of bits, b_j is the upper boundary and a_j is the lower boundary of each individual chromosome's searching parameter.

Each chromosome's binary string is converted into an associated real value of PID parameters to propagate to the discrete PID controller.

The decoding process into a real value is done as:

$$x_j = a_j + Dec \times \frac{(b_j - a_j)}{2^{m_j} - 1} \tag{5.5}$$

where x_j is the respective real value of the chromosome's search parameter and Dec is the decimal value of respective binary string. A complete simulated system response of each PID set and its initial fitness value is evaluated by using a defined objective function.

According to the chromosome's fitness value by a defined objective function, a

new generation (offspring) is produced by the process of genetic operators. The genetic operators manipulate the binary strings of the chromosome directly, by means of selection rate (S_{rate}), crossover rate (X_{rate}) and mutation rate (M_{rate}) to produce fitter chromosomes for the next generation.

After completion of the genetic operator process, the new set of binary strings for each chromosome in the population is required to be decoded into real values and propagated again to the discrete PID controller to evaluate for a new fitness value. This process is sequentially repeated until a maximum number of generations, where the optimal fitness is attained.

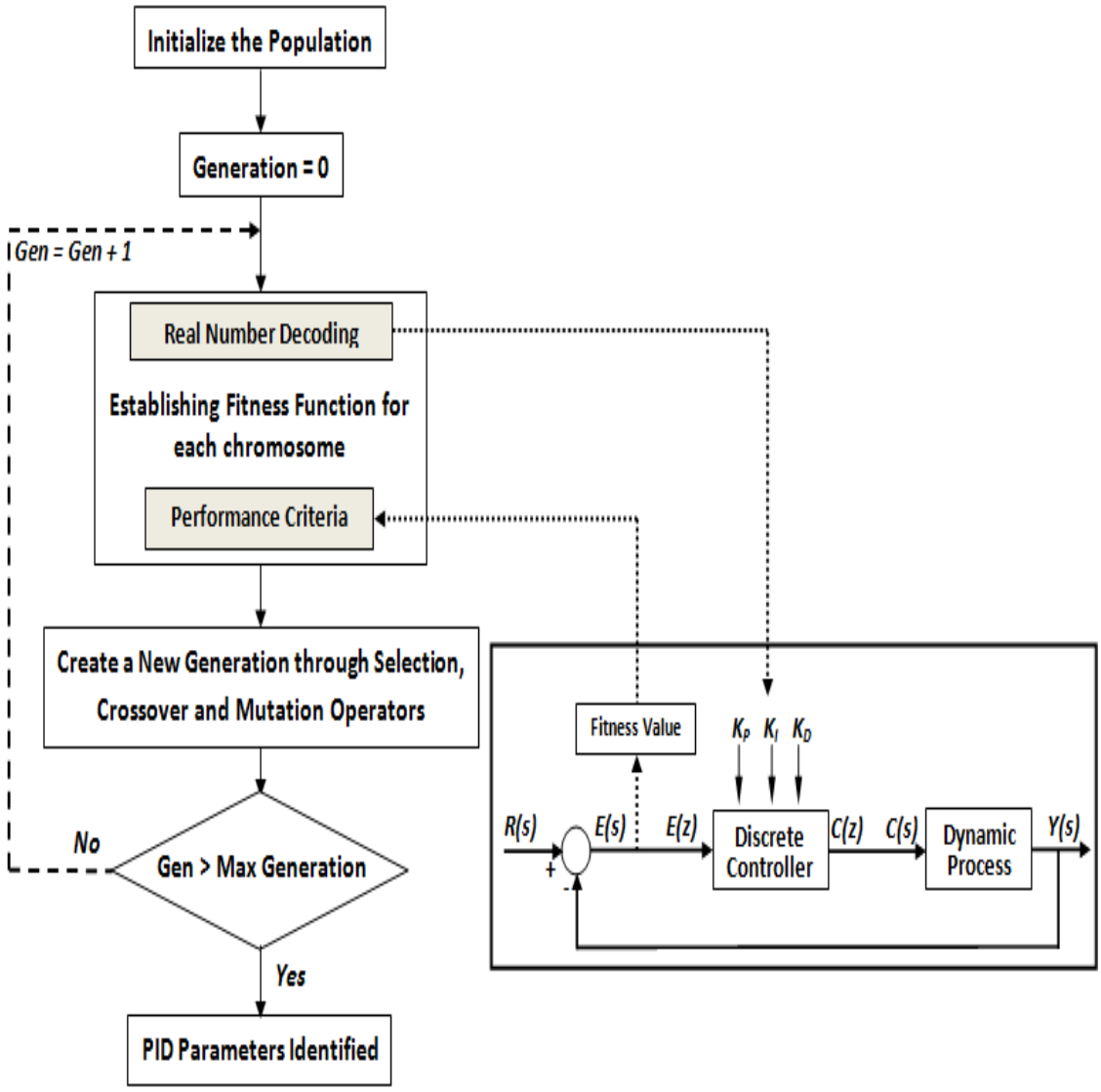

Figure 5.2: Flow chart of discrete PID control parameters optimisation by SGAs (Saad et. al., 2012)

5.4.1 Selection of Genetic Parameters

As a result of no prior information available for genetic operator values for both T_g and EO_2 control parameters optimisation, several trial and error were conducted with respective sampling time where variations of the genetic operator values were tested individually without loop interaction for enhancing the searching mechanism.

Similar types of first-order with and without dead time processes are referred as a guideline for selection of genetic parameters (Nithya et. al., 2007) (Rathikarani et. al., 2007) (Nithyarani et. al., 2013). Author preferred to calibrate the genetic operator parameters, at each testing to reduce the performance criterion (J_i) between the real plant and model as simplified in follows;

1. For the number of individuals, the J_i has improved when the $N_{ind} = 50$. While, the J_i is higher when $N_{ind} < 50$ and the J_i has sustained and the simulation time slowed when $N_{ind} > 50$.

2. For the generation gap, the J_i and simulation time are improved when $G_{gap} = 0.7$ for EO_2 and $G_{gap} = 0.6$ for T_g. However, higher generation gap, $G_{gap} > 0.7$ for EO_2 and $G_{gap} > 0.6$ for T_g have not the improved the J_i and when $G_{gap} < 0.7$ for EO_2 and $G_{gap} < 0.6$ for T_g, the J_i is higher.

3. For the maximum number of generation, the J_i has sustained well approximately 30 for both EO_2 and T_g. However, 50 as number of generation is selected for further genetic evolution. Generally, the maximum number of generation is required higher than 30 for better J_i. However, based on the trial and error method, the J_i has sustained well approximately 30 due to small precision of binary representations. According to the variation test, the higher $PRECI > 10$ has to slowed down the simulation period and the J_i has not improved as expected. The selected $PRECI = 6$ may not improved the J_i much, but the simulation time is faster. Therefore, the better J_i attained and sustained with the minimum number of generations.

4. For selection, crossover and mutation, the default values are selected due to the J_i has not improved as expected and also generally suggested by selected

research papers for first-order with or without dead time process.

As described by Vlachos (2000), the T_g and EO_2 performances are not affected much by several trial and error on genetic operators variations. Therefore, the genetic operators are reasonably selected for sustaining the performance accuracy and simulation period. Table 5.1 illustrates the selected genetic operator parameters and sampling time for both T_g and EO_2.

Table 5.1: Selected genetic operators of T_g and EO_2

Genetic Operators	$T_g(K)$	$EO_2(\%)$
No. of Individuals	50	50
Max. No. of Generation	30	35
Generation Gap	0.6	0.7
Precision of Binary Rep.	6	6
Selection	SUS	SUS
Crossover	Single Point, 0.6	Single Point, 0.7
Mutation	Binary Rep., $0.6/L_{ind}$	Binary Rep., $0.6/L_{ind}$
Sampling Time	$2min$	$5sec$

5.5 Simulation Results of Control Oriented Models

The identified control oriented models in chapter 4 for both T_g and EO_2 were applied individually to evaluate the optimum objective function and search space boundary region to achieve the desired performance criteria. In the first attempt initial guesses were made for the search space boundaries in the SGAs.

The improved boundary constraints were subsequently introduced. For better approximation of improved search space boundary values, conventional tuning methods, Ziegler-Nichols and Direct Synthesis (DS) were applied to approximate initial PID parameters. With these initially approximated PID parameters, the b_j and a_j were resized accordingly to ensure an optimal solution for the desired dynamic response characteristics.

5.5.1 Performance Criteria Formulation

The performance criteria for both T_g and EO_2 processes are formulated individually under closed-loop SISO control based on the following desired dynamic response characteristics. Theses specifications were developed in this research.

1. For T_g; Overshoot $\leq 2\%$, Settling time $(ts) \approx 5hrs$. Based on the design specifications of selected chamber's refratories (Fenton Art Glass), the selection of settling time as $5hrs$ is to avoid a sudden rise in temperature which could cause a lessening in the life time of chamber refratories (Carniglia, 1992) (Morris, 2007). The T_g has a slow and strong dynamic progression response without oscillations. Therefore, the overshoot limit as 2% is selected also, to avoid excessive fuel consumption due to oscillations.

2. For EO_2; Overshoot $\leq 2\%$, Settling time $(ts) \approx 5min$. Based on the open-loop response from numerical data, the EO_2 has a fast and strong dynamic progression response without oscillations. Therefore, the overshoot limit as 2% is selected. However, $5min$ of settling time is selected as a reasonable value, as there have been no research works undertaken for EO_2.

3. For both variables; zero steady state error to a constant set-point.

5.5.2 Objective Function and Boundary Constraint Formulation on EO_2

Two objective functions, sum of absolute error, SAE and sum of squared error, SSE were applied to evaluate and improve the set-point error for EO_2.

$$J_i(SAE) = \sum_{k=0}^{k=max} \mid e(k) \mid \tag{5.6}$$

$$J_i(SSE) = \sum_{k=0}^{k=max} e^2(k) \tag{5.7}$$

As illustrated in figure 5.3, the simulations result for control of both 1st and 2nd order control oriented models are exhibiting significant oscillatory responses with respective wide range of search space boundaries. With identified PID parameters by SGAs for 1st ($K_P = 2$; $K_I = 0$; $K_D = 30.33$) and 2nd ($K_P = 2.222$; $K_I = 0$; $K_D = 87.36$) order control oriented models responses have fast rise time, $T_r \approx 188sec$ caused high oscillation, long settling time (ts) and failed to attain the desired EO_2 output, 3%.

A wide range of search space boundaries, are inadequate and lead the SGAs trapped at local minima. As wide range of search space boundaries trapped the K_P at upper search boundary, the SGAs failed to converge the K_I and caused the response offset (2.8%).

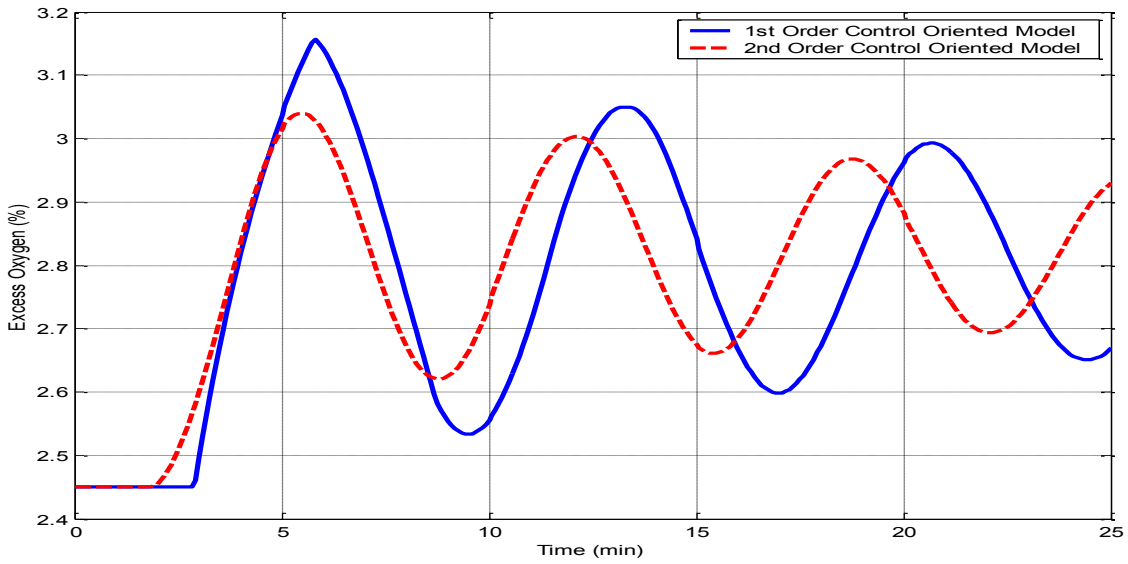

Figure 5.3: Wide range of search space boundary responses with respective control oriented models by SGA's

As discussed earlier, the conventional tuning techniques Ziegler-Nicholas and DS are applied to identify initial PID parameters to approximate the upper (b_j) and lower (a_j) search space boundaries. According to figures 5.4, 5.5 and table 5.2, the dynamic responses of 1st order models by both conventional tuning techniques are significantly suffering to attain the desired criteria performance.

On other hand, the dynamic responses of 2nd order models are significantly improved than the 1st order models, but, suffering to attain the desired criteria perform-

ance. Further analysis illustrates that the DS technique's K_I parameter (5.527e-3) of 2nd order model improves the dynamic response then the K_I parameter (2.211e-3) of 1st order model with approximately similar K_P parameters.

Table 5.2: Control Oriented of EO_2 Model's PID Parameters

Tuning Methods	Model Orders	Control Oriented		
		K_P	K_I	K_D
Ziegler-Nichols	1	0.765	2.235e-3	65.63
	2	0.822	3.497e-3	71.5
Direct-Synthesis	1	0.4225	2.211e-3	101.1
	2	0.4576	5.527e-3	89.5
Wide Range Bound SGAs	1	2	0	36.67
	2	2.222	0	87.36
Improved Bound SGAs	1	0.8153	4.418e-3	35.87
	2	0.8643	4.347e-3	83.75

Tuning Methods	Model Orders	SSE	SAE	$Ts(2\%)$ $(5min)$
Ziegler-Nichols	1	305.3214	629.8317	28.3min
	2	184.5971	428.1247	21.6min
Direct-Synthesis	1	367.2647	784.3981	34.7min
	2	258.6312	567.2941	16.9min
Wide Range Bound SGA's	1	273.7449	734.9646	-
	2	343.5467	1133.7102	-
Improved Bound SGA's	1	148.7341	326.8098	5min
	2	142.3723	319.7658	5.2min

The table 5.2 illustrates that the approximately similar K_I parameter of 1st order model by both conventional techniques is primary root for the immature dynamic response. While, the PID parameters of 2nd order model has better dynamic response than the 1st order model by Ziegler-Nicholas technique. Also, the table 5.2 illustrates inconsistencies in K_D parameter for both 1stand 2nd order models by both conventional techniques.

Based on analysis by Ziegler-Nicholas and DS techniques, an optimal PID parameters are have located within the region, $0.4 < K_P < 0.9$, $0.002 < K_I < 0.006$ and $60 < K_D < 105$. Therefore, the search space boundaries (a_j and b_j) are improved by resizing the $K_P \in [0:1]$, $K_I \in [0.001:0.01]$ and $K_D \in [10:150]$ accordingly to provide better exploitation with minimum constraints.

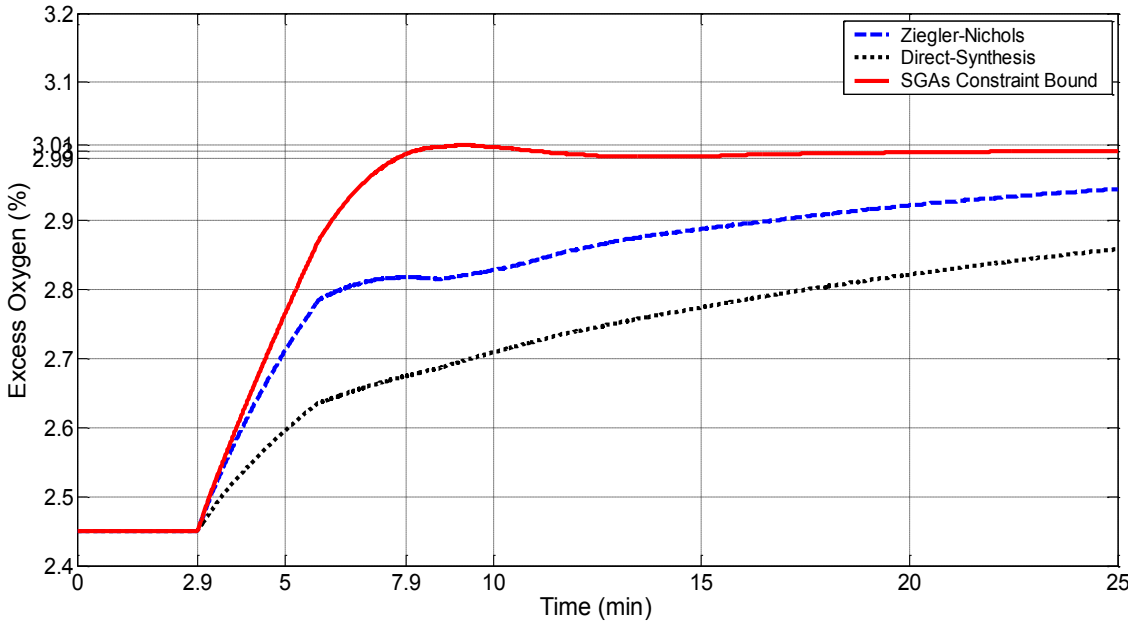

Figure 5.4: 1st order control oriented EO_2 model responses; ZN, DS and SGAs improved search space boundaries

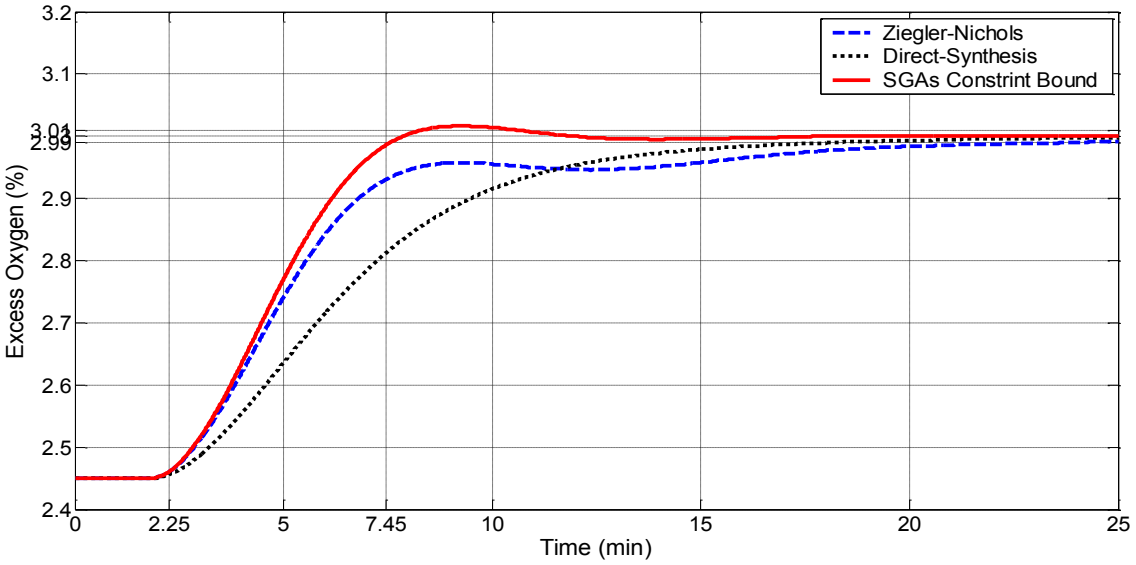

Figure 5.5: 2nd order control oriented EO_2 model responses; ZN, DS and SGAs improved search space boundaries

As illustrated in figure 5.6 and table 5.2, the SGAs with parameter vectors of improved bound both 1st and 2nd order control oriented linear models attained the desired performance criteria, $ts = 5min$ and $OS \leq 2\%$, as expected. Even though, the 2nd order model has an insignificant long period of $ts = 5.2min$ due to short dead time. By limiting the b_j of K_P, the SGAs consolidate well within the boundary constraint with K_I and K_D to converge the global minima. Initially

approximated the SGAs with PID parameter vectors of improved bound, $K_P \in [0:1]$, $K_I \in [0.001:0.01]$, $K_D \in [10:130]$ of EO_2 has provide better exploitation and dynamic response and higher degree of accuracy while reducing the SSE and SAE by adapting the fitness value.

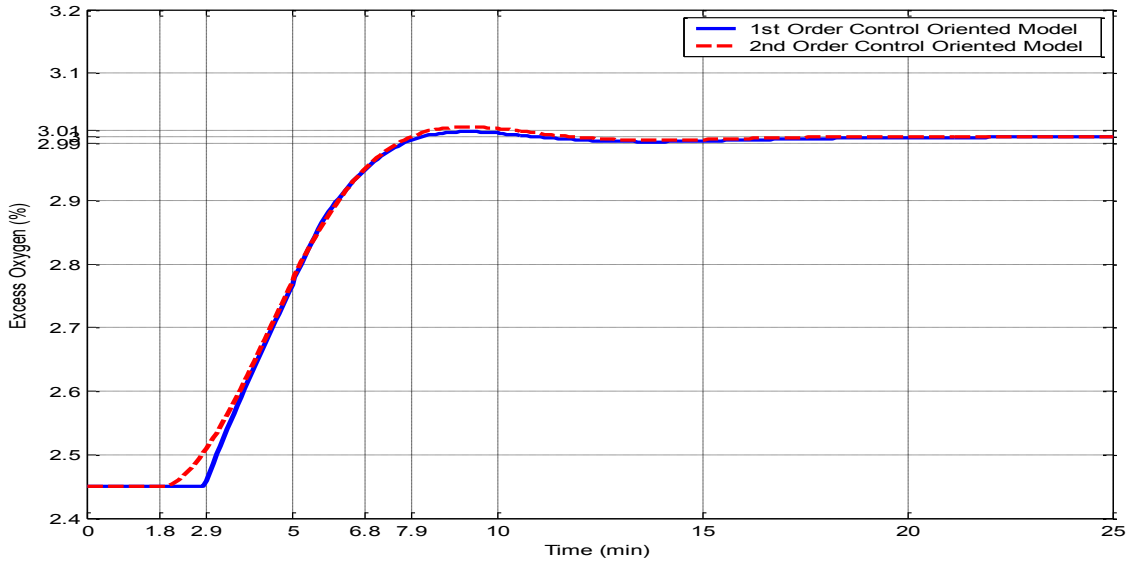

Figure 5.6: EO_2 improved boundaries responses of 1^{st} and 2^{nd} orders control oriented linear models by SGA's

Therefore, further resizing on search space boundary is not required. The initial PID parameters by conventional techniques have provided better suggestion to approximate the improved bound range than assigning the bound range by randomly.

5.5.3 Objective Function and Boundary Constraint Formulation on T_g

The approaches of improved search space boundary used for EO_2 control were also applied for T_g control oriented model. But, unlike the EO_2 process there is only one initially approximated PID parameters set for T_g, which is by Direct Synthesis technique. Thus, the search space boundaries for PID parameters $K_P \in [0.0005:0.005]$, $K_I \in [0.00001:0.0001]$, $K_D \in [1:7]$ are resized accordingly.

The improved search space boundaries by DS with conventional objective functions for control oriented model of T_g exhibited insufficiencies to attain the desired performance criteria.

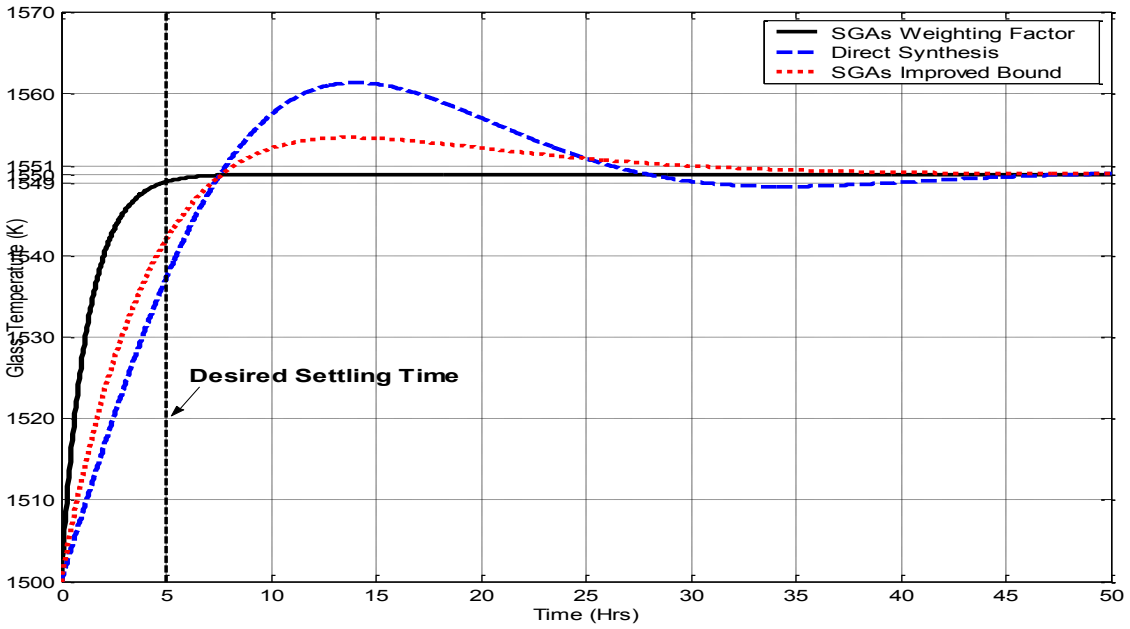

Figure 5.7: Improved boundaries and λ of T_g responses by SGA's with conventional techniques

Table 5.3: PID parameters for control oriented T_g by different tuning methods

Tuning Methods	K_P	K_I	K_D
Direct Synthesis	2.235e-3	5.15e-5	3.563
Improved Bound SGAs	3.675e-3	2.54e-5	6.322
Weighting Factor SGAs	9.863e-3	9.46e-6	1.701

Tuning Methods	Set-point Error	$Ts(2\%)$ $(5hrs)$
Direct Synthesis	1.981e5	40hrs
Improved Bound SGAs	8.438e4	30hrs
Weighting Factor SGAs	7.029e4	4.9hrs

As illustrated in figure 5.7 and table 5.3, an overshoot of 10% $(1555K)$ occurred in the transient response with long settling time of $30hrs$ for T_g with improved boundaries. The optimised PID parameters by improved bound SGAs are exploited near to b_j for K_P and near to a_j for K_I boundary search region.

Further resizing on search space boundary is ineffective to attain the desired performance criteria. The desired response may achieved by significantly constrained the search boundary regions, but no guarantee on the identified PID parameters are optimal. The small overshot $(5K)$ of T_g by improved search space bound may be perhaps acceptable, but it will cost unnecessary fuel consumption.

To enhance the searching mechanism for the PID parameters and achieve more global optima, a modified objective function is applied. Li and Bo (2012) proposed the use of absolute time integral performance parameters as the minimum objective function with the purpose of attaining the acceptable dynamic characteristics for the period of the transition process, Also, the quadratic component is added on the control input on target function to avoid the excessive control energy in the objective function.

The proposed formula is modified by adding the weighting factor (λ) with input term of the controller output of objective function to reduce the fast rising effect of the transient response. The modified objective function applied for T_g is given by the relation,

$$J_i(IAE + \lambda ISU) = \sum_{k=0}^{k=max} \left(\mid T_g(k) - 1550 \mid + \left(\lambda u^2(k) \right) \right) \tag{5.8}$$

where k is the sampling number and u is the controller output.

The selection of optimal value of λ is done by trial and error technique by varying the λ in the range [100 : 1000].

Table 5.4: Weighting factor identification with $IAE + \lambda ISU$

λ	Set-point Error	IAE	λISU	K_P	K_I	K_D
100	1.847e4	8.783e2	1.759e4	2.094e-2	8.545e-6	1.635
250	4.456e4	1.510e3	4.306e4	1.248e-2	9.461e-6	7.981e-2
350	6.173e4	1.799e3	5.993e4	1.052e-2	9.461e-6	1.996e-1
400	7.029e4	1.922e3	6.836e4	9.863e-3	9.461e-6	1.701
550	9.585e4	2.324e3	9.352e4	8.196e-3	9.155e-6	3.052e-3
850	1.467e5	2.918e3	1.438e5	6.529e-3	9.155e-6	1.115e-1
1000	1.721e5	3.192e	1.689e5	5.985e-5	9.155e-6	2.441e-3

λ	Set-point Error	$T_{Fuel}(kg)$	$Ts(2\%)$ $(5hrs)$
100	1.847e4	548.1	1.9hrs
250	4.456e4	547.9	3.7hrs
350	6.173e4	547.8	4.6hrs
400	7.029e4	547.8	4.9hrs
550	9.585e4	547.7	6.2hrs
850	1.467e5	547.5	7.6hrs
1000	1.721e5	547.5	8.3hrs

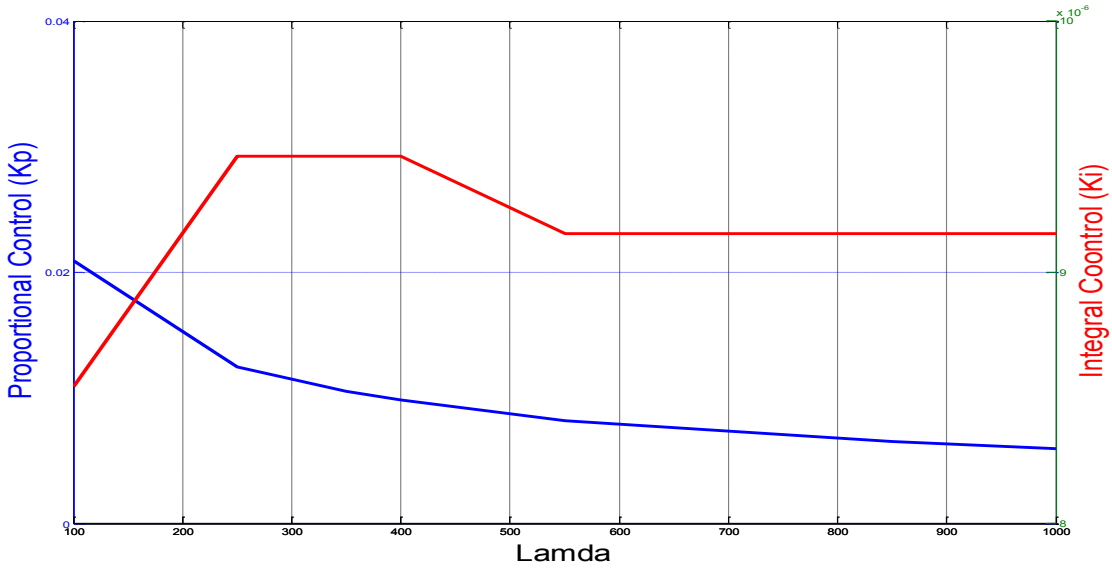

Figure 5.8: Effect of $P-term$ and $I-term$ with λ of modified objective function, $IAE+\lambda ISU$

As illustrated in table 5.4 and figure 5.8, the weighting factor associated with the desired response characteristics was set to be $\lambda = 400$ to give more emphasis to the set point tracking objectives.

According to the table 5.4 and figure 5.8, the $P-term$ reduces as the λ increases. However, the $I-term$ increases at the very initial phase ($\lambda = 100 \rightarrow 250$) and then saturated ($\lambda = 250 \rightarrow 400$) with λ to maintain the overall controller output.

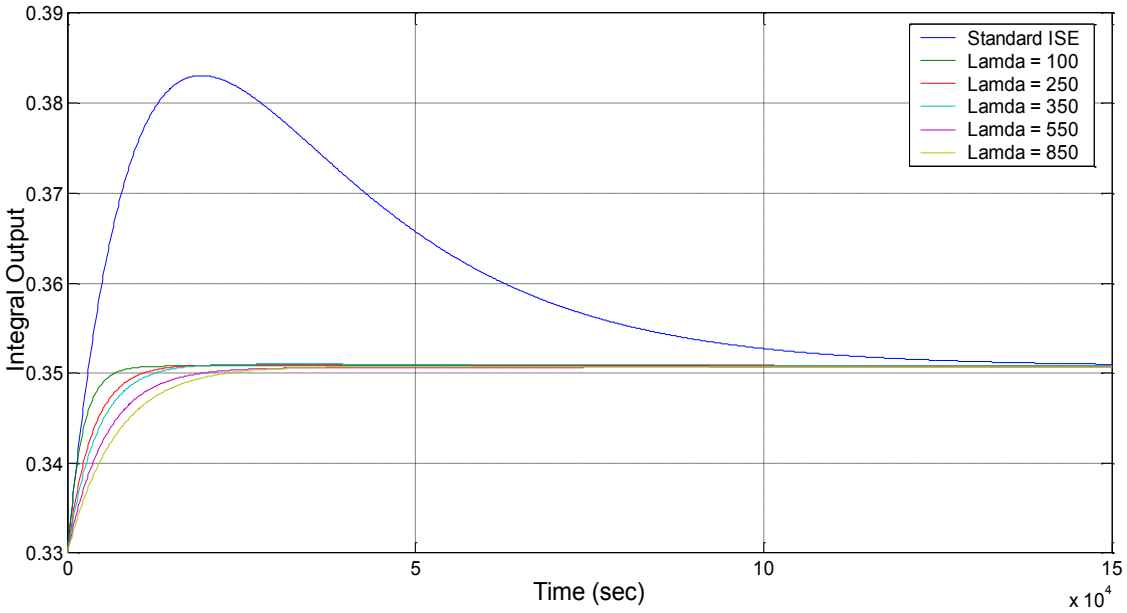

Figure 5.9: Integral output of $IAE+\lambda ISU$ objective function with $\lambda = 100 \rightarrow 850$ for T_g

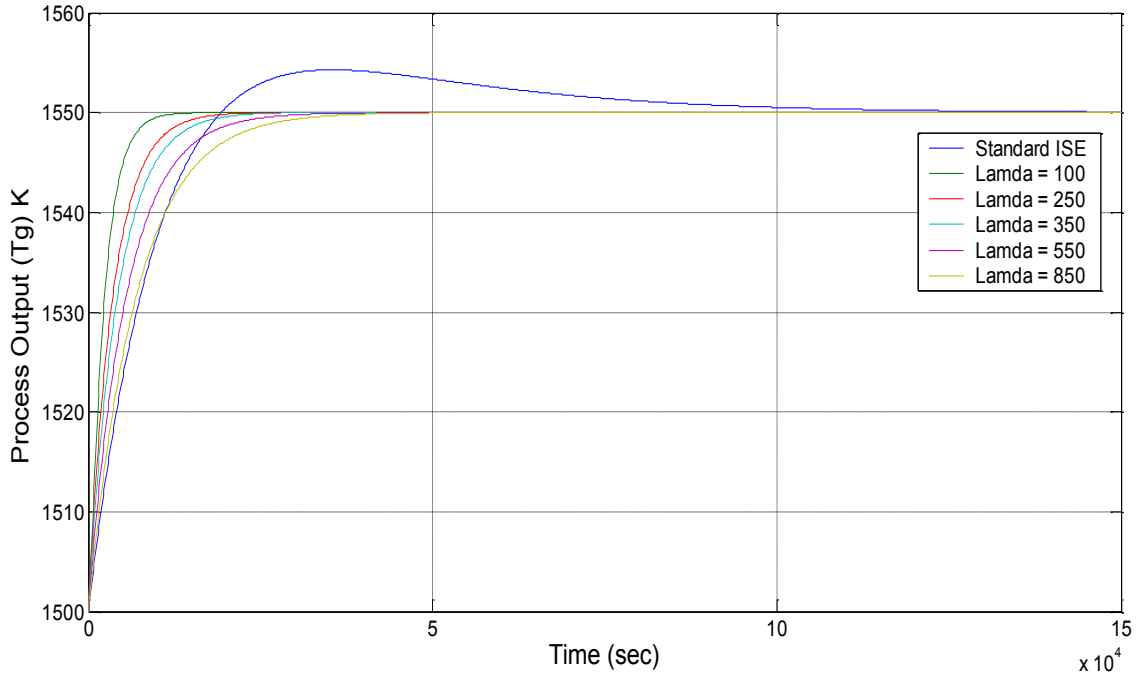

Figure 5.10: Process output of $IAE + \lambda ISU$ objective function with $\lambda = 100 \rightarrow 850$ for T_g

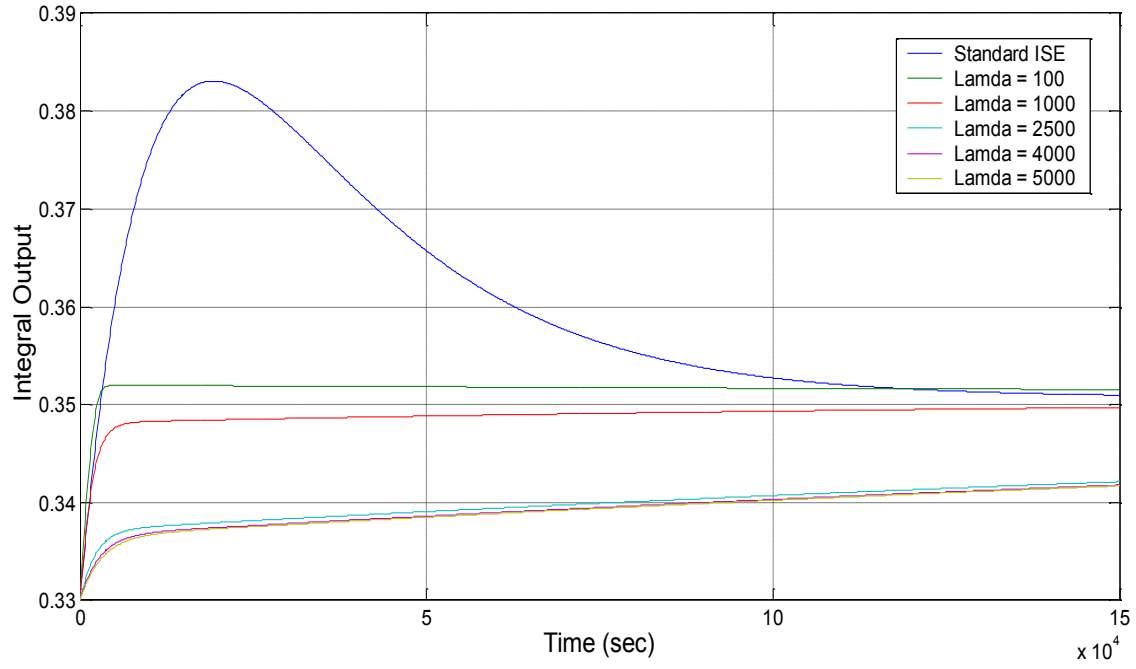

Figure 5.11: Integral output of $ISE + \lambda ISU$ objective function with $\lambda = 100 \rightarrow 5000$ for T_g

Subsequently, the $I - term$ is reduced at final phase with λ and $P - term$. The standard objective function ($\lambda = 0$) produced high integral value, which results in an overshoot in T_g response as illustrated in figures 5.9 and 5.10.

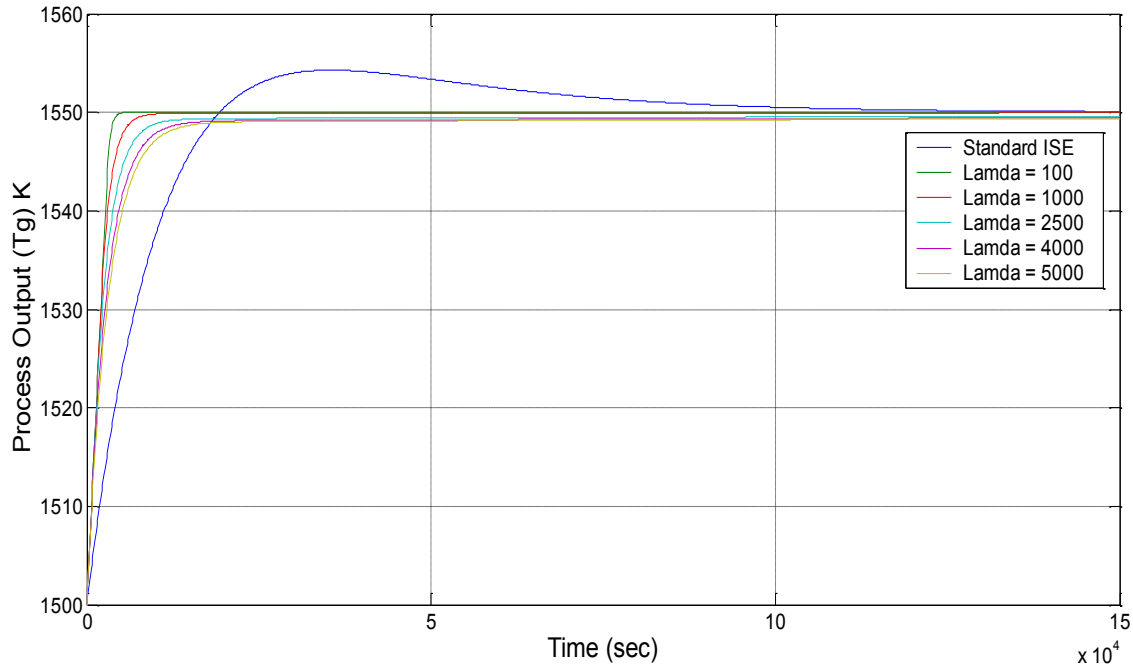

Figure 5.12: Process output of $ISE+\lambda ISU$ objective function with $\lambda = 100 \rightarrow 5000$ for T_g

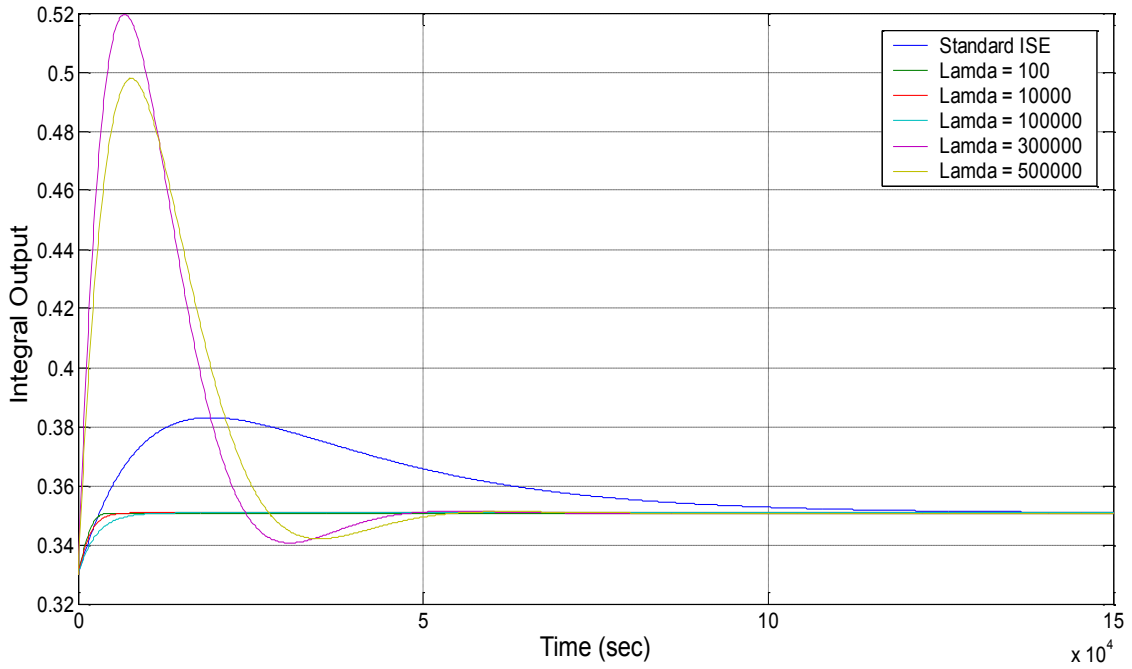

Figure 5.13: Integral output of $IAE + \lambda IS\Delta U$ objective function with $\lambda = 100 \rightarrow 500000$ for T_g

Therefore, the ts increases accordingly as the $P-term$ and $I-term$ (decreases) consolidated well and λ increases. As a results, its maintain the controller parameters to prevent the oscillatory behaviour of T_g response by smoothing the controlled

variable. In general, the desired response characteristics which are reduction of set-point error, overshoot and settling time, are achieved for T_g with the modified objective function, $IAE + \lambda ISU$.

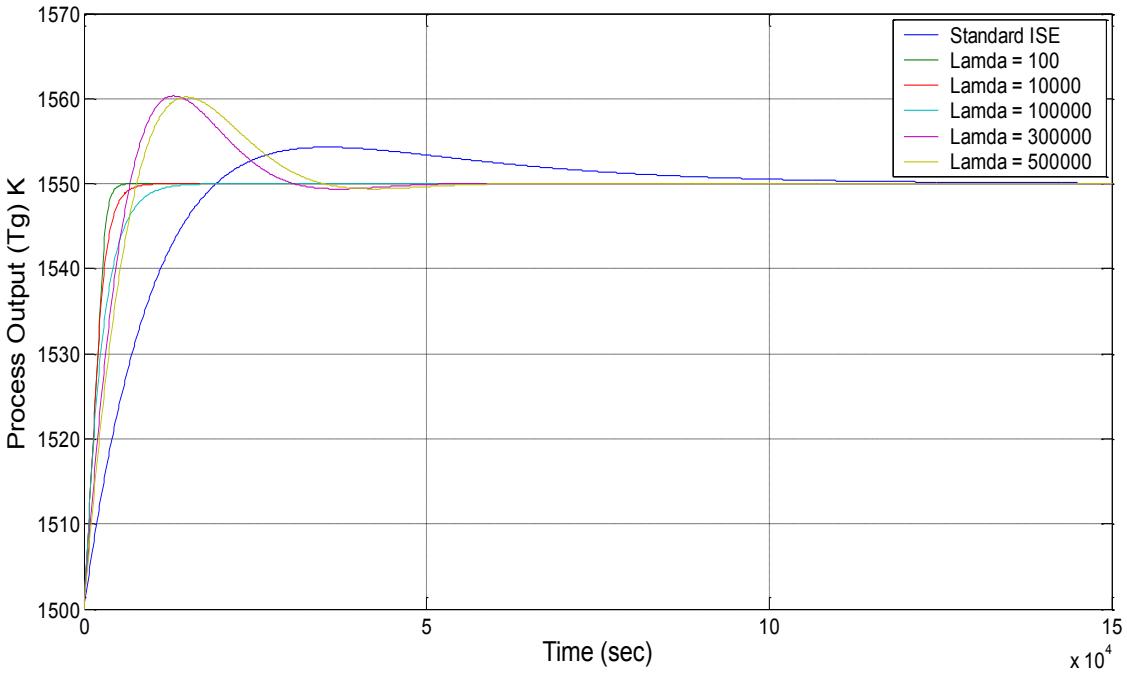

Figure 5.14: Process output of $IAE + \lambda IS\Delta U$ objective function with $\lambda = 100 \rightarrow 500000$ for T_g

Further, three other modified objective functions were analysed to compare with $IAE + \lambda ISU$ for better dynamic characteristics for the T_g response. The following modified objective functions are:

$$J_i(ISE + \lambda ISU) = \sum_{k=0}^{k=max} \left((T_g(k) - 1550)^2 + \left(\lambda u^2(k)\right)\right) \tag{5.9}$$

$$J_i(IAE + \lambda IS\Delta U) = \sum_{k=0}^{k=max} \left(\mid T_g(k) - 1550 \mid + \left(\lambda \Delta u^2(k)\right)\right) \tag{5.10}$$

$$J_i(ISE + \lambda IS\Delta U) = \sum_{k=0}^{k=max} \left((T_g(k) - 1550)^2 + \left(\lambda \Delta u^2(k)\right)\right) \tag{5.11}$$

where Δu is the change of fuel input.

For $ISE + \lambda ISU$, the effect of varying $\lambda = 100 \rightarrow 5000$ is insufficient to optimise the PID parameters as illustrated in figure 5.11 and 5.12. The $I - term$ is suffered

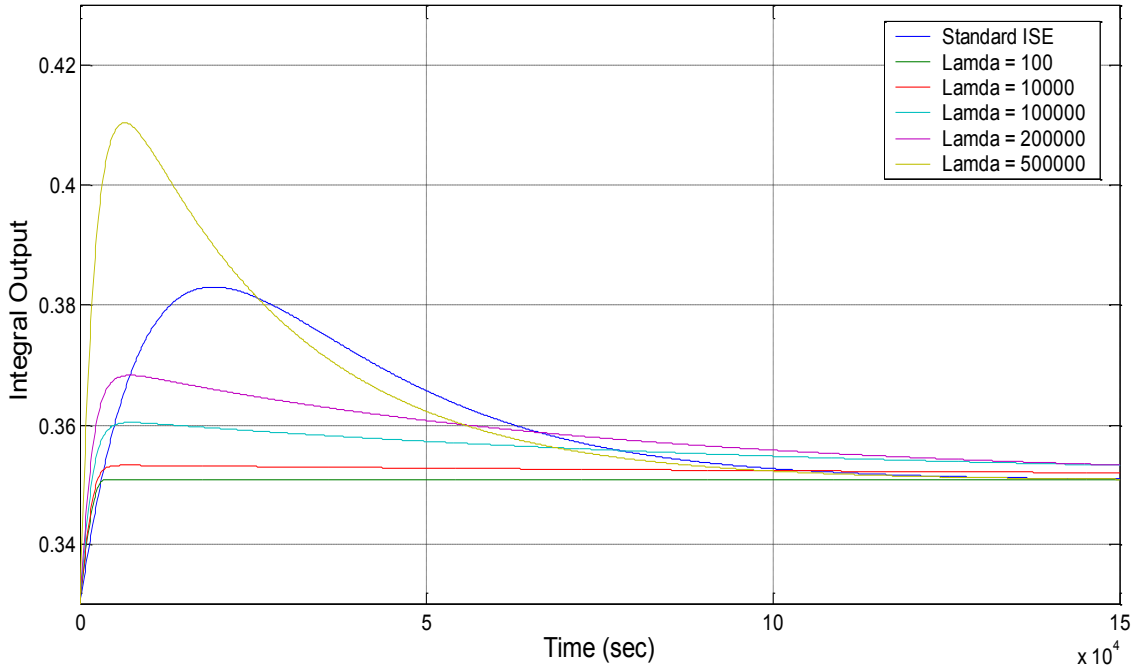

Figure 5.15: Integral output of $ISE + \lambda IS\Delta U$ objective function with $\lambda = 100 \rightarrow 500000$ for T_g

to attain zero steady-state condition as the λ increases. As a result, the T_g response has similar rise time and produce steady-state error $(1K)$.

Whereas, the other two modified objective functions, $IAE + \lambda IS\Delta U$ and $ISE + \lambda IS\Delta U$ with Δu are exhibiting dissimilar response characteristics than $ISE + \lambda ISU$ as illustrated in figure 5.13, 5.14, 5.15 and 5.16. The $I - term$ for the $IAE + \lambda IS\Delta U$ decreases insignificantly at the initial phase and increases significantly at final phase as the λ increases. Subsequently, an overshoot is produced in T_g response. For $ISE + \lambda IS\Delta U$, the $I - term$ increases significantly as the λ increases. Therefore, no improvement on T_g response's.

According to the further analysis on the modified objective function, the $IAE + \lambda ISU$ has 4.15% better fuel consumption, $\dot{m}$, when the λ increases from $100 \rightarrow 1000$. By comparing with the other modified objective functions, $ISE + \lambda ISU$, $IAE + \lambda IS\Delta U$ and $ISE + \lambda IS\Delta U$ have 0.965%, 0.153% and 0.181% fuel consumption respectively, when the λ varies from $100 \rightarrow 1000$. This illustrates that the added λ on the control input, u, avoids the excessive control energy in the objective function by suppressing the u. For the $IAE + \lambda ISU$, as the u is suppressed, the $\dot{m}$ and T_{Fuel} are decreased and J_i is increased, accordingly. Despite the differences in fuel

consumption, the effect of variation of λ for the $ISE + \lambda ISU$ exhibits similar effect as $IAE + \lambda ISU$.

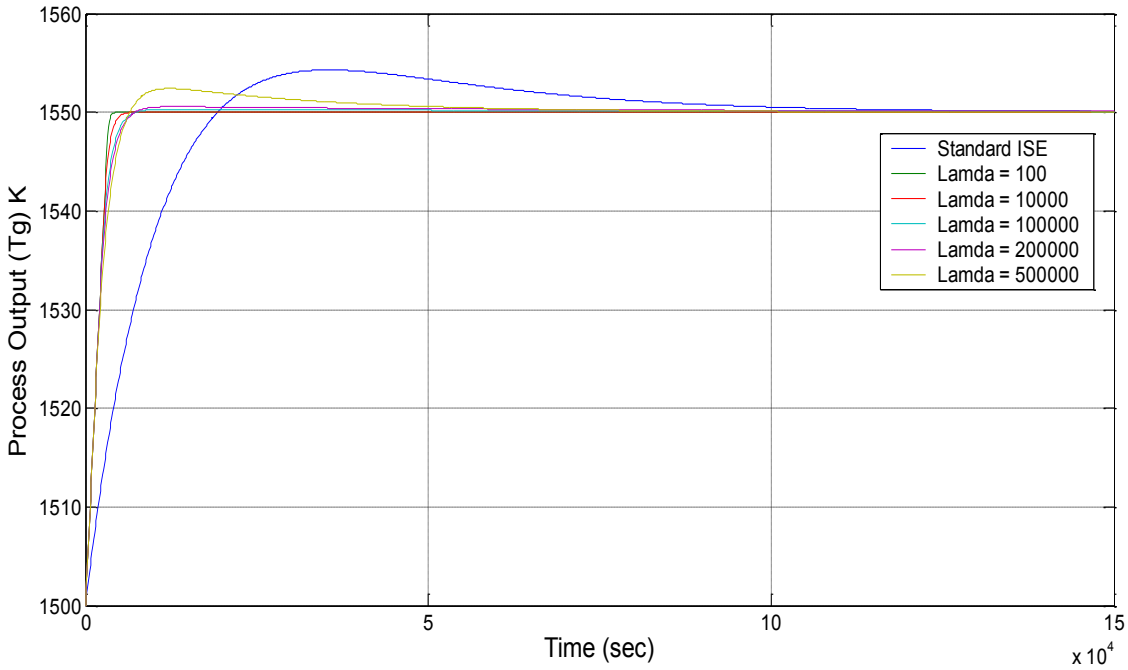

Figure 5.16: Process output of $ISE + \lambda IS\Delta U$ objective function with $\lambda = 100 \rightarrow 500000$ for T_g

However, the effect of variation of λ for the $IAE+\lambda IS\Delta U$ and $ISE+\lambda IS\Delta U$ exhibits insignificant changes in fuel consumption. The ΔU is exhibiting ineffectiveness in suppressing u to avoid the excessive control energy which results in insignificant changes in $\dot{m}$ as the λ increases. Therefore, the T_{Fuel} is relatively constant.

The effect of variation on λ for all the modified objective functions can be simplified and tabulated as follows (table 5.5);

- $IAE + \lambda ISU$; As the λ increases, the u, $\dot{m}$ and T_{Fuel} are decreased and J_i is increased, accordingly.
- $ISE + \lambda ISU$; As the λ increases, the u, $\dot{m}$ and T_{Fuel} are decreased and J_i is increased, accordingly.
- $IAE+\lambda IS\Delta U$; As the λ increases, the u and $\dot{m}$ is decreased and J_i is increased, accordingly. However, the T_{Fuel} is constant as the λ increases.

Table 5.5: Effect of λ variations for the modified objective functions

Objective Function	λ	u	$\dot{m}$	J_i	$T_{Fuel}(kg)$
$IAE + \lambda ISU$	Increase $(100 \rightarrow 1000)$	Decrease	Decrease	Increase	Decrease
$ISE + \lambda ISU$	Increase $(100 \rightarrow 5000)$	Decrease	Decrease	Increase	Decrease
$IAE + \lambda IS\Delta U$	Increase $(100 \rightarrow 500000)$	Decrease	Decrease	Increase	Constant
$ISE + \lambda IS\Delta U$	Increase $(100 \rightarrow 500000)$	Decrease	Decrease	Increase	Constant

- $ISE+\lambda IS\Delta U$; As the λ increases, the u and $\dot{m}$ is decreased and J_i is increased, accordingly. However, the T_{Fuel} is constant as the λ increases.

In general, the simulation results of the three modified objective functions are exhibiting ineffectiveness of achieving the desired performance criteria compared to the $IAE + \lambda ISU$ objective function.

5.6 Chapter Summary

The improved search space boundary technique for the optimal discrete PID parameters were demonstrated by using the 1st and 2nd orders control oriented models of EO_2. The initial PID parameters by the conventional techniques, Ziegler-Nichols and Direct Synthesis provides a better suggestion and prior knowledge of upper and lower search boundaries of EO_2 models. Based on analysis by conventional techniques, an optimal PID parameters are have located within the region, $0.4 < K_P < 0.9$, $0.002 < K_I < 0.006$ and $60 < K_D < 105$. Therefore, the search space boundaries (a_j and b_j) are improved by resizing the $K_P \in [0:1]$, $K_I \in [0.001:0.01]$ and $K_D \in [10:150]$ accordingly to provide better exploitation with minimum constraints.

According to the simulation results the SGAs with improved bound of both 1st and 2nd order control oriented linear models attained the desired performance criteria, $ts = 5min$ and $OS \leq 2\%$, as expected. Even though, the 2nd order model has an insignificant long period of $ts = 5.2min$ due to short dead time. By limiting the b_j of K_P, the SGAs consolidate well within the boundary constraint with K_I

and K_D to converge the global minima. Initially approximated the SGAs with PID parameter vectors of improved bound, $K_P \in [0:1]$, $K_I \in [0.001:0.01]$, $K_D \in [10:130]$ of EO_2 has provide better exploitation and dynamic response and higher degree of accuracy while reducing the SSE and SAE by adapting the fitness value.

However, the improved search space boundary technique is insufficient to optimise the discrete PID parameters for the T_g, where the transient response has an overshoot of 10% ($1555K$) with long settling time of $30hrs$. The optimised PID parameters by improved bound SGAs are exploited near to b_j for K_P and near to a_j for K_I boundary search region. Therefore, the modified objective function, $IAE + \lambda ISU$, with added weighting factor (λ) at the input term of the controller output of objective function to reduce the fast rising effect of the transient response. According to the simulation result, the $\lambda = 400$ gives more emphasis to the set point tracking objectives. The settling time increases accordingly as the $P - term$ and $I - term$ (decreases) consolidated well with λ increases. As a results, its maintain the controller parameters to prevent the oscillatory behaviour of T_g response by smoothing the controlled variable. In general, the desired response characteristics which are reduction of set-point error, overshoot and settling time, are achieved for T_g with the modified objective function.

Further, three other modified objective functions, $ISE + \lambda ISU$, $IAE + \lambda IS\Delta U$ and $ISE + \lambda IS\Delta U$ are analysed and compared with the selected objective function. The simulation results of three modified objective functions are exhibiting ineffectiveness of achieving the desired performance criteria as the $I - term$ is suffered to attain zero steady-state condition as the λ increases. In general, the improved search space boundary technique for EO_2 and modified objective function with weighting factor for T_g has improved the discrete control parameter optimisation and attained the desired dynamic performance criteria.

Chapter 6

Decentralised PID Controller Tuning for Multivariable Glass Furnace Process

6.1 Introduction

In this chapter, the decentralised discrete PID control tuning techniques are primarily focused here for multivariable glass furnace process. A literature review of multivariable PID control strategies and tuning issues are briefly discussed and addressed. Three tuning approaches with respective objective functions are investigated to optimise the control performances for control oriented multivariable glass furnace models.

The improved and modified objective function which includes the total effect is proposed with other conventional tuning techniques, based on SGAs. This modified objective function is shown to exhibit improved control robustness and disturbance rejection under loop interaction.

This is achieved by combining both optimal objective functions of T_g and EO_2 on control oriented models which developed individually in chapter 5. Further, the set of discrete PID parameters are applied on multivariable realistic model of T_g and EO_2 to optimise fuel consumption reduction and excess oxygen while sustaining the

glass temperature. Simulation results are presented to illustrate the effectiveness of the proposed method.

6.2 Decentralised PID Control of Multivariable Glass Furnace Process

A 2×2 (two-input two-output, TITO) multivariable control oriented glass furnace process model associated with a discrete decentralised 2 PID controllers structure and single loops, as illustrated in figure 6.1.

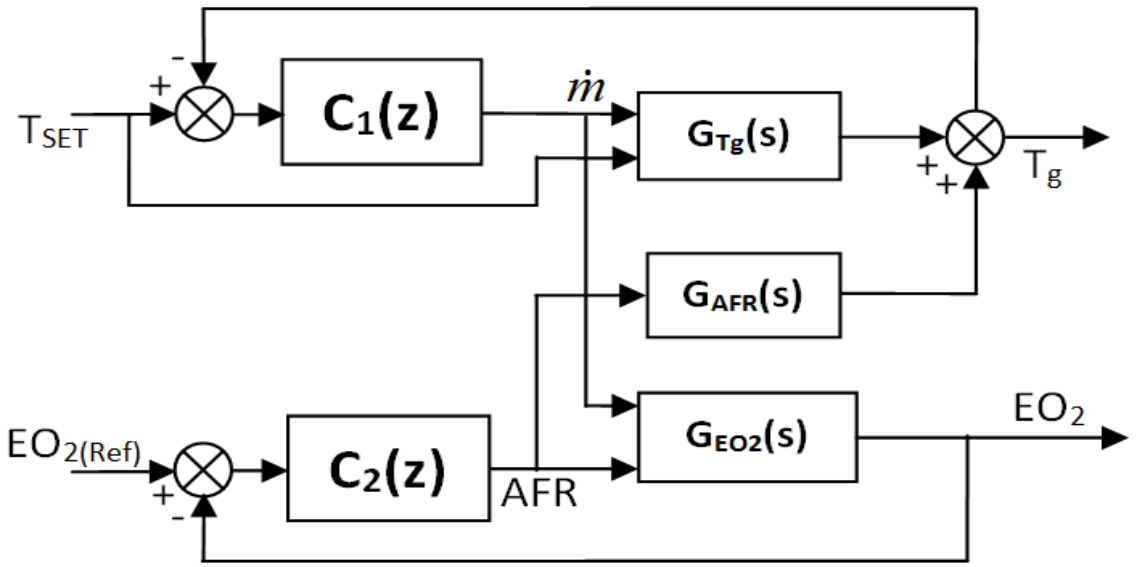

Figure 6.1: 2-input, 2-output (TITO) multivariable control oriented model under closed-loop discrete decentralised PID controllers

The pairing of controlled variables T_g and EO_2; with manipulated variables $\dot{m}$ and AFR can be performed by examining the process's relative gain array, either in the steady state or within the desired closed-loop bandwidth (Bristol, 1966). The discrete PID controllers can be arranged in the standard decentralised structure shown below,

$$C(z) = \begin{bmatrix} C_1(z) & 0 \\ 0 & C_2(z) \end{bmatrix} \tag{6.1}$$

The elements in the diagonal of the controller transfer function matrix $C(z)$ are single-input, single-output discrete PID controllers of the following standard form.

$$C_i(z) = K_{P_i}\left(1 + K_{I_i}\frac{T}{2}\frac{(z+1)}{(z-1)} + K_{D_i}\frac{1}{T}\frac{(z-1)}{z}\right), i = 1, 2 \tag{6.2}$$

where $K_{P_i}(z)$, $K_{I_i}(z)$ and $K_{D_i}(z)$ denote the discrete proportional gain, integral gain and derivative gain respectively, of the discrete PID controller in loop i.

In general, the loops interactions within the process may cause the output of the controller in loop i to appear as a disturbance in all other loops. Therefore, the $i-th$ optimised PID controller must be well suitable for loop i to achieve the desired set point tracking performance, while the disturbances caused by the PID controller outputs of the remaining i loops are rejected.

According to the collected data of EO_2, the model is designed based on a step input of air ratio ($AFR_{(Mass)} = 17.2 : 1$). As discussed in section 3.4.1, any real numerical value of fuel in kg/s is representing in ratio of 1. Thus, there will be no effect on the EO_2 when $\dot{m}$ is changed. However, any variation in air-fuel ratio will affect the outputs of f_1 and f_2 (figure 3.2) which leads directly to changes in $\dot{m}$ and hence, T_g. Therefore, the multivariable glass furnace process has single loop interaction from AFR to T_g under closed-loop influences. The identified control oriented model of the interaction was,

$$G_{AFR}(s) = \frac{\Delta T_g(s)}{\Delta AFR(s)} = \frac{-61.5}{2e5s + 1} \tag{6.3}$$

The dynamics of the glass furnace process are represented by the following low order 2×3 transfer function matrix which is developed in chapter 4 for controller optimisation. The developed models are,

$$\begin{bmatrix} \Delta T_g(s) \\ \Delta EO_2(s) \end{bmatrix} = \begin{bmatrix} G_{T_g1} & G_{T_g2} & G_{AFR} \\ 0 & 0 & G_{EO_2} \end{bmatrix} \begin{bmatrix} \Delta\dot{m}(s) \\ \Delta T_{SET}(s) \\ \Delta AFR(s) \end{bmatrix} \tag{6.4}$$

For T_g control oriented model,

$$\Delta T_g(s) = G_{T_g1}(s)\Delta\dot{m}(s) + G_{T_g2}(s)\Delta T_{SET}(s) + G_{AFR}(s)\Delta AFR(s) \tag{6.5}$$

$$\Delta T_g(s) = \frac{4566.2}{1.98e5s+1}\Delta\dot{m}(s) + \frac{-0.92}{1.98e5s+1}\Delta T_{SET}(s) + \frac{-61.5}{2e5s+1}\Delta AFR(s)$$

For 1st order EO_2 control oriented model,

$$G_{EO_2} = \frac{\Delta EO_2(s)}{\Delta AFR(s)} = \frac{1.6299}{152.4s+1}e^{-174s} \tag{6.6}$$

For 2st order EO_2 control oriented model,

$$G_{EO_2} = \frac{\Delta EO_2(s)}{\Delta AFR(s)} = \frac{1.5544}{1.446e4s^2+181s+1}e^{-110s} \tag{6.7}$$

6.2.1 Control Oriented Optimisation Techniques

The optimisation of discrete decentralised control strategies are analysed by three SGAs tuning approaches, associated with the 2×2 control oriented multivariable glass furnace model as illustrated in figure 6.1. The three SGAs tuning approaches are applied individually on closed-loop step input tests for both 1st and 2nd order control oriented EO_2 models associated with the control oriented T_g model. The performance criteria for both T_g and EO_2 remain unchanged as discussed in section 5.3.1.

The three tuning approaches are:

- SGAs-1: the discrete PID parameters of both T_g and EO_2 are optimised individually with their respective closed-loop control oriented models without loop interactions. $C_1(z)$ is optimised with respective cost function $\left(J_{i(T_g)}\right)$; $T_{SET} = 1500K \longrightarrow 1550K$; $EO_{2(Ref)}$ is constant (2.45%). $C_2(z)$ is optimised with respective cost function $\left(J_{i(T_g)}\right)$; $EO_{2(Ref)} = 2.45\% \longrightarrow 3\%$; T_{SET} is constant $(1500K)$.

$$\begin{aligned} J_{i(T_g)} &= (IAE + \lambda ISU)_{T_g} \\ J_{i(EO_2)} &= IAE_{EO_2} \end{aligned} \tag{6.8}$$

- SGAs-2: the discrete PID parameters of both T_g and EO_2 are optimised

individually with their respective closed-loop control oriented models with loop interactions. $C_1(z)$ is optimised with respective cost function $\left(J_{i(T_g)}\right)$; $T_{SET} = 1500K \longrightarrow 1550K$; $EO_{2(Ref)}$ is constant (2.45%). $C_1(z)$ and $C_2(z)$ are optimised with respective cost function $\left(J_{i(T_g)}\right)$; $EO_{2(Ref)} = 2.45\% \longrightarrow 3\%$; T_{SET} is constant $(1500K)$.

$$\begin{aligned} J_{i(T_g)} &= (IAE + \lambda ISU)_{T_g} + 0 \\ J_{i(EO_2)} &= IAE_{T_g} + IAE_{EO_2} \\ J_{i(Total)} &= T_{i(T_g)} + J_{i(EO_2)} \end{aligned} \tag{6.9}$$

- SGAs-3: the discrete PID parameters of both T_g and EO_2 are optimised simultaneously by multivariable closed-loop control oriented models with loop interaction. The optimised cost function is modified to include the total loop effect of T_g and EO_2 by applying step inputs on both set points, T_{SET} and $EO_{2(Ref)}$ at two different time periods in one simulation as illustrated in equation 6.10. $C_1(z)$ and $C_2(z)$ are optimised with modified cost function $\left(J_{i(Total)}\right)$: $T_{SET} = 1500K \longrightarrow 1550K$ at EO_2 is constant (2.45%); $EO_{2(Ref)} = 2.45\% \longrightarrow 3\%$ at T_{SET} is steady-stae $(1500K)$.

$$J_{i(Total)} = (IAE + \lambda ISU)_{T_g} + IAE_{EO_2} \tag{6.10}$$

6.2.2 Simulation Results of Decentralised Control Oriented Model

Simulation results of the optimal set of discrete PID control parameters by the three tuning approaches are tabled (table 6.1, 6.2) and the respective responses are figured (figure 6.2, 6.3, 6.4, 6.5) for comparison, accordingly. The converged values of J_i for both T_g and EO_2 as tabulated in table 6.3 by three SGAs tuning approaches.

As discussed earlier, the output response of EO_2 will not be affected by any variation in $\dot{m}$ as the AFR is constant. Therefore, the optimised discrete PID

parameters for 1st and 2nd order control oriented models of EO_2 by the three tuning approaches are exhibiting similarities to the individually optimised PID parameters in section 5.5.1.

Table 6.1: Identified PID parameters for T_g and 1st order control oriented model of EO_2 by three SGAs tuning approaches

Tuning Approach	T_g				EO_2			
	K_P	K_I	K_D	Ts(2%)	K_P	K_I	K_D	Ts(2%)
SGA-1	1.042e-2	7.771e-5	7.211	4.9Hrs	0.8152	4.417e-3	35.92	4.9min
SGA-2	1.053e-2	7.827e-5	7.681	4.9Hrs	0.8151	4.418e-3	35.38	4.9min
SGA-3	1.076e-2	8.253e-5	7.458	4.9Hrs	0.8149	4.418e-3	36.17	4.9min

Table 6.2: Identified PID parameters for T_g and 2nd order control oriented model of EO_2 by three SGAs tuning approaches

Tuning Approach	T_g				EO_2			
	K_P	K_I	K_D	Ts(2%)	K_P	K_I	K_D	Ts(2%)
SGA-1	1.041e-2	8.812e-5	7.317	4.9Hrs	0.8642	4.348e-3	83.81	5.2min
SGA-2	1.067e-2	8.767e-5	7.539	4.9Hrs	0.8639	4.349e-3	83.79	5.2min
SGA-3	1.083e-2	8.558e-5	7.745	4.9Hrs	0.8634	4.348e-3	84.27	5.2min

Table 6.3: Error criteria with respective cost function by three SGAs tuning approaches

Tuning Approach	1st Order EO_2			2nd Order EO_2		
	$J_{i(T_g)}$	$J_{i(EO_2)}$	$J_{i(Total)}$	$J_{i(T_g)}$	$J_{i(EO_2)}$	$J_{i(Total)}$
SGA-1	3.111e4	175.2	3.129e4	3.111e4	159.1	3.127e4
SGA-2	3.111e4	625.8	3.174e4	3.111e4	609.7	3.172e4
SGA-3	-	-	3.461e4	-	-	3.459e4

This is clearly noticeable in figures 6.2 and 6.4, where both order control oriented models of EO_2 by these tuning approaches are significantly exhibiting similarities in responses as only a single loop interaction is present, $AFR \longrightarrow T_g$.

Despite, the similarities in K_P and K_I values of both control oriented models of EO_2, the K_D value of 2nd order model is significantly higher (approximately, 134.3%) than 1st order model. This significant higher K_D value is required to consolidate the curvature dynamic of the initial rising of the output response after the transport delay for 2nd order model. Apart from the differences in K_D, the settling time of 2nd order model is 4% higher than desired settling time ($5mins$) and 6.12% higher

than 1st order model (4.9*mins*). This is due to the differences in rise time between the transport delay and settling time of both order models, which are illustrated in figures 6.2 and 6.4.

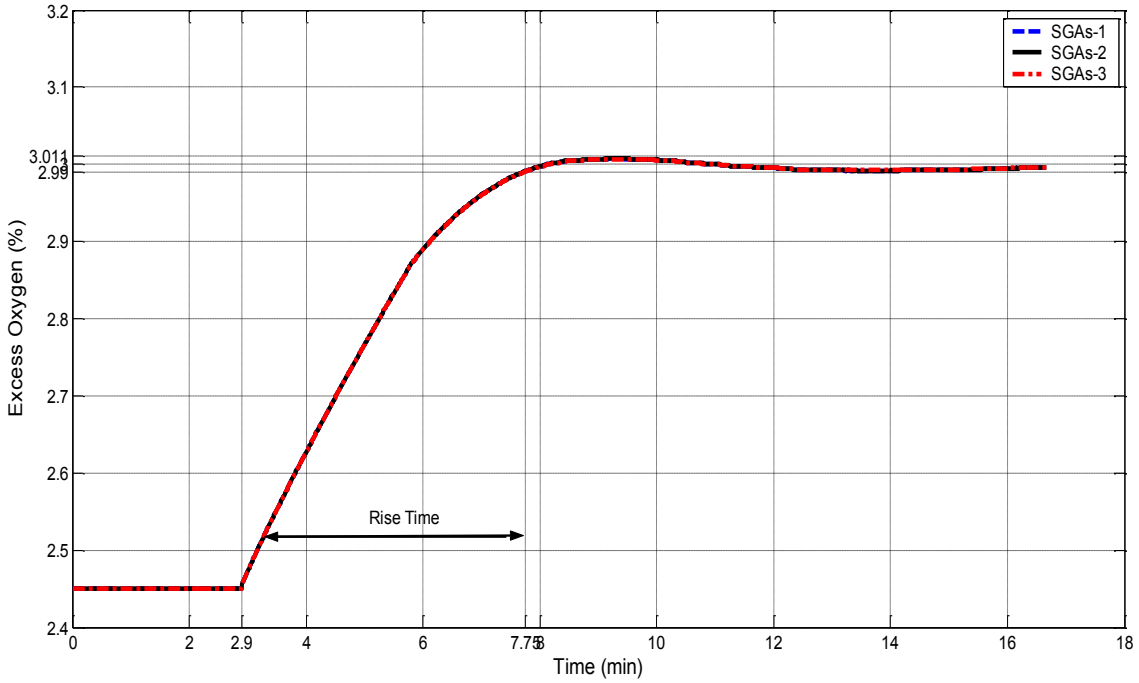

Figure 6.2: Transient responses of 1st order control oriented model of EO_2 by three SGAs tuning approaches

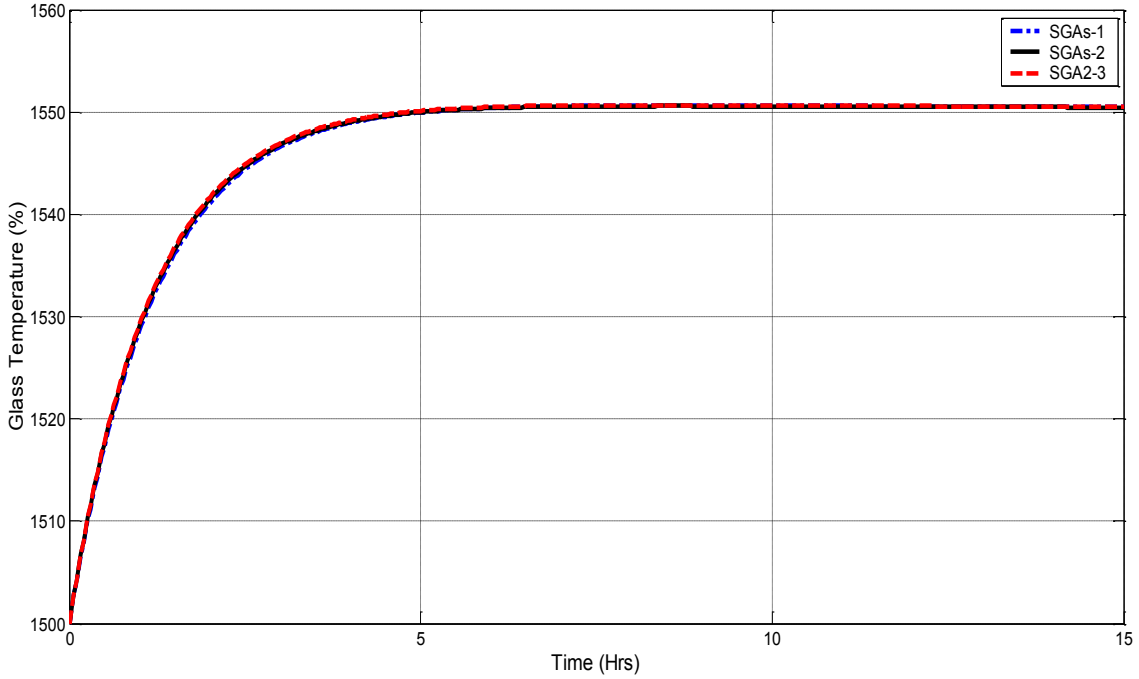

Figure 6.3: Transient responses of T_g with single-loop interaction by 2nd order control oriented model of EO_2 by three SGAs tuning approaches

For T_g, the K_P and K_D values by 1st order EO_2 model (table 6.1) are exhibiting similarities by three tuning approaches. But, the K_I value of 1st order model by SGAs-3 is insignificantly higher than SGAs-1 and SGAs-2 by 6.2% and 5.4%, respectively. Whereas, the three discrete control parameters, K_P, K_I and K_D by 2nd order EO_2 model for T_g are similar for the three tuning approaches as illustrated in table 6.2.

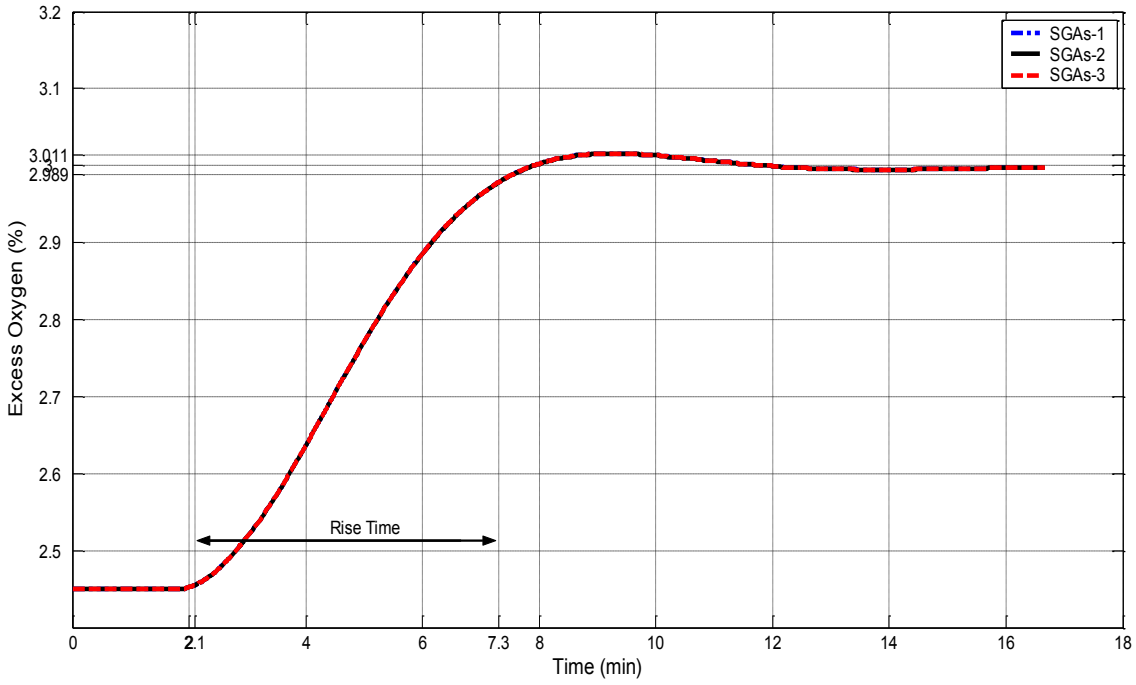

Figure 6.4: Transient responses of 2nd order control oriented model of EO_2 by three SGAs tuning approaches

Further comparison, the K_I value by SGAs-3 by 2nd order EO_2 model is similar with 1st order EO_2 model. While, the K_I values by SGAs-1 and SGAs-2 for the 2nd order model are 12.7% higher than the 1st order EO_2 model. This is illustrated in table 6.3 that the tuning approaches of SGAs-1 and SGAs-2 for the 2nd order model have improved the cost function by 9.1% (SGAs-1) and 3% (SGAs-2) compared to the 1st order model.

On the other hand, all three tuning approaches with the single loop interaction ($AFR \longrightarrow T_g$) have significantly varied the discrete PID parameters to sustain the T_g according to the performance criterion. This can be noticed in tables 6.1, 6.2 and 6.3 that the consolidation of discrete PID parameter and the similarities in $J_{i(T_g)}$ (3.111×10^4) by SGAs-1 and SGAs-2 to maintain the T_g, accordingly.

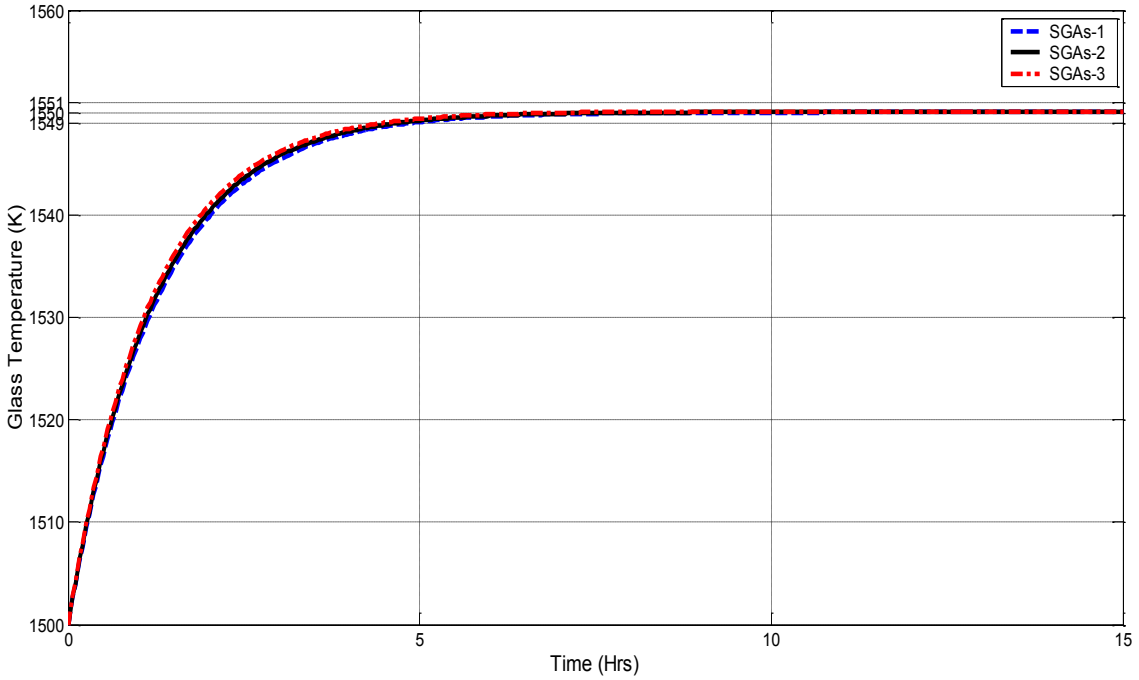

Figure 6.5: Transient responses of T_g with single-loop interaction by 1st order control oriented model of EO_2 by three SGAs tuning approaches

The SGAs-3 is a new PID parameter tuning approach to compensate the loop interaction by including the total effect in one cost function for the whole multivariable process in one simulation period. As illustrated in figure 6.6, at $t_1 = 0hrs$, a step input is applied on $T_{SET} = 1500K \longrightarrow 1550K$ while the $EO_2 = 2.45\%$ (constant). At $t_2 = 8hrs$, step input applied on $EO_2 = 2.45\% \longrightarrow 3\%$ while the $T_{SET} = 1550K$ (steady-state attained according to performance criterion). From t_1 to t_2, technically the cost function of T_g $(IAE + \lambda ISU)$ is optimising the $C_1(z)$ without any loop interaction effect of step input of the $EO_{2(Ref)}$ cost function (IAE), which is cancelled by the AFR relationship inherent in the process.

Then, from t_2 the total effect of T_g and EO_2 cost functions $(J_{i(Total)})$ are integrate together for further optimisation of PID parameters of $C_1(z)$ to compensate the loop interaction while optimising the $C_2(z)$, individually. The whole SGAs-3 tuning approach is illustrated in figure 6.6. However, as illustrated in table 6.3, the simulation result exhibits that the SGAs-3 tuning approach has higher $J_{i(Total)}$ than the SGAs-1 and SGAs-2 while compensating the loop interaction.

In overall, the optimised discrete PID parameters by the three tuning approaches are exhibiting significant performances for T_g and EO_2 with the respective model

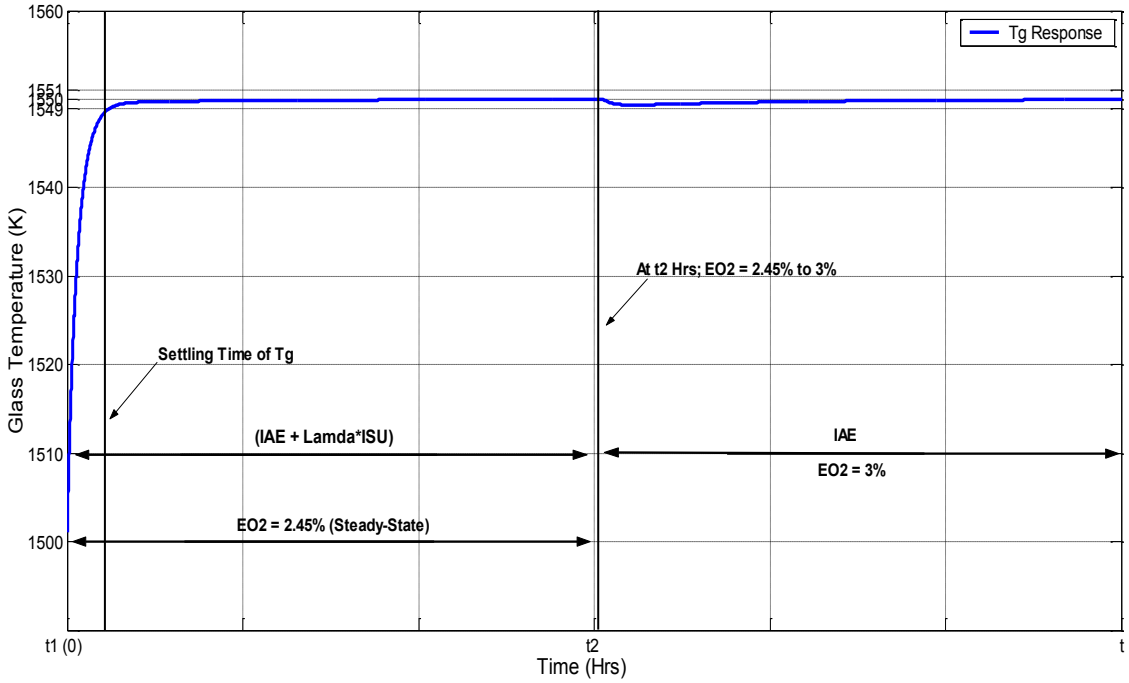

Figure 6.6: Response of T_g by SGAs-3 to include the total effect of loop compensation in one cost function, $J_{i(Total)}$

orders. Based on the tables 6.1 and 6.2, the optimised discrete PID parameters by the three tuning approaches using 2^{nd} order control oriented model of EO_2 may be more suitable on the realistic model application. But, it is still difficult to conclude at this stage which discrete PID parameters are well suitable and applicable for the realistic multivariable model.

Therefore, the optimised discrete PID parameters by all three tuning approaches with respective control oriented models will be applied on the realistic model to further evaluate and assess the performances.

6.3 Decentralised PID Control of Realistic Multivariable Glass Furnace Model

Figure 6.7 illustrated the 2×2 complete realistic multivariable glass furnace model with decentralised control. The 24 state-space T_g model, as discussed in chapter 3, and the complete 4^{th} order EO_2 model with nonlinearity effect, as discussed in section 4.8.2, are selected as the realistic model to assess the control performance.

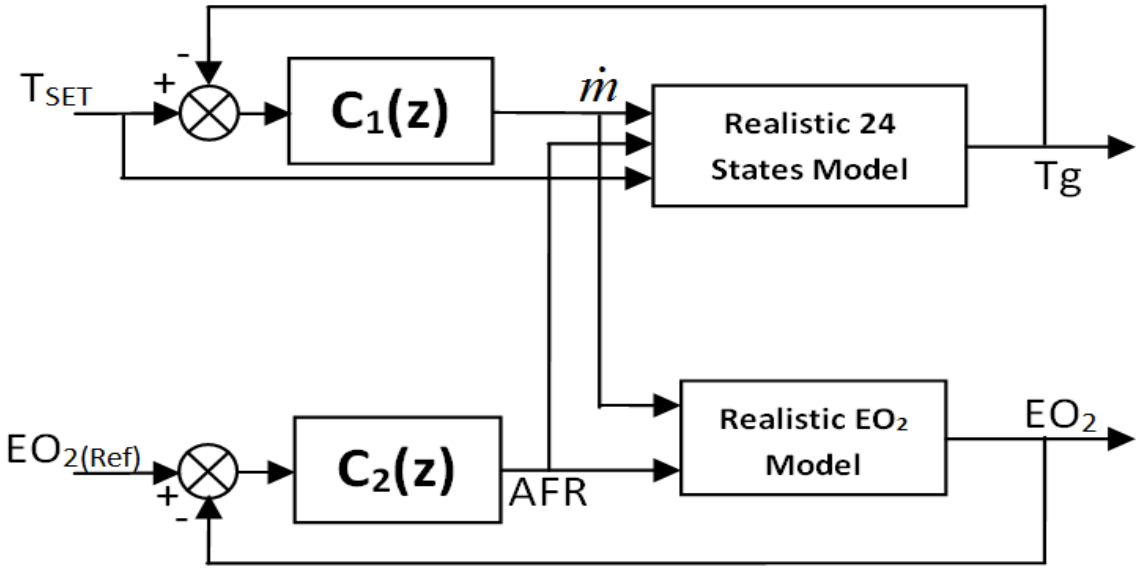

Figure 6.7: 2-input, 2-output (TITO) realistic multivariable model under closed-loop discrete decentralised PID control

According to the stoichiometric methane combustion processes, the optimum region of highest efficiency is 10% to 20% of excess air, which is approximately 1.5% to 3% of EO_2. In addition, the permissible maximum limit of EO_2 for furnace type industries is 3% (SEPA, 2005). Theoretically, the EO_2 should not be traced for stoichiometric $AFR_{(Mass)}$ (17.2). However, the EO_2 does trace in stoichiometric combustion for the industrial data used in this research.

Therefore, a reduction of EO_2 within the optimum region to reduce fuel consumption while sustaining the thermal efficiency of combustion is the main concern here. The performances criteria for both T_g and EO_2 are formulated in section 5.3.1 are unchanged for the closed-loop decentralised realistic multivariable process.

6.3.1 Simulation Results of Realistic Multivariable Process Model

The optimised discrete PID parameters for $C_1(z)$ and $C_2(z)$ by all three tuning approaches with their respective model orders of EO_2 and T_g (table 6.1 and 6.2) will be applied for performance assessment on the realistic multivariable glass furnace process by two simulation tests:

1). control robustness and loop stability,

2). minimum fuel consumption.

6.3.1.1 Control Robustness and Loop Stability

Figure 6.8 and 6.9 illustrate the performance assessment of optimised discrete PID parameters for T_g and EO_2 by decentralised control oriented model on realistic multivariable process with loop interaction.

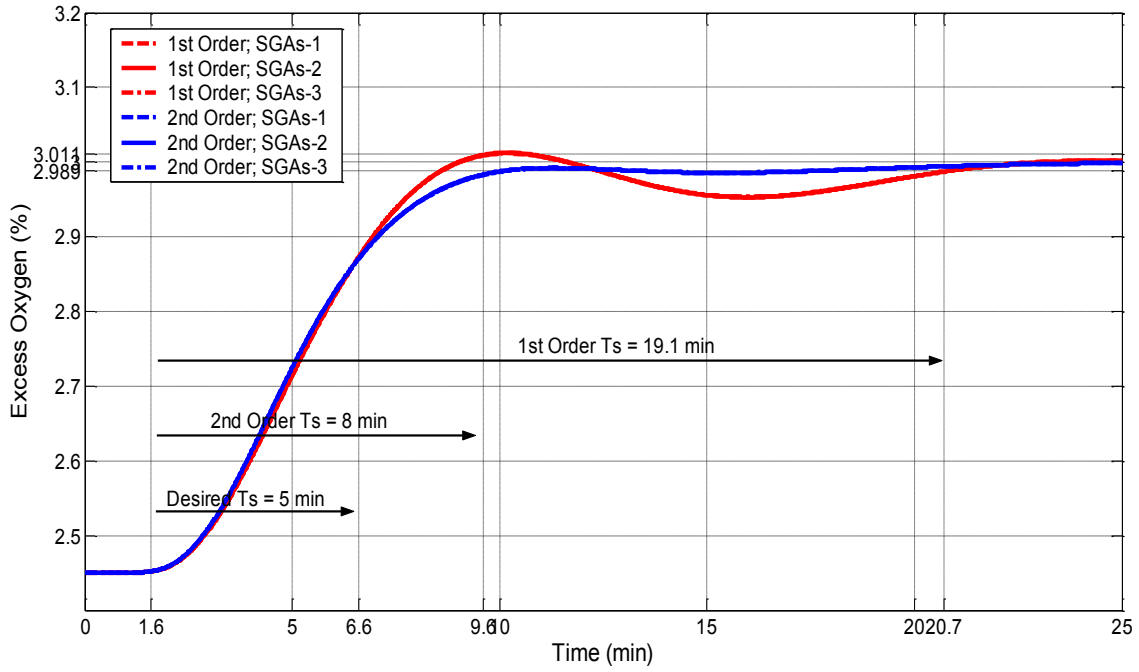

Figure 6.8: Comparison of EO_2 control responses on 4^{th} order nonlinear realistic model

According to the figure 6.7, all three tuning approaches (SGAs-1, SGAs-2 and SGAs-3) using 1^{st} and 2^{nd} order control oriented EO_2 linear models for EO_2, the discrete PID parameters demonstrate incomparable responses on the realistic model.

The simulation result discloses that the 2^{nd} order model's discrete PID parameters exhibits a better performance and dynamic characteristics than the 1^{st} order model's discrete PID parameters on the 4^{th} order nonlinear realistic model.

However, the settling time ($ts = 9.6mins$) is lagged about $3mins$ caused by the nonlinear effect and initial transport delay of the realistic model. While, the 1^{st} order model's discrete PID parameters exhibits insignificant oscillatory response and long settling time ($19.1mins$) on the realistic model.

As discussed in EO_2 control response comparison on 4^{th} order nonlinear realistic model, the identified discrete PID parameters for T_g by SGAs-1 and SGAs-2 of 1^{st}

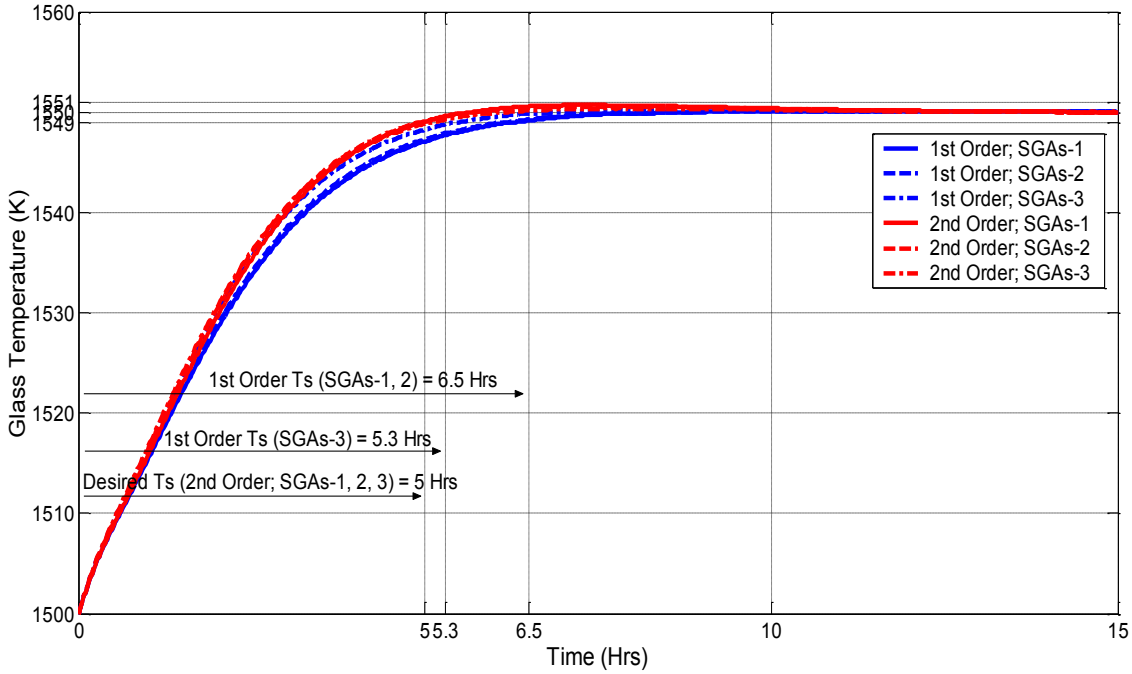

Figure 6.9: Comparison of T_g control responses on 24 state-space realistic model

control oriented EO_2 linear model exhibits ineffectiveness and inabilities to attain the desired performance criterion ($ts = 6.5hrs$) due to loop interaction. While, the SGAs-3 demonstrated the effectiveness of compensating the loop interaction even though the settling time is lagged about $0.3hrs$ ($18mins$).

As expected, the SGAs-1, SGAs-2 and SGAs-3 with 2^{nd} order control oriented linear EO_2 model exhibits better dynamic characteristics for T_g according to the desired settling time, $ts = 5hrs$.

However, insignificant differences between all three tuning approaches by 2^{nd} order EO_2 model for T_g responses on realistic model is insufficient to distinguish the discrete control parameters suitability.

Further, the loop stability and control robustness are investigated due to nonlinearity effects which may have occurred in step input variations due to the methane chemical relationship of stoichiometric $\text{AFR}_{(\text{Volumetric})}$ with $EO_{2(\%)}$.

As a result, figures 6.10 and 6.11 illustrate the robust responses of T_g for the three sets of optimised discrete PID parameters (SGAs-1, SGAs-2 and SGAs-3) by EO_2 models under loop interaction on the multivariable process.

The simulations of the two EO_2 step input tests are elaborated as follows;

By 1st order control oriented EO_2 model's three tuning approaches,

- At $T_g = 1550K$ (steady state); $EO_2 = 2.45\% \longrightarrow 3.45\%$; causes a reduction in $T_g = 1550K \longrightarrow 1548.7K$ (approximately).
- At $T_g = 1550K$ (steady state); $EO_2 = 2.45\% \longrightarrow 1.45\%$; causes a reduction in $T_g = 1550K \longrightarrow 1551.2K$ (approximately).

By 2nd order control oriented EO_2 model's three tuning approaches,

- At $T_g = 1550K$ (steady state); $EO_2 = 2.45\% \longrightarrow 3.45\%$; causes a reduction in $T_g = 1550K \longrightarrow 1548.9K$ (approximately).
- At $T_g = 1550K$ (steady state); $EO_2 = 2.45\% \longrightarrow 1.45\%$; causes a reduction in $T_g = 1550K \longrightarrow 1551.2K$ (approximately).

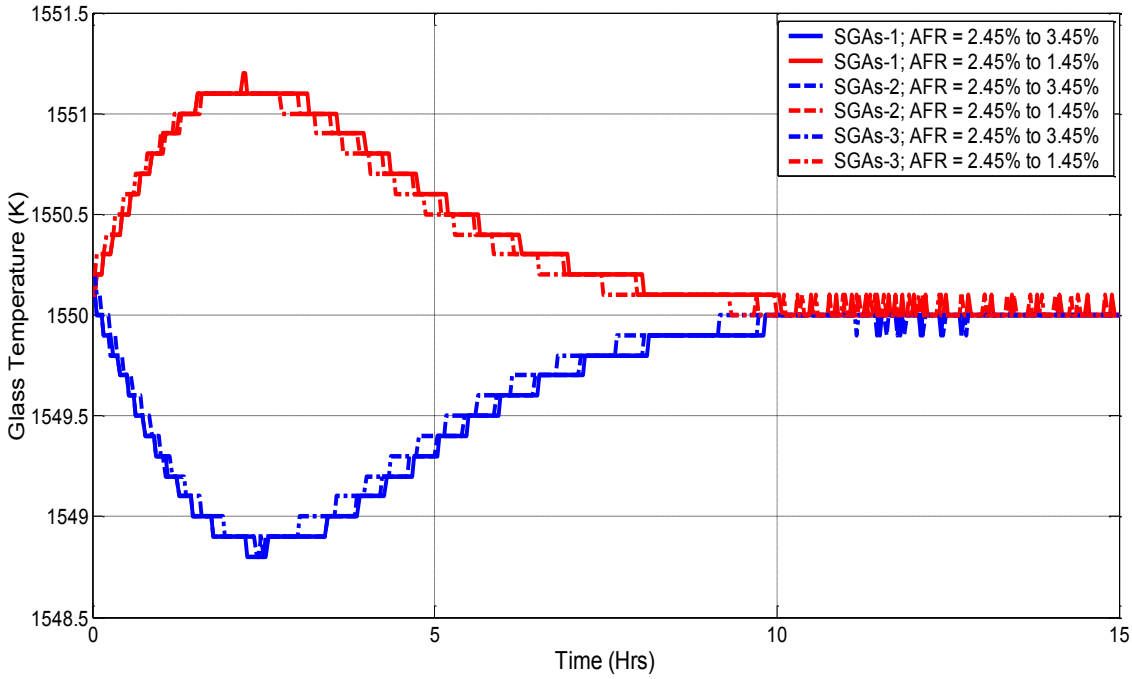

Figure 6.10: T_g responses under loop interaction of multivariable process by 1st order EO_2 model's discrete PID parameters ($\Delta 1\%_{(AFR)}$)

According to the simulation results, the T_g responses under loop interaction with 1st and 2nd order EO_2's discrete PID parameters exhibits a very similar and insig-

nificant effect on loop stability with all three tuning approaches by EO_2 step input variation as a disturbance. However, the 2nd order EO_2 model's control parameters has better zero steady-state error ($8.5hrs$) than the 1st order EO_2 model's control parameters ($9.7hrs$), which illustrate a 12.4% faster steady-state error.

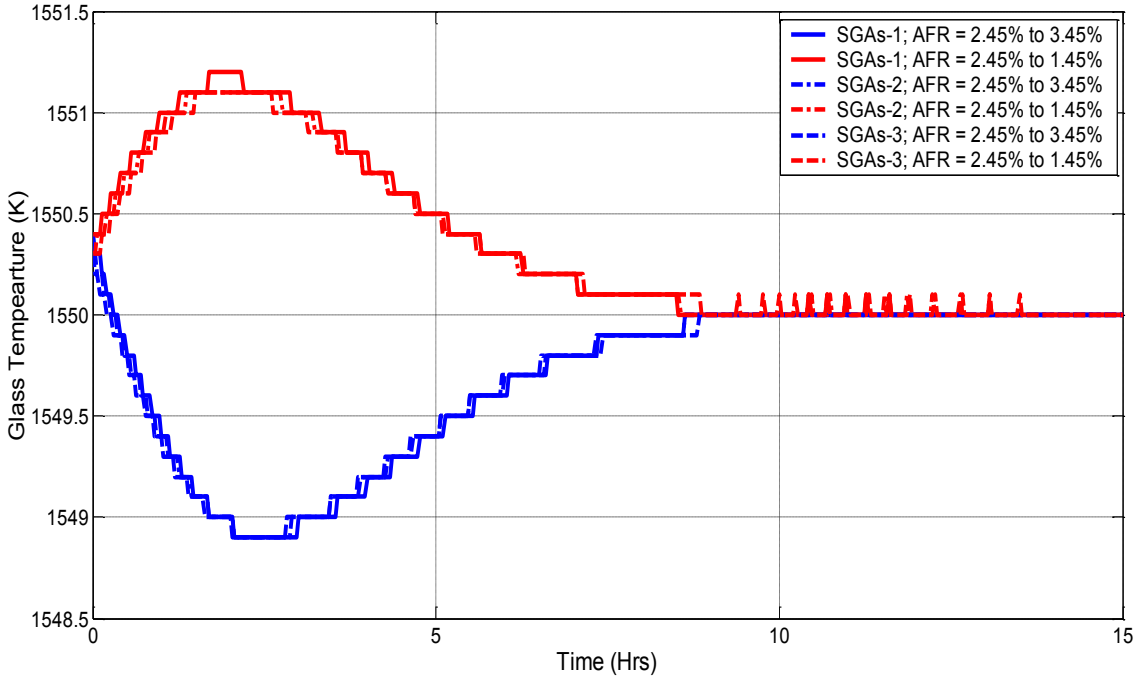

Figure 6.11: T_g responses under loop interaction of multivariable process by 2nd order EO_2 model's discrete PID parameters ($\Delta 1\%_{(AFR)}$)

Therefore, the 2nd order EO_2 model's control parameters has better loop interaction compensation and control robustness than the 1st order EO_2 model's control parameters.

6.3.1.2 Minimum Fuel Consumption

Another performance of loop interaction and discrete control parameters can be assessed according to the fuel and air consumption. An increase and a decrease in air consumption are causing a reduction and an increase in glass temperature, respectively. In actual condition, high excess air ratio will blow away the heat from the combustion chamber and can cause a reduction in T_g (Carniglia and Barna, 1992). As discussed in section 6.4, the optimum thermal efficiency of the combustion process is within the range of 1.5% to 3% of EO_2, which is equivalent to about 10%

to 20% of excess air. Therefore, a reduction in air ratio approximately 2% of EO_2 is primarily of concern here to minimise the fuel consumption.

Under closed-loop steady-state of T_g; the $T_{SET} = 1500K$ and stoichiometric $AFR_{(Mass)} = 17.2$, the air consumption is $0.04684kg/s$ and the fuel consumption is $0.002723kg/s$. Whereas, at $T_{SET} = 1550K$ and stoichiometric $AFR_{(Mass)} = 17.2$, the air consumption is $0.05060kg/s$ and the fuel consumption is $0.002942kg/s$.

Table 6.4: Fuel consumption for multivariable process by 2% of EO_2 reduction

Tuning Approach	1st Order Linear EO_2Model		2nd Order Linear EO_2Model	
	2(%) EO_2 Reduction	Fuel Reduction (%)	2(%) EO_2 Reduction	Fuel Reduction (%)
SGAs-1	0.002873	2.345	0.002871	2.413
SGAs-2	0.002872	2.379	0.002870	2.447
SGAs-3	0.002870	2.447	0.002868	2.515

Simulation results in figures 6.12, 6.13 and table 6.4 illustrate the comparison of fuel consumption under closed-loop two step inputs of multivariable loop interaction. The three tuning approaches with two step inputs in EO_2 are elaborated as follows;

By 1st order control oriented EO_2 model's three tuning approaches,

- SGAs-1 – At $T_{SET} = 1550K$ (steady state); $EO_2 = 2.45\% \longrightarrow 2\%$; The $AFR_{(Mass)}$ is decreased $17.2 \longrightarrow 16.75$, accordingly. To obey a decrease in $AFR_{(Mass)}$, the air ratio and fuel ratio are decreased to $0.04812kg/s$ and $0.002873kg/s$ while maintaining T_{SET}.

- SGAs-2 – At $T_{SET} = 1550K$ (steady state); $EO_2 = 2.45\% \longrightarrow 2\%$; The $AFR_{(Mass)}$ is decreased $17.2 \longrightarrow 16.75$, accordingly. To obey a decrease in $AFR_{(Mass)}$, the air ratio and fuel ratio are decreased to $0.04811kg/s$ and $0.002872kg/s$ while maintaining T_{SET}.

- SGAs-3 – At $T_{SET} = 1550K$ (steady state); $EO_2 = 2.45\% \longrightarrow 2\%$; The $AFR_{(Mass)}$ is decreased $17.2 \longrightarrow 16.75$, accordingly. To obey a decrease in $AFR_{(Mass)}$, the air ratio and fuel ratio are decreased to $0.04807kg/s$ and $0.002870kg/s$ while maintaining T_{SET}.

By 2nd order control oriented EO_2 model's three tuning approaches,

- SGAs-1 – At $T_{SET} = 1550K$ (steady state); $EO_2 = 2.45\% \longrightarrow 2\%$; The $AFR_{(Mass)}$ is decreased $17.2 \longrightarrow 16.75$, accordingly. To obey a decrease in $AFR_{(Mass)}$, the air ratio and fuel ratio are decreased to $0.04809kg/s$ and $0.002871kg/s$ while maintaining T_{SET}.

- SGAs-2 – At $T_{SET} = 1550K$ (steady state); $EO_2 = 2.45\% \longrightarrow 2\%$; The $AFR_{(Mass)}$ is decreased $17.2 \longrightarrow 16.75$, accordingly. To obey a decrease in $AFR_{(Mass)}$, the air ratio and fuel ratio are decreased to $0.04807kg/s$ and $0.002870kg/s$ while maintaining T_{SET}.

- SGAs-3 – At $T_{SET} = 1550K$ (steady state); $EO_2 = 2.45\% \longrightarrow 2\%$; The $AFR_{(Mass)}$ is decreased $17.2 \longrightarrow 16.75$, accordingly. To obey a decrease in $AFR_{(Mass)}$, the air ratio and fuel ratio are decreased to $0.04804kg/s$ and $0.002868kg/s$ while maintaining T_{SET}.

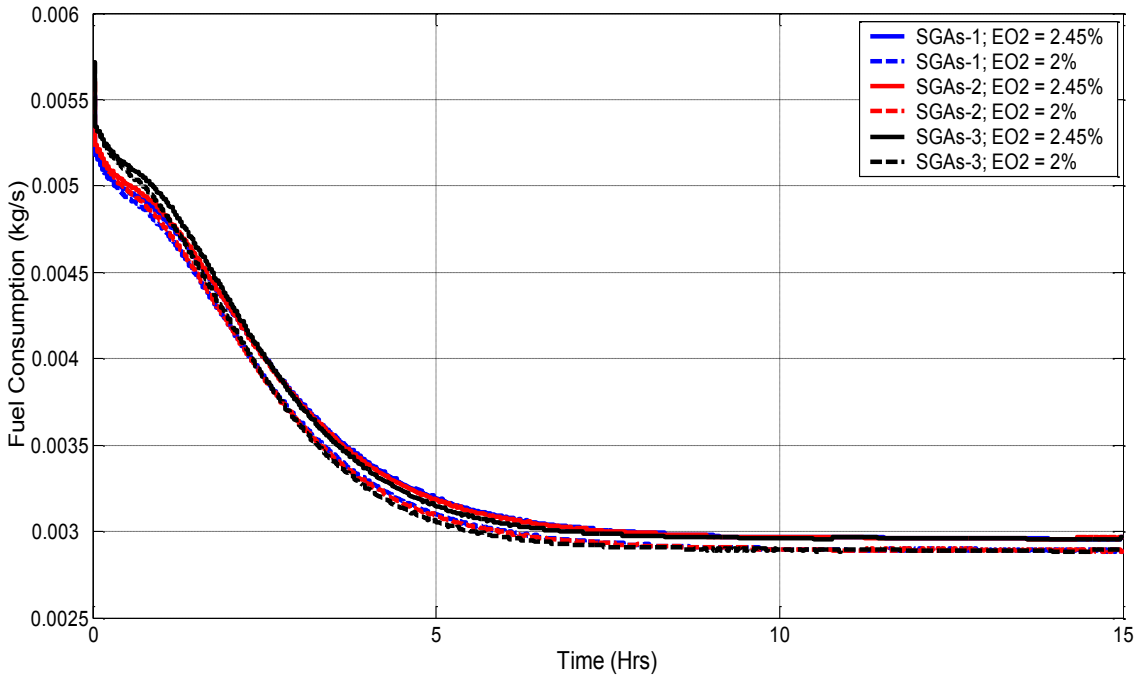

Figure 6.12: Fuel consumption under loop interaction of realistic multivariable process by 1st order EO_2 model's discrete PID parameters ($\Delta 1\%_{(AFR)}$)

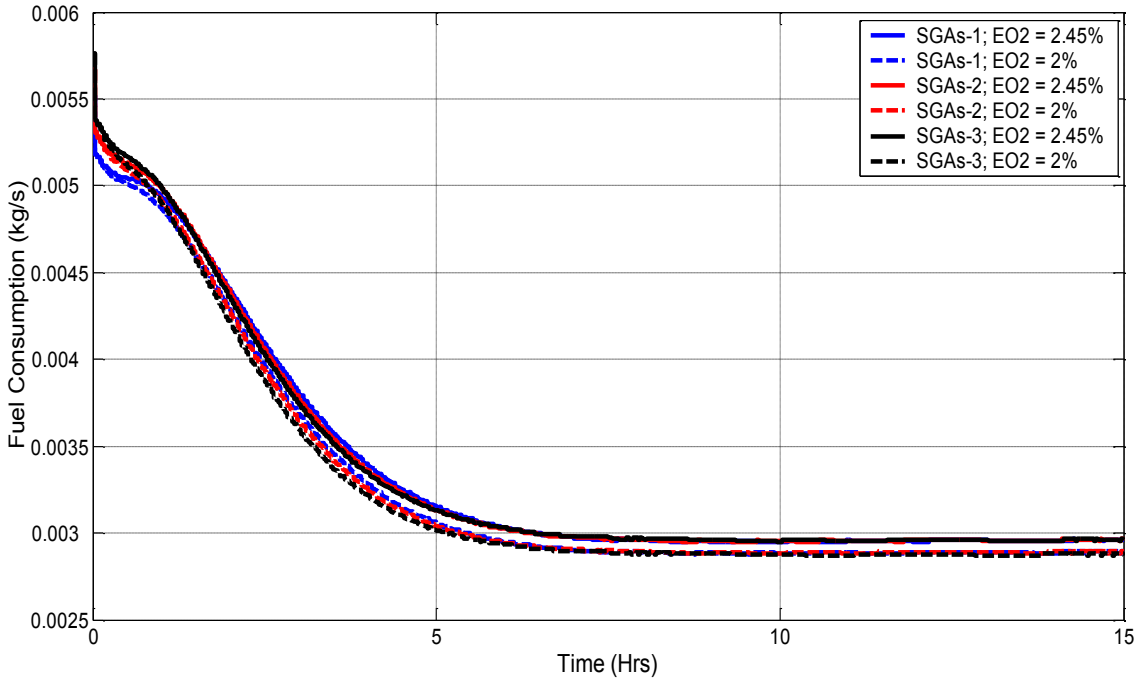

Figure 6.13: Fuel consumption under loop interaction of realistic multivariable process by 2nd order EO_2 model's discrete PID parameters ($\Delta 1\%_{(AFR)}$)

According to the figures 6.12 and 6.13, the initial dynamic progression of fuel consumption by SGAs-3 on both EO_2 models discrete control parameters are exhibiting a stronger dynamic than the SGAs-1 and SGAs-2. Such a dynamic response causes fast settling time and minimum fuel consumption as the dynamic response is in progression towards the steady-state value.

Further, the tuning approach, SGAs-3 of 1st order EO_2 model's control parameters has similar fuel consumption ($2.447\%_{(EO_2=2\%)}$) with SGAs-2 of 2nd order EO_2 model's control parameters. This illustrates that the 2nd order EO_2 model's control parameters on the 4th order realistic model of EO_2 is compensating well the loop interaction.

In overall, the SGAs-3 of 2nd order EO_2 model has 2.5% better fuel consumption than SGAs-1 and SGAs-2 with their respective discrete control parameters under loop interaction for the multivariable process.

Therefore, the tuning approach of SGAs-3 with respective PID discrete parameters for $C_1(z)$ and $C_2(z)$ by 2nd order EO_2 model is well acceptable for control of the multivariable process of EO_2 and T_g.

Table 6.5 illustrates the total fuel consumption of realistic multivariable process

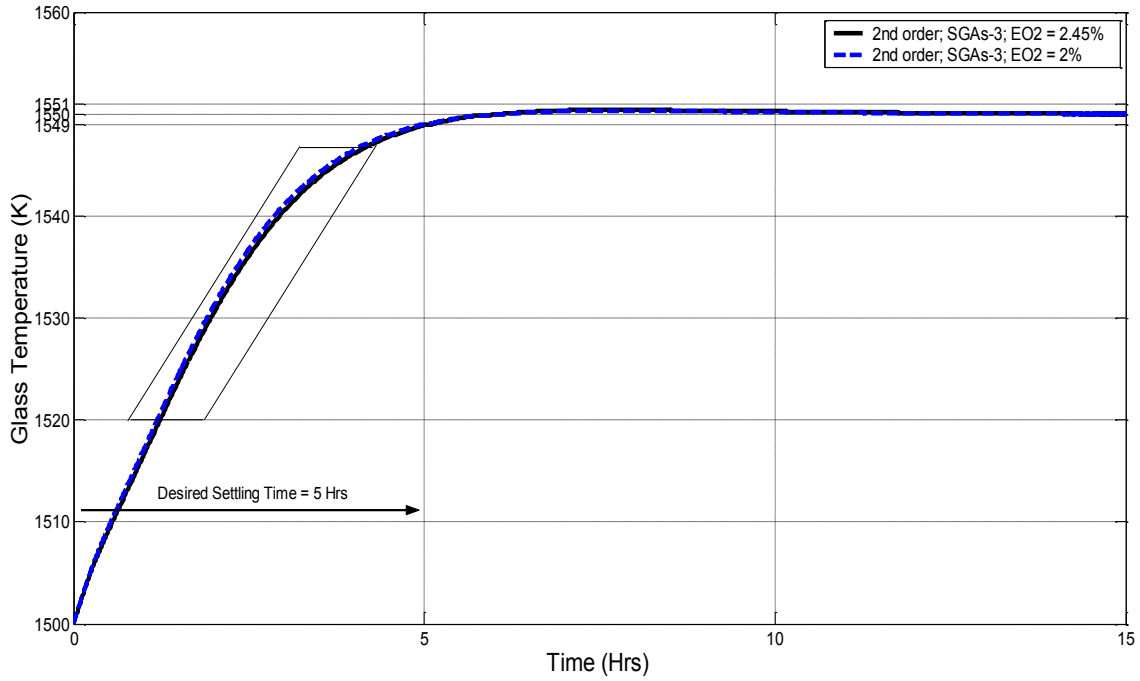

Figure 6.14: Comparison of steady-state of T_g responses by two set-points of EO_2

by 2% of EO_2 reduction. A fraction of EO_2 reduction (2.5%) for methane combustion causes vast amount of saving in methane fuel consumption, $2334kg$ in a year of operation.

In addition, figure 6.14 illustrates the comparison of dynamic responses for T_g by two set-point changes of EO_2. A reduction in $EO_{2(2.45\% \longrightarrow 2\%)}$, the steady-state of T_g still maintained even if there is an insignificant glitch on dynamic progression.

Despite the single objective function is applied, three objectives have been achieved relatively as a multi-objective function by SGAs. Apart from the fuel minimisation, the EO_2 emissions associated with undesirable emissions can be tightly controlled within the permitted limit at any glass melting period and the steady-state of T_g is still maintained.

In the end, a reduction of EO_2 within the optimum thermal efficiency region of methane combustion ($1.5\% \leftrightarrow 3\%$) will be beneficial for minimising the undesirable emissions and fuel consumption while sustaining the thermal efficiency of combustion.

6.4 Summary

In this chapter, the improved and modified objective function, equation 6.10 ($(IAE+\lambda ISU_{T_g}) + IAE_{EO_2}$), is introduced here to optimise the discrete PID parameters ($C_1(z)$ and $C_2(z)$) according to the desired performance criteria. The modified objective function includes the total effect of loop interaction of both T_g and EO_2 processes in a single simulation period (SGAs-3).

Based on simulation result, the optimised discrete PID parameters for 1st and 2nd order control oriented models of EO_2 by the three tuning approaches are exhibiting similarities to the individually optimised PID parameters as only a single loop interaction is present, $AFR \longrightarrow T_g$.

For T_g, the K_P and K_D values by 1st order EO_2 model are exhibiting similarities by three tuning approaches. But, the K_I value of 1st order model by SGAs-3 is insignificantly higher than SGAs-1 and SGAs-2 by 6.2% and 5.4%, respectively to compensate the loop interaction. Whereas, the K_I values by SGAs-1 and SGAs-2 for the 2nd order model are 12.7% higher than the 1st order EO_2 model.

While, the three tuning approaches of the 2nd order model have improved the $J_{i(T_g)}$ by 9.1% (SGAs-1) and 3% (SGAs-2) and 2.1% (SGAs-3) compared to the 1st order model. In overall, the 2nd order liner control oriented model of EO_2 with SGAs-3 well characterises and compensates the dynamic loop interaction effect for control parameters optimisation.

The simulation result discloses that the 2nd order model's discrete PID parameters exhibits a better performance and dynamic characteristics than the 1st order model's discrete PID parameters on the realistic multivariable process. The 2nd order EO_2 model's control parameters has better zero steady-state error ($8.5hrs$) than the 1st order EO_2 model's control parameters ($9.7hrs$), which illustrate a 12.4% faster steady-state error.

Further, the 2nd order EO_2 model with SGAs-3 has 2.52% better fuel consumption than SGAs-1 and SGAs-2 on the 4th order realistic model of EO_2 while compensating well the loop interaction for the multivariable process.

According to the table 6.5, the total fuel consumption of realistic multivariable

Table 6.5: Simulation result of fuel consumption by 2% $EO_{2(Ref)}$ reduction

EO_2 (%)	AFR (Mass)	Closed-Loop Steady State Fuel Flow (kg/s)	Fuel Consumption (kg)($24hrs$ Operation)	Fuel Consumption (kg)($1year$ Operation)
2.45	17.2	0.002942	254.19	92778.9
2	16.75	0.002868	247.8	90445.2

process by 2% of EO_2 reduction. A reduction in $EO_{2(2.45\% \longrightarrow 2\%)}$, the fuel consumption is minimised by 2.52% ($0.002942kg/sec \rightarrow 0.002868kg/sec$) while the T_g is sustained at steady state, T_{SET}. Also, such a reduction is saving $2334kg$ of methane fuel consumption in $1year$ of operation.

In general, the optimised discrete PID parameters are applied on the multivariable realistic model of T_g and EO_2 to optimise fuel reduction and undesirable emissions while sustaining the glass temperature.

Chapter 7

CONCLUSION – MAIN CONTRIBUTIONS AND FUTURE WORK

7.1 Introduction

The first part of this chapter summarises the key results and main contributions with achieved research novelties of this research project. A number of recommendations for further work in this direction, which will extend an improvement of SGAs in the area of model parameters identification and state-space model extension with respective thermal energy as input, are given in the second part of this chapter.

7.2 Summary of Main Contributions

This research work explored the prospective of the use of SGAs as a basis for finding the optimal function solutions in system identification and control optimisation structures, focusing on applications to a multivariable glass furnace process. A predetermined time constant approximation (PT_CA) technique was developed and proposed for higher order model's parameters identification. Also, a realistic excess oxygen (EO_2) model's parameters with nonlinearity effect were identified and

integrated with the available multivariable furnace process model.

A number of novel discrete PID controller design/tuning approaches were developed and proposed. The main contributions and novel aspects of this work are summarised in the following subsections. References to the published parts of this work are also given.

7.2.1 Realistic EO_2 Model Development

A full scale of realistic EO_2 model with nonlinearity effect was developed and its parameters identified by SGAs as discussed in chapter 4, section 4.8.2. The developed realistic complete EO_2 model consists of three sub-models to characterise the plant response. First, an air-fuel ratio (AFR) conversion model converts the real value of $AFR_{(Mass)}$ to respective $AFR_{(Volumetric)}$ derived from the methane gas law. Second, a transfer function was identified to characterise the dynamic response of real EO_2 plant data.

Finally, an EO_2 look-up table was developed according to the nonlinear methane chemical relationship of stoichiometric $AFR_{(Volumetric)}$ as an input and $EO_{2(\%)}$ as an output. Such a complex development of EO_2 model is essentially required to represent a complete realistic EO_2 model.

The developed EO_2 model was evaluated and compared with a real plant dynamic response, which illustrates the higher degree of accuracy of the developed model. A complete realistic EO_2 model parameter identification approach is under preparation as a journal publication.

7.2.2 PT_CA Method for Higher Order Model Parameters Identification

A new method called predetermined time constant approximation (PT_CA) was proposed to approximate an initial predetermined time constant ($Ts_{p(Initial)}$) value, whose purpose is to enable the SGAs to explore and exploit an optimal value (X_i) for higher order model parameter identification. The proposed PT_CA method in chapter 4, section 4.2.5 was divided into two sub-processes. First sub-process is

a $Ts_{p(Initial)}$ value identification from the dynamic response of a real plant process. This proposed sub-process provides a better approximation of prior knowledge ($Ts_{p(Initial)}$ value) of higher order poles coefficients of a transfer function from the dynamic response.

Then, the second sub-process is search space boundary optimisation (SB_O) by approximated $Ts_{p(Initial)}$ value. The second sub-process improves the search space boundaries by resizing the upper search boundary (SB_{Upper}) and lower search boundary (SB_{Lower}) by $Ts_{p(Initial)}$ value for better SGAs convergence. This sub-process approximates the distribution of the elite group well within the resized feasible boundary region $[X_i - \Delta_{GO}, X_i + \Delta_{GO}]$ at subsequent SGAs executions and offers the genetic operators an opportunity to locate the X_i rapidly without any constraint. Also, the PT_CA method demonstrated that an optimised SB_O well sustaining the population diversity by exploring the feasible search region while exploiting to X_i.

In general, the proposed method improved the SGAs convergence rate towards the global optimum and illustrated the effectiveness. Parts of these results have been published in Rajarathinam K., Gomm J. B. and Yu D.L. (2015) and Rajarathinam K., Gomm J. B., Yu D.L. and Abdelhadi A. S. (2015).

7.2.3 Automatic Tuning Technique for Multivariable Processes

A new technique for the automatic tuning of decentralised discrete PID controllers for multivariable processes, based on SGAs, was proposed in chapter 6, section 6.3.1. The main advantage of the proposed technique is the competence to improve the control robustness and to optimise discrete PID parameters by compensating the loop interaction of a multivariable process.

For the glass furnace process, this is achieved by adding the individually optimised objective functions of glass temperature (T_g) and EO_2 processes as one objective function, $J_{i(Total)} = (IAE + \Delta ISU)_{T_g} + IAE_{EO_2}$ (section 6.3.1 and equation 6.10), to include the total effect of the loop interaction by applying step inputs on both set points, T_{SET} and $EO_{2(Ref)}$, at two different time periods in one simulation.

As single loop interaction is present between AFR to T_g, the discrete PID parameter for T_g is optimised when the respective step input, T_{SET} is applied with no step input of $EO_{2(Ref)}$ is applied (steady-state). After the T_g attained the steady-state, the step input of $EO_{2(Ref)}$ is applied while the simulation is still running with loop interacted.

This process optimises the discrete PID parameters of T_g further and EO_2 while considering the effect of loop interaction in one simulation period. Thus, considering the total loop interaction effect of both multivariable processes is well compensating the loop interaction and improves the control robustness.

The effectiveness of the proposed tuning technique was supported by a number of simulation results using two other SGAs conventional techniques with 1^{st} and 2^{nd} order control oriented models. It was illustrated that, in all cases, the resulting discrete PID control parameters completely satisfied all performance specifications. Parts of these results have been published in Rajarathinam K., Gomm J. B., Yu D. L. and Abdelhadi A. S. (2014), and Rajarathinam K., Gomm J. B., Yu D. L. and Abdelhadi A. S. (2015).

7.2.4 Reduction of Fuel Consumption for Glass Furnace Process

A new technique to minimise the fuel consumption for glass furnace processes while sustaining the T_g is proposed in chapter 6, section 6.4.1.2. This proposed technique is achieved by reducing the EO_2 within the optimum thermal efficiency region ($EO_2 \approx 1.7\% \longrightarrow 3.2\%$), which is approximately equal to about 10% to 20% of excess air. A deep investigation of the methane combustion process offered a great prime understanding about the interaction of chemical properties of methane. This facilitated to develop the complete realistic EO_2 model which well characterised the real plant response, as discussed earlier.

Therefore, by reducing the $EO_{2(Ref)}$ within the optimum region ($2.45\% \longrightarrow 2\%$) the fuel consumption is minimised ($0.002942kg/sec \longrightarrow 0.002868kg/sec$) while the thermal efficiency of T_g is sustained at the desired set point ($1550K$).

In addition, a reduction in EO_2 within the methane combustion guideline will assure that the undesirable emissions are in control throughout the combustion process. The efficiencies of the proposed technique were supported by a number of simulation results applying the three SGAs tuning techniques. It was illustrated that, in all cases, the fraction of EO_2 reduction resulted in a great minimisation in fuel consumption. Parts of these results have been published in Rajarathinam K., Gomm J. B. and Abdelhadi A. S. (2014).

7.3 Achieved Objectives

The achieved objectives of this thesis and how they were met are as follows

1. The dynamic characteristics of a realistic 24 state-space glass temperature (T_g) model is identified. Based on investigation, the realistic T_g model is unstable due to incorrect eigenvalues. The incorrect eigenvalues are corrected by recalculating by energy balance equation and the realistic T_g model is stabilised (chap. 3). Then, a control oriented glass T_g simulation model developed by SGAs (chap.specifiations 4).

2. Methane chemical compounds and combustion process are studied. A 4^{th}order realistic simulation model with nonlinear effect and 1^{st} and 2^{nd}order control oriented simulation models without nonlinear effect of excess oxygen (EO_2) from numerical data of real plant are developed as discussed in section 7.2.1. The predetermined time constant approximation (PT_CA) technique is developed to enable the SGAs prevent premature convergence in model parameter identification as discussed in section 7.2.2.

3. The discrete control parameters according to the performance criteria of T_g and EO_2, individually are optimised (chap. 5). For EO_2, the SGAs with improved bound by resizing the search space boundaries are optimising the discrete PID parameters. While, for T_g, discrete PID parameters are optimised by SGAs with modified objective function by added the weighting factor.

4. The discrete decentralised control strategies by control oriented models of T_g and EO_2 are developed (chap.6). Then, the dynamic discrete control strategies are optimised by three tuning approaches. The tuning approach, SGAs-3 included the total effect of the loop interaction by applying step inputs on both set points, T_{SET} and $EO_{2(Ref)}$, at two different time periods in one simulation as discussed in section 7.2.3.

5. The optimised discrete control strategies are implemented and evaluated on realistic multivariable process for attaining the desired performances (chap.6). The desired performance criteria are atained by reducing the $EO_{2(Ref)}$ within the optimum region the fuel consumption is minimised while the thermal efficiency of T_g is sustained at the desired set point as discussed in section 7.2.4.

7.4 Recommendations for Further Work

In this section, a number of recommendations for further work are given, comparison on multiobjective optimisation associate with other tuning methods, focusing on an improvement of the predetermined time constant approximation method, designing a code for automatic search space boundary optimisation, and an extension of the 24 state-space single-stage furnace model to a multistage furnace process.

7.4.1 Comparison of SGAs with other Tuning Approaches

The optimised discrete PID parameters by SGAs for T_g and EO_2 can be optimised and compared the tuning performance assessment by considering other tuning approaches such as PID auto-tuning, model predictive control, adaptive self-tuning and other promising tuning techniques. Further, the SGAs tuning performance assessment can be compared and improved by personalised performance criterion with respective tuning techniques.

As discussed in sections 2.4.1. and 6.3.1.2, the multiobjective function by SGAs (MOGA) is relatively achieved even though a single objective function was applied

in this research. Therefore, the MOGA can be applied here for further comparison in performances with other single objective tuning approaches.

7.4.2 Improvement on PT_CA Method

The optimum model parameters identification by PT_CA method can be improved by considering the zeros with poles. The proposed PT_CA method is only considered and suitable for higher order polynomial coefficients (poles) identification. If a system has a response that is significantly affected by the presence of zeros, e.g. more rapid response or undershoot (inverse) response, subsequently the zeros need to be considered for characterising the observed response. However, it is a complicated process to develop a method to approximate the initial zero values, as the system response is affected according to the zeros placement on the s-plane.

When a zero is negative ($s = -z$), corresponding to the left half-side of s-plane, the derivative is also positive causing more rapid response. However, when a zero is positive ($s = +z$), corresponding to the right half-side of s-plane, the derivative is negative causing an overshoot going in the opposite direction (undershoot) and an increase in the delay before the response approaches its final value.

Therefore, developing a complete method by considering both zeros and poles for model parameters identification would provide a stronger foundation for an optimum search space boundary and improve the SGAs convergence diversity with minimum constraints.

Further improvement on PT_CA can be done on optimising the size of SB_{Upper} and SB_{Lower} extensions. Here, a 100% extension on SB_{Upper} and 75% extension on SB_{Lower} are applied to provide a better population diversity for characterising the dynamic response of higher order model's parameters without constraints. Such a boundary extension required a higher number of iteration (generation) for better exploration and time consuming.

Therefore, minimising or adjusting the SB_{Upper} and SB_{Lower} with respective model orders complexity may improve the time consumption while sustaining the population diversity.

7.4.3 Automatic Search Space Boundary Resizing

The proposed technique for resizing the search space boundary by manually using Ts_p to optimise the search space boundary, SB_O, and to locate an optimal value, X_i, can be improved by resizing the search space boundary, automatically. This can be achieved by designing a set of Matlab coding to be integrated with SGAs to automatically resize the SB_{Upper} and SB_{Lower} at initial and each consecutive SGAs execution until the SB_O and X_i are attained.

The process of automatic search space boundary resizing is a similar process as described in the second sub-process of PT_CA method. With initially identified, $Ts_{p(Initial)}$ by the first sub-process of the PT_CA method and desired extension of SB_{Upper} and SB_{Lower}, the entire process of optimising the search space boundaries and locating the optimal value can be carried out by automatically.

7.4.4 Extension of Single Stage Multivariable Process to Multistage Multivariable Process

The applied single-stage multivariable glass furnace process can be developed and extended to a multistage multivariable process for further research. Some work has been undertaken for model extension for further analysis about the system's dynamic behaviours and characteristics. The development of an electrode extension model for the gas metal arc welding process based on the process voltage was presented by Bingul & Cook (2006). The full dynamic model for the electrode extension is derived by combining a dynamic resistivity model with the voltage model. The electrode extension model was found to be represented mathematically by a nonlinear, time-varying, second order ordinary differential equation. This model is applied in through-the-arc sensing and arc length control systems. However, literally no research work has been done on state-space model extension.

Preliminary work has been undertaken in this research to extend the 24 state-space, single-stage furnace model to a multistage state-space furnace model under a few assumptions. As illustrated in figure 7.1, the only state variables non-flame

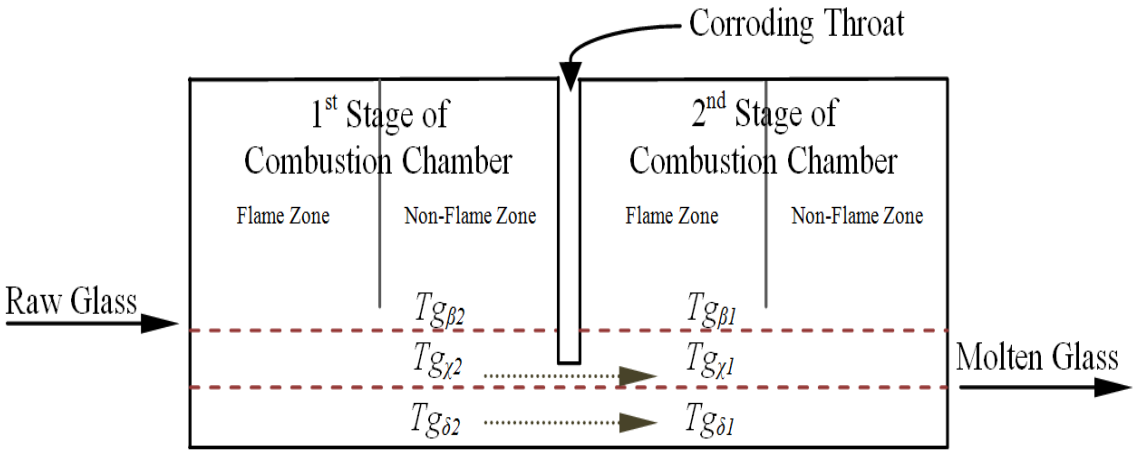

Figure 7.1: An extension of 24 state-space combustion chamber models to multistage

top-half glass zone temperature ($Tg_{\chi 2}$) of 1st stage combustion chamber is selected and considered as primary process outputs to be fed-in on flame top-half glass zone temperature ($Tg_{\chi 1}$) of 2nd stage combustion chamber as secondary process inputs. While, the other two state variables, non-flame bottom-half glass zone temperature ($Tg_{\delta 2}$) and non-flame top layer glass surface temperature ($Tg_{\chi 2}$) are discarded as the temperature gradients are approximately equal, $1500K$ with $Tg_{\chi 2}$. A further assumption is that the other 23 state variables of the 2nd stage of combustion chamber are entirely isolated from the 1st stage of combustion chamber.

The single-stage combustion response requires strong dynamic progression to raise the T_g from $1300K$ to $1500K$. Therefore, the objective of the model extension of the combustion chamber is to isolating the glass temperature's dynamic progression process into two sub-processes to analyse and improve the glass homogeneity and fuel consumption. The beginning part of 1st combustion chamber is where the raw materials containing all the ingredients needed for glass forming are introduced as wet packets into the combustion chamber. They float on the melt surface until the chemical reaction of melting occurs thanks to heat transfers. During melting, the newly formed glass sinks in the lower section of the chamber at the end of 1st combustion chamber.

At the 2nd combustion chamber, the molten glass is further homogenised and refined. The molten glass temperature gradients and residence periods in the chamber create laminar natural convection streams that allow this homogenising to occur.

The end part of 2nd combustion chamber is known as a buffer zone which the end-product is complete for glass formation.

The described physical phenomena of a glass process; melting, mixing, homogenising and refining, strongly depend on temperature gradients and requires sufficient periods to perform well. A difficulty arose in estimating an appropriate energy level of the state variable, $Tg_{\chi 1}$, for the glass refining process for the 2nd stage chamber, as the respective chamber does not require similar inputs as the 1st stage chamber. Therefore, the energy distribution technique with different steady-states of dynamic progressions is introduced based on the total fuel consumption for $Tg_{\chi 1}$ as a 2nd stage chamber's input, to divide the total dynamic progression of the T_g response. The complete simulation results of energy distribution with different steady-state of dynamic progressions are tabulated and listed in appendix.

Based on the preliminary simulation results, the 35% of total energy distribution of $Tg_{\chi 1}$ is exhibiting a well promising result by isolating the dynamic progression of chamber 1, $1300K \longrightarrow 1350K$ and chamber 2, $1350K \longrightarrow 1500K$. The total fuel consumption by isolated dynamic progression is reduced to $2\%_{(\text{approximately})}$ ($0.002723kg/sec \longrightarrow 0.002670kg/sec$). This is just a preliminary proposal in state-space model extension based on the dynamic progression isolation while optimising the fuel consumption. Further works of extension are required to design a more realistic multistage state-space model.

7.5 Summary

In this chapter, a summary was given of the key results and main contributions with achieved objectives of this research work. A number of recommendations for further work in this direction, that will broaden the application of SGAs in the area of control systems engineering, were then outlined, concentrating on an improvement of predetermined time constant approximation method for higher order model's parameters, code design for automatic search space boundary optimisation, and an extension of the 24 state-space single-stage furnace to a multistage furnace process model.

References

Abo-Hammour Z. S., Alsmadi O. M. K., Bataineh S. I., Al-Omari M. A. and Affach N. (2011), "Continuous Genetic Algorithms for Collision-Free Cartesian Path Planning of Robot Manipulators", International Journal of Advanced Robotic Systems (IJARS), vol. 8 (6), pp. 14-36.

Adewole A. P., Otubamowo K. and Egunjobi T. O. (2012), "A Comparative Study of Simulated Annealing and Genetic Algorithm for Solving the Travelling Salesman Problem", International Journal of Applied Information Systems (IJAIS), vol. 4 (4), pp. 6-12.

Aloysius G., Rajakumar B. R. and Binu D. (2012), "Genetic Algorithm based Airlines Booking Terminal Open/Close Decision System", International Conference on Advances in Computing, Communications and Informatics, (ICACCI), pp. 174-179.

Altinten, A., Karakurt S., Erdogan, S. and Alpbaz, M. (2010), " Application of Self-tuning PID Control with Genetic Algorithm to a Semi-batch Polystyrene Reactor", Indian Jounal of Chemical Technology, vol. 17, pp. 356-365.

Altinten, A., Ketevan lioglu, F., Erdogan, S., Hapoglu, H. and Alpbaz, M. (2008), "Self-tuning PID Control of Jacketed Batch Polystyrene Reactor using Genetic Algorithm", Journal of Chemical Engineering, vol. 138, pp. 490–497.

Arturo Y. J. C., Rene de J. R. T., Luis M. V. and Roque A. O. R. (2013), "PID-Controller Tuning Optimisation with Genetic Algorithms in Servo Systems", International Journal of Advanced Robotic Systems (IJARS), vol. 10 (324), pp. 1-14.

Astrid P. (2004), "Reduction of Process Simulation Models: A Proper Orthogonal Decomposition Approach", PhD Thesis, Technical University Eindhoven, The Netherlands.

Astrid P. and Weiland S. (2005), "Reduction Method to a Computational Fluid Dynamic (CFD) Model of a Glass Feeder", Preprints of the 16th IFAC World Congress 2005, International Federation of Automatic Control, Prague.

Auchet O. (2005), "Contribution to Simplified Modelling of Glass Furnaces", PhD Thesis, Institute National Polytechnique de Lorraine, France.

Auchet O., Riedinger P., Malasse O. and Iung C. (2008), "First-Principles Simplified Modelling of Glass Furnaces Combustion Chambers", Control Engineering Practice, vol. 16, pp. 1443-1456.

Aydin M. E. and Fogarty T. C. (2004), "A Distributed Evolutionary Simulated Annealing Algorithm for Combinatorial Optimization Problems", Journal of Heuristics, vol. 24 (10), pp. 269-292.

Bajeh A. O. and Abolarinwa K. O. (2011), "Optimization: A Comparative Study of Genetic and Tabu Search Algorithms", International Journal of Computer Applications (IJCA), vol. 31 (5), pp. 43-48.

Battiti R. (1996), "Reactive Search Towards Self-tuning Heuristics", in Modern Heuristic Search Methods. Wiley&Sons, pp. 61-83.

Beni G. and Wang J. (1989), "Swarm Intelligence in Cellular Robotic Systems", NATO Advanced Workshop on Robots and Biological Systems, Tuscany, Italy.

Benjamin K. K., Ammanuel A. N., David A. and Benjamin Y. K. (2008), "Genetic Algorithm using for a Batch Fermentation Process Identification", Journal of Applied Sciences, vol. 8 (12), pp. 2272-2278.

Bennett S. (2000), "The past of PID controllers", IFAC Workshop on Digital Control PID, pp. 3-13.

Bertsekas D. P. (2000), "Dynamic Programming and Optimal Control", vols. 1 & 2, 2nd Edition, Athena Scientific. ISBN 1-886529-09-4.

Bijaya K. N. and Gyanesh Das (2011), "Ant Colony Optimization. A Computational Intelligence Technique", International Journal of Computer & Communication Technology (IJCCT), vol. 2 (4).

Bingul Z. and Cook G. (2006), "A Real-Time Prediction Model of Electrode Extension for GMAW", IEEE/ASME Transactions on Mechatronics, vol. 11(1), pp. 47-54.

Bitschnau L. and Kozek M. (2009), "Modeling and Control of an Industrail Continuous Furnace", International Conference on Computational Intelligence, Modeling and Simulation (ICCIMS), pp. 231-236.

Bristol E. H. (1966), "On a New Measure of Interaction for Multivariable Process Control". IEEE Transaction on Automatic Control, AC-11, pp. 133-134.

Callendar A., Hartree D. R. and Porter A. (1935), "Time-lag in a control system", Phil. Transaction Royal Society of London, Series-A, 235, pp. 415-444.

Carniglia S. C. and Barna G. L. (1992), "Handbook of Industrial Refractories Technology Principles, Types, Properties and Applications", Noyes Publications, USA.

Carvahlo M. G., Speranskaia N., Wang J. and Nogueira M. (1997), "Modelling of Glass Melting Furnaces Applications to Control, Design, and Operation Optimization", Advances in Fusion and Processing of Glass II, Ceramic Transactions, vol. 82, pp. 109-135.

Chaiwat J. and Prabhas C. (2011), "Self-Adaptation Mechanism to Control the Diversity of the Population in Genetic Algorithm" International Journal of Computer Science & Information Technology (IJCSIT), vol. 3 (4), pp. 111-127.

Chien K. L., Hrones J. A. and Reswick J. B. (1952), "On the Automatic Control of Generalized Passive Systems", Transactions of the American Society of Mechanical Engineers, vol. 74, pp. 175-185.

Ching H. L. and Chang F. K. (2010), "Fractional-Order PID Controller Optimization via Improved Electromagnetism-like Algorithm, ISA Transactions, vol. 37, pp. 8871-8878.

Chipperfield A. J., Fleming P. J. and Fonseca, C. M. (1994), "Genetic Algorithm Tools for Control Systems Engineering", Proceedings of Adaptive Computing in Engineering Design and Control, Plymouth Engineering Design Centre, pp. 128-133.

Cohen G. H. and Coon G. A. (1953), "Theoretical consideration of retarded control", Transactions of the American Society of Mechanical Engineers, vol. 75, pp. 827-834.

Cormen T. H., Leiserson H. C. E. and Rivest R. L. (2000), "Introduction to Algorithms", MIT Press.

Darwin C. (1859), "The Origin of Species", London: John Murray.

De Jong K. A. (1975), "An Analysis of the Behaviour of a Class of Genetic Adaptive Systems", PhD Thesis, University of Michigan, USA.

Deepti G. and Shabina G. (2012), "An Overview of Methods Maintaining Diversity in Genetic Algorithms", International Journal of Emerging Technology and Advanced Engineering (IJETAE), vol. 2 (5), pp. 2250-2459.

Dorigo M. (1992), "Optimization, Learning and Natural Algorithms", PhD thesis, Politecnico di Milano, Italy.

Engineeringtoolbox, Combustion Efficiency and Excess Air, [online] at: http://www.engineeringtoolbox.com/boiler-combustion-efficiency-d_271.html [Accessed 02 March 2012].

Environmental, Health, & Safety (EHS) Guidelines, (2007), International Finance Corporation (IPC)

Fernando M., Francisco V. and Juan G. (2008), "Centralised PID Control by Decoupling for TITO Processes", IEEE International Conference on Emerging Technologies and Factory Automation (ICETFA), pp. 1318-1325.

Fisher R. A. (1930), "The Genetical Theory of Natural Selection", Oxford: Clarendon Press.

Fleming P. J. and Purshouse R. C. (2002), "Evolutionary Algorithms in Control Systems Engineering: A Survey", Control Engineering Practice, PERGAMON, vol. 10, pp. 1223-1241.

Fogel L. J., Owens A. J. and Walsh (1966), "Artificial Intelligence through Simulated Evolution", New York: Wiley.

Fogel D. B. (1994), "An Introduction to Simulated Evolutionary Optimization", IEEE Transactions on Neural Networks, vol. 5 (1), pp. 3-14.

Fonseca C. M. and Fleming P. J. (1995), "Multiobjective Genetic Algorithms Made Easy: Selection Sharing and Mating Restriction", First International Conference on Genetic Algorithms in Engineering Systems: Innovations and Applications, No. 414, pp. 45-52.

Fonseca C. M. and Fleming P. J. (1998), "Multiobjective Optimisation and Multiple Constraint Handling with Evolutionary Algorithms", IEEE Transactions System, Man and Cybernetics, Part A, vol. 28 (1), pp. 26-37.

Gamal A. El-N, Abeer M. M. and El-Sayed M (2014), "A Comparative Study of Meta-heuristic Algorithms for Solving Quadratic Assignment Problem", International Journal of Advance Computer Science and Applications (IJACSA), vol. 5 (1), pp. 1-6.

Gauri M. and Kulkarni N. R. (2013), "Design and Optimisation of PID Controller using Genetic Algorithm", International Journal of Research in Engineering and Technology (IJRET), vol. 2 (6), pp. 926-930.

Ghanbari A. and Noorani SMRS. (2011), "Optimal Trajectory Planning Design of a Crawling Gait in a Robot Using Genetic Algorithm", International Journal of Advanced Robotic Systems (IJARS), vol. 8 (1), pp. 29-36.

Goldberg D. E. (1989), "Genetic Algorithm in Search Optimization and Machine Learning", Reading, MA: Addison-Wesley.

Goldberg, D. E. (1994), "Genetic and Evolutionary Algorithms Come of Age", Communications of the Association for Computing Machinery, vol. 37 (3), pp. 113 -119.

Gondro C. and Kinghorn B. P. (2007), "A Simple Genetic Algorithm for Multiple Sequence Alignment". Genetics and Molecular Research, vol. 6 (4), pp. 964–982.

Graves A., Liwicki M., Fernandez S., Bertolami R., Bunke H. and Schmidhuber J. (2009), "A Novel Connectionist System for Improved Unconstrained Handwriting Recognition", IEEE Transactions on Pattern Analysis and Machine Intelligence, vol. 31 (5).

Grosdidier P. and Morari M. (1987), "A Computer Aided Methodology for the Design of Decentralised Controllers", International Conference on Computer and Chemical Engineering (ICCCE), vol. 11, pp. 423-433.

Gy¨ongy I. J. and Clarke D. W. (2006), "On the Automatic Tuning and Adaptation of PID Controllers", Control Engineering Practice, vol. 14, pp. 149-163.

Hamamci S. E. and Tan N. (2006), "Design of PI Controllers for Achieving Time and Frequency Domain Specifications Simultaneously, ISA Transactions, vol. 45 (4), pp. 529- 543.

Haupt R. L. and Haupt S. E. (2004), "Practical Genetic Algorithms", Second Edition, John Wiley & Sons, Inc., Publication.

Heris J. E. A. and Oskoei M. A. (2014), "Modefied Genetic Algorithm for Solving N-Queens Problem", Iranian Conference on Inteligence Systems (ICIS), pp. 1-5.

Hitay Ö., Catherine B. and André R. F. (2012), "PID Controller Design for Fractional-Order Systems with Time Delays", Elsevier, Systems & Control Letters, vol. 61, pp. 18-23.

Hohwald H., Thayer I. and Korf R. E. (2003), "Coamparing Best-First Search and Dynamic Programming for Optimal multiple Sequence Alignment", 18th International Joint Conference on Artificial In telligence, pp. 1239-1245.

Holland J. H. (1975), "Adaption in Natural and Artificial Systems", Ann Arbor: The University of Michigan Press.

Holladay A. R. (2005), "Modelling and Control of a Small Glass Furnace", Master's Thesis, Department of Mechanical Engineering, West Virginia University, Morgantown, USA.

Hoskins J. W. and Chirino A. W. (1981), "Controlling Excess Oxygen in Glass Furnaces for Energy Conservation", IEEE Transactions on Industry Applications, vol. IA-17 (2), pp. 230-235.

Hottel H. C. and Cohen E. S. (1958), "Radiant Heat Exchange in a Gas-Filled Enclosure: Allowance for Non-Uniformity of Gas Temperature", AIChE, vol. 4 (1), pp. 3-14.

Hottel H. C. and Sarofim A. F. (1967), "Radioactive Transfer", McGraw-Hill Book Cooperation.

Hovd M. and Skogestad S. (1994), "Sequential Design of Decentralised Controllers", Automatica, vol. 30 (10), pp. 1601-1607.

Huisman L. (2005), "Control of Glass Melting Process Based on Reduced CFD Models", PhD Thesis, Technical University Eindhoven, The Netherlands.

Huang H. P., Jeng J. C., Chiang C. H. and Pan W. (2003), "A Direct Method for Decentralised PI/PID Controller Design", Journal of Process Control, vol. 13 (8), pp. 769-786.

Iruthayarajan M. W. and Baskar S. (2009), "Evolutionary Algorithms Based Design of Multivariable PID Controller", Expert Systems with Applications, vol. 36 (5), pp. 9159-9167.

Jan R. M., Tseng C. S. and Liu R. J. (2008), "Robust PID Control Design for Permanent Magnet Synchronous Motor: A Genetic Approach", Electric Power Systems Research, vol. 78, pp. 1161-1168.

Jayachitra A. and Vinodha R. (2014), "Genetic Algorithm Based PID Controller Tuning Approach for Continuous Stirred Tank Reactor", Advances in Artificial Intelligence, Hindawi Publishing Corporation, vol. 2014, pp. 1-9.

Jensen M. T. (2003), "Reducing The Run-Time Complexity of Multiobjective EAs: The NSGA-II and other Algorithms", IEEE Transactions Evolutionary Computing, vol. 7 (5), pp. 503-515.

Jin J. L., Yang X. H. and Ding J. (2001), "An Improved Simple Genetic Algorithm-Accelerating Genetic Algorithm", Systems Enginnering Theory & Practice, pp. 8-13.

Joao M. P. and Pedro U. L. (2003), "A Glass Furnace Operation System using Fuzzy Modeling and Genetic Algorithms for Performance Optimisation", Engineering Applications of Artificial Intelligence, vol. 16(7), pp. 681-690.

Juang J. N. and Phan M. (1994), "Linear System Identification via Backward-Time Observer Models", Journal on Guidance Control and Dynamic, vol. 17 (3), pp. 505-512.

Kachitvichyanukul V. (2012), "Comparison of Three Evolutionary Algorithms: GA, PSO and DE", Industrial Engineering & Management Systems, vol. 11 (3), pp. 215-223.

Kai H., Jun Z., Zu-hua X. and Ji-xin Q. (2008), "A Closed-Loop Particle Swarm Optimizer for Multivariable Process Controller Design", Journal of Zhejiang University-Science, vol. 9 (8), pp. 1050-1060.

Kalyanmoy D. (2001), "Multi-Objective Optimisation Using Evolutionary Algorithms", Wiley Interscience Series in Systems and Optimisation. John Wiley & Sons, Inc., New York, USA, 2001.

Kampisios K., Zanchetta P., Gerada C. and Trentin A. (2008), "Induction Motor Parameters Identification using Genetic Algorithm for Varying Flux Levels", Power Electronics and Motion Control (EPE-PEMC), pp. 887-892.

Kennedy J. and Eberhart R. (1995), "Particle Swarm Optimization", IEEE International Conference on Neural Networks IV. pp. 1942-1948.

Kim J. S., Kim J. H., Park J. M., Park S. M., Choe M. Y. and Heo H. (2008), "Auto Tuning PID Controller Based on Improved Genetic Algorithm for Reverse Osmosis Plant", International Journal of Intelligent Systems and Technologies (IJIST), vol. 3 (4), pp. 232-237.

Kiperwasser E., David O. and Netanyahu N. S. (2013), "A Hybrid Genetic Approach for Stereo Matching", Genetic and Evolutionary Computation Conference, New York, USA, ACM, pp. 1325-1332.

Kokash and Natallia (2005), "An Introduction to Heuristic Algorithms", Research Methodology course, Department of Informatics and Telecommunications, University of Trento, Italy.

Kr¨ose B. and P. Smagt. (1996), "An introduction to Neural Networks", University of Amsterdam.

Kyoto Protocol (1998), "United Nations Framework Convention on Climate Change", UNFCCC.

Koza J. R. (1992), "Genetic Programming-On The Programming of Computers by Means of Natural Selection", Cambridge, MA: The MIT Press.

Lee T. K., Shen J. and Chiu M. S. (2001), "Independent Design of Robust Partially Decentralized Controllers", Journal of Process Control (JPC), vol. 11, pp. 419-428.

Lin Y., Hao J. M., Ji Z. S. and Dai Y. S. (2000), "A Study of Genetic Algorithm based on Isolation Niche Technique", Journal of Systems Engineering (JSE), vol. 15, pp. 86-91.

Li L. and Bo W. (2012), "Study on PID Control System Based on Genetic Algorithms", 2nd International Conference on Computer Application and System Modelling, pp. 510-513.

Li D., Gao F., Xue Y. and C. Lu C. (2007), "Optimisation of Decentralised PI/PID Controllers based on Genetic Algorithm", Asian Journal of Control, vol. 3 (3), pp. 306-316.

Liu J. and Guo S. (2013), "Fuzzy Neural Network Temperature Control System of Resistance Furnace Based on Genetic Algorithm", International Journal of Digital Content Technology and its Applications (IJDCTA), vol. 7 (6), pp. 1046-1053.

Liu X., Zhou Y., Hua Z., Chu K., Wang P., Gu L. and Chen L. (2014), "Parameter Identification of River Water Quality Models using a Genetic Algorithm", Journal Water Science Technology, vol. 69 (4), pp. 687-693.

Loh A. P., Hang C. C., C.K. Quek C. K. and Vasnani V. U. (1993), "Auto-tuning of Multi-loop Proportional-Integral Controllers using Relay Feedback", Industrial Engineering Chemical Res., vol. 32, pp. 1102-1107.

Ljung L. (1999), "System Identification - Theory for the User with Matlab", 2nd edition, PTR Prentice Hall, Upper Saddle River, New Jersey.

Luyben W. L. (1986), "Simple Method for Tuning SISO Controllers in Multivariable Systems", Industrial Engineering Chemistry Process Design and Development, vol. 25 (3), pp. 654-660.

Mahendra K. S., Gupta R. and Bhave P. R. (2008), "Optimal Design of Water Networks using Genetic Algorithm with Reduction in Search Space", Journal Water Resource Planning Management., ASCE, vol. 134 (2), pp. 147-160.

Majhi S. and Atherton D. P. (2000), "Obtaining Controller Parameters for a New Smith Predictor using Auto Tuning, Automatica, vol. 36, pp. 1651-1658.

Malik S. and Wadhwa S. (2014), "Preventing Premature Convergence in Genetic Algorithm using DGCA and Elitist Technique", International Journal of Advanced Research in Computer Science and Software Engineering. (IJARCSSE), vol. 4 (6), pp. 410-413.

Malwatkara G. M., Sonawaneb S. H. and Waghmare L. M. (2009), "Tuning PID Controllers for Higher-Order Oscillatory Systems with Improved Performance", ISA Transactions, vol. 48, pp. 347-353.

Mathew G., Arun J. S., Kalpana K., Jaya J., Jaina G. and Janardhanan S. (2014), "A Genetic Algorithm based Approach for Segmenting and Identifying Defects in Glass Bottles", American Journal of Engineering Research (AJER), vol. 3 (2), pp. 132-140.

MathWorks (2015), "Exploring Variable-Step Solvers using a Stiff Model", MathWorks Documentation, R2015b.

Maria A., Stoyan T. and Tania P. (2011), "Genetic Algorithms based Parameter Identification of Yeast Fed-Batch Cultivation", International Conference Numerical Methods and Applications (ICNMA), vol. 6046, pp. 224-231.

Michalewicz, Z. and Fogel, B. D. (2004), "How to Solve It Modern Heuristics", Springer, 2nd revised and extended edition, ISBN: 978-3-54022-494-5.

Mitchell, M. (1996), "An Introduction to Genetic Algorithms", MIT Press.

Morris H. A. (2007), "Advanced Modelling for Small Glass Furnaces", Master Thesis, Department of Mechanical Engineering, West Virginia University, Morgantown, USA.

Monica T. J.,Yu C. C. and Luyben W. L. (1998), "Improved Multi-loop Single-Input/Single-Output (SISO) Controller for Multivariable Process", Industrial Engineering Chemical Res., vol. 27, pp. 969-973.

Müller J., Chmelaø J., Bodi R. and Muysenberg E. (2003), "7th International Seminar on Mathematical Modelling and Advanced Numerical Methods of Furnace Design and Operation, Glass Service", Horní Beèva, Czech Republic, pp. 157-170.

Müller J., Bodi R., Chmelar J. (2005), "8th International Seminar on Mathematical Modelling and Advanced Numerical Methods of Furnace Design and Operation, Glass Service, Horní Becva, Czech Republic, pp. 200-211.

Nagaraj B. and Murugananth N. (2010), "A Comparative Study of PID Controller Tuning Using GA, EP, PSO and ACO", IEEE International Conference on Communication Control and Computing Technologies, (ICCCCT), pp. 305-313.

Nakisa B., Nazri A. M. Z., Rastgoo M. N. and Salwani A. (2014), "A Survey: Particle Swarm Optimization Based Algorithms To Solve Premature Convergence Problem", Journal of Computer Science, vol. 10 (10), pp. 1758-1765.

National Risk Management Research Laboratory (2004), "Minergy Corporation Glass Furnace Technology Evaluation Report", Report No. EPA/540/R-03/500.

Neumaier A., Bomze I., Emiris I. and Wolsey L. (2006), "Global Optimization and Constraint Satisfaction", Proceedings of GICOLAG workshop (Global Optimization, Integrating Convexity, Optimization, Logic Programming and Computational Algebraic Geometry).

Nithyarani N., Girirajkumar S. M. and Anantharaman N. (2013), "Modeling and Control of Temperature Process using Genetic Algorithm", International Journal

of Advanced Research in Electrical, Electronics and Instrumentation Engineering (IJAREEIE), vol. 2 (11), pp. 5355-5364.

Nithya S., Gour A. S., Sivakumaran N., Radhakrishnan T. K. and Anantharaman N. (October 2007), "Model Based Controller Design for Shell and Tube Heat Exchanger", Sensors and Transducers Journal, vol. 84 (10), pp. 1677-1686.

Nur H. K., Hairudin A. M. and Azurah A. S. (2012), "Parameter Estimation of Warranty Cost Model using Genetic Algorithm", International Journal of Soft Computing and Engineering (IJSCE), vol. 2 (5), pp. 163-166.

Okaeme N. (2008), "Automated Robust Control System Design for Variable Speed Drives", PhD Thesis, University of Nottingham, UK.

Patel H. B. and Chaphekar S. N. (2012), "Development in PID Controllers: Literature Survey", International Journal of Engineering Innovation & Research (IJEIR), vol. 1 (5), pp. 425-430.

Patrascu M., Hanchevici A. B. and Dumitrache I. (2011), "Tuning of PID Controllers from Non-Linear MIMO Systems using Genetic Algorithms", Proceedings of the 18th World Congress, International Federation of Automatic Control (IFAC) , vol. 18 (1), pp. 12644-12649.

Pereira D. S. (2005), "Genetic Algorithm Based System Identification and PID Tuning for Optimum Adaptive Control", International Conference on Advanced Intelligent Mechatronics, Monterey, California, USA, pp. 801-806.

Perez J. R. and Basterrechea J. (2004), "Near to Far-Field Transformation using GA based Optimisation: Real versus Binary Encoding Schemes", IEEE transactions, pp. 1122-1125.

Ping G., Xiaohe L. and Yuezhao G. (2014), "Predictive Control of Arc Furnace based on Genetic Algorithm", 26th Chinese Control and Decision Conference (CCDC), pp, 3385-3390.

Rajarathinam K., Gomm J. B., Yu D. L. and Abdelhadi A. S. (2014), "Decentralised Control Optimisation for a Glass Furnace by SGA's", ACM International Conference Proceeding Series, vol. 883, pp. 248-255.

Rajarathinam K., Gomm J. B., Yu D. L. and Abdelhadi A. S. (2014), "Decentralised PID Control Tuning for a Multivariable Glass Furnace by Genetic Algorithm", Proceeding of the 20th International Conference on Automation and Computing (ICAC), pp. 14-19.

Rajarathinam K., Gomm J. B. and Yu D. L. (2015), "Predetermined Time Constant Approximation Method for Optimising Search Space Boundary by Standard Genetic Algorithm", ACM International Conference Proceeding Series, vol. 1008, pp. 38-45.

Rajarathinam K., Gomm J. B., Yu D. L. and Abdelhadi A. S. (2015), "An Improved Search Space Resizing Method for Model Identification by Standard Genetic Algorithm", Proceeding of the 21st International Conference on Automation and Computing (ICAC), pp. 1-6, 2015.

Rajarathinam K., Gomm J. B., Yu D. L. and Abdelhadi A. S. (2016), "PID Controller Tuning for a Multivariable Glass Furnace Process by Genetic Algorithm", International Journal of Automation and Computing (IJAC), vol. 13 (1), pp. 64-72, 2016. (accepted, June 2015).

Ramadan S. Z. (2013), "Reducing Premature Convergence Problem in Genetic Algorithm: Application on Travel Salesman Problem", Internatioal Journal of Computer and Information Science (IJCIS), vol. 6 (1), pp. 47-57.

Ramin R., Farzad H., Esmaeil A-G., Bahman M., and Farzad R. S. (2008), "Decentralized PID Controller Design for a MIMO Evaporator based on Colonial Competitive Algorithm", Proceedings of the 17th World Congress, The International Federation of Automatic Control (IFAC), vol. 41 (2), pp. 9952-9957.

Randy L. H. and Sue E. H. (2004), "Practical Genetic Algorithms", 2nd Edition, John Wiley & Sons, Inc., Hoboken, New Jersey.

Rani M. R., Selamat H., Zamzuri H. and Ibrahim Z. (2012), "Multi-Objective Optimisation for PID Controller Tuning using the Global Ranking Genetic Algorithm", Journal of Innovative Computing, Information and Control (JICIC), vol. 8 (1A), pp. 269-284.

Rathikarani D., Sivakumar D. and Anita J. M. S. (2007), "Genetic Algorithm based Optimization of Controller Tuning for Processes with Dead Time", Proceedings of the International conference on Advances in control and optimization of dynamical systems (ACDOS).

Rechenberg I. (1973), "Evolutionsstrategie – Optimierung technischer Systeme nach Prinzipien der biologischen Evolution", PhD thesis, 1971. Reprinted by From- man-Holzboog.

Reeves C. R. (1995), "Modern Heuristic Techniques for Combinatorial Problems", London: McGraw-Hill.

Roeva O. (2008), "Parameter Estimation of a Monod-type Model based on Genetic Algorithms and Sensitivity Analysis", LNCS, Springer, vol. 4818, pp. 601-608.

Saad M. S., Jamaluddin H. and Darus I. Z. M. (2012), "Implementation of PID Controller Tuning using Differential Evolution and Genetic Algorithms", International Journal of Innovative Computing, Information and Control (IJICIC), vol. 8 (11), pp. 7761-7779.

Saptarshi D., Indranil P., Shantanu D. and Amitava G. (2011), "A Novel Fractional Order Fuzzy PID Controller and its Optimal Time Domain Tuning based on Integral Performance Indices", ISA Transactions, vol. 25, pp. 430-442.

Scarf P. A. and Majid H. A. (2011), "Modelling Warranty Extensions: A Case Study in the Automotive Industry", Proceedings of the Institution of Mechanical Engineers, Part O: Journal of Risk and Reliability, pp. 225- 251.

Schaffer J. D. (1985), "Multi Objective Optimisation with Vector Evaluated Genetic Algorithms", International Conference on Genetic Algorithms (ICGA), pp. 93-100.

Seested G. T. (2013), "Time-Delay System Identification using Genetic Algorithms", AAU Master Thesis, Aalborg University, Denmark.

SEPA (Scottish Environment Protection Agency) (2005), "Guidance for Monitoring Enclosed Landfil Gas Flares", Report No. GEHO1104BHZI-E-P.

Shopova E. G. and Vaklieva B. N. G. (2006), "Basic-A Genetic Algorithm for Engineering Problems Solution 2", Computer and Chemical Engineering, vol. 30 (8), pp. 1293-1309.

Shin G. W., Song Y. J., Lee T. B. and Choi H. K. (2007), "Genetic Algorithm for Identification of Time Delay Systems from Step Responses", International Journal of Control Automation and Systems (IJCAS), vol. 5 (1), pp. 79-85.

Silberholz J. and Golden B. (2010), "Comparison of Meta-heuristic-Handbook of Meta-heuristic algorithms", International Series in Operations Research & Management Science, vol. 146, pp. 625-640.

Skogestad S. (2003), "Simple Analytic Rules for Model Reduction and PID Controller Tuning", Journal of Process Control, vol. 13, pp. 291-309.

Slavov T. and Roeva O. (2012), "Application of Genetic Algorithm to Tuning a PID Controller for Glucose Concentration Control", WSEAS transactions on systems, vol. 11 (7), pp. 223-233.

Srisertpol J., Tantrairatn S., Tragrunwong P. and Khomphis V. (2011), "Estimation of the Mathematical Model of the Reheating Furnace Walking Hearth Type in Heating Curve Up Process", International Journal Mathematical Models & Methods in Applied Science, vol. 5 (1), pp. 167-174.

Srinivas, M. and Patnaik, L.M. (1994), "Adaptive Probabilities of Crossover and Mutation in Genetic Algorithms", IEEE Transactions on Systems, Man and Cybernetic, vol. 24 (4), pp. 656-667.

Suri P. K., Rakesh K. and Pardeep K. M. (2013), "A Simulator to Prevent Premature Convergence in YM using GA", International Journal of Emerging Technologies in Computational and Applied Sciences (IJETCAS), pp. 99-106.

Syswerda G. (1989), "Uniform Crossover in Genetic Algorithms", International Computer Games Association, vol. 3, pp. 2-9.

Tavakoli S., Griffin I. and Fleming J. (2006), "Tuning of Decentralised PI (PID) Controllers for TITO Processes", Control Engineering Practice, vol. 14 (9), pp. 1069-1080.

Truong N. L. V., Seungtaek H. and Lee M. (2009), "Analytical Design of Robust Multi-loop PI Controller for Multivariable Process", ICCAS-SICE International Joint Conference, pp. 2961-2966.

Tu Q. Y. and Mei Y. D. (2008), "Comparison of Genetic Simulated Annealing Algorithm and Niche Genetic Algorithm for reservoir Optimal Operation", Hydropower Automation and Dam Monitoring, vol. 32, pp. 1-4.

Ungan A. (1996), "Numerical Simulation of Glass Melting Furnaces", International Symposis On Glass Problems, Istanbul, Turkey, vol. 1, pp. 351-366.

Ursem R. K. (2003), "Models for Evolutionary Algorithms and Their Applications in System Identification and Control Optimisation", PhD Thesis, University of Aarhus, Denmark.

Vairavamoorthy K. and Ali M. (2005), "Pipe Index Vector: A Method to Improve Genetic Algorithm-Based Pipe Optimisation", Journal Hydraulic Engineering, ASCE, vol. 131 (12), pp. 1117-1125.

Valarmathi R., Theerthagiri P. R. and Rakeshkumar S. (2012), "Design and Analysis of Genetic Algorithm Based Controllers for Non Linear Liquid Tank System" International Conference on Advances In Engineering, Science And Management (ICAESM), pp. 616-620.

Vanaret C., Gotteland J. B., Durand N. and Alliot J. M.(2013), "Preventing Premature Convergence and Proving the Optimality in Evolutionary Algorithms" International Conference on Artificial Evolution, Bordeaux, vol. 1 (7), pp. 84-94.

Veynante D. and Vervisch L. (2002), "Turbulent Combustion Modelling", Progress in Energy and Combustion Science, vol. 28, pp. 193-266.

Vijula A. and Devarajan N. (2014), "Design of Decentralised PI Controller using Model Reference Adaptive Control for Quadruple tank Process", International Journal of Engineering and Technology (IJET), vol. 5 (6), pp. 5057-5066.

Viskanta R. and Menguc M. P.(1987), "Radiation Heat Transfer in Combustion Systems", Proceeding Energy and Combustion Science, vol. 13, pp. 97-160.

Vlachos C. (2000), "Optimal Design of Controller for Multivariable Processes using Genetic Algorithms", PhD Thesis, Liverpool John Moores University.

Vlachos C., Williams D. and Gomm J. B. (1999), "Genetic Approach to Decentralised PI Controller Tuning for Multivariable Processes", IEE Proceeding Control Theory Application, vol. 146 (1), pp. 58-64.

Vladu E. E. (2003), "Contributions in Using Genetic Algorithms in Engineering", PhD Thesis, "Politehnica" University of Timisoara.

Wang Q. G., Hang C. C. and Yang X. P. (2001), "Single-Loop Controller Design via IMC Principles", Automatica, vol. 37, pp. 2041-2048.

Wang X., Lu T. and Zhang P. (2012), "State Generation Method for Humanoid Motion Planning Based on Genetic Algorithm", International Journal of Advanced Robotic Systems (IJARS), vol. 9, pp. 1-8.

Wang Y. G., and Shao H. H. (2000), "Optimal Tuning for PI Controller, Automatica, vol. 36, pp. 147-152.

Wang S., Wang Y., Du W., Sun F., Wang X., Zhou C. and Liang Y. (2007), "A Multi-Approaches-Guided Genetic Algorithm with Application to Operon Prediction", Artificial Intelligence in Medicine, vol. 41 (2), pp. 151-159.

Weise T. (2009), "Global Optimisation Algorithms - Theory and Application", 2nd edition

Wei D. C. (2007), "A Multi-Crossover Genetic Approach to Multivariable PID Controllers Tuning", Expert Systems with Applications, vol. 33, no. 3, pp. 620-626.

Whitely D. (1993), "A Genetic Algorithm Tutorial", Technical Report CS-93-103, Colorado State University.

Wong K. C., Peng. C, Wong M. H., and Leung K. S. (2011), "Generalizing and Learning Protein-DNA Binding Sequence Representations by An Evolutionary Algorithm", Soft Computing, vol. 15 (8), pp. 1631-1642.

Wu Y. and Ji P. (2007), "Solving the Quadratic Assignment Problems by a Genetic Algorithm with a New Replacement Strategy". International Journal of Mathematical, Computational, Natural and Physical Engineering, vol. 1 (6), pp. 263-267.

Wu Z. Y. and Simpson A. R. (2002), "A Self-Adaptive Boundary Search Genetic Algorithm and its Application to Water Distribution Systems", Journal of Hydraulic Research, vol. 40 (2), pp. 191-203.

Wu Z. Y. and Wang Y. T. (1992), "Arch Dam Optimisation Design Under Strength Fuzziness and Fuzzy Safety Measure", Proceeding Of International Conference on Arch Dam, Hehai University, Nanjing, China, pp. 129-131.

Xiang Z., Zhang Q., Zhu W., Zhang Z. and Zhang Y. Q. (2004), "Peer-to-Peer Based Multimedia Distribution Service", IEEE Transactions on Multimedia, vol. 6 (2), pp. 343-355.

Xiujuan L. and Zhongke S. (2004), "Overview of Multi-objective Optimisation Method", Journal of Systems Engineering and Electronics (JSEE), vol. 15 (2), pp. 142-146.

Xu B., Zhong P. and Tang L. (2012), "Improvement on Boundary Searching of Accelerating Genetic Algorithm", International Conference on Intelligent Design and Engineering Application, pp.301-305.

Yang Z. and Seested,G. T. (2013), "Time-Delay System Identification Using Genetic Algorithm", International Conference on Intelligent Control and Automation Science, vol. 3 (1), pp. 561-567.

Yin F., Wang J. and Guo C. (2004), "Design of PID Controllers Using Genetic Algorithms Approach for Low Damping Slow Response Plants", Advances in Neural Networks, Springer-Verlag Berlin Heidelberg. pp. 219-220.

Zain B. A. M., Tokhi M. O. and Toha S. F. (2009), "PID-Based Control of a Single-Link Flexible Manipulator in Vertical Motion with Genetic Optimisation", Proceeding of the 3rd UKSim European Symposium on Computer Modeling and Simulation, Athens, Greese, pp. 355-360.

Zarko C., Vlastimir N., Ivan C. and Sorin G. (2010), "Advanced Evolutionary Optimisation for Intelligent Modeling and Control of FBC Process", Facta Universitatis, Mechanical Engneering, vol. 8 (1), pp. 47-56.

Zhang H., Cai Y. and Chen Y. (2010), "Parameter Optimisation of PID Controllers Based on Genetic Algorithm", International Conference E-Health Networking, Digital ecosystems and technologies (EDT), vol. 1, pp. 47-49.

Zhao S. Z., Iruthayarajan M. W., Baskar S. and Suganthan P. N. (2012), "Multi-Objective Robust PID Controller Tuning using Two lbests Multiobjective Particle Swarm Optimization", Information Sciences, vol. 181 (16), pp. 3323-3335.

Zhu B. F., Li Z. M. and Zhang B. C. (1984), "Structural Optimal Design: Theory and Applications", Hydro-Electrical Press, Beijing, China, 1984.

Ziegler J. G. and Nichols N. B. (1942), "Optimum Settings for Automatic Controllers", Transactions of the American Society of Mechanical Engineers, vol. 64, pp. 759-768.

Ziegler J. G. and Nichols N. B. (1943), "Process Lags in Automatic Control Circuits", Transactions of the American Society of Mechanical Engineers, vol. 65, pp. 422-444.

Appendix

State-space Model Representation

The 24 state-space matrix of glass furnace process that was employed in chapter 3 can be written in following general form;

$$\dot{x}(t) = A(t)x(t) + B(t)u(t)$$
$$y(t) = C(t)x(t) + D(t)u(t)$$

where, $x(\cdot)$ is the state vector, $x(t) \in \Re^{24}$; $y(\cdot)$ is the output vector, $y(t) \in \Re^{1}$; $u(\cdot)$ is the input (control) vector, $u(t) \in \Re^{2}$; $A(\cdot)$ is the state (system) matrix, $\dim[A(\cdot)] = 24 \times 24$; $B(\cdot)$ is the input matrix,$\dim[B(\cdot)] = 24 \times 2$; $C(\cdot)$ is the output matrix,$\dim[C(\cdot)] = 1 \times 24$; $D(\cdot)$ is the feedforward matrix,$\dim[D(\cdot)] = 1 \times 2$. The $A(\cdot)$ of glass furnace are the individual temperatures in respective volumes. The $B(\cdot)$ consists of the heat input (Q_{Fuel}) and the ambient air temperature (T_{amp}). The $C(\cdot)$ consist the glass temperature (T_g) for control. The $D(\cdot)$ is zero since there is no direct connection between inputs and T_g.

The list of state variables with respective state orders and state variable descriptions applied here is illustrated below.

Order	State Variables	State Variables Description
1	$Ta_{\alpha 1}$	Flame gas zone temperature
2	$Tbw_{\alpha 1}$	Flame back-wall gas zone temperature
3	$Tc_{\alpha 1}$	Flame crown gas zone temperature
4	$Tsw_{\alpha 1}$	Flame side-wall gas zone temperature
5	$Ta_{\alpha 2}$	Non-flame gas zone temperature
6	$Tc_{\alpha 2}$	Non-flame crown gas zone temperature
7	$Tsw_{\alpha 2}$	Non-flame side-wall gas zone temperature
8	$Tfw_{\alpha 2}$	Non-flame forward-wall gas zone temperature

9	$Tg_{\beta 1}$	Flame glass surface zone temperature
10	$Tg_{\beta 2}$	Non-flame glass surface zone temperature
11	$Tg_{\chi 1}$	Flame top-half glass zone temperature
12	$Tbw_{\chi 1}$	Flame back-wall top-half glass zone temperature
13	$Tsw_{\chi 1}$	Flame side-wall top-half glass zone temperature
14	$Tg_{\chi 2}$	Non-flame top-half glass zone temperature
15	$Tsw_{\chi 2}$	Non-flame side-wall top-half glass zone temperature
16	$Tfw_{\chi 2}$	Non-flame forward-wall top-half glass zone temperature
17	$Tg_{\delta 1}$	Flame bottom-half glass zone temperature
18	$Tbw_{\delta 1}$	Flame back-wall bottom-half glass zone temperature
19	$Tsw_{\delta 1}$	Flame side-wall bottom-half glass zone temperature
20	$Tfl_{\delta 1}$	Flame floor bottom-half glass zone temperature
21	$Tg_{\delta 2}$	Non-flame bottom-half glass zone temperature
22	$Tsw_{\delta 2}$	Non-flame side-wall bottom-half glass zone temperature
23	$Tfw_{\delta 2}$	Non-flame forward-wall bottom-half glass zone temperature
24	$Tfl_{\delta 2}$	Non-flame floor bottom-half glass zone temperature

The list of input and output variables with respective state orders and state variable descriptions applied here is illustrated below.

Input Variables	Variables Description
T_{amp}	Ambient temperature
Q_{Fuel}	Pressurised fuel flow in form of energy

Output Variable	Variable Description
$Tg_{\chi 2}$	Non-flame top-half glass zone temperature

The updated A, B, C and D matrix of glass furnace process are given below, with their states truncated to three significant digits.

$$A = \begin{bmatrix}
-3.05e+1 & 4.20e-1 & 8.40e-1 & 5.64e-1 & 2.78e+1 & 0 \\
1.09e-4 & -2.82e-4 & 0 & 0 & 0 & 0 \\
1.09e-4 & 0 & -3.49e-4 & 0 & 0 & 7.88e-5 \\
1.09e-4 & 0 & 0 & -3.70e-4 & 0 & 0 \\
5.56e+1 & 0 & 0 & 0 & -5.88e+1 & 8.19e-1 \\
0 & 0 & 1.61e-4 & 0 & 1.09e-4 & -4.15e-4 \\
0 & 0 & 0 & 1.62e-4 & 1.09e-4 & 0 \\
0 & 0 & 0 & 0 & 1.09e-4 & 0 \\
7.20e-4 & 3.24e-4 & 8.74e-4 & 4.44e-4 & 4.17e-5 & 1.58e-4 \\
3.10e-5 & 2.99e-5 & 3.17e-4 & 9.56e-5 & 7.02e-4 & 5.81e-4 \\
4.95e-5 & 2.23e-5 & 6.01e-5 & 3.06e-5 & 2.87e-6 & 1.09e-5 \\
0 & 2.70e-4 & 0 & 0 & 0 & 0 \\
0 & 0 & 0 & 2.71e-4 & 0 & 0 \\
2.19e-6 & 2.11e-6 & 2.23e-5 & 6.74e-6 & 4.96e-5 & 4.10e-5 \\
0 & 0 & 0 & 0 & 0 & 0 \\
0 & 0 & 0 & 0 & 0 & 0 \\
2.21e-4 & 9.98e-5 & 2.69e-4 & 1.37e-4 & 1.28e-5 & 4.87e-5 \\
0 & 0 & 0 & 0 & 0 & 0 \\
0 & 0 & 0 & 0 & 0 & 0 \\
0 & 0 & 0 & 0 & 0 & 0 \\
9.76e-6 & 9.43e-6 & 9.98e-5 & 3.01e-5 & 2.21e-4 & 1.83e-4 \\
0 & 0 & 0 & 0 & 0 & 0 \\
0 & 0 & 0 & 0 & 0 & 0 \\
0 & 0 & 0 & 0 & 0 & 0
\end{bmatrix}$$

0	0	$1.51e-1$	$3.25e-3$	$1.26e-1$	0
0	0	$1.76e-5$	$8.14e-7$	$1.47e-5$	$6.58e-5$
0	0	$2.38e-5$	$4.31e-6$	$1.98e-5$	0
$7.90e-5$	0	$1.80e-5$	$1.94e-6$	$1.50e-5$	0
$5.51e-1$	$8.40e-1$	$1.75e-2$	$1.47e-1$	$1.46e-2$	0
0	0	$8.83e-6$	$1.62e-5$	$7.36e-6$	0
$-4.444-4$	0	$3.98e-6$	$1.44e-5$	$3.32e-6$	0
0	$-2.47e-4$	$1.39e-5$	$5.33e-5$	$2.14e-6$	0
$4.80e-5$	$4.59e-5$	$-3.46e-3$	0	$8.00e-4$	0
$3.48e-4$	$3.53e-4$	0	$-3.24e-3$	0	0
$3.30e-6$	$3.16e-6$	$6.61e-5$	0	$-7.96e-4$	$1.35e-4$
0	0	0	0	$3.64e-4$	$-7.46e-4$
0	0	0	0	$3.66e-4$	0
$2.45e-5$	$2.49e-5$	0	$6.61e-5$	$2.01e-4$	0
$2.71e-4$	0	0	0	0	0
0	$2.70e-4$	0	0	0	0
$1.48e-5$	$1.41e-5$	0	0	$1.32e-4$	0
0	0	0	0	0	$1.06e-4$
0	0	0	0	0	0
0	0	0	0	0	0
$1.10e-4$	$1.11e-4$	0	0	0	0
0	0	0	0	0	0
0	0	0	0	0	0
0	0	0	0	0	0

0	$2.71e-3$	0	0	$5.63e-1$	0
0	$6.78e-7$	0	0	$6.56e-5$	0
0	$3.59e-6$	0	0	$8.85e-5$	0
$6.59e-5$	$1.61e-6$	0	0	$6.70e-5$	0
0	$1.23e-1$	0	0	$6.51e-2$	0
0	$1.35e-5$	0	0	$3.29e-5$	0
0	$1.20e-5$	$6.59e-5$	0	$1.48e-5$	0
0	$7.25e-6$	0	$6.58e-5$	$4.65e-5$	0
0	0	0	0	0	0
0	$7.81e-4$	0	0	0	0
$1.81e-4$	$9.82e-5$	0	0	$1.32e-4$	0
0	0	0	0	0	$1.06e-4$
$-8.26e-4$	0	$7.92e-5$	0	0	0
0	$-1.03e-3$	$1.81e-4$	$2.76e-4$	0	0
$1.63e-4$	$3.66e-4$	$-9.11e-4$	0	0	0
0	$3.64e-4$	0	$-7.46e-4$	0	0
0	0	0	0	$-2.47e-3$	$1.35e-4$
0	0	0	0	$3.64e-4$	$-4.76e-4$
$1.06e-4$	0	0	0	$3.66e-4$	0
0	0	0	0	$3.65e-4$	0
0	$1.32e-4$	0	0	$2.01e-4$	0
0	0	$1.06e-4$	0	0	0
0	0	0	$1.06e-4$	0	0
0	0	0	0	0	0

$$
\begin{bmatrix}
0 & 0 & 1.21e-2 & 0 & 0 & 0 \\
0 & 0 & 3.03e-6 & 0 & 0 & 0 \\
0 & 0 & 1.60e-5 & 0 & 0 & 0 \\
0 & 0 & 7.20e-6 & 0 & 0 & 0 \\
0 & 0 & 5.49e-1 & 0 & 0 & 0 \\
0 & 0 & 6.04e-5 & 0 & 0 & 0 \\
0 & 0 & 5.37e-5 & 0 & 0 & 0 \\
0 & 0 & 4.82e-6 & 0 & 0 & 0 \\
0 & 0 & 0 & 0 & 0 & 0 \\
0 & 0 & 0 & 0 & 0 & 0 \\
0 & 0 & 0 & 0 & 0 & 0 \\
0 & 0 & 0 & 0 & 0 & 0 \\
1.06e-4 & 0 & 0 & 0 & 0 & 0 \\
0 & 0 & 1.32e-4 & 0 & 0 & 0 \\
0 & 0 & 0 & 1.06e-4 & 0 & 0 \\
0 & 0 & 0 & 0 & 1.06e-4 & 0 \\
1.82e-4 & 1.11e-3 & 9.83e-5 & 0 & 0 & 0 \\
0 & 0 & 0 & 0 & 0 & 0 \\
-5.56e-4 & 0 & 0 & 7.92e-5 & 0 & 0 \\
0 & -4.08e-4 & 0 & 0 & 0 & 3.87e-5 \\
0 & 0 & -2.67e-3 & 1.81e-4 & 2.76e-4 & 1.11e-3 \\
1.63e-4 & 0 & 3.66e-4 & -6.40e-4 & 0 & 0 \\
0 & 0 & 3.64e-4 & 0 & -4.76e-4 & 0 \\
0 & 1.61e-4 & 3.65e-4 & 0 & 0 & -5.31e-4
\end{bmatrix}
$$

$$B^T = \left[\begin{array}{cccccccc} 0 & 5.25e-6 & 5.25e-6 & 5.25e-6 & 0 & 5.25e-6 & 5.25e-6 & 5.25e-6 \\ 5 & 0 & 0 & 0 & 0 & 0 & 0 & 0 \end{array} \right.$$

$$\left. \begin{array}{cccccccc} 0 & 0 & 0 & 5.25e-6 & 5.25e-6 & 0 & 5.25e-6 & 5.25e-6 \\ 0 & 0 & 0 & 0 & 0 & 0 & 0 & 0 \end{array} \right]$$

$$\left[\begin{array}{cccccccc} 0 & 5.25e-6 & 5.25e-6 & 5.25e-6 & 5.25e-6 & 5.25e-6 & 5.25e-6 & 5.25e-6 \\ 0 & 0 & 0 & 0 & 0 & 0 & 0 & 0 \end{array} \right]$$

$$C = \left[\begin{array}{cccccccccccccccccccccccc} 0 & 0 & 0 & 0 & 0 & 0 & 0 & 0 & 0 & 0 & 0 & 0 & 1 & 0 & 0 & 0 & 0 & 0 & 0 & 0 & 0 & 0 & 0 \end{array} \right]$$

$$D = \left[\begin{array}{cc} 0 & 0 \end{array} \right]$$

24 State Variables Equation

The 2 updated energy balance equations with the respective state variables are;

- For $\dot{Q}fw_{\alpha 2}$,

$$\begin{aligned} Cfw_{\alpha 2}\frac{dTfw_{\alpha 2}}{dt} = & \dot{Q}a_{\alpha 2} + \dot{Q}g_{\beta 1} + \dot{Q}g_{\beta 2} + \dot{Q}g_{\chi 1} + \\ & \dot{Q}g_{\chi 2} + \dot{Q}fw_{\chi 2} + \dot{Q}g_{\delta 1} + \dot{Q}g_{\delta 2} \\ \frac{dTfw_{\alpha 2}}{dt} = & Ta_{\alpha 2} - Tfw_{\alpha 2} + Tg_{\beta 1} + Tg_{\beta 2} + Tg_{\chi 1} + \\ & Tg_{\chi 2} + Tfw_{\chi 2} + Tg_{\delta 1} + Tg_{\delta 2} \end{aligned}$$

- For $\dot{Q}g_{\beta 2}$,

$$\begin{aligned} Cg_{\beta 2}\frac{dTg_{\beta 2}}{dt} = & \dot{Q}a_{\alpha 1} + \dot{Q}bw_{\alpha 1} + \dot{Q}c_{\alpha 1} + \dot{Q}sw_{\alpha 1} + \dot{Q}a_{\alpha 2} + \\ & \dot{Q}c_{\alpha 2} + \dot{Q}sw_{\alpha 2} + \dot{Q}fw_{\alpha 2} + \dot{Q}g_{\chi 2} \\ \frac{dTg_{\beta 2}}{dt} = & Ta_{\alpha 1} + Tbw_{\alpha 1} + Tc_{\alpha 1} + Tsw_{\alpha 1} + Ta_{\alpha 2} + \\ & Tc_{\alpha 2} + Tsw_{\alpha 2} + Tfw_{\alpha 2} - Tg_{\beta 2} + Tg_{\chi 2} \end{aligned}$$

Energy Distribution with Isolated Dynamic Progressions

The respective test patterns of energy distribution to estimate the energy level for both chamber 1 and 2 with different steady-state are; 1). $1350K_{(Chamber1)} \longrightarrow 1500K_{(Chamber2)}$, 2). $1400K_{(Chamber1)} \longrightarrow 1500K_{(Chamber2)}$, 3). $1450K_{(Chamber1)} \longrightarrow 1500K_{(Chamber2)}$ and 4). $1500K_{(Chamber1)} \longrightarrow 1550K_{(Chamber2)}$.

Table 7.1: Energy Distribution, $1350K_{(Chamber1)} \longrightarrow 1500K_{(Chamber2)}$

Energy Distribution (%)	StateVariable of Chamber 1 ($T_{g_{\chi 1}}$)	Fuel Consumption of Chamber 1 $(1350K)(kg/s)$	Fuel Consumption of Chamber 2 $(1500K)(kg/s)$	Total Fuel Consumption (kg/s)
100	2.01e-4	0.002152	x	x
0.1	2.01e-7	0.002148	0.002714	0.004862
0.5	1.01e-6	0.002149	0.002690	0.004839
1	2.01e-6	0.002153	0.002663	0.004816
5	1.61e-5	0.002156	0.002413	0.004569
10	2.01e-5	0.002150	0.002092	0.004242
15	3.02e-5	0.002156	0.001783	0.003939
20	4.02e-5	0.002162	0.001474	0.003636
25	5.03e-5	0.002161	0.001157	0.003318
30	6.03e-5	0.002134	0.000814	0.002948
35	7.04e-5	0.002152	0.000518	0.002670
40	8.04e-5	0.002176	x	x

Table 7.2: Energy Distribution, $1400K_{(Chamber1)} \longrightarrow 1500K_{(Chamber2)}$

Energy Distribution (%)	StateVariable of Chamber 1 ($T_{g_{\chi 1}}$)	Fuel Consumption of Chamber 1 $(1400K)(kg/s)$	Fuel Consumption of Chamber 2 $(1500K)(kg/s)$	Total Fuel Consumption (kg/s)
100	2.01e-4	0.002308	x	x
0.1	2.01e-7	0.002319	0.002713	0.005032
0.5	1.01e-6	0.002337	0.002705	0.005042
1	2.01e-6	0.002306	0.002641	0.004947
5	1.61e-5	0.002330	0.002403	0.004733
10	2.01e-5	0.002315	0.002061	0.004376
15	3.02e-5	0.002330	0.001749	0.004079
20	4.02e-5	0.002320	0.001400	0.003720
25	5.03e-5	0.002331	0.001095	0.003426
30	6.03e-5	0.002313	0.000751	0.003064
35	7.04e-5	0.002326	0.000437	0.002763
40	8.04e-5	0.002329	x	x

Table 7.3: Energy Distribution, $1450K_{(Chamber1)} \longrightarrow 1500K_{(Chamber2)}$

Energy Distribution (%)	StateVariable of Chamber 1 ($T_{g_{\chi 1}}$)	Fuel Consumption of Chamber 1 $(1450K)(kg/s)$	Fuel Consumption of Chamber 2 $(1500K)(kg/s)$	Total Fuel Consumption (kg/s)
100	2.01e-4	0.002522	x	x
0.1	2.01e-7	0.002523	0.002718	0.005241
0.5	1.01e-6	0.002523	0.002692	0.005215
1	2.01e-6	0.002517	0.002652	0.005169
5	1.61e-5	0.002525	0.002389	0.004914
10	2.01e-5	0.002535	0.002061	0.004596
15	3.02e-5	0.002535	0.001721	0.004256
20	4.02e-5	0.002518	0.001365	0.003883
25	5.03e-5	0.002572	0.001080	0.003652
30	6.03e-5	0.002496	0.000665	0.003161
35	7.04e-5	0.002572	0.000402	0.002974
40	8.04e-5	x	x	x

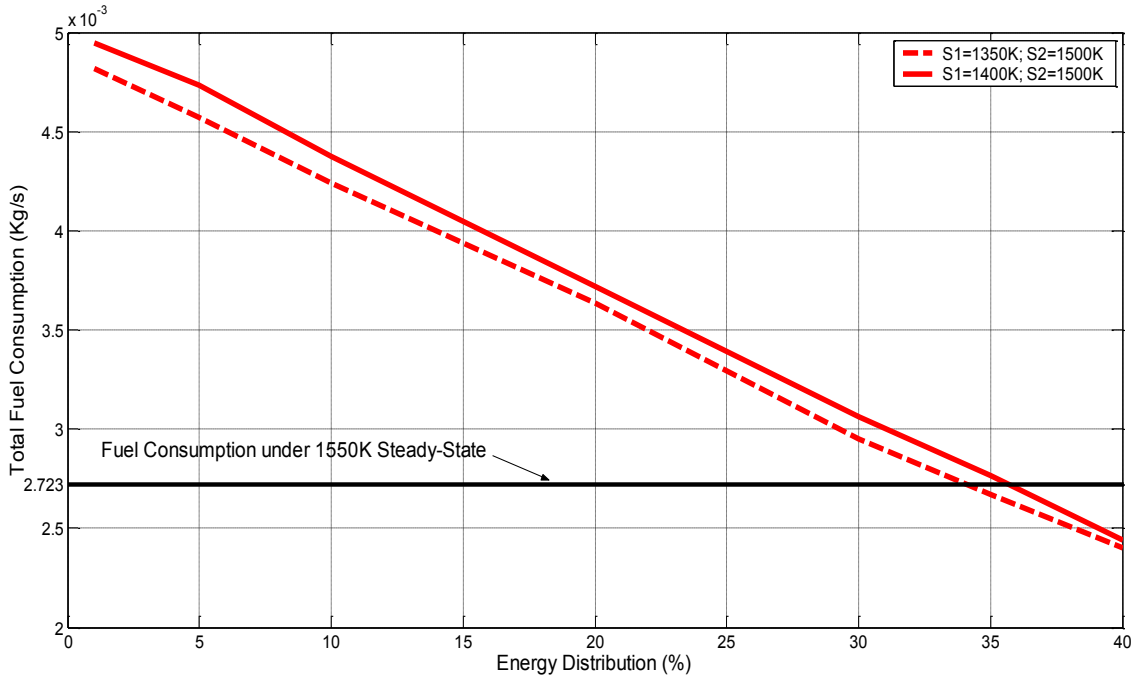

Figure 7.2: 2 Energy Distributions$(1350K_{(Chamber1)} \longrightarrow 1500K_{(Chamber2)})$,$(1400K_{(Chamber1)} \longrightarrow 1500K_{(Chamber2)})$

Table 7.4: Energy Distribution, $1500K_{(Chamber1)} \longrightarrow 1550K_{(Chamber2)}$

Energy Distribution (%)	StateVariable of Chamber 1 ($T_{g_{\chi 1}}$)	Fuel Consumption of Chamber 1 $(1500K)(kg/s)$	Fuel Consumption of Chamber 2 $(1550K)(kg/s)$	Total Fuel Consumption (kg/s)
100	2.01e-4	0.002733	x	x
0.1	2.01e-7	0.002698	0.002919	0.005617
0.5	1.01e-6	0.002743	0.002929	0.005672
1	2.01e-6	0.002735	0.002879	0.005614
5	1.61e-5	0.002709	0.002562	0.005271
10	2.01e-5	0.002726	0.002226	0.004952
15	3.02e-5	0.002717	0.001836	0.004553
20	4.02e-5	0.002737	0.001497	0.004234
25	5.03e-5	0.002738	0.001134	0.003872
30	6.03e-5	0.002726	0.000769	0.003495
35	7.04e-5	0.002708	0.000376	0.003084
40	8.04e-5	x	x	x

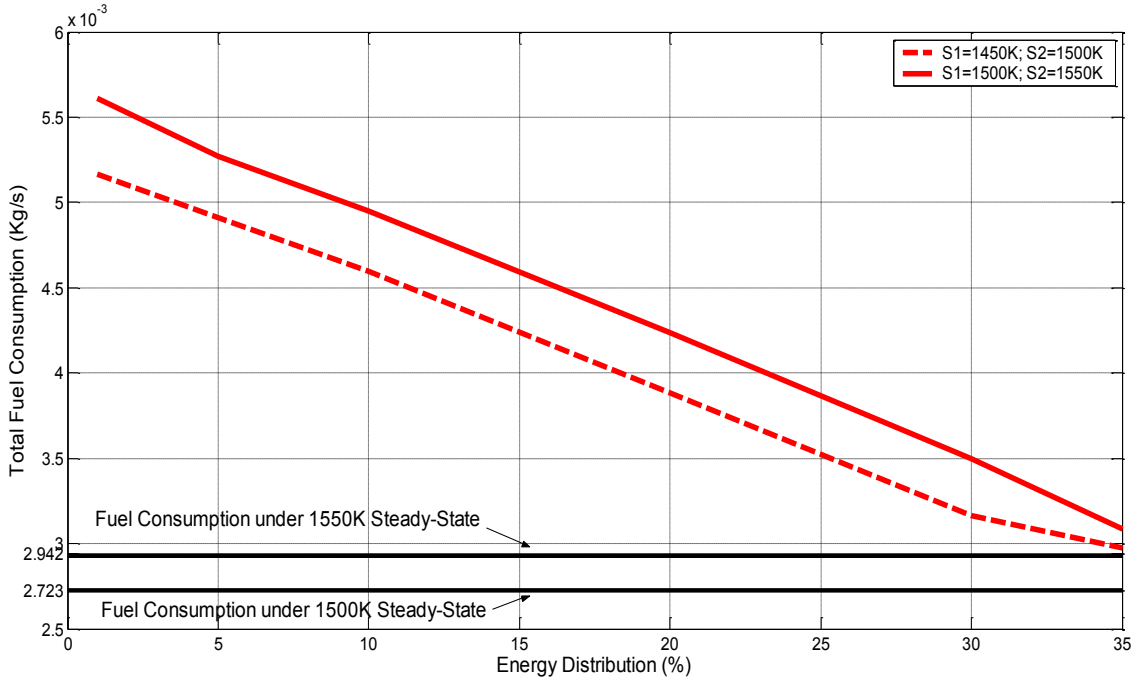

Figure 7.3: 2 Energy Distributions$(1450K_{(Chamber1)} \longrightarrow 1500K_{(Chamber2)})$,$(1500K_{(Chamber1)} \longrightarrow 1550K_{(Chamber2)})$